

**EXPLOITING PASSIVE GAMMA SIGNALS FROM WEAPONS
GRADE PLUTONIUM AND HIGHLY ENRICHED URANIUM FOR
WEAPONS PIT STORAGE**

A Thesis
Presented to
The Academic Faculty

by

Jessica N. Paul

In Partial Fulfillment
of the Requirements for the Degree
Master of Science in Nuclear and Radiological Engineering in the
School of Mechanical Engineering

Georgia Institute of Technology
December 2013

COPYRIGHT 2013 BY JESSICA N. PAUL

**EXPLOITING PASSIVE GAMMA SIGNALS FROM WEAPONS
GRADE PLUTONIUM AND HIGHLY ENRICHED URANIUM FOR
WEAPONS PIT STORAGE**

Approved by:

Dr. Glenn E. Sjoden, Advisor
School of Mechanical Engineering
Georgia Institute of Technology

Dr. Chris Wang
School of Mechanical Engineering
Georgia Institute of Technology

Dr. Bojan Petrovic
School of Mechanical Engineering
Georgia Institute of Technology

Dr. Ce Yi
School of Mechanical Engineering
Georgia Institute of Technology

Date Approved: April 24, 2013

ACKNOWLEDGEMENTS

This material is based upon work supported by the U.S. Department of State and the U.S. Department of Homeland Security under Grant Award Number, 2012-DN-130-NF0001-02. The views and conclusions contained in this document are those of the authors and should not be interpreted as necessarily representing the official policies, either expressed or implied, of the U.S. Department of Homeland Security.

TABLE OF CONTENTS

	Page
ACKNOWLEDGEMENTS	iii
LIST OF TABLES	vi
LIST OF FIGURES	vii
LIST OF SYMBOLS AND ABBREVIATIONS	xi
SUMMARY	xii
 <u>CHAPTER</u>	
1 INTRODUCTION	1
Background	1
Purpose	2
Technical Background	2
2 MODEL DEVELOPMENT	10
Computational Methods	10
MCNP	11
PENTRAN	11
Models	12
3 SOURCE TERMS	19
Source Book	25
4 PASSIVE AGE DATING OF SNM	32
Highly Enriched Uranium	32
Weapons Grade Plutonium	39
Spoof Testing	47
5 NEUTRON DETECTION	52

Transport Methodology	54
Detector Block I	56
Detector Block III	65
Detector Block V	71
6 CONCLUSIONS	79
APPENDIX A: Source Book	81
APPENDIX B: Sample MCNP Source Box Input	171
APPENDIX C: Sample MCNP GEB Input	175
REFERENCES	179

LIST OF TABLES

	Page
Table 2.1: SNM canister configurations [12, 14].	15
Table 2.2: SNM pit dimensions.	16
Table 3.1: Isotopic makeup of HEU used in this study.	20
Table 3.2: Isotopic makeup of WGpu used in this study.	20
Table 3.3: Bugle 47 group structure for neutron emissions [18].	22
Table 3.4: 30 group structure for neutron emissions.	22
Table 3.5: 24 group structure for gamma emissions.	23
Table 4.1: Ratios of regions of interest in HEU, NORM, and 50y rods [19].	33
Table 4.2: FWHM data for a typical CsI as a function of energy.	37
Table 4.3: GEB parameters for MCNP f8 tally.	37
Table 4.4: Total gamma leakages through +x plane of the Source Box for various ages of the WGpu shell source.	42
Table 4.5: Gamma leakage through one surface of source box for various HEU masses using a hollowed out solid core diversions with an outer radius of 6.79cm. All cases had an average relative 1 sigma error of ~0.5%.	50
Table 5.1: Uncollided fraction of neutrons in the He-3 detectors per forward energy group.	65
Table A.1: 1year HEU Shell Source Inner Source Box.	83
Table A.2: 1 year Shell Source Outer Source Box.	85
Table A.3: 1 year HEU Shell spatial distributions at Outer Source Box.	87
Table A.4: 1 year HEU Solid Source Inner Source Box.	88
Table A.5: 1 year HEU Solid Source Outer Source Box.	90
Table A.6: 1 year HEU Solid spatial distributions at Outer Source Box.	92
Table A.7: 22.5 year HEU Shell Source Inner Source Box.	94

Table A.8: 22.5 year HEU Shell Source Outer Source Box.	96
Table A.9: 22.5 year HEU Solid Source Inner Source Box	98
Table A.10: 22.5 year HEU Solid Source Outer Source Box.	100
Table A.11: 50 year HEU Shell Source Inner Source Box.	102
Table A.12: 50 year HEU Shell Source Outer Source Box.	104
Table A.13: 50 year HEU Shell spatial distributions at Outer Source Box surfaces.	106
Table A.14: 50 year HEU Solid Source Inner Source Box.	107
Table A.15: 50 year HEU Solid Source Outer Source Box.	109
Table A.16: 50 year HEU Solid spatial distributions at Outer Source Box surfaces.	111
Table A.17: 75 year HEU Shell Source Inner Source Box.	113
Table A.18: 75 year HEU Shell Source Outer Source Box.	115
Table A.19: 75 year HEU Solid Source Inner Source Box.	117
Table A.20: 75 year HEU Solid Source Outer Source Box.	119
Table A.21: 1 year WGpu Shell Gamma spectrum Inner Source Box.	121
Table A.22: 1 year WGpu Shell Gamma spectrum Outer Source Box.	123
Table A.23: 1 year WGpu Shell Neutron spectrum Outer Source Box.	125
Table A.24: 1 year WGpu Solid Gamma spectrum Inner Source Box.	127
Table A.25: 1 year WGpu Solid Gamma spectrum Outer Source Box.	129
Table A.26: 1 year WGpu Solid Neutron spectrum Outer Source Box.	131
Table A.27: 22.5 year WGpu Shell Gamma spectrum Inner Source Box.	133
Table A.28: 22.5 year WGpu Shell Gamma spectrum Outer Source Box.	135
Table A.29: 22.5 year WGpu Shell Neutron spectrum Outer Source Box.	137
Table A.30: 22.5 year WGpu Shell 30 Group Neutron spectrum Outer Source Box.	139
Table A.31: 22.5 year WGpu Shell spatial distributions for Outer Source Box surfaces.	140
Table A.32: 22.5 year WGpu Solid Gamma spectrum Inner Source Box.	141

Table A.33: 22.5 year WGPu Solid Gamma spectrum Outer Source Box.	143
Table A.34: 22.5 year WGPu Solid Neutron spectrum Outer Source Box.	145
Table A.35: 22.5 year WGPu Solid 30 Group Neutron spectrum Outer Source Box.	147
Table A.36: 50 year WGPu Shell Gamma spectrum Inner Source Box.	151
Table A.37: 50 year WGPu Shell Gamma spectrum Outer Source Box.	153
Table A.38: 50 year WGPu Shell Neutron spectrum Outer Source Box.	155
Table A.39: 50 year WGPu Solid Gamma spectrum Inner Source Box.	157
Table A.40: 50 year WGPu Solid Gamma spectrum Outer Source Box.	159
Table A.41: 50 year WGPu Solid Neutron spectrum Outer Source Box.	161
Table A.42: 25 kg HEU unshielded.	165
Table A.43: 8 kg WGPu unshielded source gammas ($0.29 - 2.75$ MeV).	166
Table A.44: 8 kg WGPu unshielded source gammas ($1.0 \times 10^{-13} - 3.0$ MeV).	167
Table A.45: 8 kg WGPu unshielded source neutrons.	168
Table A.46: 8 kg WGPu unshielded source 30 group neutron spectrum.	170

LIST OF FIGURES

	Page
Figure 1.1: MPVS Concept, where the flat detector area shown (at Left) must be collimated as it moves past the SNM Source container, and detectors move past the source within a fixed gate time, where most all counts are recorded in close proximity to the source, as is shown on a normalized scale (Center). To prevent interference from other sources, collimators (shielding) must surround the detectors (shown at Right).	6
Figure 2.1: Lard canister storage on racks at the Hanford Site [11].	12
Figure 2.2: AL-R8 pit container used for a dismantled nuclear weapon at Pantex[13].	13
Figure 2.3: AT-400A pit container for Pantex [14].	14
Figure 2.4: MCNP geometry model of HEU shell source cut along x-z and x-y planes. The inner shell is HEU, surrounded by aluminum. Air surrounds the shells and is contained by Celotex surrounded by steel. Air makes up the remainder.	16
Figure 2.5: MCNP Monte Carlo model of HEU solid source geometry cut along x-z and x-y planes. The inner sphere is HEU, the surrounding shell is aluminum. Air surrounds the shells and is contained by Celotex, which is surrounded by a thin layer of steel. Air makes up the remaining portion of the figure.	17
Figure 3.1: Example section of an ORIGEN output file showing the gamma/s leakage rate from a 25kg HEU source.	21
Figure 3.2: Typical HEU (50 year aged) spectrum with key gamma peaks readily identified.	23
Figure 3.3: Typical WGPu spectrum (22.5 year aged) with key gamma peaks readily identified.	24
Figure 3.4: Normalized unshielded gamma emission from 25 kg of 1 year age since separation HEU.	24
Figure 3.5: Normalized unshielded gamma emission from 8 kg of 22.5 year age since separation WGPu.	25
Figure 3.6: Histogram plot for 50 year age since separation HEU shell source from both MCNP and PENTRAN gamma leakage results through the Source Box.	26
Figure 3.7: (a) The relative contributions of photon leakage across the top and bottom surfaces of the Source Box. (b) The relative contributions of photon leakage across the side surfaces of the Source Box.	27

Figure 3.8: The complicated weapon pit geometry can be simplified so that the contents no longer need to be modeled and the leakage source term can be used in a “painted” distribution on the surface of a box.	28
Figure 3.9: Sample SDEF card in MCNP for source box model of 1 year HEU shell source.	30
Figure 4.1: Normalized HEU spectrum for 1 year, 22.5 years, and 50 years since separation.	33
Figure 4.2: Ratio 1 (Eqn 4.1) for both shell and solid HEU configurations, along with the published reference ratios: (830-1060 keV)/(700-3000 keV).	35
Figure 4.3: Ratio 2 (Eqn 4.2) for both shell and solid HEU configurations, along with the published reference ratios: (830-1060 keV)/(1060-3000 keV).	36
Figure 4.4: Gamma spectrum for 1 year and 50 years since separation HEU for a CsI detector using a pulse height tally in MCNP5 with Gaussian energy broadening. Below E=1MeV, the average relative error is 28% for the 1yr case, and 21% for the 50yr case. Above 1 MeV the average relative error is 70% for both cases.	38
Figure 4.5: Ratio 2 (Eqn. 4.2) for both shell and solid HEU configurations, along with the published reference ratios: (830-1060 keV)/(1060-3000 keV). The ratio for the shell HEU configuration from the spectrum seen in a CsI detector is also included.	39
Figure 4.6: WGpu unshielded signature for various ages since separation.	40
Figure 4.7: (a) Ratio for WGpu <i>shell source</i> using the protocol Ratio 3 (Eqn 4.5). (b) Ratio (nonlinear) for WGpu <i>shell source</i> using the protocol Ratio 4 (Eqn 4.6).	44
Figure 4.8: The Gaussian Energy Broadened spectrum of 1year, 22.5year, and 50 year age since separation WGpu shell source for a 4 x 4 x 8 CsI detector placed approximately 5cm away from the surface of the pit container. The average relative errors were 28%, 23%, and 29% for the 1yr, 22.5yr, and 50yr cases.	45
Figure 4.9: Comparison between normalized total gamma leakage through the source box surface for the solid and shell configured sources for 22.5 years age since separation WGpu. The Energy range is restricted to highlight upper energy differences in the spectrum.	46
Figure 4.10: (a) Comparison of the solid and shell 22.5 year WGpu gamma leakages for ratio 4 (Eqn 4.6). (b) Comparison of the solid and shell 22.5 year WGpu source gamma leakages for ratio 5 (Eqn 4.7).	47

Figure 4.11: Neutron spectrum for a WGPu source along with a PuBe shielded surrogate source [22].	48
Figure 5.1: The normalized neutron leakage for a 22.5 year age since separation WGPu Shell. The average relative 2 sigma error was 0.12%.	52
Figure 5.2: Blocks 1 through 5 (from left to right) of the neutron detector assembly [23].	53
Figure 5.3: Block I of the neutron detector assembly and gamma detector block model in PENTRAN.	56
Figure 5.4: Block I adjoint importances for “forward” group ordering, including group 30 ($<1 \times 10^{-10}$ MeV) ceiling/floor (1.0/0.0), group 13 ($1.3 \times 10^{-6} - 3.05 \times 10^{-6}$ MeV) ceiling/floor (0.58/0.0), group 3 (3.0 – 8.19 MeV) ceiling/floor ($6.7 \times 10^{-2}/4.0 \times 10^{-5}$), and group 1 (17.3 – 20 MeV) ceiling/floor ($1.3 \times 10^{-2}/4.8 \times 10^{-5}$) at center height of Source Box.	57
Figure 5.5: Adjoint importances for forward group 30 (thermal, $< 1 \times 10^{-10}$ MeV), group 13 (epithermal, $1.3 \times 10^{-6} - 3.05 \times 10^{-6}$ MeV), group 3 (fast, 3.0 – 8.19 MeV), and 1 (high energy, 17.3 – 20 MeV) sliced at center height of the Source Box. The color map scaling is identical for all four plots. The ceiling and floor importances were 1.0 and 5×10^{-6} respectively.	58
Figure 5.6: Block I adjoint importances along the source box surface 30 cm away from detector surface at center height. The vertical lines represent the detector block separations and collimation.	60
Figure 5.7: Block I adjoint importances along source box surface 30 cm away from detector surface at center height.	61
Figure 5.8: Visualization of the section that the adjoint model includes from the source box.	62
Figure 5.9: a.) Block I detector model for collided neutrons in MCNP5. b.) Block I detector model for uncollided neutrons in MCNP5.	64
Figure 5.10: Block III of the neutron detector assembly and gamma detector block model in PENTRAN.	66
Figure 5.11: Block III adjoint importances for “forward” groups 30 ($<1 \times 10^{-10}$ MeV) ceiling/floor (1.0/0.0), 13 ($1.3 \times 10^{-6} - 3.05 \times 10^{-6}$ MeV) ceiling/floor (0.58/0.0), 3 (3.0 – 8.19 MeV) ceiling/floor ($6.7 \times 10^{-2}/4.0 \times 10^{-5}$), and 1 (17.3 – 20 MeV) ceiling/floor ($1.3 \times 10^{-2}/4.8 \times 10^{-5}$) at center height of Source Box.	67

Figure 5.12: Block III adjoint importances for “forward” group 30 (thermal, $< 1 \times 10^{-10}$ MeV), group 13 (epithermal, $1.3 \times 10^{-6} - 3.05 \times 10^{-6}$ MeV), group 3 (fast, 3.0 – 8.19 MeV), and 1 (high energy, 17.3 – 20 MeV) sliced at center height of the Source Box. The color map scaling is identical for all four plots. The ceiling and floor importances were 1.0 and 5×10^{-6} respectively. 68

Figure 5.13: Block III adjoint importances along source box surface 30 cm away from detector surface at center height. The vertical lines represent the detector block separations and collimation. 70

Figure 5.14: Block III adjoint importances along source box surface 30 cm away from detector surface at center height. Group numbers refer to forward group. 71

Figure 5.15: Block V of the neutron detector assembly and gamma detector block model in PENTRAN. 72

Figure 5.16: Block V adjoint importances for “forward” groups 30 ($< 1 \times 10^{-10}$ MeV) ceiling/floor (1.0/0.0), 13 ($1.3 \times 10^{-6} - 3.05 \times 10^{-6}$ MeV) ceiling/floor (0.58/0.0), 3 (3.0 – 8.19 MeV) ceiling/floor ($6.7 \times 10^{-2} / 4.0 \times 10^{-5}$), and 1 (17.3 – 20 MeV) ceiling/floor ($1.3 \times 10^2 / 4.8 \times 10^5$) at center height of Source Box. 73

Figure 5.17: Block V adjoint importances for “forward” group 30 (thermal, $< 1 \times 10^{-10}$ MeV), group 13 (epithermal, $1.3 \times 10^{-6} - 3.05 \times 10^{-6}$ MeV), group 3 (fast, 3.0 – 8.19 MeV), and 1 (high energy, 17.3 – 20 MeV) sliced at center height of the Source Box. The color map scaling is identical for all four plots. The ceiling and floor importances were 1.0 and 5×10^{-6} respectively. 74

Figure 5.18: Block V adjoint importances for “forward” group 23 (thermal, $3 \times 10^{-8} - 4 \times 10^{-8}$), and group 20 (thermal, $7 \times 10^{-8} - 1 \times 10^{-7}$) sliced at center height of the Source Box. The color map scaling is identical for both plots. The ceiling and floor importances were 1.0 and 5×10^{-6} respectively. 75

Figure 5.19: Block V adjoint importances along source box surface 30 cm away from detector surface at center height. The vertical lines represent the detector block separations and collimation. 76

Figure 5.20: Block V adjoint importances along source box surface 30 cm away from detector surface at center height. 77

Figure A.1: Visualization of how gammas and neutrons are leaking through the Source Box surfaces. The data is presented as gammas or neutrons leaking through an individual side or top or bottom of the source box. 81

Figure A.2: HEU 1 year Shell Outer Source Box Histograms. 93

Figure A.3: HEU 50 year Shell Outer Source Box Histograms of gamma leakage. 112

Figure A.4: 22.5 year WGPu Shell Histograms for gamma and neutron leakages through outer source box side surfaces.	148
Figure A.5: 22.5 year WGPu Solid Histograms for gamma and neutron leakages through outer source box side surfaces.	149
Figure A.6: 22.5yr WGPu Solid vs. Shell Comparison.	150
Figure A.7: HEU 10keV binned unshielded 25kg mass gamma spectrum.	163
Figure A.8: WGPu 10keV binned unshielded 8kg mass gamma spectrum.	164

LIST OF SYMBOLS AND ABBREVIATIONS

FOV	Field of View
IAEA	International Atomic Energy Agency
HEU	Highly Enriched Uranium
LANL	Los Alamos National Laboratory
MPVS	Mobile Pit Verification System
ORNL	Oak Ridge National Laboratory
PFR	Probability of False Alarm
POD	Probability of Detection
SNM	Special Nuclear Material
SNR	Signal-to-Noise Ratio
SQ	Significant Quantity
WGPu	Weapons Grade Plutonium

SUMMARY

Using computational deterministic and Monte Carlo methods, I present an analysis of the gamma and neutron signatures emitted from special nuclear material (SNM) in weapons stockpile storage scenarios. My efforts are focused on 1 year old, 25 year old, 50 year old, and 75 year old highly enriched uranium (HEU), and 1 year old, 22.5 year old, and 50 year old weapons grade plutonium (WGPu). HEU gammas are easily shielded, and when reasonably shielded, do not produce a definable signature at low energies; however, using new methods applied in this work that involve analyzing the higher energy, penetrating gammas from HEU, it can be shown that not only the presence of the HEU can be verified, but also the age since separation of the material can be discerned. Through computational modeling, I am able to verify that the novel methods investigated are both unique and effective for HEU detection. In addition, I also present my investigation of similar methods applied to the detection of WGPu. From this work I determined that WGPu age discrimination is more challenging compared to that of HEU (in spite of more radiation per unit mass) due to the high rate of induced gammas from n-gamma interactions taking place within the Pu metal and container; however, I believe that by combining neutron detection with gamma signature verification of WGPu, the approach identified can be successful. I present the neutron signature of the WGPu and how it would be observed in the detector used for material verification. I calculated the detector response for a pre-determined neutron detector design using adjoint calculations in order to determine whether the detector will perform as designed. In addition to developing a new protocol for WGPu detection, I present in this work, a

comprehensive source book as a product of this research, detailing the gamma and neutron signatures for both solid and shell configurations of HEU and WGPu. This can serve as a very beneficial guide for anyone interested in modeling SNM, since the many steps needed to obtain this radiation leakage data will save a significant amount of researcher time. The results from my work have contributed to a collaborative effort supporting funded US department of State research towards designing a mobile detection system that can rapidly validate and verify the presence of SNM in weapons pit containers.

CHAPTER 1

INTRODUCTION

Background

The main component of a nuclear weapon is the special nuclear material (SNM) that is used as the fuel. Because of the grave potential damage a nuclear device can cause, all SNM must be properly accounted for in various storage facilities maintained by nuclear weapon states, and diversions of this material must be prevented. The work presented in this thesis has provided foundational technical data supporting the design of a Mobile Pit Verification System in a research effort for the US Department of State.

One of the main steps one can take to prevent a loss of control of nuclear material is to ensure that SNM in weapons stockpile storage facilities has not been diverted for undeclared nuclear activities through Verification and Validation (V&V) of SNM storage containers. Matthew Bunn, an associate Professor at Harvard University's John F. Kennedy School of Government, states that nuclear weapon terrorism could be prevented if all of the existing stockpiles are effectively guarded [1]. Currently, some procedures in place to do this can require considerable time and effort via interrogation of individual storage containers using radiation detectors. In large facilities, potentially only a fraction of all SNM storage containers are subjected to content authentication, and therefore a potential opportunity for the diversion of materials can arise if the diverter is willing to assume the risk of an empty container not being inspected. In the past, Al-Qaeda's leadership has shown a desire to acquire nuclear weapons by any means, and views the acquisition of such to be a "religious duty" [1]. Therefore, the risk for diversion and the need for vigilant monitoring of SNM materials in storage facilities must not be underestimated.

Purpose

In order to mitigate risk of SNM diversion or to detect a diversion, full inspection of every SNM container is considered ultimately necessary by many arms control experts. The US Department of State funded our research team to design a mobile pit detector system, capable of rapidly validating and verifying SNM in stockpile storage. As a result, using computational tools, a mobile detector platform, or *Mobile Pit Verification System* (MPVS), has been designed to make this goal attainable in a rapid time frame with a high probability of detection. In order to satisfy the many complex issues in designing the MPVS to detect and verify that SNM has not been diverted, comprehensive neutron and gamma signatures were needed to assess what passive radiation is available for detection. In this work, I will discuss how I constructed credible SNM sources using both deterministic and Monte Carlo models to describe the leakage of photons and neutrons from weapon storage container sources that will reach a detector employed for safeguards verification. I will also discuss how I performed research to utilize and create new methods for verifying Highly Enriched Uranium (HEU) and Weapons Grade Plutonium (WGPu) materials stored in containers via passive means. This information was ultimately used in the design of the MPVS.

Technical Background

HEU verification and age dating

For many years researchers have been carefully examining how to detect and verify HEU. It is noted by Thomas Gosnell [2], that an estimate of enrichment can be found by analyzing the concentration of ^{235}U and ^{238}U by scrutinizing their prominent intrinsic gamma ray emissions. This method is a major challenge, especially for shielded HEU, because the principal characteristic gamma for ^{235}U is at an energy of 186 keV, and the characteristic gamma for ^{238}U is 1001 keV. This large separation in energy

introduces many issues in cases with unknown shielding. The 186 keV gamma is easily shielded, whereas the 1001 keV gamma can penetrate materials without significant attenuation. This can substantially shift the detected enrichment of the uranium in question, and can even make material appear below the HEU enrichment threshold of 20% U-235 if only looking at these two gamma energies. An alternative method to passively detect HEU that has been examined is performing gamma spectrometry analysis for the presence of ^{232}U . ^{232}U does not occur in nature; instead it is a product of reactor irradiation, and has a characteristic gamma at 2615 keV (from ^{208}Tl in the decay chain). Trace quantities of ^{232}U contaminate the HEU in the United States (US) since it was introduced in the 1960's in US gaseous diffusion cascades from reprocessed spent reactor fuel [2]. The relatively short half-life of ^{232}U and its daughters results in a high specific activity, which makes it clearly observable in the HEU spectrum. The difficulty, however, presses the need for longer counting times to be able to detect it, and this line can't be used alone as a way to detect HEU, since not all HEU may be mixed with reprocessed uranium, and this gamma line is also associated with the decay of ^{228}Th [2] and thorium fuel cycles. It also depends immensely on the quantity of contamination. In the literature, Thomas Gosnell concluded that the simplest technique to detect shielded HEU would be to detect the 1001 keV line to confirm the presence of uranium, and also the 2615 keV line, but in order to verify the material in question is in fact HEU, both the 911 keV (from Th decay chain) and 414 keV (WGpu) lines must also be absent. Verifying all four conditions would take considerable time, depending on the relative contamination level or use of large, costly high-resolution gamma-ray detectors, not ideal for weapons pit verification applications. It is also important to note that the 2615 keV line from ^{232}U will not show up in HEU stockpiles from other countries if they have not enriched with feed from previously irradiated uranium; therefore this isotope cannot be used as a general identifying signature of HEU.

Other researchers acknowledge these difficulties, and therefore, have recommended that *active* interrogation be an alternative method to detecting shielded HEU. It is claimed that passive detection is not reliable, since the 186 keV principal ^{235}U line is easily attenuated, however, high energy gammas are only slightly attenuated by intervening material [3]. Active interrogation employs the use of an external radiation source (typically a D-T, or in some cases a D-D neutron generator) to interrogate the unknown object and induce a response [4]. This method is also met by limitations in the intensity of the radiation source and the intensity of background and interferences, but in active interrogation “background” measurements can be taken before interrogation begins (estimation of performance). This method would be challenging for the MPVS format since it requires additional equipment and would not be adequate for drive-by rapid detection. Also, the US Department of State, the sponsor of this related work, specifically requested that active interrogation not be investigated for SNM verification; instead, only passive methods should be used for the MPVS capabilities, because subjecting weapon pits to fast neutron sources can potentially alter the stored materials and make them less stable. Many facilities, especially facilities in the international community, may not allow the use of neutron generators for active interrogation inside their storage facilities.

In a joint hearing before the Subcommittee on Prevention of Nuclear and Biological Attack with the Subcommittee on Emergency Preparedness, Science, and Technology of the Committee on Homeland Security, the current conditions of SNM detection at portals were addressed. The capabilities as described in 2005 show that only passive detection is available, which is adequate for plutonium detection, but is difficult and limited for HEU detection when the SNM is placed in a vehicle at speed [5]. These same challenges must be faced with the MPVS, where in the case of the MPVS, detectors are ‘at speed,’ while the sources are stationary and shielded. As discussed in the preceding paragraphs, measurement time is a major limitation. In order to successfully

and passively detect HEU, measurement time must be decreased. A new protocol proposed by Sjoden, Maniscalco, and Chapman in 2012 responds to these issues by investigating alternative signatures that enable the use of low resolution spectral detectors in a rapid time frame, along with a multiple detector synthetic aperture approach. This new protocol will be thoroughly investigated here, applied to pit storage container leakage signatures.

Neutron Detection

Due to its significant neutron signature (on the order of 10^3 neutrons per second per steradian), WGPu (typically <7% Pu-240) can be detected two ways: by examining the gamma signature as mentioned previously, and by analyzing the neutron signature. WGPu has a unique neutron signature, which can be detected by utilizing multiple neutron detectors. I will calculate the neutron detection capabilities for three out of the five blocks that make up a detector assembly developed in other research and applied here to analyze how the neutron spectrum leaking from the storage cans will be detected. It was important to examine different energy ranges to get a unique signature which will help aid the inspector in verifying the presence of WGPu.

This thesis will further detail computational, theoretical, and analytical aspects that must be considered the design of the MPVS. Much of my efforts went into the culmination of leakage source terms, “age since separation” material dating, and neutron detection potential for WGPu in this application. This thesis will discuss each topic in detail in the following chapters.

Basic Design Concept

The key to the successful design of a *Mobile Pit Verification System* using passive signatures from SNM comes from the proposed use of a time-phased radiation signal capture methodology (akin to a “synthetic aperture” approach) in a set of detectors geometrically positioned along each shelf containing SNM storage containers. The

detectors are intended to be stack-mounted in “train cars” towed on a moving MPVS inspection platform (e.g. a “motorized cart”) as they move past shelved SNM masses. As noted in Figure 1.1, there are many items to consider for optimization of the MPVS using transport methods using collimation, source geometry, speed, etc. If required, depending upon background interference count rates, multiple detector “trains” must be used to pass by the source with time gating and count integration, detecting when the source and detector are in the proper “Field of View” (FOV), delimited by the collimation; the minimum detector accumulation of radiation counts (“signal”) from an SNM source is determined from vehicle speed.

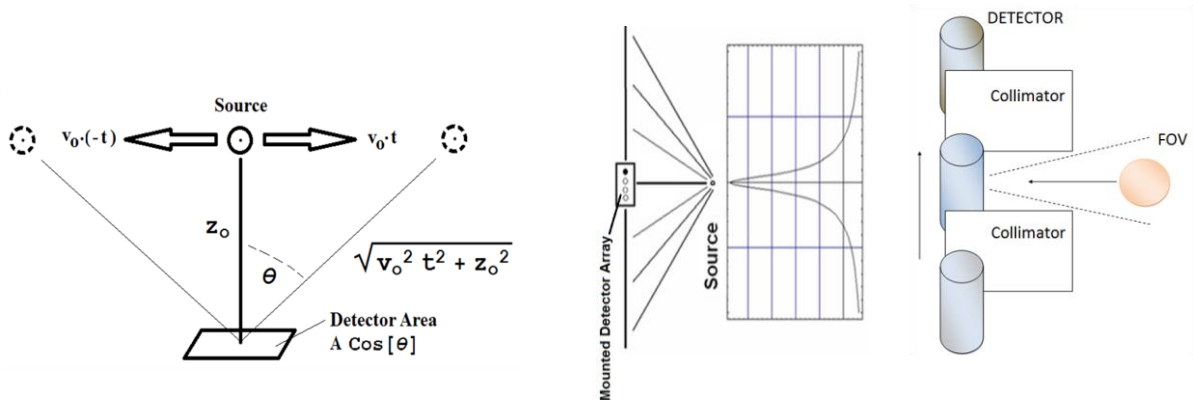


Figure 1.1. MPVS Concept, where the flat detector area shown (at Left) must be collimated as it moves past the SNM Source container, and detectors move past the source within a fixed gate time, where most all counts are recorded in close proximity to the source, as is shown on a normalized scale (Center). To prevent interference from other sources, collimators (shielding) must surround the detectors (shown at Right).

As the MPVS detectors pass by each SNM source, each detector can be focused along a line integral aliased to each source using a shield-collimated aperture placed on each detector along with a time-gated signal capture, based on vehicle speed, to yield an optimum detection time and distance window that maximizes signal to noise, *only*

collecting the signal when geometrically in an optimum configuration, not accumulating when the geometry is dominated by background (as the slant range to the source increases) or when crossing into the solid angle contribution of the neighboring source in storage for a given detector collimation. This is the detector “Field of View” (FOV). In a single instant of time, the number of incident neutrons or gammas arriving (uncollided) on the detector front surface at a single position x can be estimated with Eq. 1.1.

$$R_g(x) = \frac{(S_g)}{4\pi(z_0^2 + x^2)} A_d \cos\theta = \frac{(S_g)}{4\pi(z_0^2 + x^2)} \frac{(A_d \cdot z_0)}{(z_0^2 + x^2)^{1/2}} \quad (1.1)$$

where:

- $R_g(x)$ is the incident response rate (#/sec) for energy group g for an SNM source located at position x ; x is tangent to the vehicle path;
- $x = v_0 t$ is the distance from SNM to the center of the Field of View (FOV), where v_0 is the detector platform speed;
- S_g is the number of (point isotropic) source particles for energy group g (#/sec);
- θ is the source-detector angle, up to a maximum detector-FOV angle bounded by a competing source adjacent to the source undergoing a scan (as shown in Figure 1.1)
- A_d is the area of the detector front surface
- z_0 is the fixed distance to the shelved SNM source

Note that in Eq. (1.1), $(z_0^2 + x^2)$ is the distance squared from the detector to the SNM, and $\frac{(A_d \cdot z_0)}{(z_0^2 + x^2)^{1/2}}$ is the cosine-projected detector front surface area viewed relative to a minimum fixed detector-SNM distance direction. The peak rate at a detector face C_{peak} is obtained from

$$C_{peak} = \lim_{x \rightarrow 0} R_g(x) = \left(\frac{S_g A_d}{4\pi z_0^2} \right) \quad (1.2)$$

If the SNM source area is small compared to the separation distance (which can be corrected for with a transport correction if this is not the case) and most of the region between SNM and detector is filled with air, the total counts that detected can be determined from the integration of Eq. (1) over the gate time $[-\tau, \tau]$ when the detector platform crosses the detector FOV (with a minimum source-detector distance at time = 0):

$$C_{g,uncollided} = \int_{-\tau}^{\tau} dt R_g(x) = \int_{-\tau}^{\tau} dt \frac{S_g}{4\pi(z_0^2 + (v_0 t)^2)} \frac{(A_d \cdot z_0)}{(z_0^2 + (v_0 t)^2)^{1/2}} \quad (1.3)$$

Or, completing the integration analytically, with $L = v_0 \tau$ being the “half time distance” at constant speed, the path length covered over the time for the platform to pass at the vehicle speed to cover half of the maximum FOV; the total path traveled is $2L$, from $[-L, L]$:

$$C_{g,uncollided} = \frac{S_g A_d}{4\pi z_0^2} \left(\frac{2Lz_0}{v_0(z_0^2 + L^2)^{1/2}} \right) = C_{peak} \left(\frac{2Lz_0}{v_0(z_0^2 + L^2)^{1/2}} \right) \quad (1.4)$$

Simplifying the second term in Eq. (1.4), this is effectively a cosine corrected counting time:

$$T_p = \frac{2L}{v_0} \left(\frac{z_0}{(z_0^2 + L^2)^{1/2}} \right) = T_r \left(\frac{z_0}{(z_0^2 + L^2)^{1/2}} \right) = T_r \cdot \cos \theta_{max} \quad (1.5)$$

where $\left(T_r = \frac{2L}{v_0} \right)$ is the “Real” Counting Time and θ_{max} is the maximum slant angle for the path geometry as noted. Therefore, T_r is the total time period when the detector array platform is moving through the detector FOV over the gate time $[-\tau, \tau]$ accumulating counts from the SNM source storage container package.

Considering $L = 90$ cm, and $v_0 = 5$ mph = 223.52 cm/s, with $z_0 = 40$ cm, $T_r = 0.805$ s and $T_p = 0.327$ s; for 2.5 mph = 111.8 cm/s, $T_r = 1.610$ s and $T_p = 0.654$ s. Given that these times are very short for a modest vehicle speed, depending upon the background, and source terms, several detector modules may be required to integrate the signal as the detector train passes a source. Therefore, the real source terms are

investigated here for both gamma and neutron signatures, and I perform transport calculations with coupled detector responses to quantify the neutron signatures. A practical count time for consideration is on the order of a range from [0.25 to 0.75] seconds, depending upon “Field of View” versus vehicle speed, or an average of ~0.5 seconds of signal+background accumulation.

With multiple time-gated detectors operating on the mobile platform, this forms an enlarged “synthetic aperture” detector if needed when detector signals are summed. If the source signature has low intensity and/or must reject a high background, the synthetic aperture approach enables verification of the SNM presence as the detector platform vehicle passes each SNM source at speeds that make the system tractable for rapid, large scale facility monitoring of each stored container mass. As a result, the work presented in this thesis will be instrumental to the overall design of the MPVS. I will present my approach to developing source leakage terms necessary to determine proper time-gating and collimation (investigated as a separate, complimentary effort to the sponsored effort), along with verifying and developing new protocols for SNM detection and “age since separation” determinations, and investigating the detector responses for neutron detection and verification. I will begin with discussing the development of models for the source term calculations.

CHAPTER 2

MODEL DEVELOPMENT

Computational Methods

The first step to designing a mobile detector system is to determine the kinds of computations required to obtain the data necessary for analyzing specific design parameters. Since the MPVS is a detector system that will examine both gamma and neutron signatures leaking from weapons storage containers at a distance away from the containers, models of the particles leaking from the surfaces of the containers into the detector are necessary. This requires that all physics and radiation transport be considered in the reactions taking place between particles inside of the containers and their surrounding mediums to determine an accurate representation of the quantity and energy distributions of the particles leaking. This can be done by solving the multi-group linear Boltzmann equation. There are currently two widely used methods of solving the linear Boltzmann equation: Discrete Ordinates and Monte Carlo. Both methods are successful at producing accurate results. For my work, I employed both methods to demonstrate that results did not significantly change depending on the applied method, and also to show that I can utilize results from the Monte Carlo method to use in hybrid models that make use of Discrete Ordinates methods. The popular code, MCNP5, was used to accomplish particle transport via the Monte Carlo method, and the deterministic code, PENTRAN, was used for the Discrete Ordinates (Sn) method. I will discuss each code in further detail in the following sections.

MCNP

The Monte Carlo computational method is currently the most extensively used, straight forward technique applied for particle transport, and it has been widely demonstrated as being capable of representing very complex geometries in a rigorous manner using robust particle physics by statistically tracking the outcome of individual particle histories [6]. MCNP5 is a globally used general-purpose, continuous-energy, coupled neutron-photon-electron Monte Carlo transport code developed at the Los Alamos National Laboratory. It can be used in several transport modes, and was developed with over 500 person-years of effort. It operates in neutron only, photon only, electron only, and combined neutron-photon transport problems where the photons are produced by neutron interactions, neutron-photon-electron interactions, photon-electron, or electron-photon interactions. The capability to calculate k_{eff} eigenvalues for fissile systems (“kcode” computations) is also a standard feature.

PENTRAN

The PENTRAN code system, developed by Sjoden and Haghigat, can be used for 3-D multigroup forward or adjoint discrete ordinates (Sn) simulations. The Sn method is a deterministic approach that discretizes the angle, energy, and physical spatial variables into a finite number of discrete angular ordinates, energy groups, and spatial grids over the entire phase space system. The PENTRAN system is actually a suite of codes that allow one to readily generate mesh geometries, solve 3-D transport models, and automatically collate parallel data. PENTRAN is a multi-group, anisotropic Sn code for 3-D Cartesian geometries; it has been specifically designed for distributed memory, scalable parallel computer architectures using the Message Passing Interface library [7]. Automatic domain decomposition of the phase space among the angular, energy, and spatial variables with an adaptive differencing algorithm and other numerical enhancements make PENTRAN an extremely robust solver with a 0.996 parallel code

fraction (based on Amdahl's law). Numerous simulations have been performed using the PENTRAN code system, including many international benchmark computations [8, 9]. The many advanced numerical features in PENTRAN, including adaptive differencing with a two-level parallel angular memory structure in a scalable architecture, are such that it is well-suited for deterministic work in this research. Both PENTRAN and MCNP5 were used to create the models discussed in the next section.

Models

In order to show the effects of the weapons pit containers on the overall HEU and WGPU signatures, I began with a review of the literature (limited to open-source publications) to determine the geometry and types of source material configurations seen in weapons storage facilities, and I created models of the weapons containers based on the International Atomic Energy Agency (IAEA) Significant Quantities (SQ) for plutonium and uranium. These models were used to determine the minimum detection limits necessary for distinguishing between naturally occurring radiation materials (NORM) and types of SNM [10]. SNM is normally stored within steel canisters placed in racks. Figure 2.1 shows a sample configuration of this type of canister storage.



Figure 2.1. Lard canister storage on racks at the Hanford Site [11].

I investigated the types of storage containers used in the US and types of material configurations typically seen at weapons pit storage facilities. Specifically, weapons grade/component material in the US is stored in a solid sphere or spherical shell configuration which is placed in one of several different types of canister configurations. These canister configurations include AL-R8 containers and more recently, AT-400A containers. The AL-R8 container is composed of a confinement canister, fiberboard, refractory insulation, and a pit support frame [12]. The fiberboard is Celotex material of equal parts carbon, hydrogen, and oxygen with a minimum density of 0.24 g/cm^3 [12]. Figure. 2.2 depicts the AL-R8 configuration.

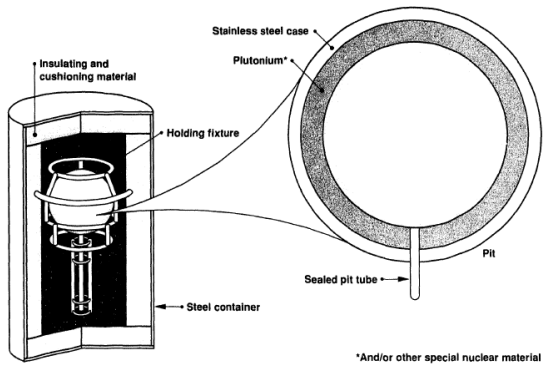


Figure. 2.2. AL-R8 pit container used for a dismantled nuclear weapon at Pantex [13].

The AT-400A pit containers differ from the AL-R8 containers in that they have an additional inner confinement liner; polyurethane foam fills the space between the liner and outside container, and is also placed at the bottom and top of the container. The pit is held in place in the center of the liner by an aluminum support frame [12]. Figure. 2.3 shows this pit structure.

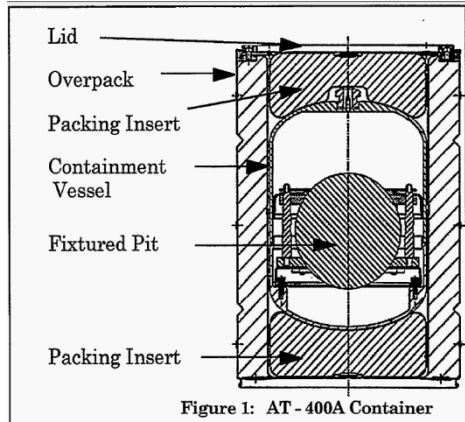


Figure 2.3. AT-400A pit container for Pantex [14].

The overall dimensions and structure of both the AL-R8 and AT-400A containers were very similar; therefore, I generalized both designs into a single, “hybrid geometry” model, and viewed this as sufficient to create standardized leakage source terms for HEU and WGPu SNM materials that could be stored in the canister. Table 2.1 depicts the dimensions for the AL-R8, the AT-400A, and the finalized “hybrid” geometry model for the MPVS source terms. For simplicity, the AL-R8 container was the principal basis for the “hybrid” geometry model.

Table 2.1. SNM canister configurations [12, 14]

	Hybrid Model	AL-R8	AT-400A
Inner container radius/diam (cm)	None	None	17.15/34.3
Outer container radius/diam (cm)	26.924	23/46	25.1/50.2
Outer container height (cm)	76.2	76.0 ¹	68.45
Outer container wall thickness (cm)	0.122	0.122	0.122
Packing material (thickness-cm) [composed of Celotex at 0.24g/cc or Polyurethane at 0.482g/cc]	7.0 side 5.0 top/bot	7.0 side 5.0 top/bot	6.98 side (14.07 edge 6.65 center) top/bot
Refractory fiber insulation (cm) [equivalent density at 0.128g/cc]	none	30.5x30.5x1.27 Below lid	none

Two “source boxes” were used as tallying regions of interest. The “inner” source box is a cube of dimensions equal to the outermost radius of the source ball. The “outer” source box encompasses the entire outer boundaries of the model. See Table 2.2 for specific dimensions of the inner and outer source boxes. Both boxes were defined to be used as a standardized metric for comparisons between continuous energy MCNP5 and multigroup PENTRAN. Intrinsic photons resulting from the decay of parent nuclides were added with photons from spontaneous and induced fission to form a total photon leakage term. The outward streaming photon leakage of the outer source box for a single surface will be also used as a source term in my MPVS deterministic models.

For most of the PENTRAN runs, a volumetric source was used where the HEU/WGPu shell or solid resides. This was performed on a fine-mesh basis, and was automatically generated with the PENTRAN geometry meshing tool PENMSH-XP [15]. Since there are spectral boundary conditions along the edges of the problem, the volumetric sources were defined to be spatially isotropic.

¹ AL-R8 can also be manufactured in heights of 102.0, 127.0, and 152.0 cm depending on load size.

Table 2.2. SNM pit dimensions².

	HEU (25kg)	WG Pu (8kg)
Solid Radius (cm)	6.7918	4.581
Solid Inner Source Box length(cm) × width(cm) × height(cm)	15.58 × 15.58 × 15.58	11.17 × 11.17 × 11.17
Solid Outer Source Box length(cm) × width(cm) × height(cm)	60 × 60 × 77.2	60 × 60 × 77.2
Shell Inner radius (cm) Outer radius (cm)	12.458 13.087	6.909 7.524
Shell Inner Source Box length(cm) × width(cm) × height(cm)	28.17 × 28.17 × 28.17	17.05 × 17.05 × 17.05
Shell Outer Source Box length(cm) × width(cm) × height(cm)	60 × 60 × 77.2	60 × 60 × 77.2

Each SNM sphere was additionally surrounded by 1 cm of Aluminum cladding.

In all models, the inner source box immediately surrounds this surface, and the outer source box surrounds the steel canister. Figures 2.4 and 2.5 show cutaway views along the x-z and x-y planes, respectively for the HEU shell and HEU solid sphere sources.

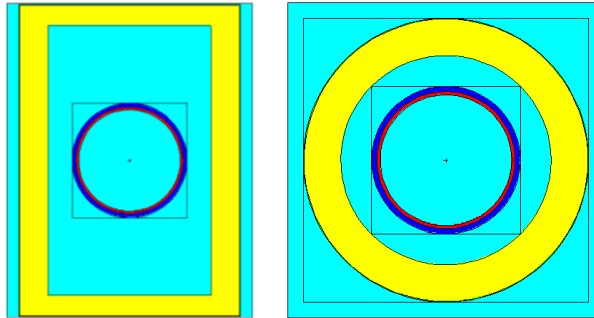


Figure 2.4. MCNP geometry model of HEU shell source cut along x-z and x-y planes. The inner shell is HEU, surrounded by aluminum. Air surrounds the shells and is contained by Celotex surrounded by steel. Air makes up the remainder.

² Isotopes are described in Chapter 3, Tables 3.1 and 3.2.

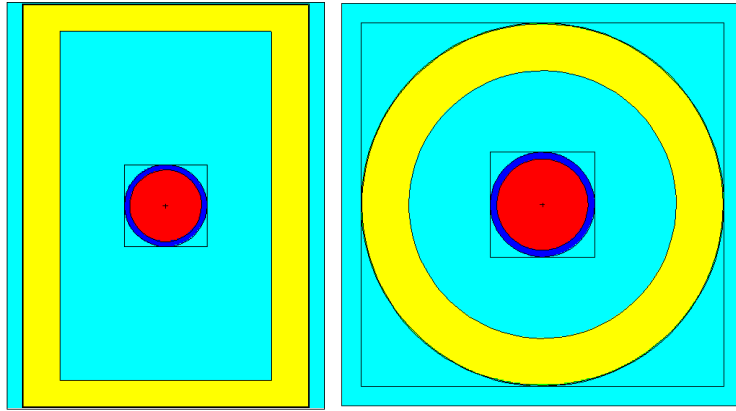


Figure 2.5. MCNP Monte Carlo model of HEU solid source geometry cut along x-z and x-y planes. The inner sphere is HEU, the surrounding shell is aluminum. Air surrounds the shells and is contained by Celotex, which is surrounded by a thin layer of steel. Air makes up the remaining portion of the Figure.

Only intrinsic gammas were considered for the HEU pit, since the total neutron contribution is very weak (on the order of ~ 10 's of n/s over 4π sr and at 1 m away on the order of 10^{-5} n/s per sr) and not useful to have detectable significance. However, intrinsic gammas, neutrons, and gammas resulting from (n, γ) reactions must be considered for the WGPu pit (neutrons on the order of 10^5 n/s over 4π sr). I gathered the source specification information defined from the gamma and neutron distributions per energy group derived from the ORIGEN code from the SCALE6 coded system, and I used the ORIGEN output to create the probability cards in MCNP5 to describe the sources [16]. I will discuss how this is performed in further detail in the next chapter.

To get a description of the particle leakages through the weapons pit storage containers, I used surface current tallies in MCNP with a cosine card along with the corresponding tally multiplier of source intensity as a function of time referenced from the ORIGEN output. These photon and/or neutron particle currents were recorded based

on the energy grouping introduced in Chapter 3. For the WGPu pit, each MCNP model was executed twice, first for the determination of the intrinsic gammas via photon only transport mode, and then again looking at the neutron, (n, γ) and fission photons via neutron transport mode with induced photons. The NONU card was included for all intrinsic gamma runs in the WGPu models so that no fission gammas were included. The TOTNU card was included for the fission induced/spontaneous gamma runs to account for all fission events. The results for both runs were combined to yield an integrated WGPu gamma signature. These tallies were used to create “source terms” describing the signature of the SNM leaking through the weapons container. In Chapter 3, I will further detail how these signatures were obtained, and how they will be utilized in the MPVS design.

CHAPTER 3

SOURCE TERMS

In the previous chapter, I discussed how the geometry and source terms would be treated in the models of the weapons pit containers. In this chapter, I will further detail the specifics of these source terms, and how they will change depending on the type of SNM. In order to design the MPVS for optimal detection and verification of the material under inspection, the unique gamma and neutron leakage terms must be known for un-tampered SNM. As stated in Chapter 2, I will determine these leakages from MCNP current tallies (F1 tallies) through each surface of the source box. I compiled the tally results into a single self-standing guide, a “*Source Book*” that can be used for future research needs. The Source Book is described in more detail later in this chapter and in Appendix A. First, it is important to discuss the types of materials for weapons pit scenarios, and how the source terms for these materials were generated.

I first considered both 1 year old and 50 year old HEU (age since separation) to show how the HEU signature changes with age due to the in-growth of decay daughters, specifically the Pa^{234} and Bi^{214} isotopes, and how this can affect the “detectability” of stored HEU. The average age of plutonium in the US stockpile ranges from 20 to 26 years, so 22.5 year old plutonium was used as a basis [17]. The isotopes considered for each SNM source are given in Tables 3.1 and 3.2.

Table 3.1. Isotopic makeup of HEU used in this study³.

Isotope	Concentration (w%)
U-235	90.0
U-236	0.664
U-238	8.5027
U-234	0.8334

Table 3.2. Isotopic makeup of WGPu used in this study.

Isotope	Concentration (w%)	Isotope	Concentration (w%)
Pu-238	0.02	C-Natural	0.023
Pu-239	93.279	Zr-Natural	0.01
Pu-240	5.911	Na-Natural	0.005
Pu-242	0.2	Fe-Natural	0.001
Pu-241	0.028	Mo-Natural	0.0009
Am-241	0.256	Al-Natural	0.0005
Ga-Natural	0.0335	U-238	0.2321

The initial source terms for SQ masses, 25 kg of HEU and 8 kg of WGPu, were generated using ORIGEN/ORIGEN-ARP modules that are isotopic depletion and decay analysis tools that are part of the Oak Ridge National Laboratory SCALE6 code system [16]. This code system produces a detailed output file accounting for all decay daughter products and their radiation contributions based on mass yield without consideration of transport effects. It also provides the unique gamma and neutron spectra as a function of age since separation per energy group for the material in question, as shown in Figure 3.1. I extracted this information from the output files and normalized the photon/neutron leakages for each energy group with respect to the total leakage of each age to be used in the probability distribution cards in MCNP. Neutron contributions were based on both the BUGLE-96 47 group structure, and a 30 group structure with upscatter shown in Tables 3.3 and 3.4 [18]. Gamma contributions were based on a 24 group structure as

³ U-232 was not included since it may not be seen for every case.

shown in Table 3.5 [19]. It should be noted that this 24 group structure was used in previous research, and it was selected because it isolates the key uranium and plutonium gamma emissions (photopeaks), such as the 1001 keV line for U²³⁸ in equilibrium with Pa^{234m}, and similar gamma emissions in a minimal but adequate gamma cross section multigroup library applicable to this problem [19, 20]. When looking at the plots (Figures. 3.2 and 3.3) showing the energy spectrum from gamma emissions for both HEU and WGpu, it is seen that this group structure from Table 3.3 does indeed focus on the key energy peaks (the 1 MeV line, between 1.2 and 1.24 MeV, and between 1.736 and 1.74 MeV). The fine detail is only important for the most probable gamma lines so broader grouping was used for the less probable, minor lines.

gamma source intensity as a function of time					
Decay Case 1					
gamma spectra, photons/sec/basis basis = 0.025 MTU					
grp	boundaries, mev	1.0 y	22.5 y	50.0 y	
1	2.90E-01 - 3.00E-01	7.636E+05	7.997E+05	8.798E+05	
2	3.00E-01 - 7.41E-01	1.998E+06	2.135E+06	2.536E+06	
3	7.41E-01 - 7.43E-01	2.571E+04	2.573E+04	2.587E+04	
4	7.43E-01 - 7.65E-01	1.145E+03	1.215E+03	1.484E+03	
5	7.65E-01 - 7.67E-01	5.503E+04	5.795E+04	6.774E+04	
6	7.67E-01 - 9.54E-01	6.871E+04	8.280E+04	1.281E+05	
7	9.54E-01 - 9.56E-01	1.367E+03	1.393E+03	1.469E+03	
8	9.56E-01 - 9.99E-01	4.041E+03	4.238E+03	5.017E+03	
9	9.99E-01 - 1.00E+00	1.562E+05	1.561E+05	1.561E+05	
10	1.00E+00 - 1.18E+00	4.081E+03	1.349E+04	4.996E+04	
11	1.18E+00 - 1.20E+00	2.389E+03	2.419E+03	2.510E+03	
12	1.20E+00 - 1.24E+00	1.476E+03	4.607E+03	1.690E+04	
13	1.24E+00 - 1.26E+00	3.168E+02	3.168E+02	3.168E+02	
14	1.26E+00 - 1.50E+00	5.501E+03	1.054E+04	3.030E+04	
15	1.50E+00 - 1.52E+00	2.820E+03	3.871E+03	8.006E+03	
16	1.52E+00 - 1.74E+00	5.638E+03	8.106E+03	1.781E+04	
17	1.74E+00 - 1.74E+00	3.965E+03	4.692E+03	7.553E+03	
18	1.74E+00 - 1.76E+00	6.269E+02	6.266E+02	6.266E+02	
19	1.76E+00 - 1.83E+00	2.846E+03	1.038E+04	3.997E+04	
20	1.83E+00 - 1.83E+00	2.980E+03	3.071E+03	3.434E+03	
21	1.83E+00 - 2.21E+00	5.307E+03	8.700E+03	2.203E+04	
22	2.21E+00 - 2.25E+00	1.905E+01	1.209E+03	5.881E+03	
23	2.25E+00 - 2.75E+00	1.675E+01	9.567E+02	4.647E+03	
24	2.75E+00 - 2.75E+00	1.727E+01	1.727E+01	1.727E+01	
	totals	3.112E+06	3.337E+06	4.012E+06	

Figure 3.1. Example section of an ORIGEN output file showing the gamma/leakage source from a 25kg HEU source.

Table 3.3. Bugle 47 group structure for neutron emissions. [18]

Group	Upper Energy Bound (MeV)						
1	19.6	13	2.37	25	0.297	37	1.58×10^{-3}
2	14.2	14	2.35	26	0.183	38	4.54×10^{-4}
3	12.2	15	2.23	27	0.111	39	2.14×10^{-4}
4	10	16	1.92	28	0.0674	40	1.01×10^{-4}
5	8.61	17	1.65	29	0.0409	41	3.73×10^{-5}
6	7.41	18	1.35	30	0.0318	42	1.07×10^{-5}
7	6.07	19	1.00	31	0.0261	43	5.04×10^{-6}
8	4.97	20	0.821	32	0.0242	44	1.86×10^{-6}
9	3.68	21	0.743	33	0.0219	45	8.76×10^{-7}
10	3.01	22	0.608	34	0.015	46	4.14×10^{-7}
11	2.73	23	0.498	35	7.1×10^{-3}	47	1.00×10^{-7}
12	2.47	24	0.369	36	3.35×10^{-3}		

Table 3.4. 30 group structure for neutron emissions.

Group	Upper Energy Bound (MeV)	Group	Upper Energy Bound (MeV)	Group	Upper Energy Bound (MeV)
1	20	11	1.55×10^{-3}	21	7.0×10^{-8}
2	17.3	12	3.7×10^{-5}	22	5.0×10^{-8}
3	8.19	13	3.05×10^{-6}	23	4.0×10^{-8}
4	3.0	14	1.3×10^{-6}	24	3.0×10^{-8}
5	1.5	15	1.0×10^{-6}	25	2.53×10^{-8}
6	1.25	16	6.25×10^{-7}	26	1.5×10^{-9}
7	7.5	17	3.5×10^{-7}	27	1.2×10^{-9}
8	0.27	18	1.75×10^{-7}	28	7.5×10^{-10}
9	0.045	19	1.25×10^{-7}	29	5.0×10^{-10}
10	0.013	20	1.0×10^{-7}	30	1.0×10^{-10}

Table 3.5. 24 group structure for gamma emissions.

Group	Upper Energy Bound (keV)	Group	Upper Energy Bound (keV)
1	2750	13	1240
2	2749	14	1200
3	2250	15	1180
4	2210	16	1002
5	1832	17	999
6	1830	18	956
7	1760	19	954
8	1740	20	767
9	1736	21	765
10	1520	22	743
11	1500	23	741
12	1260	24	300

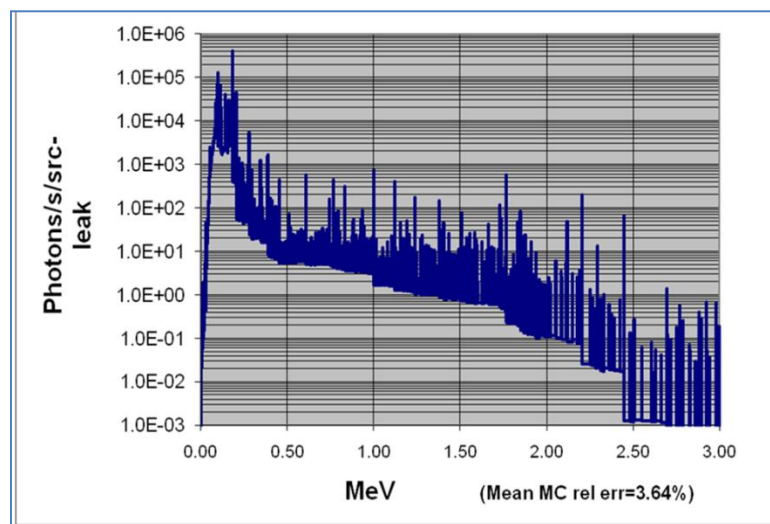


Figure 3.2. Typical HEU (50 year aged) spectrum with key gamma peaks readily identified.

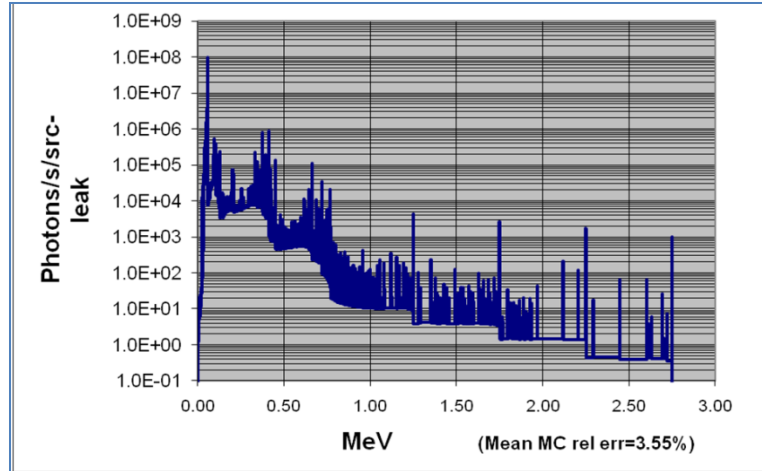


Figure 3.3. Typical WGPu spectrum (22.5 year aged) with key gamma peaks readily identified.

The ORIGEN outputted results confirm this observation when plotted by showing drastic peaks at the energies of importance. Figures 3.4 and 3.5 show these plots. Notice the peak at 1 MeV for HEU which represents the ingrowth of the Pa daughter product, which is influential in detecting the presence of HEU.

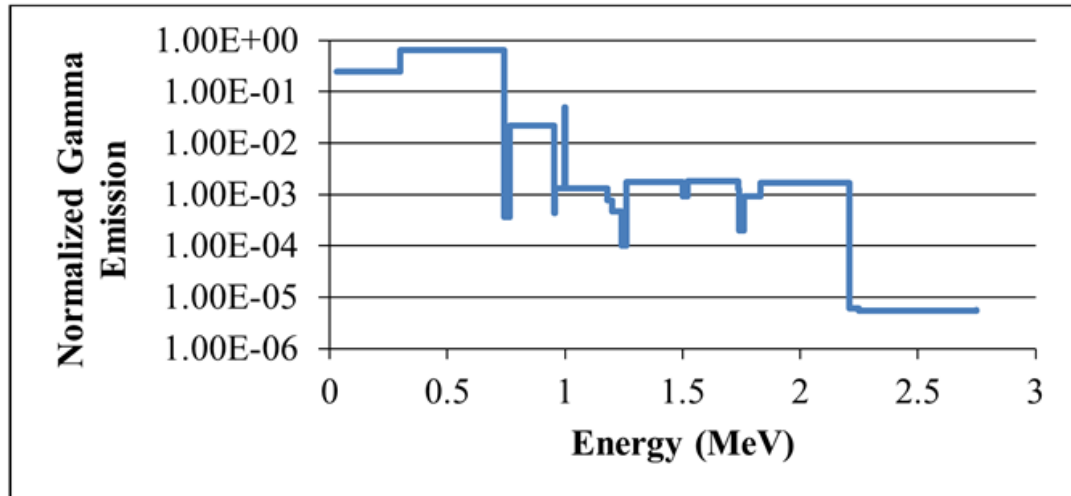


Figure 3.4. Normalized unshielded gamma emission from 25 kg of 1 year age since separation HEU.

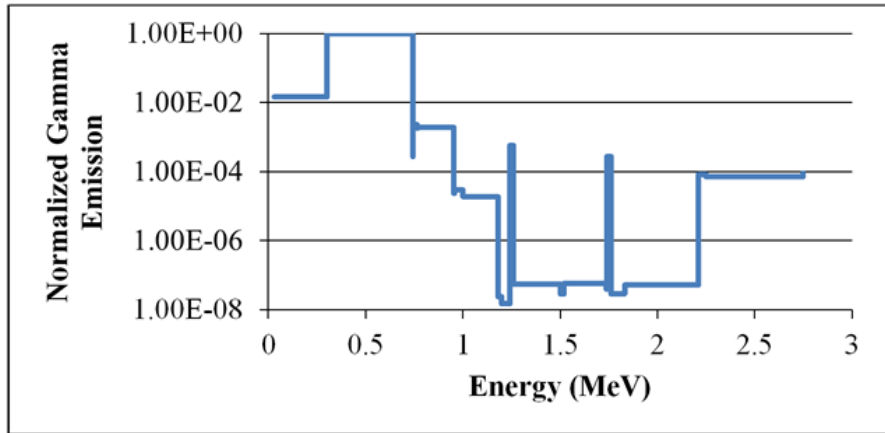


Figure 3.5. Normalized unshielded gamma emission from 8 kg of 22.5 years age since separation WGPu.

Although many key gammas of interest fall in the lower energy ranges (less than 1 MeV), especially for WGPu, fine separation in these lower energy ranges is unnecessary when using low resolution gamma detectors. Later, in Chapter 4, I will analyze how this 24 group energy spectrum can be used to determine the presence of WGPu and its possible configuration.

Source Book

I compiled the source terms described in previous sections into a comprehensive “Source Book” included in Appendix A. I compiled the results and organized them by type of SNM. I then separated each HEU and WGPu source by age and geometry configuration. I included the energy distributions for the Monte Carlo models for each source box surface, and I included the PENTRAN results for the $+x$ plane surface to compare both models. When looking at Appendix A, the leakages are given for both the “Inner Source Box” (directly surrounding the SNM source), and the “Outer Source Box” (directly surrounding the pit container). The number of particles leaking out of each individual source box surface is recorded for each energy group. I also included Neutron leakage results for the WGPu sources. This neutron data is compiled and organized in

the same manner as photon data. The normalized leakage results along with the spatial distribution (discussed in the following subsection) of the particles can be used directly in an MCNP5 or PENTRAN input file to describe the source “painted” on the surface of a box.

Source Book: Histograms

Histograms showing the relative contributions from photons and neutrons in the given energy groups are also included in Appendix A, following each type and age SNM. The graphs all start at 0.741 MeV, but they are normalized to the leakage spectrum beginning at approximately 0.0 MeV (with a lower limit cutoff) for MCNP5 models and 0.3 MeV for PENTRAN models. Energies below 0.741 MeV are likely to be shielded out, and have less chance of being counted in the detector. The comparison between the initial intrinsic photon source terms for various ages of WGpu and HEU are included in the source book to show how the in-growth of daughter products affect the overall spectrum shape. Figure 3.6 shows a representative histogram for a 50 year HEU shell source. It is noted that the MCNP and PENTRAN results match up or are very similar across each energy group.

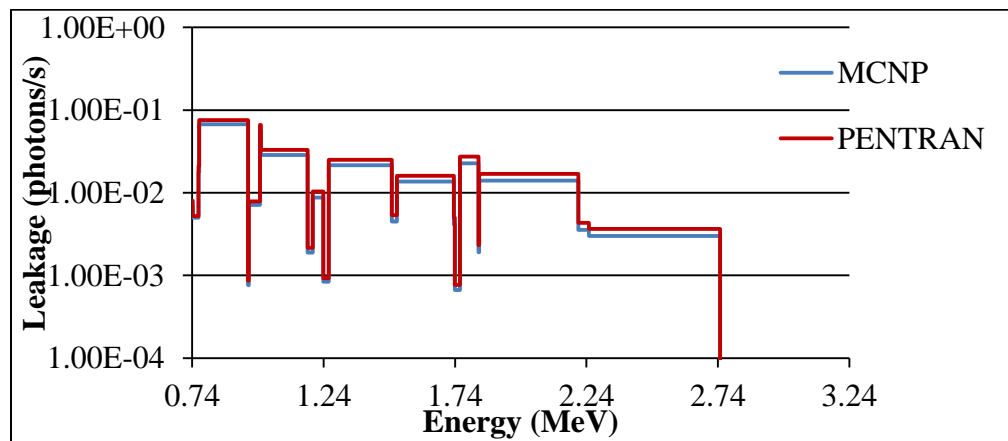


Figure 3.6. Histogram plot for 50 year age since separation HEU shell source from both MCNP and PENTRAN gamma leakage results through the Source Box.

Source Book: Spatial Distributions

The results from the PENTRAN models were used to find the spatial distribution along the surface of the outer source box for the photon leakages of the HEU. This distribution will account for the spherical shape of the actual SNM pit in the center of the box. Each side of the source box has an x and z axis or y and z axis distribution while the top and bottom surfaces have an x and y axis distribution with the maximum number of photons leaking through the center of each. Figure 3.7 shows a representation of the leakage distribution across the top and bottom surfaces of the box. These distributions can be used to “paint” the leakage source term on a simplified box surface (with zero importance set inside if using Monte Carlo) to aide in creating models as depicted in Figure 3.8.

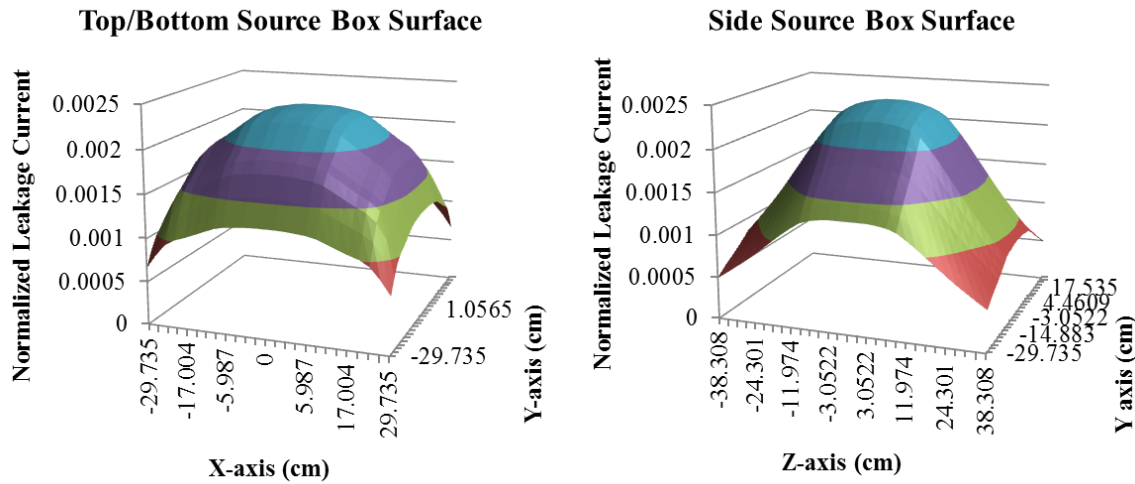


Figure 3.7. (a) The relative contributions of photon leakage across the top and bottom surfaces of the Source Box. (b) The relative contributions of photon leakage across the side surfaces of the Source Box.

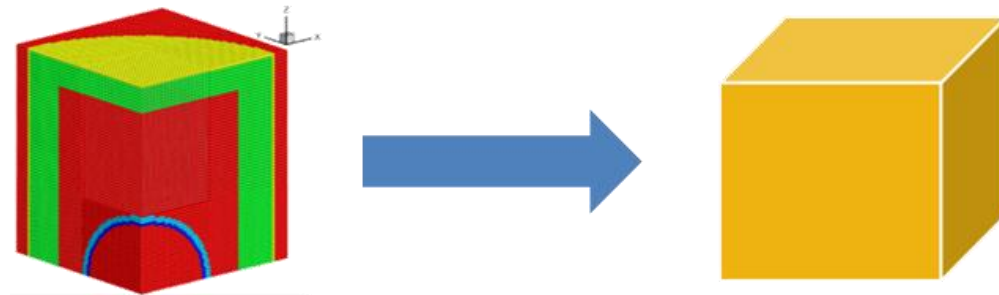


Figure 3.8. The complicated weapon pit geometry can be simplified so that the contents no longer need to be modeled and the leakage source term can be used in a “painted” distribution on the surface of a box.

I assembled a simplified distribution for the 1 year HEU case based on the side leakages from the source box and “painted” it on a cube with dimensions 30cm x 30cm x 30cm. I surrounded the box with a mesh tally in MCNP, and I executed the original 1 year HEU shell case with the same mesh tally in MCNP. I calculated the differences between the results of the two models and found that they differed on average by ~5%. As expected, the distributed “source box” source ran much faster than the exact modeled source. I also noticed that the distributed source case could run with an order of magnitude fewer particle histories than the exact case and still have errors on the order of 0.1%. The exact case ran in 2 min 12.046 s on 16 processors for 10^8 particle histories, and the distributed source case ran on 16 processors in 15.318 s for 10^7 particle histories for a 0.1% uncertainty.

Source Book: Mass Based Energy Distributions from ORIGEN

In case an exact SNM weapons pit was needed to be modeled, or a different weapons pit container required consideration, the original unshielded source terms would be needed, and therefore, I included these along with the Source Box source terms in the Source Book. The unshielded source term data per energy group from the ORIGEN code simulations were used to determine the energy distributions for the 25 kg HEU and 8 kg

WGpu sources for the full MCNP5 models. The Source book discussed previously has an additional tab marked ‘ORIGEN’ (excel file) which includes these results and corresponding normalized distributions. These distributions can also be directly entered into an MCNP or another code that requires information in this format.

A simplified case could be constructed in MCNP by creating a rectangular parallelepiped (RPP) surface with dimensions 60cm x 60cm x 60cm filled with void space. The SDEF card needs to have an energy distribution and spatial distributions for each x , y , and z axis. These distributions would be sampled directly from the source book. For example, in the case of a 1 year HEU shell source, the energy distribution would be extracted from the normalized leakage values in Table A.2, and the spatial distributions would be taken directly from Table A.3. Figure 3.9 depicts the 1 year shell HEU SDEF card for the energy distribution and the x axis distribution for the MCNP code. The distributions for the y and z axis would follow the same procedure as the x axis distribution. “CEL=1” refers to the RPP defining the source box in the initial CELL cards in the MCNP input. The complete MCNP deck for this example is included in the Appendix section. For source normalization of particle strength, the Appendix lists the particle distribution and total leakage emitted as a function of energy bin from each surface independently; therefore, the total leakage over 4π sr is determined from the sum of each total from the six respective sides of the source box.

```

SDEF ERG=d1 CEL=1 x=d2 y=d3 z=d4
c
c -----Energy Distribution-----
#   SI1           SP1
    h             d
    0.00          0.00
    3.000E-01  9.913E-01
    7.410E-01  6.871E-03
    7.430E-01  8.408E-05
    7.650E-01  3.865E-05
    7.670E-01  1.834E-04
    9.540E-01  4.726E-04
    9.560E-01  7.822E-06
    9.990E-01  5.759E-05
    1.002E+00  7.010E-04
    1.180E+00  4.210E-05
    1.200E+00  1.489E-05
    1.240E+00  1.210E-05
    1.260E+00  3.655E-06
    1.500E+00  5.284E-05
    1.520E+00  1.894E-05
    1.736E+00  4.859E-05
    1.740E+00  2.698E-05
    1.760E+00  5.036E-06
    1.830E+00  2.153E-04
    1.832E+00  2.085E-04
    2.210E+00  4.047E-04
    2.250E+00  1.433E-07
    2.749E+00  1.394E-07
    2.750E+00  1.443E-07
c
c -----X-Axis Distribution-----
#   SI2           SP2
    h             d
    -30  0.0000E+00
    -24  7.0319E-02
    -18  8.4472E-02
    -12  1.0066E-01
    -6   1.1681E-01
    0    1.2774E-01
    6   1.2774E-01
    12  1.1681E-01
    18  1.0066E-01
    24  8.4472E-02
    30  7.0319E-02

```

Figure 3.9. Sample SDEF card in MCNP for source box model of 1 year HEU shell source.

The Source Book has the potential to have a great impact on future research on SNM and SNM storage. I have found that nowhere else exists a document that clearly defines and identifies all important signatures from HEU and WGPu for various ages since separation. This guide will help myself and future researchers quickly create complex models in MCNP or other codes requiring date in similar formats which could potentially reduce months of effort of the intended research study. The results from the

Source Book can also be used to analyze how the signatures of HEU and WGPu can be utilized for verification and detection. In the following chapter I will describe how I analyzed these leakage signatures to verify a pre-existing method of HEU verification, and develop a new method for detecting WGPu.

CHAPTER 4

PASSIVE AGE DATING of SNM

Highly Enriched Uranium

Once I found and organized all of the source terms as discussed in the last chapter, I investigated how this information can be used for rapid detection. As discussed in the introduction, passively detecting HEU is a challenge, and especially difficult with low resolution detectors and short counting times. The introduction of a new method developed by Sjoden, Maniscalco, and Chapman, however, significantly changes this issue by making it possible to combine both needs.

The new protocol, as mentioned in the Introduction, was developed to passively detect and verify HEU [19]. This patented (Quintell, 2011) passive gamma technique can distinguish between different ages since separation, and also between natural and reactor grade un-irradiated uranium rods. There is no indication that this method of HEU detection has been developed or evaluated before in literature, other than its first publication by Sjoden, Maniscalco, and Chapman in Journal of Radioanalytical and Nuclear Chemistry, therefore, I set out to verify this protocol through analysis of my gamma leakage source results from the Source Book.

The ratios for ranges of gamma ray energies that should be integrated and applied for positive detection of HEU using passive gamma rays are given in Table 4.1; the method is quite powerful, since a low resolution, low cost detector (such as NaI(Tl) or CsI(Tl)) can be used to determine these passive signatures quite easily at room temperature, and with excellent efficiency. Based on an unshielded spectrum for different ages of HEU, as shown in Figure 4.1, the ratios match up with the 1 MeV line, which stays approximately stable over all ages, and regions where deviation is strong

between ages. This applies to HEU that is aged for at least 90 days to allow for equilibrium in-growth of the ^{234}Pa and related decay daughters.

Table 4.1. Ratios of Regions of Interest in HEU, NORM, and 50y Rods. [19]

	Ratio (830-1060 keV)/(700-3000 keV)	Ratio (830-1060 keV)/(1060-3000 keV)
1 year HEU	0.55	3.40
50 year HEU	0.37	0.84
NORM⁴	0.26	0.43
50 year Rods⁵	0.35 +/- 0.04 (1-sigma)	0.91 +/- 0.09 (1-sigma)

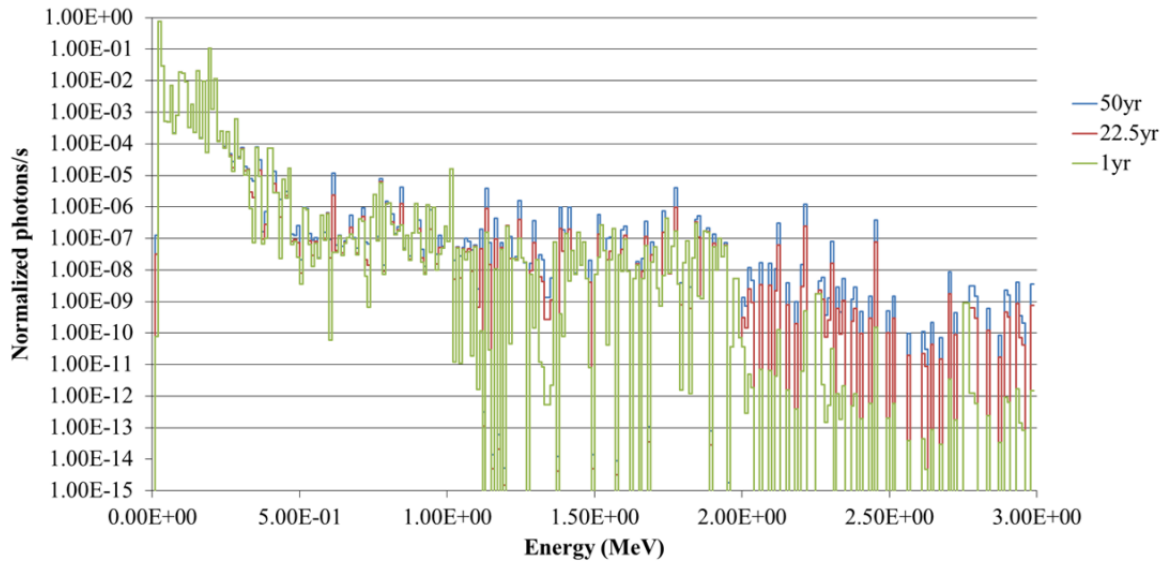


Figure 4.1. Normalized HEU spectrum for 1 year, 22.5 years, and 50 years since separation.

⁴ Naturally Occurring Radioactive Material

⁵ Uranium reactor fuel material

The 186 keV gamma line is typically regarded as the key signature gamma ray for HEU detection, however, this can only be detected reliably in the case of unshielded HEU sources. Once modest shielding is added, this signature is not practically detectable, virtually “disappearing.” This places added emphasis on the passive new protocol identified. I approached verifying this new ratio method by correlating my group structure to the ratio energy ranges defined in Table 4.1. I postulated that the gamma leakages through the weapons pit container should match up with the ratios described by the passive protocol, but I was unsure if there would be any effects from the canister’s shielding materials that would significantly shift or alter the upper energy spectrum due to Compton. I chose to first investigate the 1 year and 50 year age since separation cases by comparing the leakages through the Source Box surface per energy group, and the published ratios. For the ratios, the energy groups were matched by accumulating counts in energy groups as follows:

$$Ratio\ 1 = \frac{\int_{830keV}^{1060keV} Counts}{\int_{700keV}^{3000keV} Counts} \cong \frac{\frac{1}{2}Counts_{15} + \sum_{g=16}^{18} Counts_g + \frac{1}{2}Counts_{19}}{\sum_{g=1}^{22} Counts_g} \quad (4.1)$$

$$Ratio\ 2 = \frac{\int_{830keV}^{1060keV} Counts}{\int_{1060keV}^{3000keV} Counts} \cong \frac{\frac{1}{2}Counts_{15} + \sum_{g=16}^{18} Counts_g + \frac{1}{2}Counts_{19}}{\sum_{g=1}^{14} Counts_g + \frac{1}{2}Counts_{15}} \quad (4.2)$$

When I applied this protocol to the results of the gammas leaking through each side of the source box, I found that the ratios were very consistent with the data presented in Table 4.1. As I anticipated, the high energy gammas were not shielded enough to alter their spectrum, however, if a different type of packaging/shielding were to be used this may no longer be true. Lead, Tungsten, or other highly attenuating materials would be able to significantly impact the higher energy gamma leakages which would alter the ratios, but as cited in the literature, weapons storage facilities do not utilize such materials to shield and store SNM, so this should not be an issue. Even with only a 24 group

energy computational structure, I was able to identify and match the respective aged HEU with its published ratio. I then decided to investigate additional material ages, since separation for HEU to see if there was an identifiable trend between age and ratio. I specifically noted a clear correlation between the age of the HEU and its gamma ratios, such that an inspector could pinpoint an estimated age since separation for the material in question.

Figures 4.2 and 4.3 depict these results for both ratios as a function of material age. By analyzing a range of ages, one can see the correlation between the ratio and age since separation. As I noted, these correlations can be used to better predict any age over 90 days since separation of HEU.

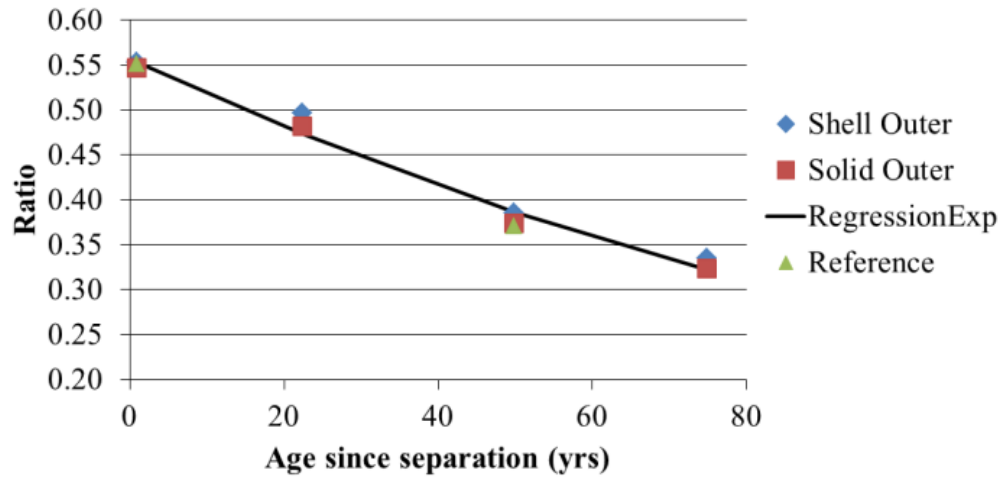


Figure 4.2. Ratio 1 (Eqn 4.1) for both shell and solid HEU configurations, along with the published reference ratios: (830-1060 keV)/(700-3000 keV).

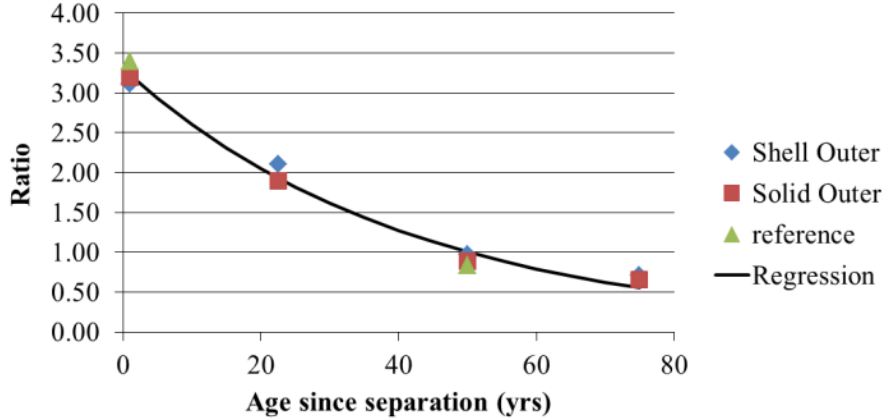


Figure 4.3. Ratio 2 (Eqn 4.2) for both shell and solid HEU configurations, along with the published reference ratios: (830-1060 keV)/(1060-3000 keV).

I analyzed pulse height tallies with Gaussian energy broadening (GEB) in a pulse height tally representing the detector's inherent performance and resolution to determine if these ratios would also be matched using an actual CsI(Na) detector. The GEB tally is represented by the equation,

$$FWHM = a + b\sqrt{E + cE^2} \quad (4.3)$$

where a , b , and c are user defined quantities that are dependent on the detector material. The FWHM at discrete energies was known for the CsI detector, allowing these parameters to be defined through a linear least squares approach. The FWHM data, and the resulting GEB parameters are shown in Tables 4.2 and 4.3. An example MCNP input is given in Appendix B, showing how this parameter is implemented.

Table 4.2. FWHM data for a typical CsI as a function of energy.

MeV	FWHM (MeV)
0.081	0.0141
0.1218	0.01828
0.3443	0.04076
0.356	0.03655
0.511	0.05039
0.6617	0.06001
0.7789	0.06049
1.1732	0.08194
1.2745	0.09503
1.3325	0.09222
1.408	0.10045
2.6145	0.15141

Table 4.2. GEB parameters for MCNP f8 tally.

a	b	c
-0.00725	0.07322	0.31329

Figure 4.4 shows the gamma spectra for both 1 year and 50 years since separation HEU produced from an MCNP “f8” pulse height tally in MCNP5. As previously noted, the gamma contribution at energies greater than 1 MeV is much higher for the 50 year HEU than the 1 year HEU due to the ingrowth of decay daughter products.

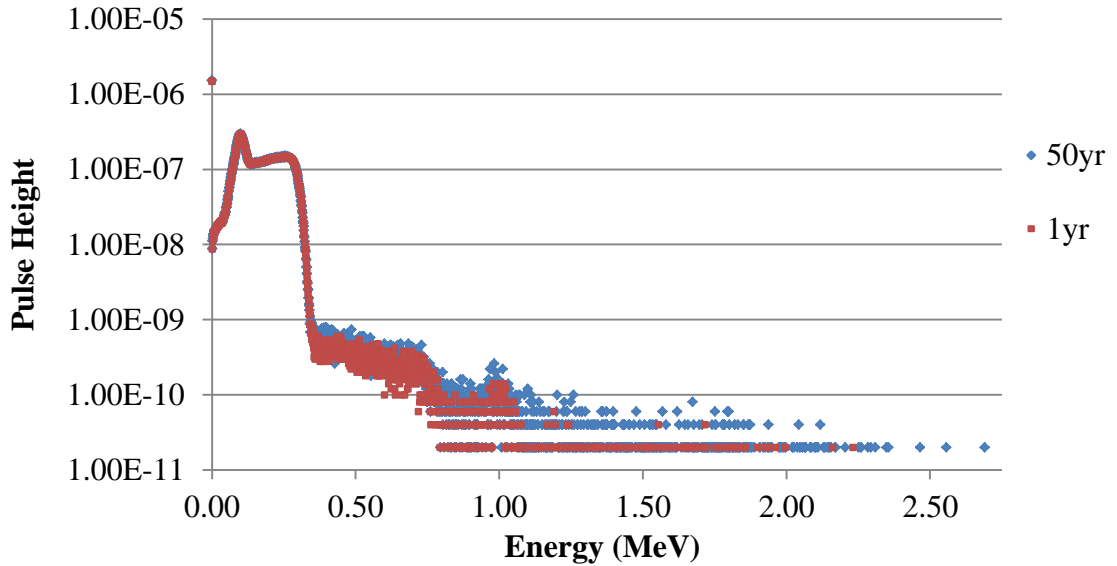


Figure 4.4. Gamma spectrum for 1 year and 50 years since separation HEU for a CsI detector using a pulse height tally in MCNP5 with Gaussian energy broadening. Below E=1MeV, the average relative error is 28% for the 1yr case, and 21% for the 50yr case. Above 1 MeV the average relative error is 70% for both cases.

Again using the protocol as described, I computed the perturbed uranium ratios as in Eq. 4.1 and 4.2, and compared them to the published data and to my ratios using gamma leakage currents through the source box surface broken up into energy group. Figure 4.5 shows that my computational approach using the gamma leakages on a broad group basis was sufficient in identifying the key regions in the spectrum for HEU identification.

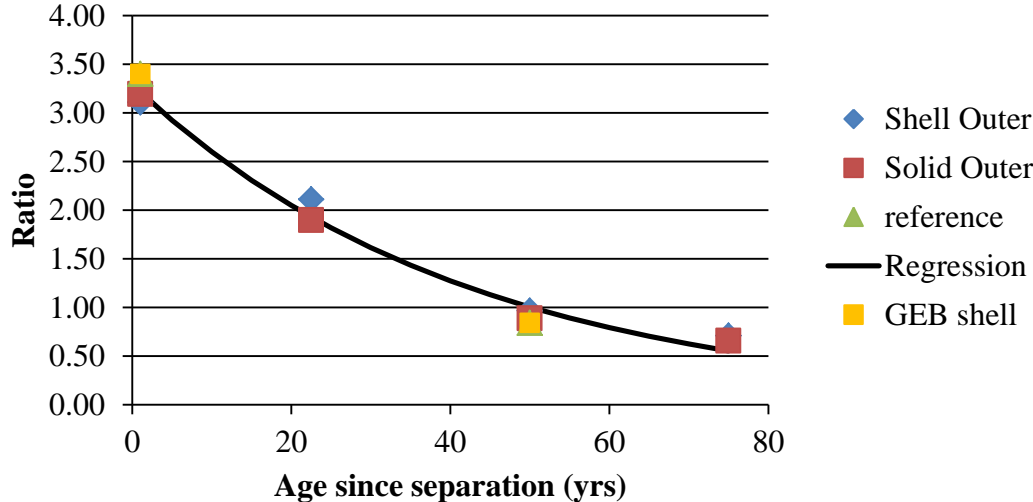


Figure 4.5. Ratio 2 (Eqn 4.2) for both shell and solid HEU configurations, along with the published reference ratios: (830-1060 keV)/(1060-3000 keV). The ratio for the shell HEU configuration from the spectrum seen in a CsI detector is also included.

The GEB case matches previous cases for each given age since separation, showing that the gamma energy spectrum seen in a CsI detector will work well when following this ratio protocol. It also shows that this protocol will work well for robust, low resolution detectors, which greatly lowers cost and maintenance issues while upholding high verification standards.

Weapons Grade Plutonium

Since this protocol was shown to work well for HEU detection, and “age since separation” determinations, I focused on developing protocols for WGPu verification to determine if a similar method could be applied. Figure 4.6 depicts an unshielded 8 kg WGPu normalized spectrum for various ages. As with the HEU spectrum, key source regions exist that show great deviations between ages. However, unlike HEU, WGPu has a strong neutron signature, which via (n,γ) reactions in the shielding, produce an induced gamma spectrum that can cause interference, but also provide some unique gamma spectrum features.

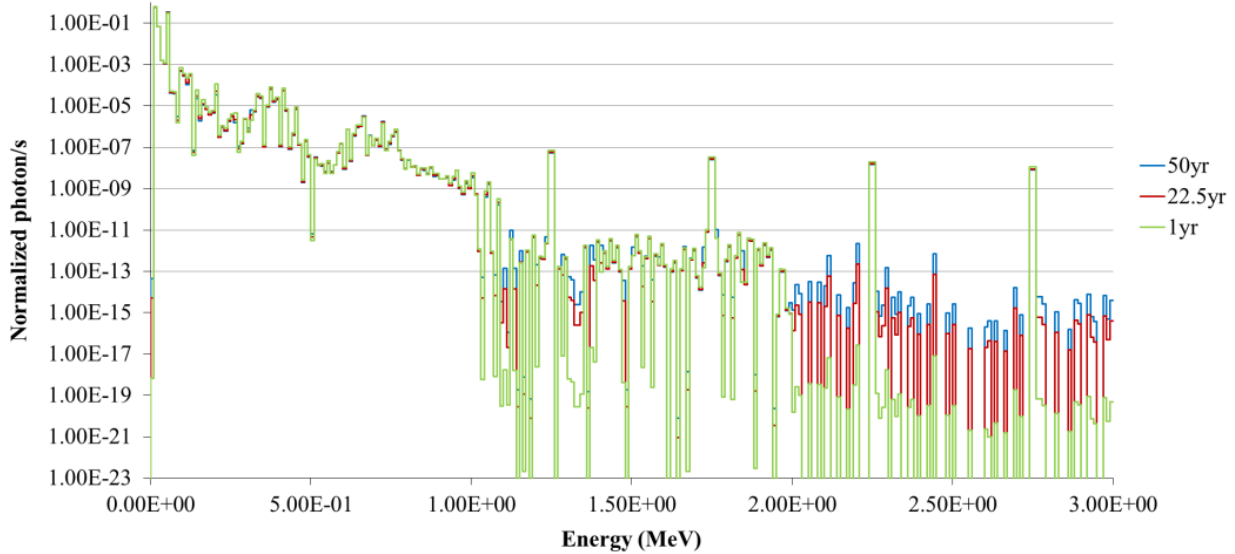


Figure 4.6. WGPu unshielded signature for various ages since separation.

I initially postulated that a clear indicator of Pu age from a passive gamma ray ratio could be determined near/below the 400 keV range due to the ingrowth of americium, but upon further investigation, the unshielded signature did not indicate a significant change, and detection of gammas at low energies is problematic, as noted previously, in the mobile pit application. Also, Compton pileup from scattering in the detector will further add to the difficulty of deciphering gamma lines in the lower energy range. From Figure 4.6, it appears that it should be easy to discern the changes in spectrum between ages, but unlike HEU, the source spectrum emission rates drop off significantly at energies greater than 1 MeV. To determine if detectable ratios can be used to identify and age date the mass as a signature, I investigated applying the 24 group structure that focuses on gamma lines and applicable regions of interest in the WGPu spectrum.

I used the original MCNP models to investigate the total (induced and intrinsic) photon leakages out of the outer source box, and I added models for 1 year and 50 year WGPu cases. The intrinsic gamma spectrum was added to the induced gamma spectrum

at the surface of the source box, and for each age since separation, the groups were compared to see how they differed. Table 4.4 depicts the gamma leakage for each WGPu mass age per energy group (analogous to the source behavior in Figure 4.6), and the percent differences between each group. Percent difference is defined as the absolute value difference between two experimental values divided by the mean of those values. This method is employed over the typical percent error calculations since there is no baseline or theoretical value for comparison. The percent difference formula is described mathematically as

$$\% \text{ Difference} = \frac{|E_1 - E_2|}{\frac{E_1 + E_2}{2}} \quad (4.4)$$

where E_1 and E_2 are the experimental values. It is possible to see percent differences greater than 100% if the relative difference between two values is greater than their average.

Table 4.4. Total gamma leakage through +x plane of the Source Box for various ages of the WGpu shell source.

Group	Upper Energy (keV)	1 year	22.5 year	% diff between 1 year & 22.5 year	50 year	% diff between 22.5 year & 50 year
24	300	4.66×10^6	4.56×10^6	2.28%	4.72×10^6	1.35%
23	741	1.74×10^7	1.71×10^7	1.96%	1.75×10^7	0.42%
22	743	7.01×10^3	5.91×10^3	16.97%	7.09×10^3	1.22%
21	765	5.46×10^4	5.20×10^4	5.01%	5.57×10^4	1.82%
20	767	3.81×10^4	3.77×10^4	1.16%	3.78×10^4	0.86%
19	954	6.58×10^4	6.13×10^4	6.98%	6.68×10^4	1.59%
18	956	9.58×10^2	7.53×10^2	23.97%	1.02×10^3	5.77%
17	999	2.87×10^3	2.88×10^3	0.35%	2.85×10^3	0.72%
16	1002	6.24×10^2	6.97×10^2	11.02%	5.48×10^2	12.97%
15	1180	9.15×10^3	9.16×10^3	0.07%	9.10×10^3	0.56%
14	1200	8.35×10^2	8.36×10^2	0.09%	8.28×10^2	0.85%
13	1240	1.67×10^3	1.67×10^3	0.09%	1.67×10^3	0.12%
12	1260	2.10×10^4	2.10×10^4	0.03%	2.10×10^4	0.32%
11	1500	5.36×10^3	5.37×10^3	0.15%	5.34×10^3	0.37%
10	1520	3.90×10^2	3.91×10^2	0.14%	3.89×10^2	0.39%
9	1736	3.97×10^3	3.98×10^3	0.13%	3.96×10^3	0.41%
8	1740	6.62×10^1	6.62×10^1	0.09%	6.64×10^1	0.32%
7	1760	1.24×10^4	1.24×10^4	0.08%	1.24×10^4	0.38%
6	1830	7.84×10^2	7.85×10^2	0.19%	7.82×10^2	0.16%
5	1832	2.27×10^1	2.27×10^1	0.19%	2.26×10^1	0.10%
4	2210	3.49×10^3	3.50×10^3	0.20%	3.48×10^3	0.37%
3	2250	4.59×10^3	4.59×10^3	0.03%	4.57×10^3	0.37%
2	2749	6.26×10^3	6.26×10^3	0.09%	6.24×10^3	0.34%
1	2750	4.63×10^3	4.63×10^3	0.04%	4.62×10^3	0.37%

I noted that the changes between leakages as a function of age were fairly small for most energy groups. A few groups, such as group 16 and group 18, stood out as being the groups with the greatest differentiation across ages. I chose to base my ratio methods around these groups to identify the most noticeable changes with respect to age. It was challenging to find ratios that would lead to a reliable age determinations, but I was able to develop three ratios that examined different energy ranges along the WGpu

gamma leakage spectrum. The ratios found with the greatest deviation between material age since separation were:

$$Ratio\ 3 = \frac{\int_{999keV}^{1002keV} Counts}{\int_{767keV}^{956keV} Counts} \cong \frac{Counts_{g=16}}{\sum_{g=18}^{19} Counts_g} \quad (4.5)$$

$$Ratio\ 4 = \frac{\int_{741keV}^{765keV} Counts \int_{767keV}^{956keV} Counts}{\left(\int_{1200keV}^{2750keV} Counts\right)^2} \cong \frac{\sum_{g=21}^{22} Counts_g + \sum_{g=18}^{19} Counts_g}{\left[\sum_{g=1}^{13} Counts_g\right]^2} \quad (4.6)$$

$$Ratio\ 5 = \frac{\int_{999keV}^{1002keV} Counts}{\int_{741keV}^{965keV} Counts} \cong \frac{Counts_{g=16}}{\sum_{g=18}^{22} Counts_g} \quad (4.7)$$

Figures 4.7a and 4.7b show ratio 3 (Eqn. 4.5) and ratio 4 (Eqn. 4.6) over ‘age since separation’ from the Gaussian energy broadening models for a CsI detector. It will be difficult to pinpoint the age of the plutonium from the model results, since the ratios found deviate very slowly with accumulated age. Each ratio alone would not be reliable enough for a definitive assessment of age since separation, but it may be possible with the application of multiple ratios that one can quickly and passively achieve an estimate of WGPu age. Examining ratios that include different ranges of the spectrum will help. For example, ratio 5 deals with gammas with energies in the middle range of the spectrum (around 1 MeV), whereas ratio 4 deals primarily with gammas with energies up into the high range of the spectrum (greater than 2 MeV). It may be problematic to achieve good enough statistics in a reasonable count time for these ratios. In addition, if the ratio is poorly resolved in one energy range, it may be easier to resolve in another.

For the Mobile Pit application, where the presence and type of mass needs to be verified rapidly, the use of multiple ratios with multiple detectors in a synthetic aperture arrangement can help one better see if another material has been used to replace a portion of the weapons pit. If all ratios appear to be in line with one another, with perhaps one

outlier, then it is likely that there is another actinide in the source that should not be present, indicating potential mass tampering. If this is identified, a closer secondary inspection should be taken of the pit/container in question.

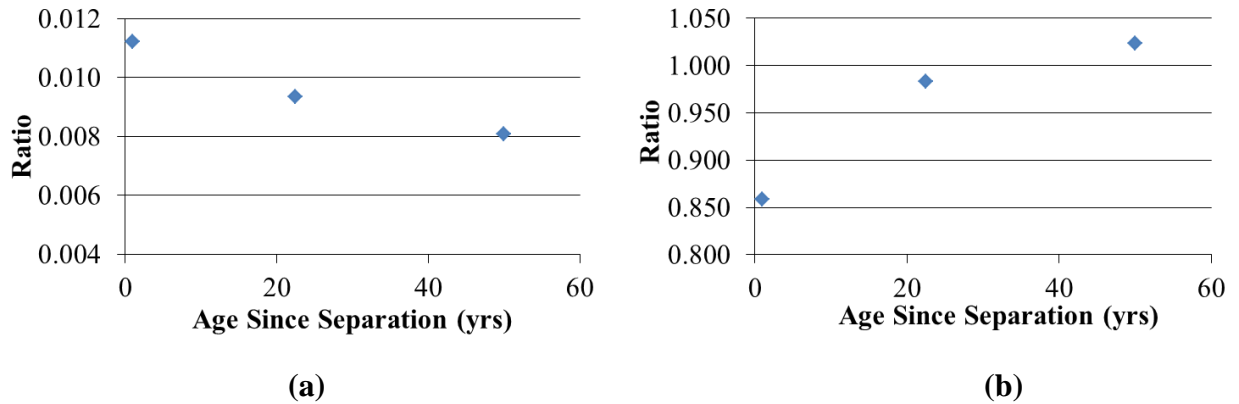


Figure 4.7. (a) Ratio for WGPu *shell* source using the protocol Ratio 3 (Eqn 4.5). (b) Ratio (nonlinear) for WGPu *shell* source using the protocol Ratio 4 (Eqn 4.6).

It is more challenging to see a differentiation between these ratios when looking at a low resolution detector spectrum as modeled by MCNP using Gaussian Energy Broadening. Figure 4.8 shows how close each spectrum for each age is. Part of this is due to the relative uncertainties in the Monte Carlo simulations. Some of the uncertainties at various energies are greater than the percent differences seen between each ratio proposed in Figure 4.7. Further laboratory experimentation or spectral clean-up may be needed to better see how these ratios come into play.

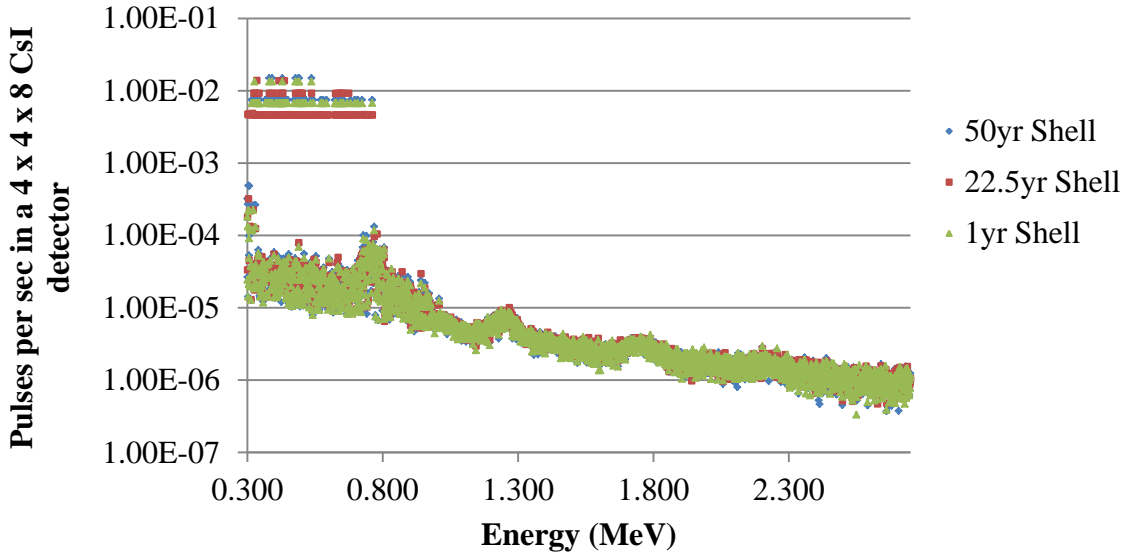


Figure 4.8. The Gaussian Energy Broadened spectrum of 1year, 22.5year, and 50 year age since separation WGpu shell source for a $4 \times 4 \times 8$ CsI detector placed approximately 5cm away from the surface of the pit container. The average relative errors were 28%, 23%, and 29% for the 1yr, 22.5yr, and 50yr cases.

Additional challenges arise when viewing different geometry configurations of the WGpu source. The ratios determined for the shell source do not hold for the solid. The effects of self-shielding on the intrinsic gammas, plus the increased number of induced gammas from neutron multiplication are great enough such that the induced gamma signature overpowers the intrinsic gamma signature at energies greater than 1 MeV by a factor of 5.5 for the 8 kg 22.5 year case. The total normalized gamma leakage through the source box surface is shown in Figure 4.9. As discussed, the spectrum has significant changes due to increased neutron multiplication in the solid configuration, resulting in increased induced gamma production, which “washes out” much of the intrinsic spectrum.

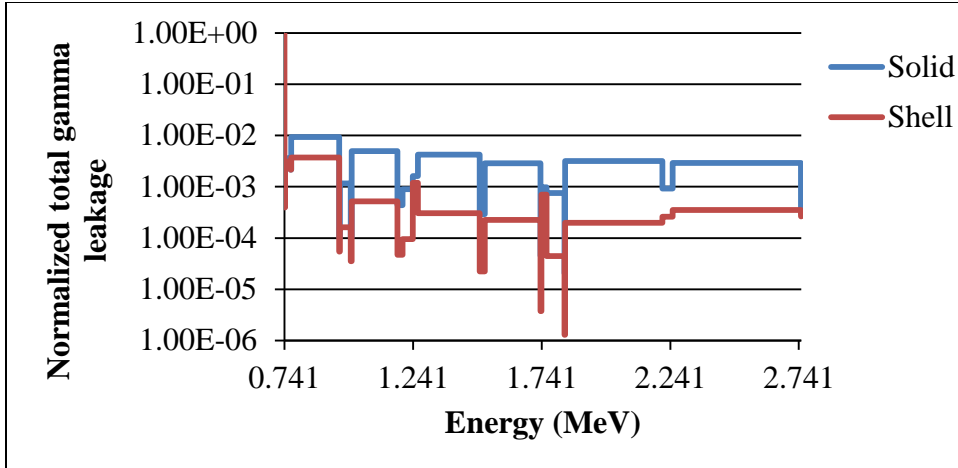
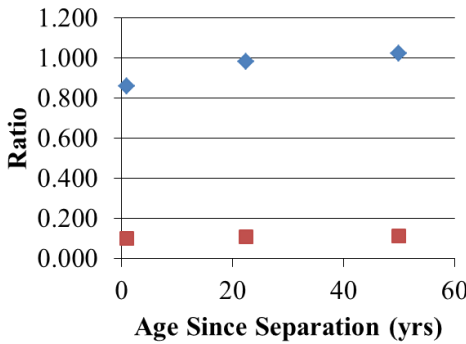
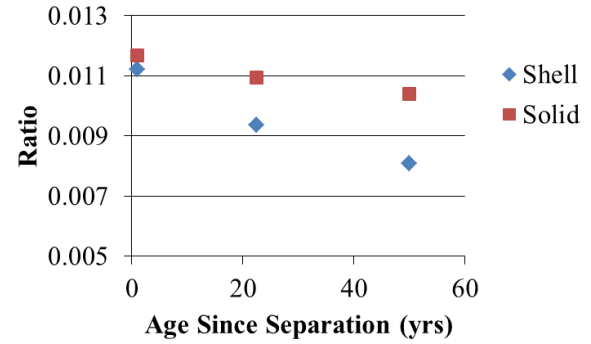


Figure 4.9. Comparison between normalized total gamma leakage through the source box surface for the solid and shell configured sources for 22.5 years age since separation WGPu. The Energy range is restricted to highlight upper energy differences in the spectrum.

Under the same protocols as described earlier in this section, I noted that ratios can still be observed, but they do not readily align with those observed for the shell configuration. Figure 4.10 depicts how large the differences are between the solid and shell configurations for ratios (4.3) and (4.4). Since the differences are considerable, and it does not appear they will overlap, these ratios can still be used to determine the presence of WGPu. It is an added bonus that the configuration of the WGPu can be determined as well. This could be very beneficial to determining whether or not any material has been removed, or if a solid source was switched with a shell. Ratio (4.3) has significant separation between the shell and solid sources as shown in Figure 4.10a, so it should be used not only for age determination, but for source configuration. Once the configuration is determined, I could apply ratio (4.3) further, and ratio (4.4) and (4.5) to narrow down the most likely age of the material.



(a)



(b)

Figure 4.10. (a) Comparison of the solid and shell 22.5 year WGPu gamma leakages for ratio 4 (Eqn 4.6). (b) Comparison of the solid and shell 22.5 year WGPu source gamma leakages for ratio 5 (Eqn 4.7).

Spoof Testing

As briefly mentioned previously, the use of multiple passive spectral ratios will augment proof of efforts to spoof or “foil” the system. Adding or replacing other actinides to produce a gamma signature similar to HEU or WGPu will alter the ratios, particularly for gamma materials that leak from the system. Even if sources are added to maintain consistency with one of the ratios, it is highly unlikely all ratios will be correct.

Since the ratios observed with WGPu are not as clearly pronounced or easy to detect, coupling the gamma signature with the neutron signature for Pu will be important and necessary for proper material classification and verification for the Mobile Pit system. Sure, one can essentially “fake” a WGPu spectrum from other fissile materials and shielding, but the associated gamma spectrum will be noticeably skewed. For example, a PuBe source can be used as a surrogate source for WGPu, but in order to do this, sufficient shielding, such as a Ni composite alloy, must be placed around the PuBe to alter the neutron spectrum so that it resembles a fission neutron spectrum surrogate for WGPu [21]. Figure 4.11 shows how the surrogate source can be shielded to resemble a

WGpu source enough so that a detector will not be able to sufficiently show noticeable differences. Due to gamma attenuation through the Ni, the gamma spectrum leaking through the weapons container will change such that the ratios will be altered. Someone who may want to spoof the system would have to not only match the ratios in the mid-range of the gamma energy spectrum, but also over the high range; they would also have to do this without altering neutron multiplication (and neutron-gamma effects) as well as overall gamma leakage. Even if the normalized neutron spectrum or gamma spectrum is similar, the overall integrated count rates for each particle type will change. The PuBe source will yield higher neutrons/s with less WGpu mass than a strictly WGpu source, but with less Pu in the surrogate source, the gammas emissions will be reduced [21]. Many variables are at play, such that it would be extremely challenging for a diverter to successfully spoof this system using a combination of ratios and signatures. Obviously, a past screening or metrics on specific container's Pu would need to be known prior to screening to flag a container that had material that was potentially diverted.

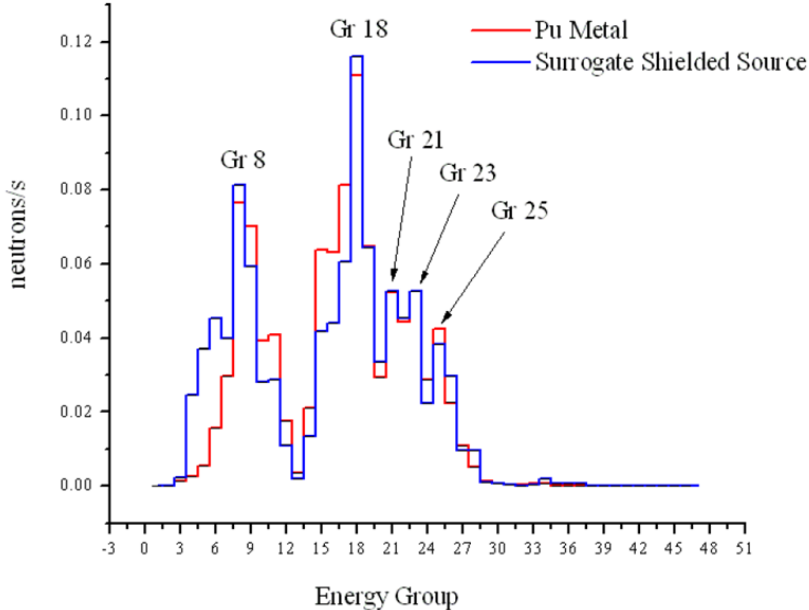


Figure 4.11. Neutron spectrum for a WGpu source along with a PuBe shielded surrogate source [22].

By applying these various methods, and considering more than just one type of radiation, I can successfully validate whether a weapons pit is in fact containing the contents as expected. Much of this could be managed in a system incorporating software and RFID tags, or similar technology in a fully engineered system design.

One approach to spoofing could be to ‘hollow out’ a solid source and increase the surface area such that it becomes a “shell” source, but potentially is counted as a solid, enabling the mass to be diverted. In theory, this would still result in a close but skewed gamma ratio signature, and like the solid source, have a lower integrated count rate. In practice, there may actually be no noticeable change in the ratios. The count rate for each energy group decreases in a uniform percentage for each group. It was postulated that self-shielding of the low energy group gammas would help skew the ratios towards being “high energy heavy”, but this is not the case. In order to mitigate self-shielding effects, the thickness of the HEU shell must be much thinner. Looking at the ratios alone would not be indicative of tampering, since an inspector can be faced with 25kg HEU shell sources as well. Even if an inspector was expecting to see a solid source and, instead, a shell source was replaced in its place, the inspector would not be able to differentiate if the material in question was HEU. The prescribed ratios between the shell and solid sources are very close for HEU, as seen in Figure 4.5. Therefore, in order to noticeably detect a diversion of this type, the inspector must pay close attention to the integral count rate in the detectors for the specified source-detector geometry, thus requiring a facility baseline measurement to be established prior to facility screening. If all solid sources yield a certain count rate, but one or two do not, then additional scrutiny of the outlier containers for a secondary protocol for inspection is warranted. Table 4.5 shows the result of Monte Carlo computations of leakages through one of the source box surfaces for 25kg, 20kg, 15kg, 10kg, and 5kg of HEU. These scenarios considered each maintained the same outer radial dimension of 6.79cm of the HEU mass, but with variations of the hollowed inner radius replaced by air. One side of the source box is

60cm x 60cm and the total photon leakage through a side is 2.35×10^4 photons/s for the 25kg case. Starting from a 25 kg SQ mass, it is noted that the overall gamma leakage rate through the container differs by 22% for 5 kg diverted, by 49% for 10 kg diverted, by 84% for 15 kg diverted, and the rate drops 129% for 20 kg diverted.

Table 4.5. Gamma leakage through one surface of source box for various HEU masses using a hollowed out solid core diversions with an outer radius of 6.79cm.

All cases had an average relative 1 sigma error of ~0.5%.

Group	Energy Bounds (MeV)	25 kg photons/s	20kg photons/s	15kg photons/s	10kg photons/s	5kg photons/s
24	0 -0.3 **	4.53×10^3	3.62×10^3	2.73×10^3	1.84×10^3	9.75×10^2
23	0.3- 0.741	1.40×10^4	1.12×10^4	8.41×10^3	5.69×10^3	3.01×10^3
22	0.741- 0.743	1.74×10^2	1.40×10^2	1.05×10^2	7.11×10^1	3.76×10^1
21	0.743- 0.765	9.87×10^1	7.90×10^1	5.94×10^1	4.02×10^1	2.13×10^1
20	0.765- 0.767	4.01×10^2	3.21×10^2	2.42×10^2	1.63×10^2	8.64×10^1
19	0.767- 0.954	1.23×10^3	9.88×10^2	7.44×10^2	5.03×10^2	2.66×10^2
18	0.954- 0.956	1.80×10^1	1.44×10^1	1.08×10^1	7.31×10	3.87×10
17	0.956- 0.999	1.50×10^2	1.20×10^2	9.05×10^1	6.12×10^1	3.23×10^1
16	0.999- 1.002	1.51×10^3	1.21×10^3	9.10×10^2	6.16×10^2	3.25×10^2
15	1.002- 1.18	2.57×10^2	2.06×10^2	1.55×10^2	1.05×10^2	5.54×10^1
14	1.18- 1.2	3.94×10^1	3.15×10^1	2.37×10^1	1.61×10^1	8.48×10
13	1.2- 1.24	7.57×10^1	6.06×10^1	4.56×10^1	3.09×10^1	1.63×10^1
12	1.24- 1.26	1.33×10^1	1.07×10^1	8.02×10^0	5.43×10	2.86×10
11	1.26- 1.5	2.42×10^2	1.93×10^2	1.45×10^2	9.84×10^1	5.20×10^1
10	1.5- 1.52	6.27×10^1	5.02×10^1	3.78×10^1	2.56×10^1	1.35×10^1
9	1.52- 1.736	1.84×10^2	1.47×10^2	1.11×10^2	7.48×10^1	3.96×10^1
8	1.736- 1.74	7.59×10^1	6.08×10^1	4.58×10^1	3.10×10^1	1.64×10^1
7	1.74- 1.76	1.39×10^1	1.11×10^1	8.35×10^0	5.65×10	2.99×10
6	1.76- 1.83	1.79×10^2	1.43×10^2	1.08×10^2	7.30×10^1	3.86×10^1
5	1.83- 1.832	5.07×10^1	4.06×10^1	3.05×10^1	2.07×10^1	1.09×10^1
4	1.832- 2.21	1.66×10^2	1.33×10^2	1.00×10^2	6.77×10^1	3.58×10^1
3	2.21- 2.25	2.22×10^1	1.78×10^1	1.34×10^1	9.05×10	4.77×10
2	2.25- 2.749	1.92×10^1	1.54×10^1	1.16×10^1	7.83×10	4.14×10
1	2.749- 2.75	3.10×10^{-1}	2.48×10^{-1}	1.88×10^{-1}	1.26×10^{-1}	6.66×10^{-2}
Total		2.35×10^4	1.88×10^4	1.41×10^4	9.57×10^3	5.06×10^3

Another possible diversion scenario would be to store additional material by increasing the mass of the solid source such that it gives off the overall number of gammas leaking out, while keeping the same “age since separation” based on the passive spectral protocols investigated here. This scenario would be much more difficult to achieve, given that the additional mass must be the same age as the original unperturbed mass, and the total mass must not violate criticality safety protocols. Also, it should be obvious for the low vs. high energy gamma yields to be affected by self-shielding for lower energy gammas compared to the high energy gammas, affecting the overall spectrum.

In the next chapter I will investigate more specifically the neutron signature for the WGPu source, and how this can be detected so that the key portions of the spectrum are preserved.

CHAPTER 5

NEUTRON DETECTION

After analyzing the passive gamma signatures for HEU and WGPu, I investigated the neutron signatures for WGPu. Unlike HEU, which has a neutron signature on the order of $0.1 \text{ n per s per sr}$, WGPu has a strong neutron signature on the order of $10^3 \text{ n per s per sr}$. Therefore, the neutron signature for HEU was not considered.

Most of the neutrons for bare WGPu are fast, with energies far above thermal energies, with the majority around 1 MeV. As shown Figure 5.1, the majority of neutrons emitted from the WGPu source are not significantly thermalized when passing through the weapons pit container. Therefore, a neutron detector system that can thermalize these neutrons so that they interact with the detectors is needed. In addition, in order to determine a signature unique to WGPu, more than one single energy band must be considered. A neutron detector assembly designed for use in similar applications that discriminates between neutrons of different energy ranges was chosen.

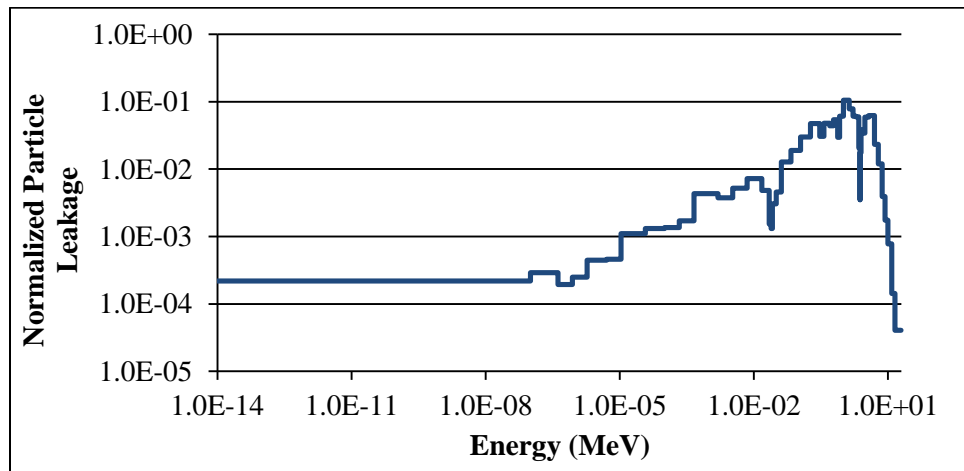


Figure 5.1. The normalized neutron leakage for a 22.5 year age since separation WGPu Shell. The average relative 2 sigma error was 0.12%.

The neutron detector array designed for the “Transport Simulation and Validation of a Synthetic Aperture SNM Detection System (“T-SADS”) project was used in this work; T-SADS is an ongoing project funded by DOE-NNSA that will be completed in FY2013 [23]. Neutron work related to spectral deconvolution performed in the NNSA project was used here as forecast. The neutron array is broken into five major sections, and uses He-3 detectors. The five sections are each layered with different materials “filtering neutrons” ahead of each bank of detectors. The materials are layered in different configurations to filter different energy neutrons in various particle energy ranges. A particle must travel through these materials, with varying absorption and scattering cross sections, before it can be counted in the He-3 detectors. Figure 5.2 shows the layout of the five detector blocks [23].

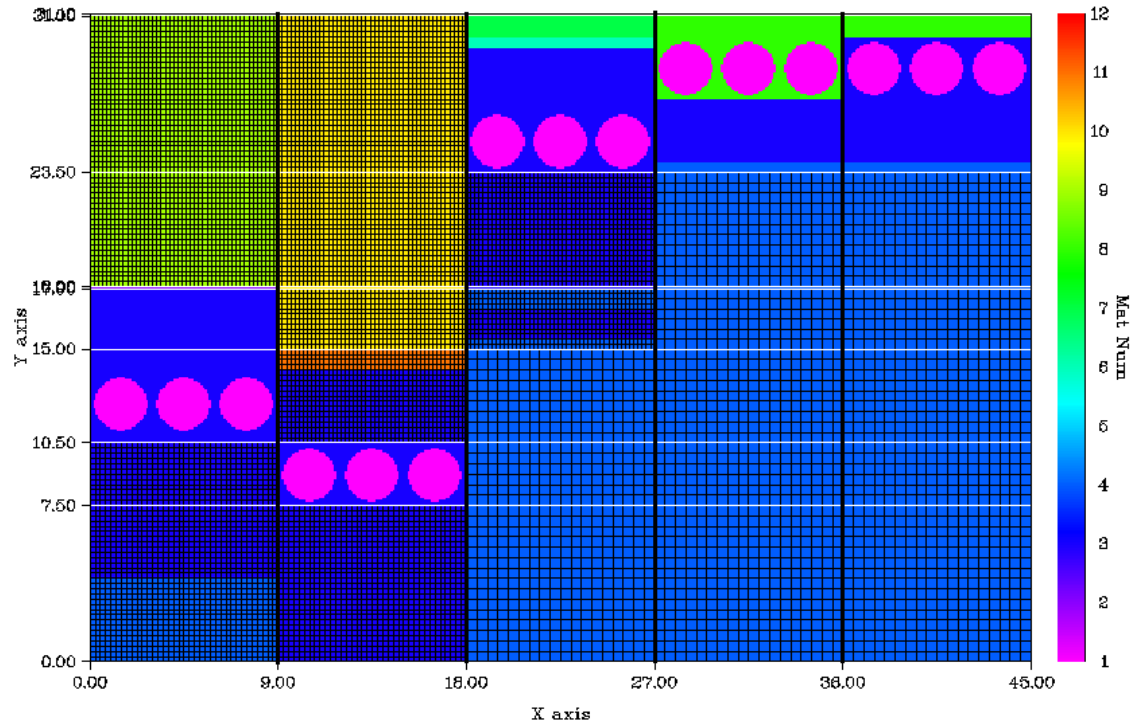


Figure 5.2. Blocks 1 through 5 (from left to right) of the neutron detector assembly [23].

Block I was designed to detect neutrons with energies greater than 3.68 MeV, and Block 2 was designed to detect neutrons in the energy range of 1 to 3.68 MeV [24].

Since a large number of neutrons leaking out of the canister were around 3.68 MeV, I focused on analyzing the detector response in Block I.

A model of Block 1 adjacent to the gamma detection block was created using PENTRAN. A tungsten collimator 1cm in thickness was placed adjacent to the CsI block, and protruded 10cm in front of the block. This collimation was carefully selected in previous work for optimal gamma detection [25]. The front face of the detector system was placed at a distance of 30 cm from the front surface of the source box. This distance was assumed to be a likely separation distance for the detector operator and sources. In addition, to further impede thermal neutrons from crossing across blocks, and increase scattering, I added a 1 mm strip of cadmium metal in along both sides of Block I.

Additional models were created for Block III and Block V of the neutron detector system to analyze the response rates of lower energy neutrons leaking out from the source box surface. Investigating the signatures at various energy ranges will aide in the discrimination of WGPu from other fissile materials. These models were used to determine the response rates found in each detector block for weapon pit sources. Each model is discussed in detail later.

Transport Methodology

Instead of running multiple models with differing detector placement to determine the detector response, a single “adjoint” run can be completed. From one model run, the response in the detector can be found from any point surrounding the detector, saving a considerable amount of time and effort.

The transport equation can be written in operator form as

$$H\psi = q_{fwd} \quad (5.1)$$

with zero incident boundary angular flux consistent with a vacuum boundary. The operator H , is defined as

$$H = \widehat{\Omega} \cdot \nabla + \sigma_g(\vec{r}) - \sum_{g'=1}^G \int_{4\pi} \sigma_{s,g' \rightarrow g}(\vec{r}, \widehat{\Omega}' \cdot \widehat{\Omega}) d\Omega' \quad (5.2)$$

where $\sigma_g(\vec{r})$ is the total cross section for a given group, $\sigma_{s,g \rightarrow g'}(\vec{r}, \widehat{\Omega}' \cdot \widehat{\Omega})$ is the scattering cross section from group g' to g and from $\widehat{\Omega}'$ to $\widehat{\Omega}$.

The adjoint equation reverses the direction of streaming and inverts the scattering group to group energy and directional term and is written as

$$H^\dagger \psi^\dagger = \sigma_d \quad (5.3)$$

with the equivalent boundary condition that particles leaving the geometry have zero importance. The adjoint operator is defined as:

$$H^\dagger = -\widehat{\Omega} \cdot \nabla + \sigma_g(\vec{r}) - \sum_{g'=1}^G \int_{4\pi} \sigma_{s,g \rightarrow g'}(\vec{r}, \widehat{\Omega} \cdot \widehat{\Omega}') d\Omega' \quad (5.4)$$

Where $\sigma_g(\vec{r})$ is the total cross section for a given group, $\sigma_{s,g \rightarrow g'}(\vec{r}, \widehat{\Omega} \cdot \widehat{\Omega}')$ is the scattering cross section from group g to g' and from $\widehat{\Omega}$ to $\widehat{\Omega}'$.

In a typical forward calculation, the detector response is represented by,

$$R \left[\frac{\text{particles}}{\text{s}} \right] = \int_{4\pi} d\Omega \int_0^\infty dE \int_{V_d} dV \sigma_d \psi(r, E, \Omega) = \langle \psi \sigma_d \rangle \quad (5.5)$$

where R is the reaction rate, V_d is the detector volume, σ_d is the reaction cross section of the detector material for a given energy, and φ is the angular flux. The adjoint response rate can be found by applying the principle of the adjoint identity, which is represented by

$$\langle \psi^\dagger H \psi \rangle = \langle \psi H^\dagger \psi^\dagger \rangle \quad (5.6)$$

Substituting equations 5.1 and 5.3 gives the expression

$$\langle \psi^\dagger q_{fwd} \rangle = \langle \psi \sigma_d \rangle \quad (5.7)$$

Plug equation 5.5 into equation 5.6 to get the adjoint and forward reaction rates,

$$R_{adj} = \langle \psi^\dagger q_{fwd} \rangle \quad (5.8)$$

$$R_{fwd} = \langle \psi \sigma_d \rangle$$

where R_{adj} is the adjoint reaction rate, ψ^\dagger is the adjoint importance, q_{fwd} is the forward source, R_{fwd} is the forward reaction rate, ψ is the forward angular flux and σ_d is the reaction cross section of the detector.

Detector Block I

Figure 5.3 shows a top down view of Block I next to the gamma detection block cut at the Z=0 plane. As previously described, this detector assembly was designed to detect high energy neutrons leaking from the source box surface. As Figure 5.3 shows, Cd, along with asphalt and polyethylene are used to thermalize these “fast” neutrons down to more important energies for detection. Additional layers of cadmium along the walls of the detector block will help reduce leakage from adjacent blocks into the detectors.

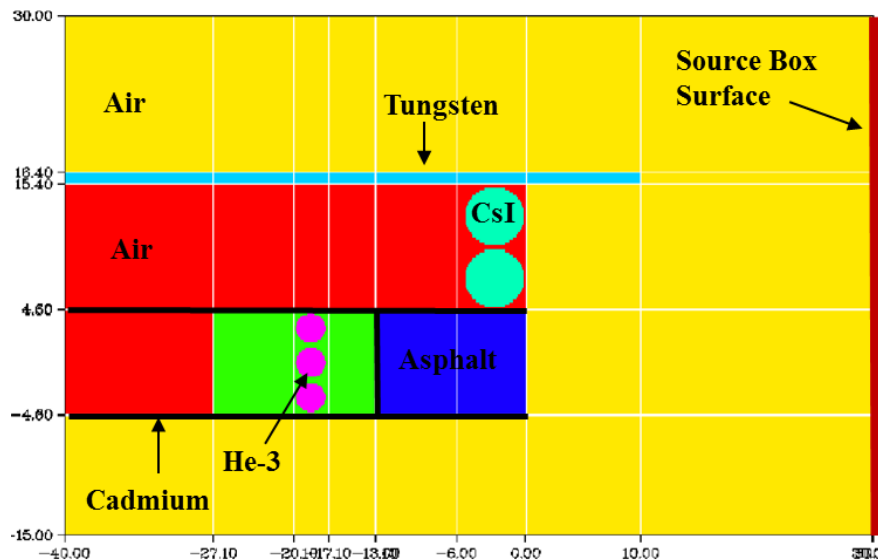


Figure 5.3. Block I of the neutron detector assembly and gamma detector block model in PENTRAN.

This model was executed in PENTRAN to find the adjoint importances at the surface of the source box using a 30 energy group library with neutron upscattering (based on other supporting research in a DOE/NNSA funded project (T-SADS) [23]. The adjoint importances (analogous to detector efficiencies) were plotted for each energy group to determine the relative likelihood of a neutron with a given energy to interact with the 4 atm He-3 detectors. Figure 5.4 shows these plots for a selected set of energy groups. These groups were chosen to show how the neutron importances change as the energy group of focus changes. Two fast neutron and two thermal groups were chosen to be represented. These groups do not necessarily represent the most responsive groups for the given model.

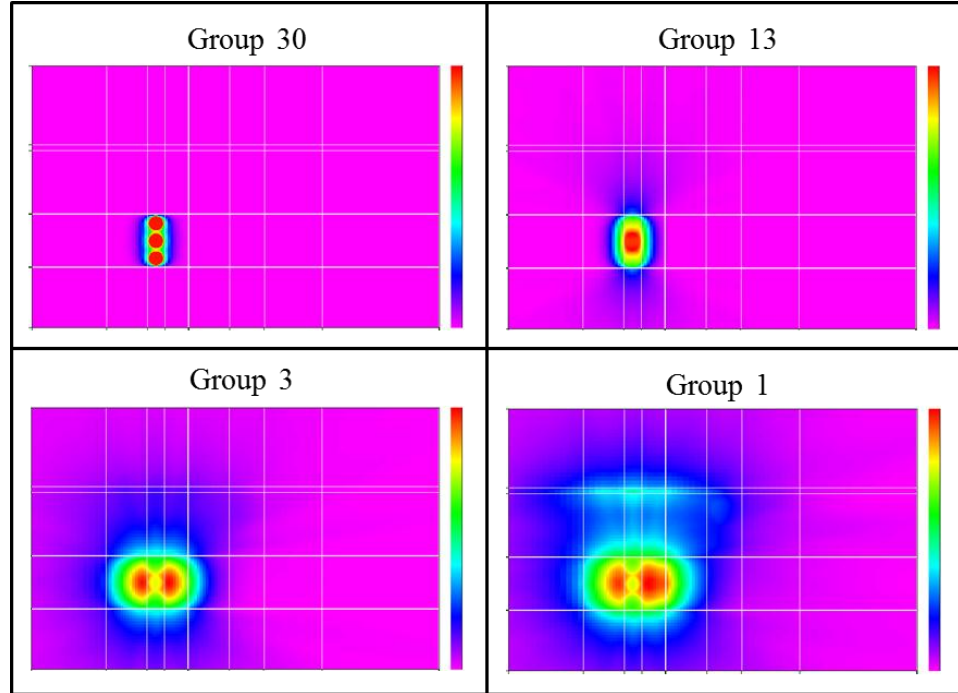


Figure 5.4. Block I adjoint importances for “forward” group ordering, including group 30 ($<1\times10^{-10}$ MeV) ceiling/floor (1.0/0.0), group 13 ($1.3\times10^{-6} - 3.05\times10^{-6}$ MeV) ceiling/floor (0.58/0.0), group 3 (3.0 – 8.19 MeV) ceiling/floor ($6.7\times10^{-2}/4.0\times10^{-5}$), and group 1 (17.3 – 20 MeV) ceiling/floor ($1.3\times10^{-2}/4.8\times10^{-5}$) at center height of Source Box.

It can be seen that Block 1 is indeed most useful for detecting fast neutrons in forward group 1. Thermal and epithermal neutrons have very little chance of creating a reaction in a He-3 detector, seen by the extreme drop off of adjoint importance in the Group 30 and 13 plots. It, however, must be noted that Figure 5.4 does not have a uniform scale across all groups, giving the sense that the adjoint importances are much greater in groups 3 and 1, respectively, when that is not necessarily the case. Figure 5.5 depicts the same groups and adjoint importances, but all plots are on a uniform scaling basis. The solid black areas in Figure 5.5 are locations where the (efficiencies) importances are values below what is included in the color scale (5×10^{-6}).

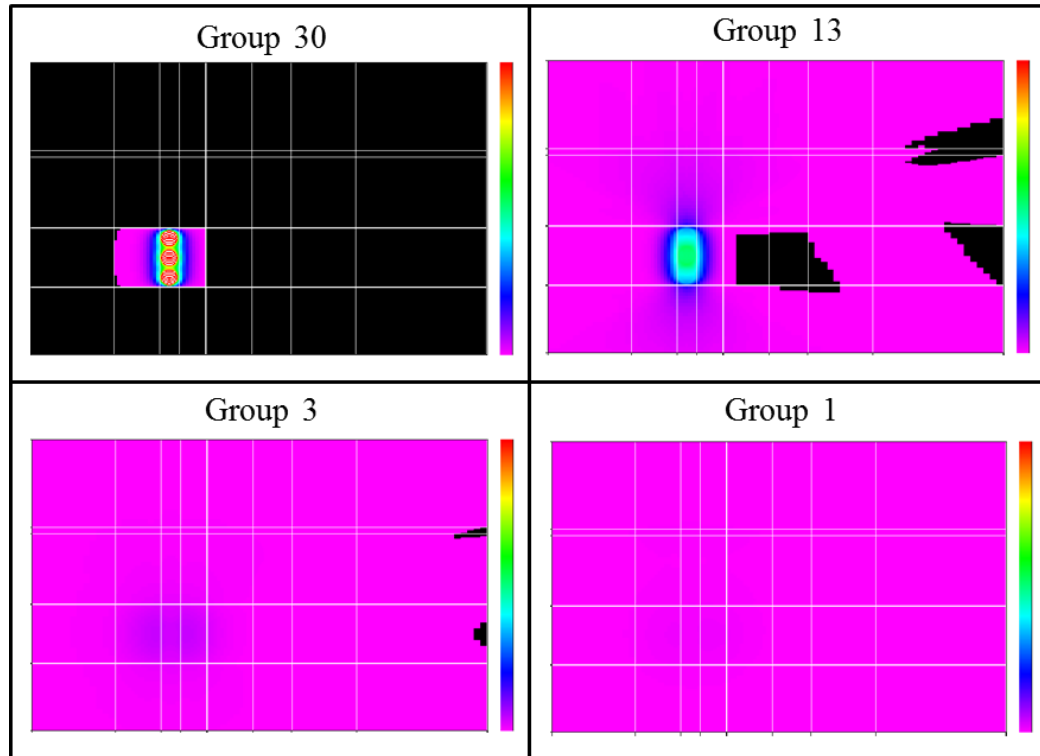


Figure 5.5. Adjoint importances for forward group 30 (thermal, $< 1 \times 10^{-10}$ MeV), group 13 (epithermal, $1.3 \times 10^{-6} - 3.05 \times 10^{-6}$ MeV), group 3 (fast, $3.0 - 8.19$ MeV), and 1 (high energy, $17.3 - 20$ MeV) sliced at center height of the Source Box. The color map scaling is identical for all four plots. The ceiling and floor importances were 1.0 and 5×10^{-6} respectively.

The regions where the importances “drop off” are indicative of large energy losses per collision. The average energy loss in a neutron collision with a material of atomic mass, A , is denoted as

$$\Delta E = \frac{(1 - \alpha)}{2} \quad (5.9)$$

where ΔE is the average energy loss in a collision and $\alpha = \frac{(A-1)^2}{(A+1)^2}$ where A is the effective atomic mass. It makes sense for group 30 (very thermal neutrons), that outside of the poly material region, there is a negligible chance that a thermal neutron will have an interaction with the detector. By the time a thermal neutron would make it through the air, it is met by additional low atomic mass compounds. The black region in front of the detector for group 13 in Figure 5.5 is indicative that importance is very low for that energy of neutrons, making it unlikely for a neutron born in that region to cause an interaction in the detector. This region represents the large asphalt region (Ref. Figure 5.3), which is made from a hybrid of hydrocarbons, giving it a relatively low effective atomic mass. The density of asphalt is also much greater than air and poly, providing more opportunities for neutron collisions. The combination of these characteristics makes it difficult for an epithermal neutron to escape.

This is a useful detector block assembly for the MPVS application, since there is likely to be a strong interference of background thermal neutrons that have thermalized in concrete and other materials over several meters from the storage container of interest, and the Block I array is not sensitive to those neutrons, having strong dependence on the most energetic sources.

Looking closer at the adjoint importances along the source plane surface shows the relative likelihood of neutrons leaving a point along the source box surface will be detected in Block I. Figure 5.6 shows this for the same four energy groups described in Figures 5.4 and 5.5. Fast neutrons will undergo many scattering collisions when traveling through the asphalt, polyethylene, and cadmium. For this reason, I will not see

a peak in the importance at the centerline of the detector. Looking back at Figure 5.1, I can see how this will pose a challenge to time gating and providing confidence that the neutrons detected are from the weapons pit container that the inspector is measuring. A possible method to reduce interference from surrounding sources is to add a layer of polyethylene surrounding the outside of the assembly, including the Tungsten collimator.

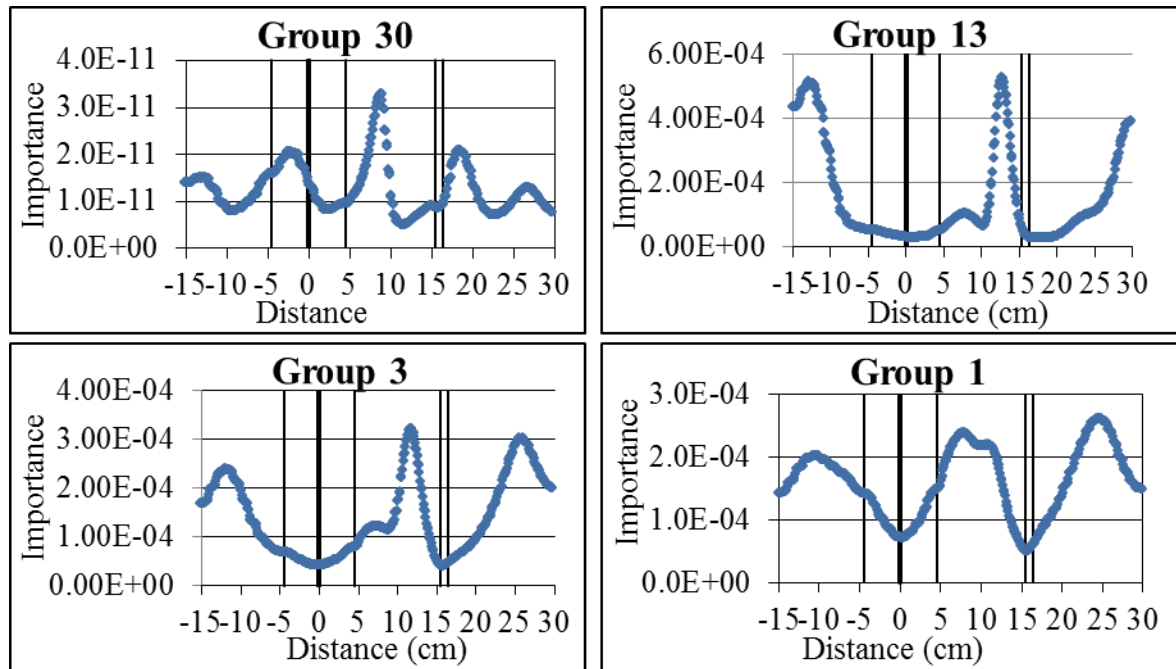


Figure 5.6. Block I adjoint importances along the source box surface 30 cm away from detector surface at center height. The vertical lines represent the detector block separations and collimation.

Figure 5.6 shows how the adjoint importances change moving along the source box surface, but in order to get a true sense of how these importances relate based on group is shown by Figure 5.7. Upon inspecting Figure 5.6, it looks as if there are significant contributions from group 1 neutrons in the detectors, but this is certainly not the case. Plotting all four groups on the same scale, it can be seen that most of the neutron contributions come from lower group numbers (higher energies). In fact, group

30 neutrons are viewed as less important by the He-3 detectors by seven orders of magnitude from group 1 neutrons. From analyzing all 30 energy groups, I found that the groups with the greatest efficiencies were, in descending order: 4, 7, 3, 6, 8, and 5. Group 4 represents neutron energies from 1.5 to 3 MeV, ideal for capturing leaking fission neutrons.

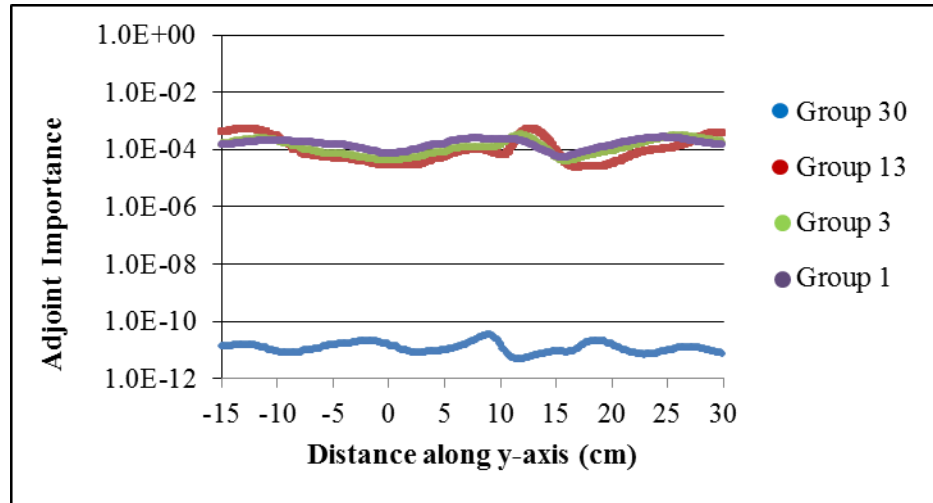


Figure 5.7. Block I adjoint importances along source box surface 30 cm away from detector surface at center height.

From equation 5.8, the following relationship between the reaction rate and source current and adjoint importance can be made. The adjoint reaction rate in the detector for energy based on leakage current discretized into groups is

$$R = \sum_g J_g \sum_{CM} J_{CM,g}^{adj} \delta A_{CM} \quad (5.10)$$

where R is the reaction rate in the detectors, J_g is the forward current source at the source box surface for a given energy group, $J_{CM,g}^{adj}$ is the adjoint importance for a given coarse mesh and energy group, and δA_{CM} is the surface area normal to the x-axis at a given course mesh.

As described in the Source Book, the leakages are given per each entire source box side. However, for our adjoint model, I only included a centralized section of the source plane. Figure 5.8 shows the projected section that is included in the adjoint model. Because of this I could not use the total leakage through the surface, and instead weighted this value with the spatial distribution of the leakage to find the approximate number of neutrons leaking through the appropriate portion of the source box surface.

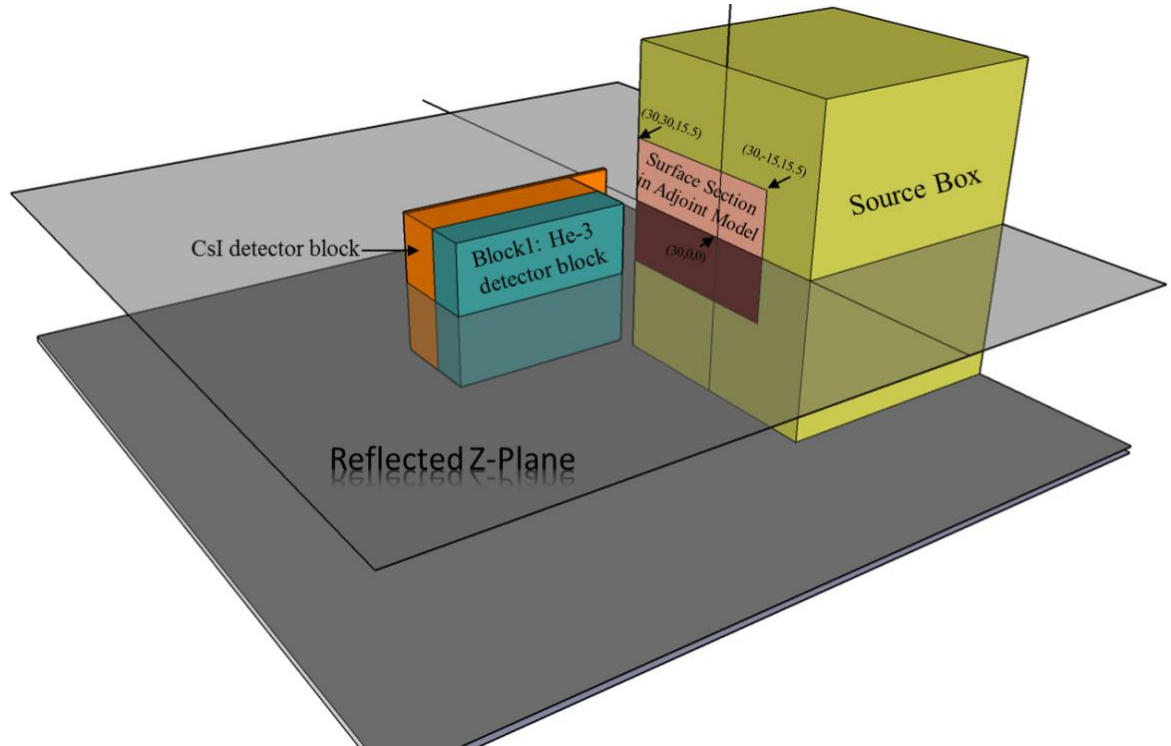
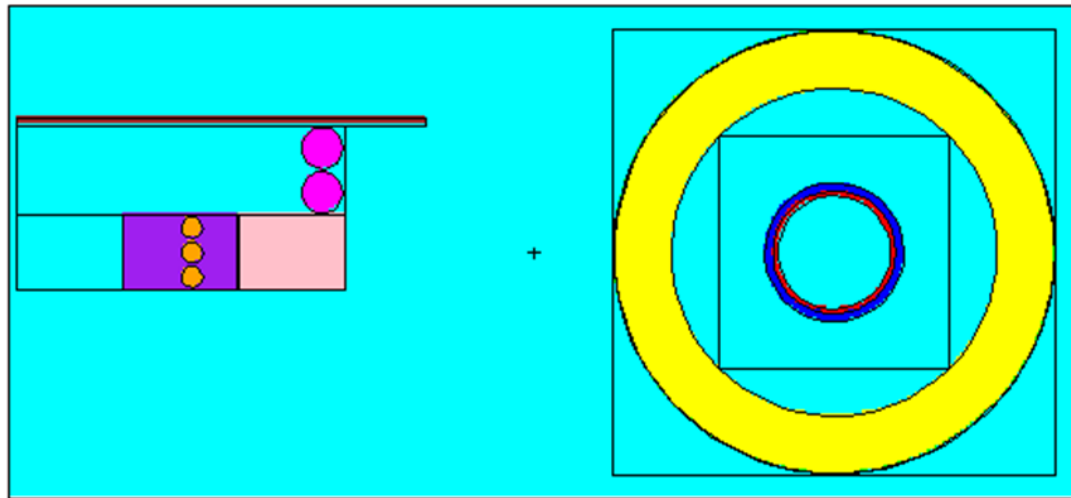


Figure 5.8. Visualization of the section that the adjoint model includes from the source box.

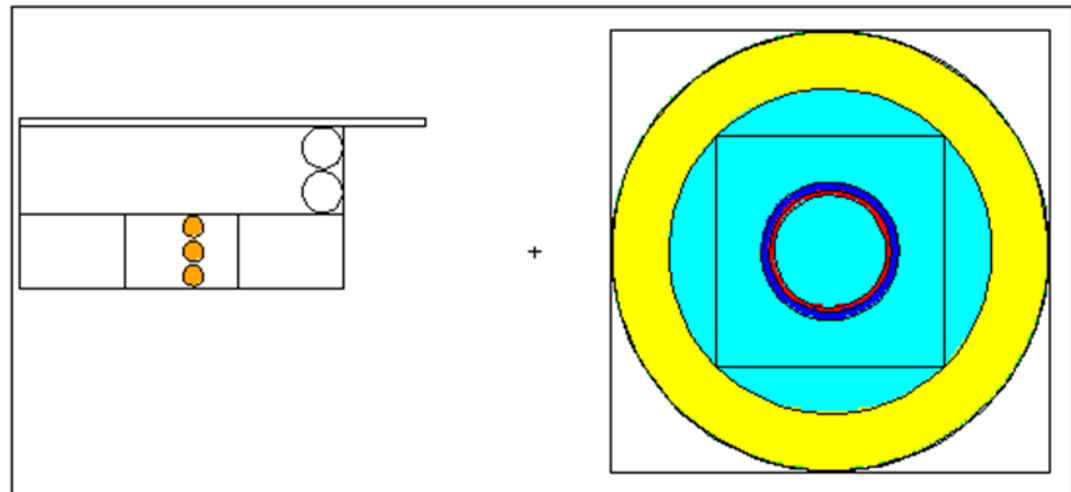
The area of the source box seen in the model is only 15.1% of the total source box side (light pink area in Figure 5.8 over the entire source box side area), but taking into account the spatial distribution of the neutron source, 20.8% of the total number of neutrons leaking from the surface are in this region (area of the block) for the WGPu shell source. Applying Eq. (5.10), I found that the reaction rate in the He-3 detectors was ~ 2.3 n/s. Due to a reflected z-plane boundary in the model, this result is actually for the

entire Block 1 He-3 detectors. This low count fraction is consistent with the results found in the T-SADS work. The average neutron energy at the source box surface that creates a reaction in the He-3 detectors ranges from 3-4 MeV. This is consistent with the design specifications of Block I (again, optimized from previous research). The neutron block could be time gated with multiple sets of detector blocks in the train, and it is important to note that the Block I design is not sensitive to thermal neutrons, and is collimated with Cd; I note that the added presence of cadmium in this Block I detector set increased the relative level of scattering and interaction in the detector at higher energies, and this increased the sensitivity for high energy neutrons, and lowered the Block1 average adjoint weighted neutron energy.

I also looked at the fraction of the neutron uncollided flux in the three He-3 detectors for the 22.5 year WG⁹⁰Pu shell case. I created two models in MCNP5, shown in Figure 5.9: one looking at the collided neutron flux in the detectors and the other looking at the uncollided flux in the detectors. I note that for the uncollided models, all materials outside of the source container and detectors were set to a void space.



(a)



(b)

Figure 5.9. a.) Block I detector model for collided neutrons in MCNP5. b.) Block I detector model for uncollided neutrons in MCNP5.

The uncollided fraction was calculated by dividing the uncollided neutron flux in the detectors by the total neutron flux in the detector (both collided and uncollided). Table 5.1 shows the results per energy group. The fraction of uncollided neutrons decreases as energy group increases (energy decreases) since this block was designed to greatly slow down fast neutrons by subjecting them to materials with high probabilities of

collisions. Since there are a large number of fast neutrons leaking from the source box, a low uncollided fraction is necessary in the higher energy groups to ensure that these are the neutrons being detected. My results show that this is true, and that this detector block will perform as designed and shown in the adjoint calculations.

Table 5.1. Uncollided fraction of neutrons in the He-3 detectors per forward energy group.

Group	Uncollided Fraction	Group	Uncollided Fraction	Group	Uncollided Fraction
1	0.91	17	0.96	33	0.76
2	0.94	18	0.95	34	0.71
3	0.95	19	0.95	35	0.66
4	0.96	20	0.94	36	0.60
5	0.96	21	0.94	37	0.53
6	0.96	22	0.93	38	0.44
7	0.97	23	0.92	39	0.40
8	0.98	24	0.92	40	0.33
9	0.98	25	0.90	41	0.27
10	0.98	26	0.88	42	0.20
11	0.97	27	0.86	43	0.17
12	0.98	28	0.83	44	0.14
13	0.97	29	0.79	45	0.12
14	0.97	30	0.77	46	0.07
15	0.97	31	0.79	47	0.02
16	0.97	32	0.78	Total	0.91

Detector Block III

Figure 5.10 shows neutron detector Block III paired with the CsI gamma detector block. As in the Block I case, 1mm thick cadmium metal is used to separate blocks and reduce leakage from one block into the other. Block III was designed to detect neutrons on the order of 100 keV. The neutrons were slowed down by including layers of indium and tantalum along with poly in between the detectors and detector block surface.

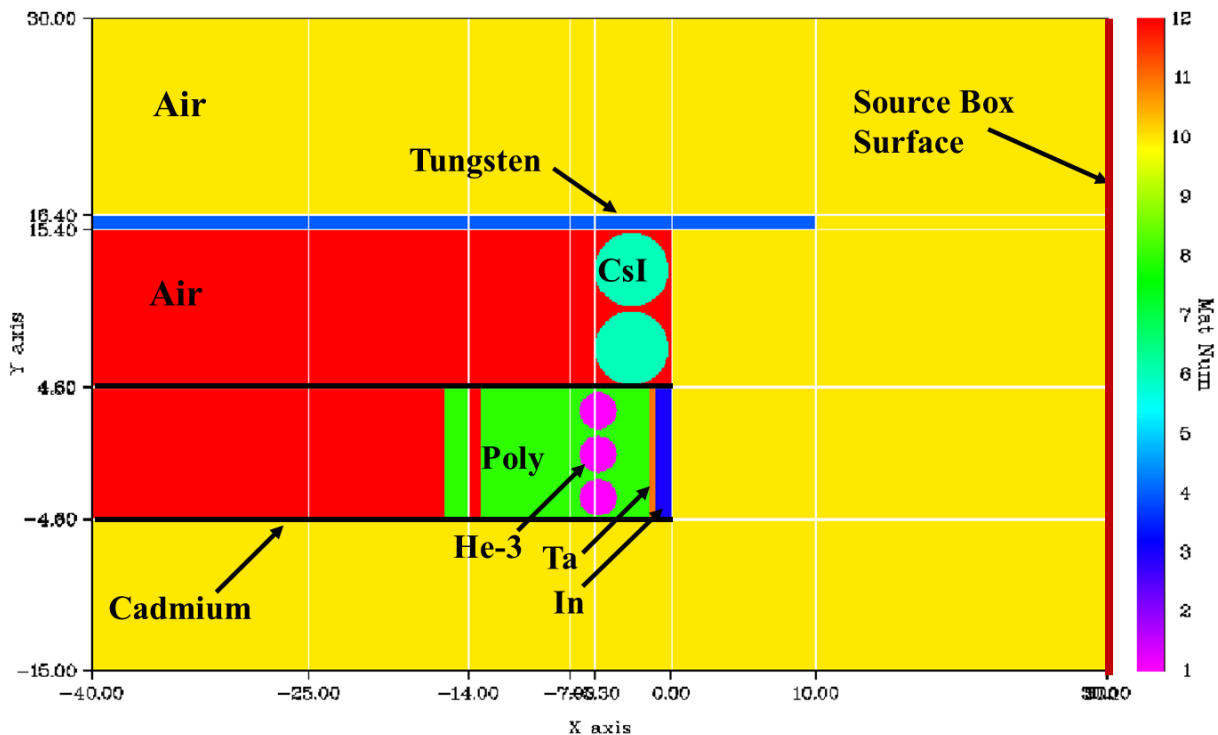


Figure 5.10. Block III of the neutron detector assembly and gamma detector block model in PENTRAN.

As in the analysis of detector Block I, the adjoint importances were computed using a 30 energy group library with neutron upscattering. Figure 5.11 shows the adjoint importance plots for the same four groups seen for Block I in Figure 5.4.

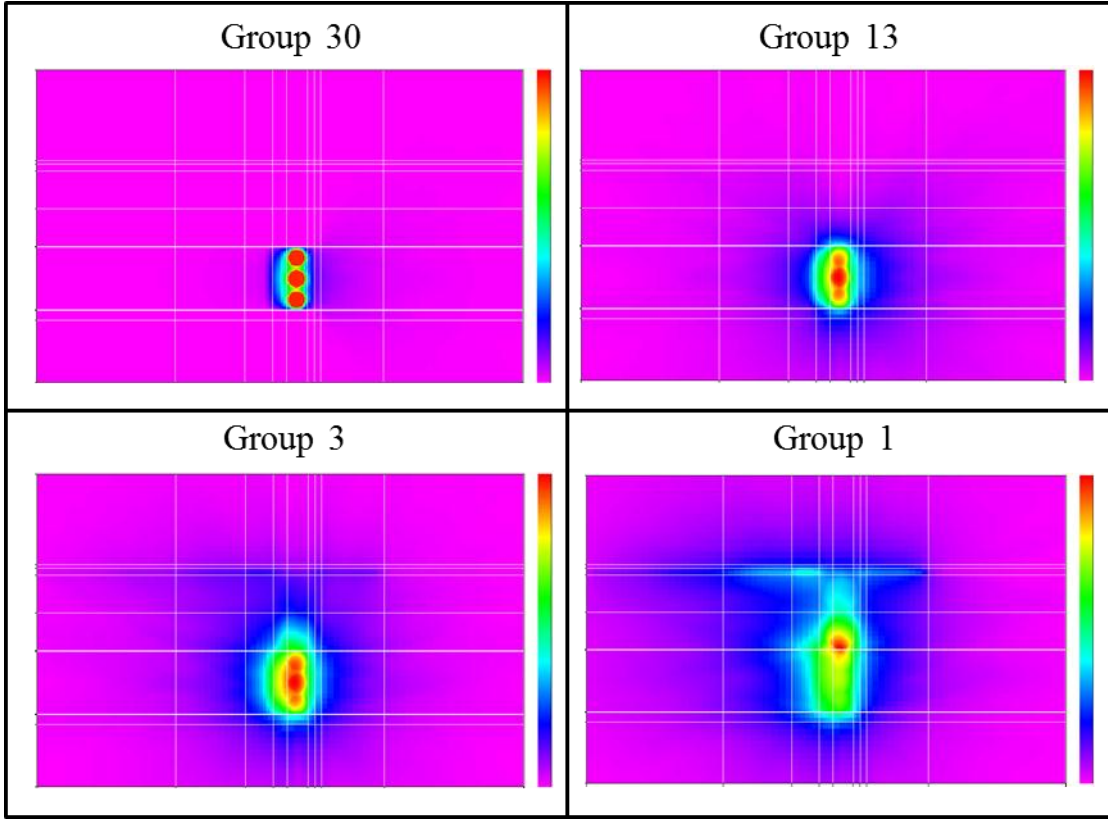


Figure 5.11. Block III adjoint importances for “forward” groups 30 ($<1 \times 10^{-10}$ MeV ceiling/floor (1.0/0.0), 13 ($1.3 \times 10^{-6} - 3.05 \times 10^{-6}$ MeV ceiling/floor (0.58/0.0), 3 (3.0 – 8.19 MeV ceiling/floor ($6.7 \times 10^{-2}/4.0 \times 10^{-5}$), and 1 (17.3 – 20 MeV ceiling/floor ($1.3 \times 10^{-2}/4.8 \times 10^{-5}$) at center height of Source Box.

The plots in Figure 5.12 differ from Figure 5.5 in that the higher groups (lower energies) seem to be more easily detected by the detectors and lower groups (higher energies) have very little chance of creating interacting with the detectors. This is consistent with the design of the detector blocks and what is expected. The lower group neutrons are practically undetectable (importances $< 5 \times 10^{-5}$) when leaking from the source box surface. Group 30 is interesting to note because it is clearly shown that the adjoint importances drop off in the CsI gamma detector material and in its surrounding air. Neutrons interacting with CsI do not result in large energy losses like those in air and poly, but the CsI is directly next to Cd, very thin and very good at scattering at energies

well above thermal. It is likely that if a neutron reaches the CsI region, it has a great chance of being scattered back into a region of air or poly where it can sustain more energy losses before scattering into the detector region. Tungsten is also has large scattering cross section, therefore neutrons have a better chance of being scattered back and forth in the region of air between the cadmium and tungsten, giving it a greater chance to interact with the low atomic mass elements in air and scattering down to undetectable energies. The higher energy neutrons starting at far distances from the He-3 detectors have little chance of slowing down to detectable energies.

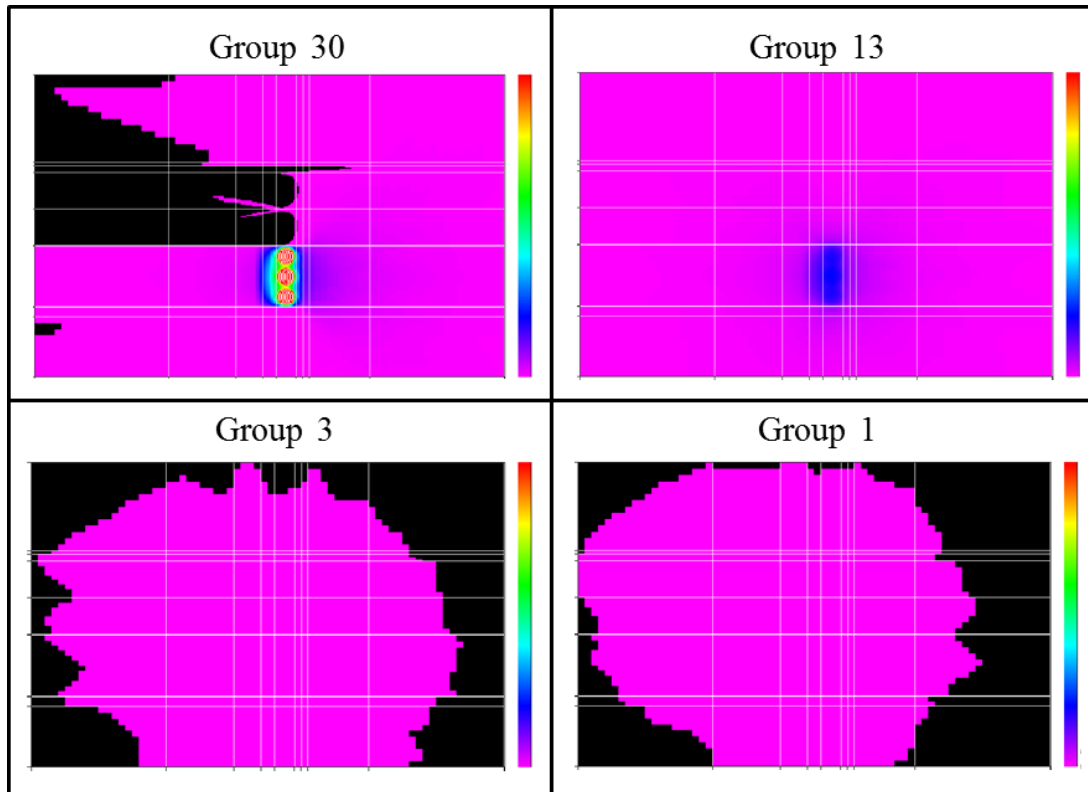


Figure 5.12. Block III adjoint importances for “forward” group 30 (thermal, $< 1 \times 10^{-10}$ MeV), group 13 (epithermal, $1.3 \times 10^{-6} - 3.05 \times 10^{-6}$ MeV), group 3 (fast, $3.0 - 8.19$ MeV), and 1 (high energy, $17.3 - 20$ MeV) sliced at center height of the Source Box.

The color map scaling is identical for all four plots. The ceiling and floor importances were 1.0 and 5×10^{-6} respectively.

Figure 5.13 shows the adjoint importances along the source box surface for each group's scaling. This shows how the location along the source box determines the likelihood of an interaction taking place in the detectors. The center of each He-3 detector is at 0 cm along the surface. Looking at group 30, there is a peak in the adjoint importance with the importance decreasing as the distance along the surface increases. This is consistent with what is known about neutron interactions in air. In order for high energy neutrons to reach the detectors they must have very few scattering interactions in air, therefore, they would most likely stream directly from the source box to the detector surface. The detector was designed to slow down higher energy neutrons at its front face, where neutrons are thermalized, resulting in the importance peak at 0 cm. Using the same logic, a depression occurs at 0 cm for lower energy neutrons. The lower energy neutrons are already closer to thermal energies and do not need to go through as many scattering interactions. The lower energy neutrons hitting the front face of the detector along the 0 cm distance will interact with the Ta, In and Poly and scatter down close to ~0 eV before they have the chance to interact with the detectors. Therefore, it is unlikely for low energy neutrons to begin at 0 cm along the source box surface and interact with the Block III detectors.

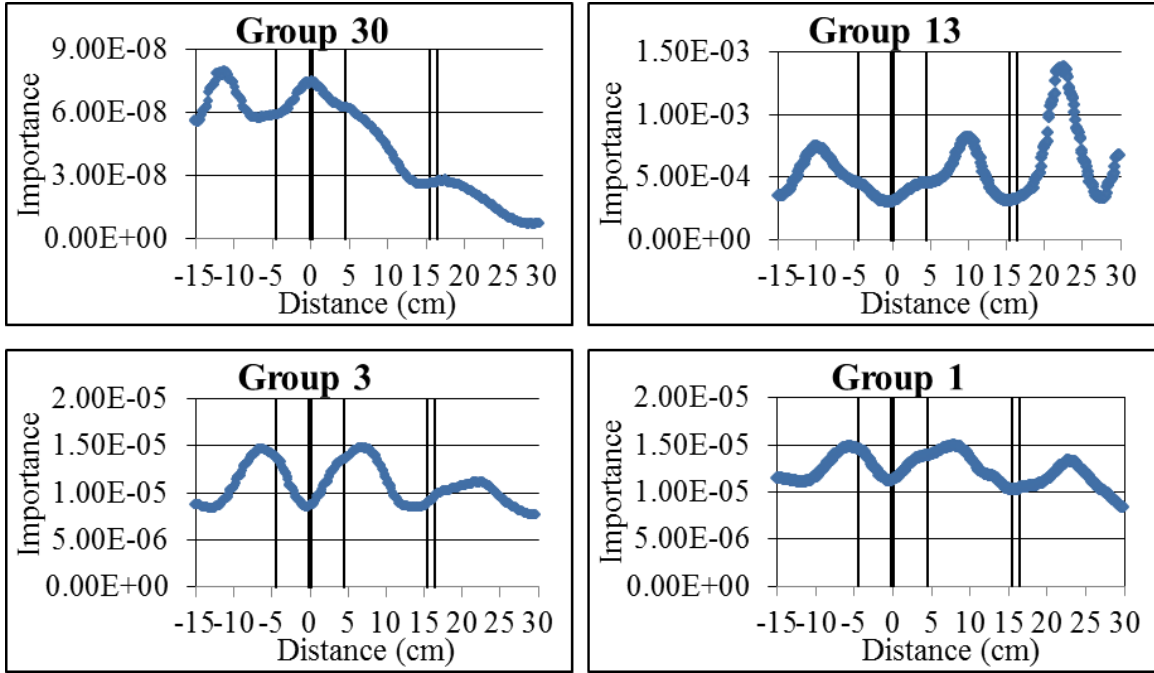


Figure 5.13. Block III adjoint importances along source box surface 30 cm away from Block III detector surface at center height. The vertical lines represent the detector Block III separations and collimation.

Figure 5.14 shows the adjoint importances of these groups on the same scale. As expected, it is noted that the detectors have higher detection efficiencies for some groups over others. Therefore, it is unlikely that neutrons in group 30 at the source box surface have little chance of interaction with the detector. Out of the four groups shown, group 13 has highest interaction probability in the neutron detectors by a few orders of magnitude over groups 3 and 1. From examining the entire neutron energy range, it is seen that neutron group with the highest efficiency is forward group 7 (0.27 to 0.75 MeV) for this block.

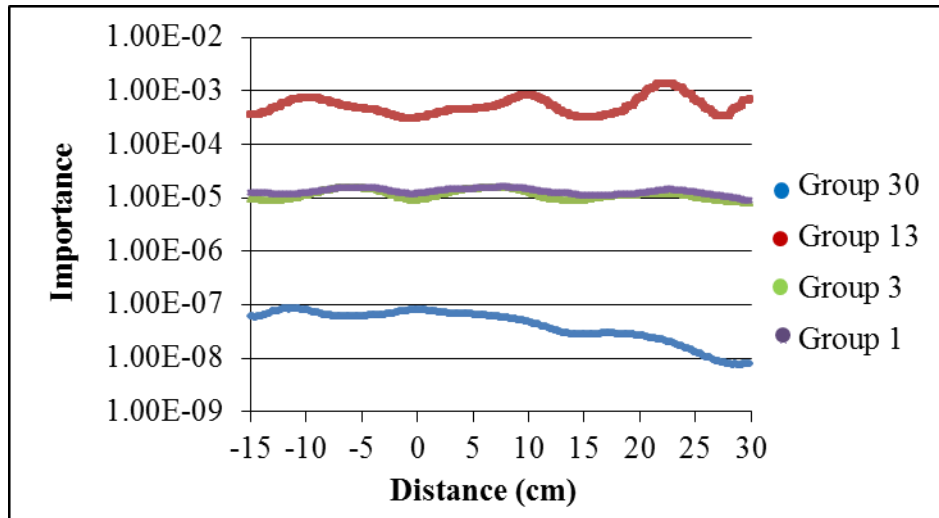


Figure 5.14. Block III adjoint importances along source box surface 30 cm away from the detector surface at center height. Group numbers refer to forward group

From the same response rate procedure as described in the previous section, and using equation 5.10, the response rate in detector Block III is ~ 1.03 n/s. The average neutron energies seen by the detector are in the range of 100 – 200 keV.

Detector Block V

Figure 5.15 shows neutron detector Block V paired with the CsI gamma detector block. As in the previous cases, 1mm cadmium is used to separate blocks and reduce leakage from one block into the other. Block V was designed to detect neutrons on the order of 10^2 eV. Since the neutron energy of interest is close to the thermal range, little shielding was used to slow the neutrons down to thermal energies. Only a thin strip of Dow Foam and poly surrounding the He-3 detectors was necessary.

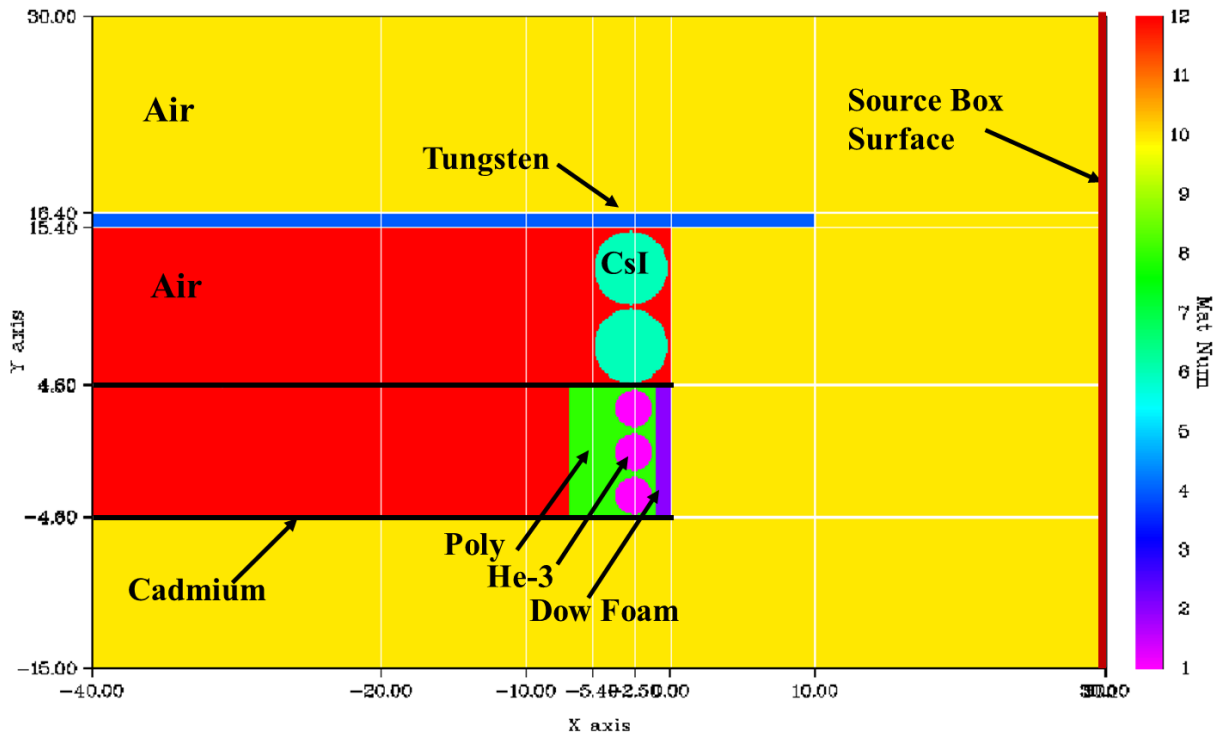


Figure 5.15. Block V of the neutron detector assembly and gamma detector block model in PENTRAN.

Following the same procedure as in the analysis of detector blocks I and III, the adjoint importances using a 30 energy group library with neutron upscattering were determined and plotted. Figure 5.16 shows the adjoint importance plots for the same four groups seen for Blocks I and III analysis.

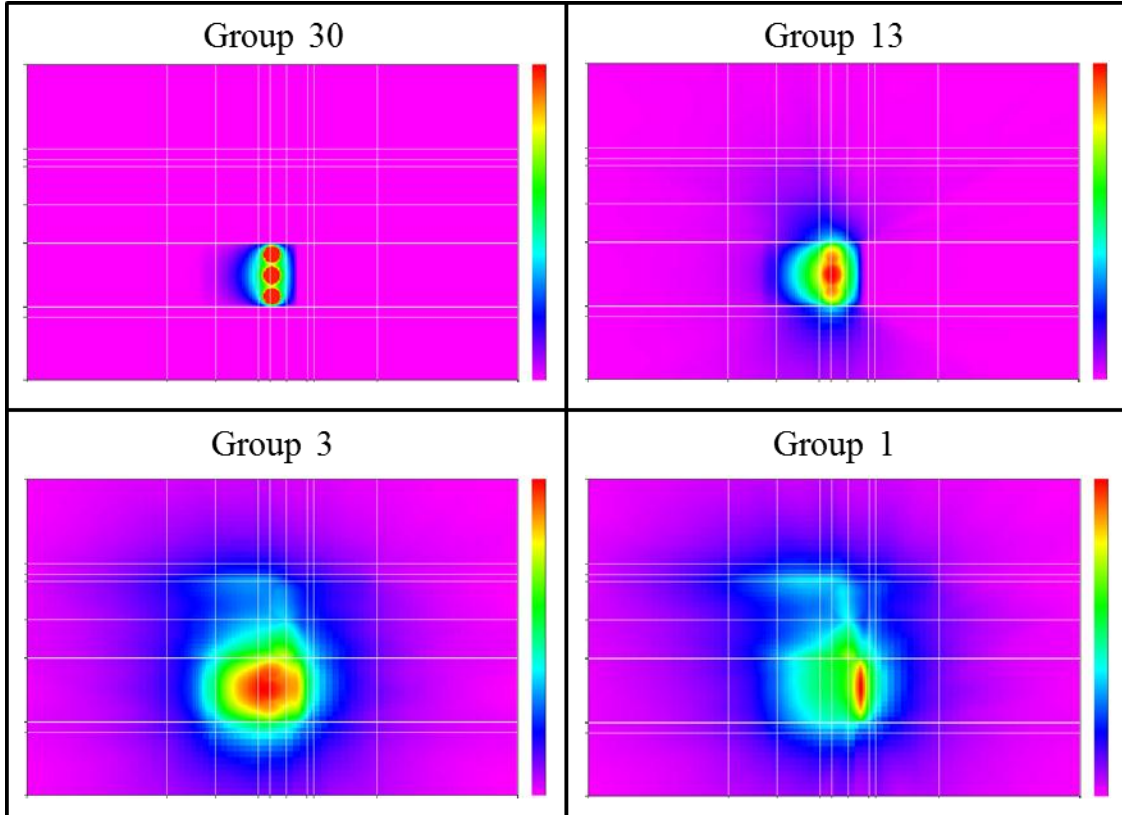


Figure 5.16. Block V adjoint importances for “forward” groups 30 ($<1 \times 10^{-10}$ MeV) ceiling/floor (1.0/0.0), 13 ($1.3 \times 10^{-6} - 3.05 \times 10^{-6}$ MeV) ceiling/floor (0.58/0.0), 3 (3.0 – 8.19 MeV) ceiling/floor ($6.7 \times 10^{-2}/4.0 \times 10^{-5}$), and 1 (17.3 – 20 MeV) ceiling/floor ($1.3 \times 10^2/4.8 \times 10^5$) at center height of Source Box.

Once again, Figure 5.16 only tells a limited amount of information. To get a better understanding of how the adjoint importances relate on a group by group basis, figure 5.17 was created. Here, it is seen that there is no clear difference between groups 13, 3, and 1, but it is highly unlikely that the detectors interact with group 30 neutrons at the surface of the source box. I investigated more carefully the remaining energy groups, and saw that these four chosen groups are not the best suited for showing how the detection efficiencies change with energy.

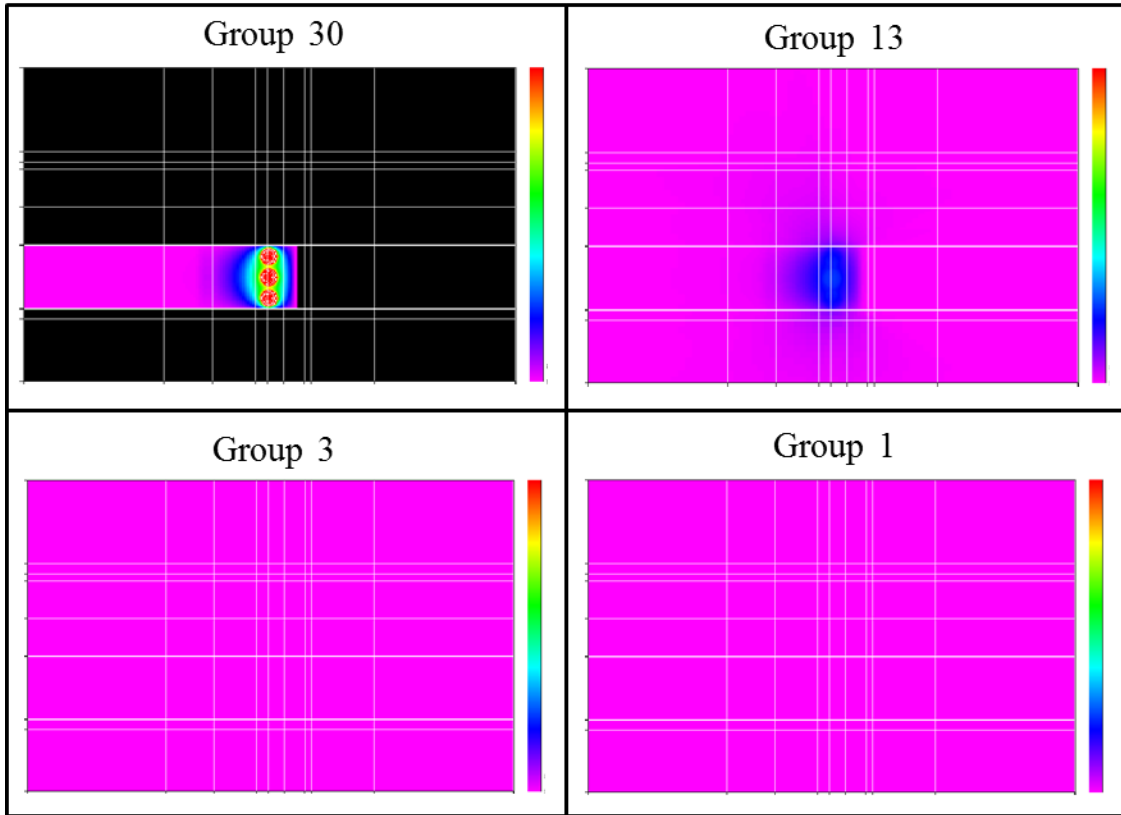


Figure 5.17. Block V adjoint importances for “forward” group 30 (thermal, $< 1 \times 10^{-10}$ MeV), group 13 (epithermal, $1.3 \times 10^{-6} – 3.05 \times 10^{-6}$ MeV), group 3 (fast, $3.0 – 8.19$ MeV), and 1 (high energy, $17.3 – 20$ MeV) sliced at center height of the Source Box.

The color map scaling is identical for all four plots. The ceiling and floor importances were 1.0 and 5×10^{-6} respectively.

Group 30 sticks out in that thermal neutrons have a very unlikely chance of interacting with the neutron detectors if born outside of the detector block. If born inside the air region inside the Block V detector there is a chance the neutron can stream to the detector without large energy loss collisions. The region of air outside the detector is large so neutrons born farther away have an increased probability of interacting with air and losing all energy. Those born closer to the detector have very little chance of escaping through the cadmium shielding due to its large scattering cross section. Group 30 neutrons also have little chance of penetrating through the Dow Foam directly in front

of the detector since it results large energy losses for neutrons during collisions. Groups 3 and 1 show little differentiation in adjoint importance across the plot indicating that for high neutron energies there is little discrimination from neutrons born far from the detector from those born close. This is not troubling since the reaction rates are still very low in the detector at these energies.

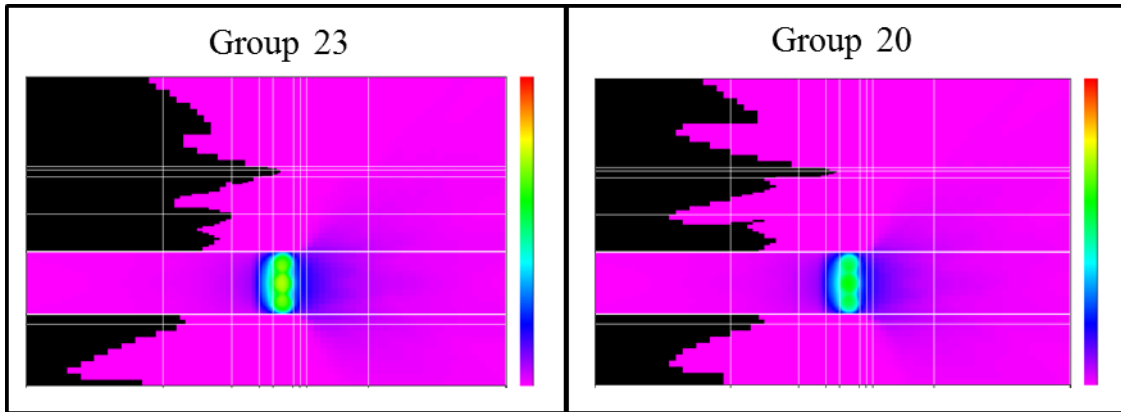


Figure 5.18. Block V adjoint importances for “forward” group 23 (thermal, $3 \times 10^{-8} - 4 \times 10^{-8}$), and group 20 (thermal, $7 \times 10^{-8} - 1 \times 10^{-7}$) sliced at center height of the Source Box. The color map scaling is identical for both plots. The ceiling and floor importances were 1.0 and 5×10^{-6} respectively.

Looking at additional energy groups shows that there is some definition between regions of low importance to regions of higher importance. Figure 15.18 shows a clear field of view for neutrons with energies in groups 23 and 20. The Dow Foam provides the right amount of shielding to thermalize them further down to detectable energies without too many scatters that could displace them outside of the He-3 region. Moving towards the back of the detector block, it is seen that the importances dramatically drop off. This again, is due to the cadmium shielding surrounding Block V. Group 23 and group 20 neutrons have high probability of scattering around in the cadmium shielding to the point where neutrons have low energies. If energy does remain, there is also the

chance of it interacting with the hydrogen in air and scattering down to near zero energy before reaching the He-3 detectors. Therefore, this is an exceptionally well designed detector block that can be used optimally for time gating and collecting groups 23 and 20 neutrons.

Figure 5.19 shows the adjoint importances along the source box surface for each group's scaling. This shows how the location along the source box determines the likelihood of an interaction taking place in the detectors. The center of the He-3 detectors is at distance 0 cm along the surface. It is seen in Figure 5.18 that if the efficiency drops at distance equals 0 cm for the lower groups (higher energies). The higher energy neutrons that stream to the front surface of the detector block cannot thermalize to detectable energies in the 1cm thick Dow Foam and small volume of Poly. Only neutrons with low energies are able to stream to the detector block surface and thermalize.

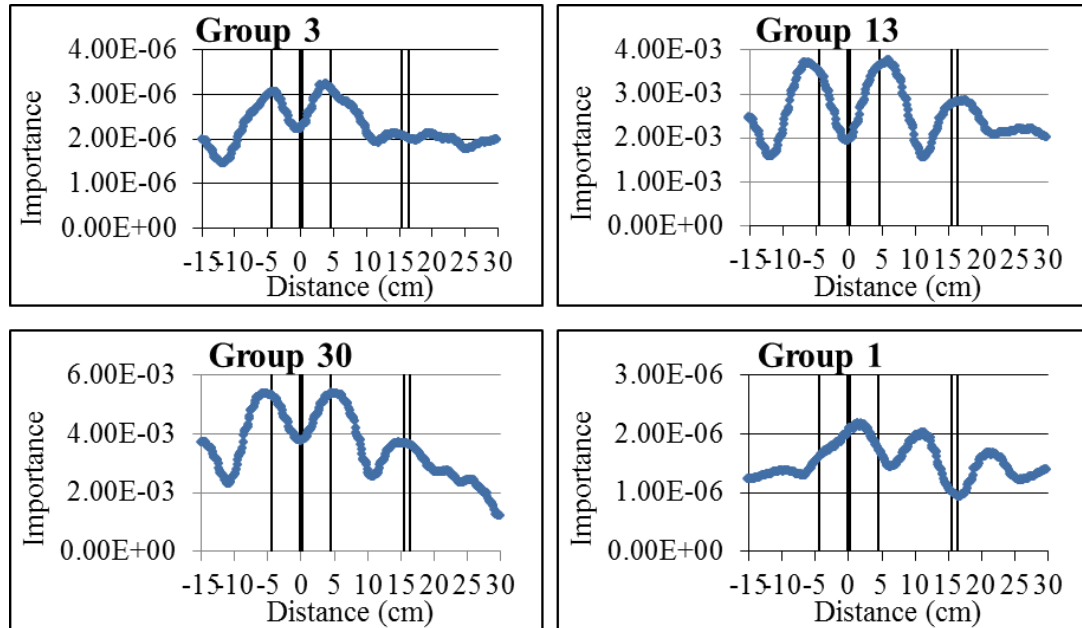


Figure 5.19. Block V adjoint importances along source box surface 30 cm away from detector surface at center height. The vertical lines represent the detector block separations and collimation.

Figure 5.20 shows these same importances from Figure 5.19 plotted on the same scale. It was found that the six energy groups with the greatest responses were, in descending order: 11, 8, 10, 12, 7, and 9. Note that group 11 is the energy range from 37 eV to 0.155 keV.

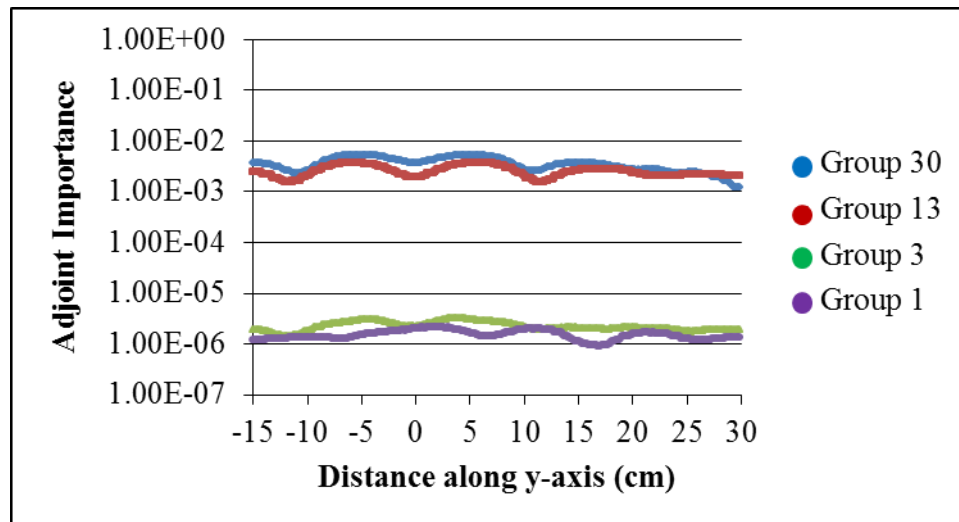


Figure 5.20. Block V adjoint importances along source box surface 30 cm away from detector surface at center height.

From the same response rate procedure as described in the previous section, and using equation 5.10, the response rate in detector Block V for the 8kg WGpu shell source is ~ 0.66 n/s. The average neutron energies seen by the detector are in the range of 0.5 – 1 keV. An item that should be noticed is that the group with the greatest response is not the group with the greatest adjoint importance. This phenomenon is a result of the spectrum leaking from the source box surface. Referring back to the neutron spectrum shown in Figure 5.1, it is seen that the contribution of neutrons leaking at energies less than 1×10^{-5} is very small in comparison to neutrons leaking with substantially higher energies. This has a significant impact on the reaction rate. The average energy seen in the detector is also skewed towards energies higher than the group with the greatest

adjoint importances because the neutron leakages through the weapons pit containers (neutrons per second) for the high energies (groups 1 to 10) were 2 to 8 orders of magnitude greater than those of the lower energies (groups 11 to 30) while the low energy group's adjoint importances were only a few orders of magnitude less than the importances at high energies. Therefore, Block V is not a reliable detector on its own, since it could have interference from the abundance of high energy neutrons leaking from the adjacent WGPu sources. It is necessary to utilize all detectors to achieve a signature that is not only representative of WGPu, but also discriminate between separated sources. For a 22.5 year WGPu shell weapons pit, the ratio of the signals recorded in the detector blocks should be approximately 7:3:2 for blocks I, III, and V respectively. This is consistent with what is known from Figure 5.1, which shows the greatest amount of neutrons leaking out of the source box have high energies.

CHAPTER 6

CONCLUSIONS

The MPVS design was based, in part, on my efforts on methods for detection of HEU and WGPu from gamma and neutron signatures. This system utilized new protocols for the passive detection of SNM that will aid in the reasonably rapid verification and validation of weapons stockpile storage SNM. I was able to verify the new protocol presented by Sjoden, et al, by investigating the gamma leakages through the surface of the weapons pit container, and by matching the energy grouping to follow the published ratios. This shows that this protocol is effective for passive detection for both presence and age since separation HEU verification. The WGPu signature was analyzed, and I presented for a hybrid approach for WGPu that utilizes both gamma and neutron signatures. For my contribution to the MPVS project, I examined the response rates noted in the neutron detectors for a few different neutron energy ranges that would be indicative of WGPu. My end results showed that the neutron detector blocks performed as designed for this application, discriminating between energy ranges by providing counts for neutrons leaking from the weapons canisters at the desired energies. The ratio of the signals recorded in the detector blocks was approximately 7:3:2 for block designs I, III, and V respectively, emphasizing the importance of detecting neutron leakage from high energies for a 22.5 year WGPu shell source.

I put forth additional efforts to create a comprehensive Source Book detailing the gamma and neutron leakages through the weapons pit container for a variety of SNM types, ages, and configurations. This is a useful guide for anyone wishing to model SNM for future studies. The Source Book is a valuable resource which will save up to months of modeling and data analysis by allowing the researcher to directly input leakage

signatures into a transport model. There is no other known guide that includes both HEU and WGPu for multiple ages since separation and SQ masses.

The signatures I analyzed leaking through the source canisters will play an integral part in the time gating and collimation studies for the MPVS. Without this work, optimal detection limits and the detector design would be much more difficult. The work presented here on the passive verification and age dating for HEU and WGPu has the potential to change the way researchers and inspectors study and validate the presence of SNM for stockpile storage. In many cases, it may remove the need for additional equipment and perceived need for active interrogation, along with the need for expensive high resolution detectors. Overall, the sponsor of this project was impressed with the outcomes of this work, and they have asked for an additional proposal for a Phase II that will build upon many of the results presented here.

APPENDIX A

SOURCE BOOK

Appendix A contains all information necessary for modeling unshielded and shielded particle leakages through the surface of a surrounding 60 cm x 60 cm x 60 cm "Source Box," which surrounds the SNM, SNM cladding, air, Celotex, and a steel drum container for uranium and plutonium weapons pits. Figure A.1 shows how the Source Box is modeled from the original detailed geometry, where in MCNP the interior is voided and particles leaking from the surfaces to simplify modeling, where particle leakages are particle currents at the Source Box surfaces. These were determined from MCNP f1 tallies and particle current data from the PENTRAN output files.

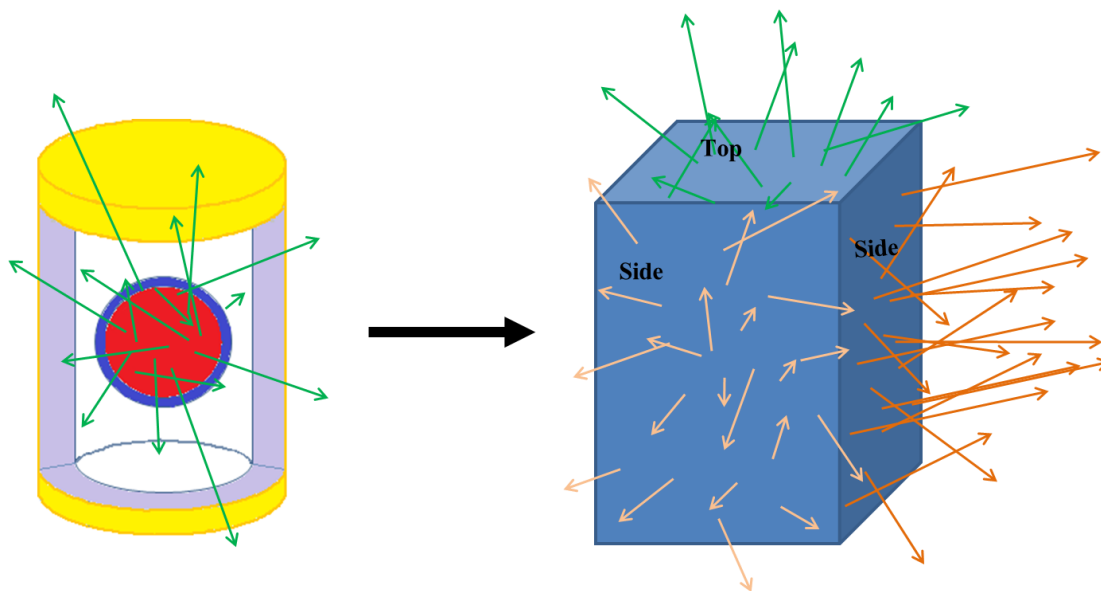


Figure A.1. Visualization of how gammas and neutrons are leaking through the Source Box surfaces. Source Book data is presented as gammas or neutrons leaking through an individual side, top, or bottom of the source box.

The data is organized by shielded or unshielded (Source Box or ORIGEN), type of SNM (HEU or WGPu), geometrical configuration (shell or solid), and type of particle radiation (gamma or neutron). The Source Box particle leakages are organized by energy group, Source Box size (inner or outer), and computational method. Both the leakage and normalized leakage gammas through each Source Box surface are listed in accordance to each energy group in a 24 group structure, while leakage neutrons and normalized leakage neutrons are listed for a 47 and/or 30 group structure. For Pu sources, neutron multiplication is accounted for, as is resulting n-gamma generation, which is significant for the solid configuration. This data can ultimately be used to model simplified sources in MCNP or similar programs. In order to do this more accurately, the spatial dependency of the leaking particles is needed. The spatial dependency is presented in a distributed form similar to that of the particle leakages or normalized leakages. The bare mass based gamma and neutron signatures were produced by ORIGEN on a mass basis (25kg HEU and 8kg WGPu), and are shown in Tables A.42 through A.47 in the Source Book.

APPENDIX A SOURCE BOOK

A.1. 1 year HEU Shell Source Inner Source Box

Side Surfaces		MCNP			PENTRAN		
Group	Energy Bounds (MeV)	Current Leakage (Photons/s)	2 sigma error	Normalized Leakage	Current Leakage (Photons/s)	Normalized Leakage	% difference
24	0 -0.3 **	7.986E+06	0.00%	9.923E-01	3.97E+03	7.560E-02	
23	0.3- 0.741	4.826E+04	0.08%	5.996E-03	3.52E+04	6.701E-01	31.33%
22	0.741- 0.743	6.620E+02	0.66%	8.226E-05	6.55E+02	1.2476E-02	1.06%
21	0.743- 0.765	2.344E+02	1.10%	2.913E-05	2.05E+02	3.9112E-03	13.22%
20	0.765- 0.767	1.438E+03	0.44%	1.787E-04	1.44E+03	2.7343E-02	0.19%
19	0.767- 0.954	3.298E+03	0.30%	4.098E-04	3.10E+03	5.9060E-02	6.15%
18	0.954- 0.956	5.706E+01	2.24%	7.090E-06	5.52E+01	1.0522E-03	3.23%
17	0.956- 0.999	3.749E+02	0.88%	4.658E-05	3.54E+02	6.7507E-03	5.61%
16	0.999- 1.002	5.389E+03	0.24%	6.696E-04	5.40E+03	1.0282E-01	0.17%
15	1.002- 1.18	2.843E+02	1.00%	3.532E-05	2.68E+02	5.1101E-03	5.78%
14	1.18- 1.2	1.097E+02	1.62%	1.363E-05	1.07E+02	2.0473E-03	2.00%
13	1.2- 1.24	8.447E+01	1.84%	1.050E-05	8.17E+01	1.5558E-03	3.35%
12	1.24- 1.26	2.473E+01	3.40%	3.072E-06	2.34E+01	4.4630E-04	5.37%
11	1.26- 1.5	3.633E+02	0.88%	4.514E-05	3.53E+02	6.7216E-03	2.91%
10	1.5- 1.52	1.382E+02	1.44%	1.717E-05	1.40E+02	2.6596E-03	1.03%
9	1.52- 1.736	3.416E+02	0.92%	4.245E-05	3.36E+02	6.4069E-03	1.54%
8	1.736- 1.74	1.964E+02	1.20%	2.440E-05	1.99E+02	3.7952E-03	1.46%
7	1.74- 1.76	3.606E+01	2.82%	4.481E-06	3.48E+01	6.6323E-04	3.50%
6	1.76- 1.83	1.544E+02	1.36%	1.919E-05	1.54E+02	2.9355E-03	0.19%
5	1.83- 1.832	1.528E+02	1.38%	1.898E-05	1.52E+02	2.9036E-03	0.21%
4	1.832- 2.21	2.881E+02	1.00%	3.580E-05	2.93E+02	5.5896E-03	1.84%
3	2.21- 2.25	9.896E-01	17.02%	1.230E-07	1.05E+00	2.0063E-05	6.25%
2	2.25- 2.749	9.968E-01	16.96%	1.239E-07	1.04E+00	1.9891E-05	4.66%
1	2.749- 2.75	9.609E-01	17.28%	1.194E-07	9.84E-01	1.8733E-05	2.33%
Total		8.0482E+06	0.00%		5.2505E+04		

**Lower bound for PENTRAN models was 0.29 MeV

APPENDIX A SOURCE BOOK

A.1. 1 year HEU Shell Source Inner Source Box

Top/Bottom Surfaces		MCNP		
Group	Energy Bounds (MeV)	Current Leakage (Photons/s)	2 sigma error	Normalized Leakage
24	0 -0.3 **	8.05E+06	0.00%	9.92E-01
23	0.3- 0.741	4.83E+04	0.08%	5.96E-03
22	0.741- 0.743	6.600E+02	0.66%	8.14E-05
21	0.743- 0.765	2.346E+02	1.10%	2.89E-05
20	0.765- 0.767	1.444E+03	0.44%	1.78E-04
19	0.767- 0.954	3.296E+03	0.30%	4.07E-04
18	0.954- 0.956	5.667E+01	2.24%	6.99E-06
17	0.956- 0.999	3.731E+02	0.88%	4.60E-05
16	0.999- 1.002	5.381E+03	0.24%	6.64E-04
15	1.002- 1.18	2.831E+02	1.00%	3.49E-05
14	1.18- 1.2	1.082E+02	1.62%	1.33E-05
13	1.2- 1.24	8.440E+01	1.84%	1.04E-05
12	1.24- 1.26	2.569E+01	3.34%	3.17E-06
11	1.26- 1.5	3.647E+02	0.88%	4.50E-05
10	1.5- 1.52	1.401E+02	1.44%	1.73E-05
9	1.52- 1.736	3.388E+02	0.92%	4.18E-05
8	1.736- 1.74	1.998E+02	1.20%	2.46E-05
7	1.74- 1.76	3.461E+01	2.88%	4.27E-06
6	1.76- 1.83	1.532E+02	1.36%	1.89E-05
5	1.83- 1.832	1.517E+02	1.38%	1.87E-05
4	1.832- 2.21	2.908E+02	1.00%	3.59E-05
3	2.21- 2.25	9.537E-01	17.34%	1.18E-07
2	2.25- 2.749	1.327E+00	14.70%	1.64E-07
1	2.749- 2.75	1.004E+00	16.90%	1.24E-07
Total		8.1069E+06	0.00%	

**Lower bound for PENTRAN models was 0.29 MeV

APPENDIX A SOURCE BOOK

A.2. 1 year HEU Shell Source Outer Source Box

Side Surfaces		MCNP	PENTRAN				
Group	Energy Bounds (MeV)	Current Leakage (Photons/s)	2 sigma error	Normalized Leakage	Current Leakage (Photons/s)	Normalized Leakage	% difference
24	0 -0.3 **	7.292E+06	0.00%	9.913E-01	3.237E+03	6.5418E-02	
23	0.3- 0.741	5.054E+04	0.08%	6.871E-03	3.392E+04	6.8541E-01	39.38%
22	0.741- 0.743	6.185E+02	0.68%	8.408E-05	5.634E+02	1.1385E-02	9.33%
21	0.743- 0.765	2.843E+02	1.00%	3.865E-05	2.331E+02	4.7116E-03	19.79%
20	0.765- 0.767	1.349E+03	0.46%	1.834E-04	1.232E+03	2.4907E-02	9.02%
19	0.767- 0.954	3.476E+03	0.28%	4.726E-04	3.016E+03	6.0948E-02	14.19%
18	0.954- 0.956	5.754E+01	2.24%	7.822E-06	5.134E+01	1.0376E-03	11.38%
17	0.956- 0.999	4.237E+02	0.82%	5.759E-05	3.704E+02	7.4859E-03	13.41%
16	0.999- 1.002	5.157E+03	0.24%	7.010E-04	4.777E+03	9.6545E-02	7.64%
15	1.002- 1.18	3.097E+02	0.96%	4.210E-05	2.728E+02	5.5139E-03	12.65%
14	1.18- 1.2	1.095E+02	1.62%	1.489E-05	1.002E+02	2.0243E-03	8.90%
13	1.2- 1.24	8.898E+01	1.80%	1.210E-05	7.964E+01	1.6095E-03	11.08%
12	1.24- 1.26	2.688E+01	3.26%	3.655E-06	2.397E+01	4.8442E-04	11.46%
11	1.26- 1.5	3.887E+02	0.86%	5.284E-05	3.510E+02	7.0934E-03	10.19%
10	1.5- 1.52	1.393E+02	1.44%	1.894E-05	1.312E+02	2.6508E-03	6.02%
9	1.52- 1.736	3.574E+02	0.90%	4.859E-05	3.287E+02	6.6421E-03	8.39%
8	1.736- 1.74	1.985E+02	1.20%	2.698E-05	1.875E+02	3.7887E-03	5.69%
7	1.74- 1.76	3.705E+01	2.78%	5.036E-06	3.352E+01	6.7743E-04	9.99%
6	1.76- 1.83	1.584E+02	1.34%	2.153E-05	1.475E+02	2.9818E-03	7.10%
5	1.83- 1.832	1.534E+02	1.36%	2.085E-05	1.440E+02	2.9111E-03	6.27%
4	1.832- 2.21	2.977E+02	0.98%	4.047E-05	2.827E+02	5.7127E-03	5.18%
3	2.21- 2.25	1.054E+00	16.50%	1.433E-07	1.017E+00	2.0546E-05	3.62%
2	2.25- 2.749	1.025E+00	16.72%	1.394E-07	1.038E+00	2.0976E-05	1.21%
1	2.749- 2.75	1.061E+00	16.44%	1.443E-07	9.618E-01	1.9438E-05	9.84%
Total		7.356E+06	0.00%		4.9482E+04		

**Lower bound for PENTRAN models was 0.29 MeV

APPENDIX A SOURCE BOOK

A.2. 1 year HEU Shell Source Outer Source Box

Top/Bottom Surfaces MCNP

Group	Energy Bounds (MeV)	Current Leakage (Photons/s)	2 sigma error	Normalized Leakage
24	0 -0.3 **	4.23E+06	0.00%	9.91E-01
23	0.3- 0.741	2.89E+04	0.10%	6.77E-03
22	0.741- 0.743	3.474E+02	0.90%	8.14E-05
21	0.743- 0.765	1.586E+02	1.34%	3.71E-05
20	0.765- 0.767	7.571E+02	0.62%	1.77E-04
19	0.767- 0.954	1.946E+03	0.38%	4.56E-04
18	0.954- 0.956	3.156E+01	3.02%	7.39E-06
17	0.956- 0.999	2.339E+02	1.10%	5.48E-05
16	0.999- 1.002	2.895E+03	0.32%	6.78E-04
15	1.002- 1.18	1.733E+02	1.28%	4.06E-05
14	1.18- 1.2	6.165E+01	2.16%	1.44E-05
13	1.2- 1.24	5.002E+01	2.40%	1.17E-05
12	1.24- 1.26	1.601E+01	4.24%	3.75E-06
11	1.26- 1.5	2.161E+02	1.16%	5.06E-05
10	1.5- 1.52	7.846E+01	1.92%	1.84E-05
9	1.52- 1.736	1.983E+02	1.20%	4.64E-05
8	1.736- 1.74	1.123E+02	1.60%	2.63E-05
7	1.74- 1.76	1.976E+01	3.80%	4.63E-06
6	1.76- 1.83	8.764E+01	1.80%	2.05E-05
5	1.83- 1.832	8.455E+01	1.84%	1.98E-05
4	1.832- 2.21	1.661E+02	1.32%	3.89E-05
3	2.21- 2.25	5.091E-01	23.74%	1.19E-07
2	2.25- 2.749	7.816E-01	19.16%	1.83E-07
1	2.749- 2.75	5.737E-01	22.36%	1.34E-07
Total		4.270E+06	0.00%	1.00E+00

**Lower bound for PENTRAN models was 0.29 MeV

APPENDIX A SOURCE BOOK

A.3. 1 year HEU Shell Spatial Distributions at Outer Source Box

TOP/BOTTOM PLANE OF BOX

X-axis distribution

Location (cm)	Normalization
-30	0.000E+00
-24	6.975E-02
-18	9.111E-02
-12	1.044E-01
-6	1.139E-01
0	1.209E-01
6	1.209E-01
12	1.139E-01
18	1.044E-01
24	9.111E-02
30	6.975E-02

Y-axis distribution

Location (cm)	Normalization
-30	0.000E+00
-24	6.975E-02
-18	9.111E-02
-12	1.044E-01
-6	1.139E-01
0	1.209E-01
6	1.209E-01
12	1.139E-01
18	1.044E-01
24	9.111E-02
30	6.975E-02

SIDE PLANES OF BOX

X/Y-axis distribution

Location (cm)	Normalization
-30	0.000E+00
-24	7.032E-02
-18	8.447E-02
-12	1.007E-01
-6	1.168E-01
0	1.277E-01
6	1.277E-01
12	1.168E-01
18	1.007E-01
24	8.447E-02
30	7.032E-02

Z-axis distribution

Location (cm)	Normalization
-38.5	0.000E+00
-33	3.867E-02
-27.5	4.808E-02
-22	5.899E-02
-16.5	7.123E-02
-11	8.425E-02
-5.5	9.584E-02
0	1.029E-01
5.5	1.029E-01
11	9.584E-02
16.5	8.425E-02
22	7.123E-02
27.5	5.899E-02
33	4.808E-02
38.5	3.867E-02

APPENDIX A SOURCE BOOK

A.4. 1 year HEU Solid Source Inner Source Box

Side Surfaces		MCNP		PENTRAN			
Group	Energy Bounds (MeV)	Current Leakage (Photons/s)	2 sigma error	Normalized Leakage	Current Leakage (Photons/s)	Normalized Leakage	% difference
24	0 -0.3 **	1.54E+06	0.02%	9.89E-01	3.676E+06	9.962E-01	
23	0.3- 0.741	1.26E+04	0.14%	8.13E-03	1.024E+04	2.774E-03	-21.1%
22	0.741- 0.743	1.77E+02	1.14%	1.14E-04	1.802E+02	4.882E-05	1.9%
21	0.743- 0.765	7.24E+01	1.78%	4.65E-05	5.955E+01	1.614E-05	-19.4%
20	0.765- 0.767	3.87E+02	0.78%	2.49E-04	3.960E+02	1.073E-04	2.4%
19	0.767- 0.954	9.67E+02	0.48%	6.22E-04	8.908E+02	2.414E-04	-8.3%
18	0.954- 0.956	1.72E+01	3.66%	1.10E-05	1.594E+01	4.320E-06	-7.4%
17	0.956- 0.999	1.16E+02	1.40%	7.45E-05	1.066E+02	2.890E-05	-8.3%
16	0.999- 1.002	1.53E+03	0.38%	9.81E-04	1.544E+03	4.185E-04	1.2%
15	1.002- 1.18	9.45E+01	1.56%	6.08E-05	8.408E+01	2.279E-05	-11.6%
14	1.18- 1.2	3.33E+01	2.62%	2.14E-05	3.237E+01	8.771E-06	-2.9%
13	1.2- 1.24	2.76E+01	2.88%	1.78E-05	2.546E+01	6.900E-06	-8.2%
12	1.24- 1.26	8.42E+00	5.22%	5.42E-06	7.589E+00	2.057E-06	-10.4%
11	1.26- 1.5	1.21E+02	1.38%	7.80E-05	1.135E+02	3.075E-05	-6.7%
10	1.5- 1.52	4.31E+01	2.30%	2.77E-05	4.337E+01	1.175E-05	0.7%
9	1.52- 1.736	1.14E+02	1.42%	7.33E-05	1.084E+02	2.939E-05	-5.0%
8	1.736- 1.74	6.12E+01	1.94%	3.94E-05	6.243E+01	1.692E-05	1.9%
7	1.74- 1.76	1.14E+01	4.48%	7.33E-06	1.114E+01	3.018E-06	-2.3%
6	1.76- 1.83	4.94E+01	2.16%	3.18E-05	4.910E+01	1.330E-05	-0.6%
5	1.83- 1.832	4.80E+01	2.18%	3.09E-05	4.803E+01	1.302E-05	0.1%
4	1.832- 2.21	9.32E+01	1.56%	6.00E-05	9.434E+01	2.557E-05	1.2%
3	2.21- 2.25	3.38E-01	26.04%	2.18E-07	3.394E-01	9.198E-08	0.3%
2	2.25- 2.749	3.10E-01	27.22%	1.99E-07	3.462E-01	9.382E-08	11.1%
1	2.749- 2.75	3.16E-01	26.96%	2.03E-07	3.203E-01	8.680E-08	1.5%
Total		1.55E+06	0.02%		3.690E+06		

**Lower bound for PENTRAN models was 0.29 MeV

APPENDIX A SOURCE BOOK

A.4. 1 year HEU Solid Source Inner Source Box

Top/Bottom Surfaces

MCNP

Group	Energy Bounds (MeV)	Current Leakage (Photons/s)	2 sigma error	Normalized Leakage
24	0 -0.3 **	1.54E+06	0.02%	9.89E-01
23	0.3- 0.741	1.27E+04	0.14%	8.13E-03
22	0.741- 0.743	1.78E+02	1.14%	1.14E-04
21	0.743- 0.765	7.09E+01	1.80%	4.55E-05
20	0.765- 0.767	3.89E+02	0.76%	2.50E-04
19	0.767- 0.954	9.68E+02	0.48%	6.22E-04
18	0.954- 0.956	1.65E+01	3.74%	1.06E-05
17	0.956- 0.999	1.18E+02	1.40%	7.54E-05
16	0.999- 1.002	1.53E+03	0.38%	9.80E-04
15	1.002- 1.18	9.59E+01	1.54%	6.16E-05
14	1.18- 1.2	3.31E+01	2.64%	2.13E-05
13	1.2- 1.24	2.74E+01	2.90%	1.76E-05
12	1.24- 1.26	8.59E+00	5.16%	5.52E-06
11	1.26- 1.5	1.22E+02	1.38%	7.84E-05
10	1.5- 1.52	4.41E+01	2.28%	2.83E-05
9	1.52- 1.736	1.13E+02	1.42%	7.23E-05
8	1.736- 1.74	6.20E+01	1.92%	3.98E-05
7	1.74- 1.76	1.13E+01	4.52%	7.24E-06
6	1.76- 1.83	4.99E+01	2.14%	3.21E-05
5	1.83- 1.832	4.74E+01	2.20%	3.05E-05
4	1.832- 2.21	9.38E+01	1.56%	6.03E-05
3	2.21- 2.25	3.27E-01	26.50%	2.10E-07
2	2.25- 2.749	3.16E-01	26.96%	2.03E-07
1	2.749- 2.75	2.70E-01	29.18%	1.73E-07
Total		1.56E+06	0.02%	

**Lower bound for PENTRAN models was 0.29 MeV

APPENDIX A SOURCE BOOK

A.5. 1 year HEU Solid Source Outer Source Box

Side Surfaces		MCNP			PENTRAN		
Group	Energy Bounds (MeV)	Current Leakage (Photons/s)	2 sigma error	Normalized Leakage	Current Leakage (Photons/s)	Normalized Leakage	% difference
24	0 -0.3 **	1.48E+06	0.02%	9.88E-01	2.805E+06	9.95E-01	
23	0.3- 0.741	1.34E+04	0.14%	8.94E-03	1.004E+04	3.56E-03	28.3%
22	0.741- 0.743	1.67E+02	1.18%	1.12E-04	1.570E+02	5.57E-05	6.1%
21	0.743- 0.765	8.58E+01	1.64%	5.75E-05	6.846E+01	2.43E-05	22.5%
20	0.765- 0.767	3.65E+02	0.80%	2.45E-04	3.442E+02	1.22E-04	5.9%
19	0.767- 0.954	1.02E+03	0.48%	6.86E-04	8.785E+02	3.12E-04	15.4%
18	0.954- 0.956	1.69E+01	3.68%	1.13E-05	1.500E+01	5.32E-06	12.0%
17	0.956- 0.999	1.31E+02	1.32%	8.78E-05	1.123E+02	3.98E-05	15.5%
16	0.999- 1.002	1.47E+03	0.40%	9.83E-04	1.381E+03	4.90E-04	6.0%
15	1.002- 1.18	1.04E+02	1.48%	6.97E-05	8.660E+01	3.07E-05	18.3%
14	1.18- 1.2	3.39E+01	2.60%	2.27E-05	3.052E+01	1.08E-05	10.4%
13	1.2- 1.24	2.89E+01	2.82%	1.93E-05	2.513E+01	8.91E-06	13.9%
12	1.24- 1.26	9.40E+00	4.94%	6.29E-06	7.834E+00	2.78E-06	18.1%
11	1.26- 1.5	1.30E+02	1.32%	8.72E-05	1.139E+02	4.04E-05	13.3%
10	1.5- 1.52	4.39E+01	2.28%	2.94E-05	4.111E+01	1.46E-05	6.6%
9	1.52- 1.736	1.19E+02	1.38%	7.97E-05	1.068E+02	3.79E-05	10.8%
8	1.736- 1.74	6.23E+01	1.92%	4.18E-05	5.921E+01	2.10E-05	5.2%
7	1.74- 1.76	1.18E+01	4.40%	7.93E-06	1.081E+01	3.83E-06	9.1%
6	1.76- 1.83	5.07E+01	2.12%	3.40E-05	4.738E+01	1.68E-05	6.8%
5	1.83- 1.832	4.90E+01	2.16%	3.28E-05	4.574E+01	1.62E-05	7.0%
4	1.832- 2.21	9.71E+01	1.54%	6.50E-05	9.154E+01	3.25E-05	5.9%
3	2.21- 2.25	3.27E-01	26.50%	2.19E-07	3.299E-01	1.17E-07	0.9%
2	2.25- 2.749	3.50E-01	25.60%	2.34E-07	3.463E-01	1.23E-07	1.0%
1	2.749- 2.75	3.79E-01	24.62%	2.54E-07	3.151E-01	1.12E-07	18.3%
Total		1.49E+06	0.02%		2.819E+06		

**Lower bound for PENTRAN models was 0.29 MeV

APPENDIX A SOURCE BOOK

A.5. 1 year HEU Solid Source Outer Source Box

Top/Bottom Surfaces		MCNP		
Group	Energy Bounds (MeV)	Current Leakage (Photons/s)	2 sigma error	Normalized Leakage
24	0 -0.3 **	8.55E+05	0.02%	9.89E-01
23	0.3- 0.741	7.63E+03	0.18%	8.82E-03
22	0.741- 0.743	9.46E+01	1.56%	1.09E-04
21	0.743- 0.765	4.83E+01	2.18%	5.58E-05
20	0.765- 0.767	2.07E+02	1.06%	2.39E-04
19	0.767- 0.954	5.70E+02	0.64%	6.59E-04
18	0.954- 0.956	9.35E+00	4.96%	1.08E-05
17	0.956- 0.999	7.27E+01	1.78%	8.40E-05
16	0.999- 1.002	8.26E+02	0.52%	9.55E-04
15	1.002- 1.18	5.91E+01	1.98%	6.83E-05
14	1.18- 1.2	1.88E+01	3.50%	2.17E-05
13	1.2- 1.24	1.61E+01	3.78%	1.86E-05
12	1.24- 1.26	5.25E+00	6.60%	6.08E-06
11	1.26- 1.5	7.24E+01	1.78%	8.37E-05
10	1.5- 1.52	2.50E+01	3.02%	2.89E-05
9	1.52- 1.736	6.62E+01	1.86%	7.66E-05
8	1.736- 1.74	3.56E+01	2.54%	4.12E-05
7	1.74- 1.76	6.42E+00	5.98%	7.42E-06
6	1.76- 1.83	2.87E+01	2.82%	3.32E-05
5	1.83- 1.832	2.64E+01	2.94%	3.05E-05
4	1.832- 2.21	5.36E+01	2.06%	6.20E-05
3	2.21- 2.25	2.01E-01	33.80%	2.32E-07
2	2.25- 2.749	1.49E-01	39.22%	1.72E-07
1	2.749- 2.75	1.55E-01	38.50%	1.79E-07
Total		8.65E+05	0.02%	

**Lower bound for PENTRAN models was 0.29 MeV

APPENDIX A SOURCE BOOK

A.6. 1 year HEU Solid Spatial Distributions at Outer Source Box

TOP/BOTTOM PLANE OF BOX

X-axis distribution

Location (cm)	Normalization
-30	0.000E+00
-24	6.740E-02
-18	9.096E-02
-12	1.060E-01
-6	1.142E-01
0	1.214E-01
6	1.214E-01
12	1.142E-01
18	1.060E-01
24	9.096E-02
30	6.740E-02

Y-axis distribution

Location (cm)	Normalization
-30	0.000E+00
-24	6.740E-02
-18	9.096E-02
-12	1.060E-01
-6	1.142E-01
0	1.214E-01
6	1.214E-01
12	1.142E-01
18	1.060E-01
24	9.096E-02
30	6.740E-02

SIDE PLANES OF BOX

X/Y-axis distribution

Location (cm)	Normalization
-30	0.000E+00
-24	7.370E-02
-18	8.675E-02
-12	1.013E-01
-6	1.141E-01
0	1.242E-01
6	1.242E-01
12	1.141E-01
18	1.013E-01
24	8.675E-02
30	7.370E-02

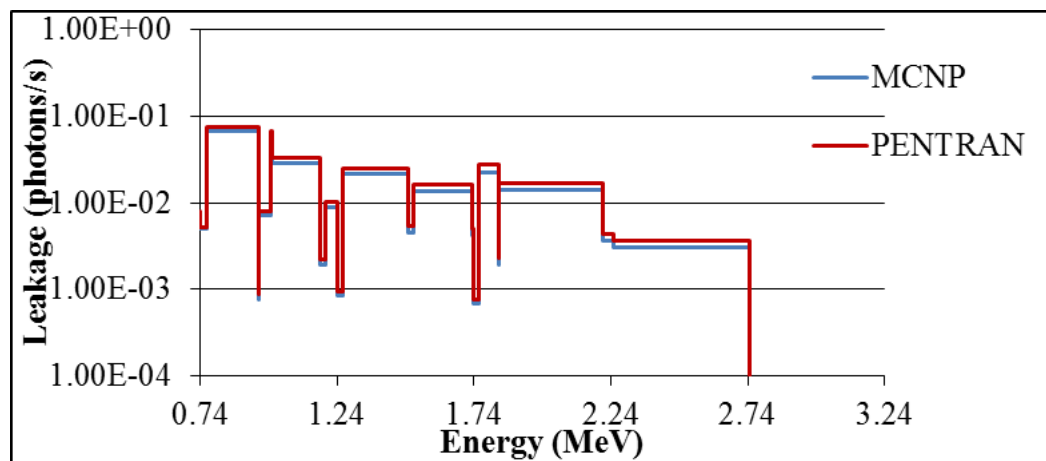
Z-axis distribution

Location (cm)	Normalization
-38.5	0.000E+00
-33	3.646E-02
-27.5	4.646E-02
-22	5.894E-02
-16.5	7.199E-02
-11	8.492E-02
-5.5	9.650E-02
0	1.047E-01
5.5	1.047E-01
11	9.650E-02
16.5	8.492E-02
22	7.199E-02
27.5	5.894E-02
33	4.646E-02
38.5	3.646E-02

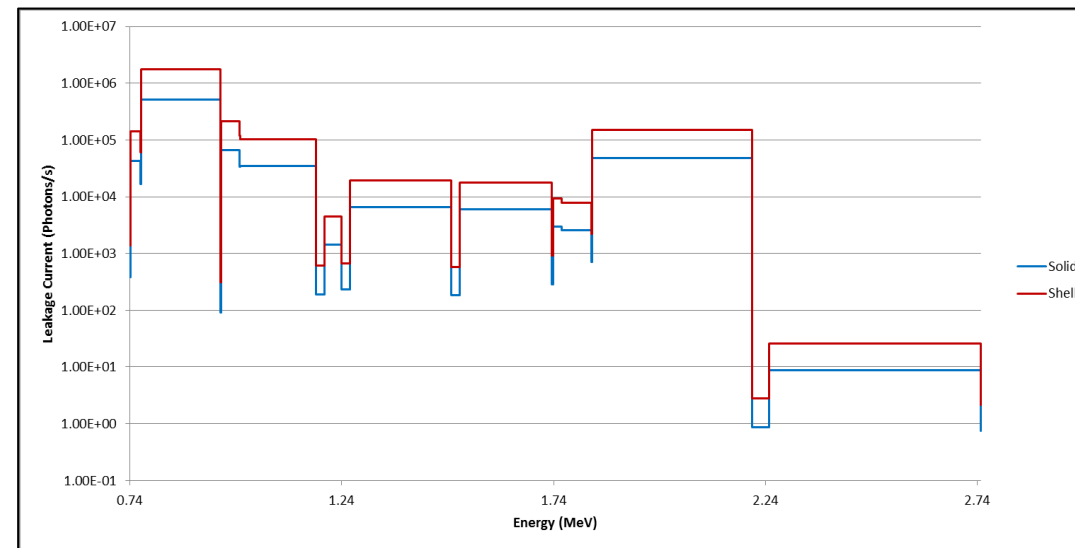
APPENDIX A SOURCE BOOK

Figure. A.2. HEU 1 year Shell Outer Source Box Histograms

Pentran vs. MCNP for 1yr HEU Shell



Solid vs. Shell for 1yr HEU Shell



APPENDIX A SOURCE BOOK

A.7. 22.5 year HEU Shell Source Inner Souce Box

Side Surfaces		MCNP		
Group	Energy Bounds (MeV)	Current Leakage (Photons/s)	2 sigma error	Normalized Leakage
24	0 -0.3 **	7.99E+06	0.00%	9.92E-01
23	0.3- 0.741	5.17E+04	0.08%	6.41E-03
22	0.741- 0.743	6.61E+02	0.66%	8.21E-05
21	0.743- 0.765	2.65E+02	1.04%	3.29E-05
20	0.765- 0.767	1.52E+03	0.44%	1.89E-04
19	0.767- 0.954	3.90E+03	0.28%	4.84E-04
18	0.954- 0.956	5.87E+01	2.22%	7.29E-06
17	0.956- 0.999	4.17E+02	0.82%	5.17E-05
16	0.999- 1.002	5.39E+03	0.24%	6.69E-04
15	1.002- 1.18	7.51E+02	0.62%	9.32E-05
14	1.18- 1.2	1.20E+02	1.54%	1.49E-05
13	1.2- 1.24	2.31E+02	1.12%	2.87E-05
12	1.24- 1.26	3.38E+01	2.92%	4.20E-06
11	1.26- 1.5	6.71E+02	0.66%	8.33E-05
10	1.5- 1.52	1.93E+02	1.22%	2.39E-05
9	1.52- 1.736	5.12E+02	0.74%	6.35E-05
8	1.736- 1.74	2.35E+02	1.10%	2.92E-05
7	1.74- 1.76	3.88E+01	2.72%	4.81E-06
6	1.76- 1.83	5.42E+02	0.72%	6.73E-05
5	1.83- 1.832	1.55E+02	1.36%	1.93E-05
4	1.832- 2.21	4.88E+02	0.76%	6.06E-05
3	2.21- 2.25	6.53E+01	2.10%	8.10E-06
2	2.25- 2.749	5.32E+01	2.32%	6.60E-06
1	2.749- 2.75	9.61E-01	17.28%	1.19E-07
Total		8.06E+06	0.00%	

**Lower bound for PENTRAN models was 0.29 MeV

APPENDIX A SOURCE BOOK

A.7. 22.5 year HEU Shell Source Inner Souce Box

Top/Bottom Surfaces

MCNP

Group	Energy Bounds (MeV)	Current Leakage (Photons/s)	2 sigma error	Normalized Leakage
24	0 -0.3 **	8.05E+06	0.00%	9.92E-01
23	0.3- 0.741	5.17E+04	0.08%	6.37E-03
22	0.741- 0.743	6.60E+02	0.66%	8.14E-05
21	0.743- 0.765	2.63E+02	1.04%	3.25E-05
20	0.765- 0.767	1.52E+03	0.44%	1.87E-04
19	0.767- 0.954	3.90E+03	0.28%	4.81E-04
18	0.954- 0.956	6.00E+01	2.18%	7.39E-06
17	0.956- 0.999	4.16E+02	0.84%	5.12E-05
16	0.999- 1.002	5.39E+03	0.24%	6.64E-04
15	1.002- 1.18	7.48E+02	0.62%	9.21E-05
14	1.18- 1.2	1.20E+02	1.54%	1.48E-05
13	1.2- 1.24	2.30E+02	1.12%	2.83E-05
12	1.24- 1.26	3.42E+01	2.90%	4.21E-06
11	1.26- 1.5	6.72E+02	0.66%	8.28E-05
10	1.5- 1.52	1.93E+02	1.22%	2.38E-05
9	1.52- 1.736	5.10E+02	0.76%	6.28E-05
8	1.736- 1.74	2.34E+02	1.10%	2.88E-05
7	1.74- 1.76	3.91E+01	2.70%	4.82E-06
6	1.76- 1.83	5.44E+02	0.72%	6.70E-05
5	1.83- 1.832	1.56E+02	1.36%	1.92E-05
4	1.832- 2.21	4.87E+02	0.76%	6.01E-05
3	2.21- 2.25	6.56E+01	2.10%	8.08E-06
2	2.25- 2.749	5.50E+01	2.28%	6.77E-06
1	2.749- 2.75	1.00E+00	16.90%	1.24E-07
Total		8.12E+06	0.00%	

**Lower bound for PENTRAN models was 0.29 MeV

APPENDIX A SOURCE BOOK

A.8. 22.5 year HEU Shell Source Outer Source Box

Side Surfaces		MCNP		
Group	Energy Bounds (MeV)	Current Leakage (Photons/s)	2 sigma error	Normalized Leakage
24	0 -0.3 **	7.30E+06	0.00%	9.90E-01
23	0.3- 0.741	5.42E+04	0.08%	7.36E-03
22	0.741- 0.743	6.22E+02	0.68%	8.44E-05
21	0.743- 0.765	3.21E+02	0.94%	4.36E-05
20	0.765- 0.767	1.42E+03	0.44%	1.93E-04
19	0.767- 0.954	4.11E+03	0.26%	5.57E-04
18	0.954- 0.956	5.98E+01	2.18%	8.12E-06
17	0.956- 0.999	4.74E+02	0.78%	6.44E-05
16	0.999- 1.002	5.16E+03	0.24%	7.00E-04
15	1.002- 1.18	7.92E+02	0.60%	1.08E-04
14	1.18- 1.2	1.23E+02	1.52%	1.67E-05
13	1.2- 1.24	2.37E+02	1.10%	3.22E-05
12	1.24- 1.26	3.75E+01	2.76%	5.09E-06
11	1.26- 1.5	7.13E+02	0.64%	9.68E-05
10	1.5- 1.52	1.95E+02	1.22%	2.65E-05
9	1.52- 1.736	5.40E+02	0.72%	7.33E-05
8	1.736- 1.74	2.37E+02	1.10%	3.22E-05
7	1.74- 1.76	4.09E+01	2.64%	5.55E-06
6	1.76- 1.83	5.52E+02	0.72%	7.50E-05
5	1.83- 1.832	1.58E+02	1.34%	2.14E-05
4	1.832- 2.21	5.05E+02	0.76%	6.86E-05
3	2.21- 2.25	6.70E+01	2.06%	9.09E-06
2	2.25- 2.749	5.59E+01	2.26%	7.58E-06
1	2.749- 2.75	1.06E+00	16.44%	1.44E-07
Total		7.37E+06	0.00%	

**Lower bound for PENTRAN models was 0.29 MeV

APPENDIX A SOURCE BOOK

A.8. 22.5 year HEU Shell Source Outer Source Box

Top/Bottom Surfaces		MCNP		
Group	Energy Bounds (MeV)	Current Leakage (Photons/s)	2 sigma error	Normalized Leakage
24	0 -0.3 **	4.24E+06	0.00%	9.91E-01
23	0.3- 0.741	3.10E+04	0.10%	7.25E-03
22	0.741- 0.743	3.49E+02	0.90%	8.17E-05
21	0.743- 0.765	1.79E+02	1.26%	4.18E-05
20	0.765- 0.767	8.01E+02	0.60%	1.87E-04
19	0.767- 0.954	2.30E+03	0.36%	5.38E-04
18	0.954- 0.956	3.43E+01	2.90%	8.02E-06
17	0.956- 0.999	2.62E+02	1.04%	6.13E-05
16	0.999- 1.002	2.90E+03	0.32%	6.78E-04
15	1.002- 1.18	4.42E+02	0.80%	1.03E-04
14	1.18- 1.2	6.84E+01	2.04%	1.60E-05
13	1.2- 1.24	1.31E+02	1.48%	3.07E-05
12	1.24- 1.26	2.17E+01	3.64%	5.08E-06
11	1.26- 1.5	3.98E+02	0.84%	9.32E-05
10	1.5- 1.52	1.10E+02	1.62%	2.57E-05
9	1.52- 1.736	3.01E+02	0.98%	7.05E-05
8	1.736- 1.74	1.31E+02	1.48%	3.07E-05
7	1.74- 1.76	2.29E+01	3.54%	5.36E-06
6	1.76- 1.83	3.09E+02	0.96%	7.22E-05
5	1.83- 1.832	8.78E+01	1.80%	2.05E-05
4	1.832- 2.21	2.78E+02	1.02%	6.50E-05
3	2.21- 2.25	3.74E+01	2.78%	8.74E-06
2	2.25- 2.749	3.21E+01	2.98%	7.51E-06
1	2.749- 2.75	5.74E-01	22.36%	1.34E-07
Total		4.28E+06	0.00%	

**Lower bound for PENTRAN models was 0.29 MeV

APPENDIX A SOURCE BOOK

A.9. 22.5 year HEU Solid Source Inner Source Box

Side Surfaces MCNP

Group	Energy Bounds (MeV)	Current Leakage (Photons/s)	2 sigma error	Normalized Leakage
24	0 -0.3 **	1.54E+06	0.02%	9.88E-01
23	0.3- 0.741	1.36E+04	0.14%	8.71E-03
22	0.741- 0.743	1.77E+02	1.28%	1.14E-04
21	0.743- 0.765	8.21E+01	1.86%	5.27E-05
20	0.765- 0.767	4.10E+02	0.84%	2.63E-04
19	0.767- 0.954	1.15E+03	0.50%	7.37E-04
18	0.954- 0.956	1.71E+01	4.10%	1.10E-05
17	0.956- 0.999	1.32E+02	1.48%	8.45E-05
16	0.999- 1.002	1.53E+03	0.44%	9.81E-04
15	1.002- 1.18	2.40E+02	1.10%	1.54E-04
14	1.18- 1.2	3.81E+01	2.74%	2.45E-05
13	1.2- 1.24	7.23E+01	2.00%	4.64E-05
12	1.24- 1.26	1.16E+01	4.98%	7.46E-06
11	1.26- 1.5	2.22E+02	1.14%	1.42E-04
10	1.5- 1.52	6.16E+01	2.16%	3.96E-05
9	1.52- 1.736	1.73E+02	1.28%	1.11E-04
8	1.736- 1.74	7.32E+01	1.98%	4.70E-05
7	1.74- 1.76	1.31E+01	4.68%	8.44E-06
6	1.76- 1.83	1.74E+02	1.28%	1.12E-04
5	1.83- 1.832	4.86E+01	2.44%	3.12E-05
4	1.832- 2.21	1.60E+02	1.34%	1.03E-04
3	2.21- 2.25	2.13E+01	3.68%	1.37E-05
2	2.25- 2.749	1.73E+01	4.08%	1.11E-05
1	2.749- 2.75	3.01E-01	30.86%	1.93E-07
Total		1.56E+06	0.02%	

**Lower bound for PENTRAN models was 0.29 MeV

APPENDIX A SOURCE BOOK

A.9. 22.5 year HEU Solid Source Inner Source Box

Top/Bottom Surfaces

MCNP

Group	Energy Bounds (MeV)	Current Leakage (Photons/s)	2 sigma error	Normalized Leakage
24	0 -0.3 **	1.54E+06	0.02%	9.88E-01
23	0.3- 0.741	1.36E+04	0.14%	8.70E-03
22	0.741- 0.743	1.79E+02	1.26%	1.15E-04
21	0.743- 0.765	8.11E+01	1.88%	5.20E-05
20	0.765- 0.767	4.09E+02	0.84%	2.62E-04
19	0.767- 0.954	1.15E+03	0.50%	7.36E-04
18	0.954- 0.956	1.76E+01	4.04%	1.13E-05
17	0.956- 0.999	1.32E+02	1.48%	8.47E-05
16	0.999- 1.002	1.53E+03	0.44%	9.80E-04
15	1.002- 1.18	2.39E+02	1.10%	1.53E-04
14	1.18- 1.2	3.82E+01	2.74%	2.45E-05
13	1.2- 1.24	7.33E+01	1.98%	4.70E-05
12	1.24- 1.26	1.20E+01	4.88%	7.70E-06
11	1.26- 1.5	2.24E+02	1.14%	1.44E-04
10	1.5- 1.52	6.04E+01	2.18%	3.88E-05
9	1.52- 1.736	1.72E+02	1.30%	1.10E-04
8	1.736- 1.74	7.25E+01	2.00%	4.65E-05
7	1.74- 1.76	1.31E+01	4.68%	8.39E-06
6	1.76- 1.83	1.73E+02	1.28%	1.11E-04
5	1.83- 1.832	4.91E+01	2.42%	3.15E-05
4	1.832- 2.21	1.58E+02	1.34%	1.01E-04
3	2.21- 2.25	2.07E+01	3.72%	1.33E-05
2	2.25- 2.749	1.80E+01	3.98%	1.16E-05
1	2.749- 2.75	3.01E-01	30.86%	1.93E-07
Total		1.56E+06	0.02%	

**Lower bound for PENTRAN models was 0.29 MeV

APPENDIX A SOURCE BOOK

A.10. 22.5 year HEU Solid Source Outer Source Box

Side Surfaces

MCNP

Group	Energy Bounds (MeV)	Current Leakage (Photons/s)	2 sigma error	Normalized Leakage
24	0 -0.3 **	1.48E+06	0.02%	9.87E-01
23	0.3- 0.741	1.44E+04	0.14%	9.60E-03
22	0.741- 0.743	1.67E+02	1.32%	1.12E-04
21	0.743- 0.765	9.77E+01	1.72%	6.53E-05
20	0.765- 0.767	3.84E+02	0.86%	2.57E-04
19	0.767- 0.954	1.21E+03	0.48%	8.11E-04
18	0.954- 0.956	1.74E+01	4.06%	1.17E-05
17	0.956- 0.999	1.49E+02	1.38%	9.96E-05
16	0.999- 1.002	1.47E+03	0.44%	9.83E-04
15	1.002- 1.18	2.55E+02	1.06%	1.70E-04
14	1.18- 1.2	3.88E+01	2.72%	2.59E-05
13	1.2- 1.24	7.47E+01	1.96%	5.00E-05
12	1.24- 1.26	1.31E+01	4.68%	8.76E-06
11	1.26- 1.5	2.37E+02	1.10%	1.59E-04
10	1.5- 1.52	6.25E+01	2.14%	4.18E-05
9	1.52- 1.736	1.83E+02	1.26%	1.22E-04
8	1.736- 1.74	7.45E+01	1.96%	4.98E-05
7	1.74- 1.76	1.38E+01	4.56%	9.24E-06
6	1.76- 1.83	1.78E+02	1.26%	1.19E-04
5	1.83- 1.832	4.95E+01	2.40%	3.31E-05
4	1.832- 2.21	1.66E+02	1.32%	1.11E-04
3	2.21- 2.25	2.17E+01	3.64%	1.45E-05
2	2.25- 2.749	1.83E+01	3.96%	1.22E-05
1	2.749- 2.75	3.73E-01	27.74%	2.49E-07
Total		1.50E+06	0.02%	

**Lower bound for PENTRAN models was 0.29 MeV

APPENDIX A SOURCE BOOK

A.10. 22.5 year HEU Solid Source Outer Source Box

Top/Bottom Surfaces MCNP

Group	Energy Bounds (MeV)	Current Leakage (Photons/s)	2 sigma error	Normalized Leakage
24	0 -0.3 **	8.55E+05	0.02%	9.87E-01
23	0.3- 0.741	8.20E+03	0.18%	9.47E-03
22	0.741- 0.743	9.55E+01	1.74%	1.10E-04
21	0.743- 0.765	5.47E+01	2.30%	6.31E-05
20	0.765- 0.767	2.17E+02	1.14%	2.51E-04
19	0.767- 0.954	6.80E+02	0.64%	7.85E-04
18	0.954- 0.956	9.92E+00	5.38%	1.15E-05
17	0.956- 0.999	8.17E+01	1.88%	9.43E-05
16	0.999- 1.002	8.29E+02	0.58%	9.57E-04
15	1.002- 1.18	1.41E+02	1.42%	1.63E-04
14	1.18- 1.2	2.17E+01	3.64%	2.51E-05
13	1.2- 1.24	4.25E+01	2.60%	4.91E-05
12	1.24- 1.26	7.27E+00	6.28%	8.39E-06
11	1.26- 1.5	1.33E+02	1.46%	1.54E-04
10	1.5- 1.52	3.41E+01	2.90%	3.93E-05
9	1.52- 1.736	1.03E+02	1.68%	1.18E-04
8	1.736- 1.74	4.11E+01	2.64%	4.74E-05
7	1.74- 1.76	7.86E+00	6.04%	9.07E-06
6	1.76- 1.83	9.87E+01	1.70%	1.14E-04
5	1.83- 1.832	2.83E+01	3.18%	3.26E-05
4	1.832- 2.21	9.01E+01	1.78%	1.04E-04
3	2.21- 2.25	1.21E+01	4.88%	1.40E-05
2	2.25- 2.749	1.02E+01	5.30%	1.18E-05
1	2.749- 2.75	1.72E-01	40.82%	1.99E-07
Total		8.66E+05	0.02%	

**Lower bound for PENTRAN models was 0.29 MeV

APPENDIX A SOURCE BOOK

A.11. 50 year HEU Shell Source Inner Source Box

Side Surfaces		MCNP			PENTRAN		
Group	Energy Bounds (MeV)	Current Leakage (Photons/s)	2 sigma error	Normalized Leakage	Current Leakage (Photons/s)	Normalized Leakage	% difference
24	0 -0.3 **	8.00E+06	0.00%	9.89E-01	1.364E+07	9.945E-01	
23	0.3- 0.741	6.22E+04	0.06%	7.70E-03	4.914E+04	3.582E-03	23.5%
22	0.741- 0.743	6.77E+02	0.66%	8.38E-05	6.692E+02	4.878E-05	1.2%
21	0.743- 0.765	3.77E+02	0.88%	4.66E-05	3.271E+02	2.384E-05	14.2%
20	0.765- 0.767	1.79E+03	0.40%	2.21E-04	1.774E+03	1.293E-04	0.7%
19	0.767- 0.954	5.93E+03	0.22%	7.34E-04	5.610E+03	4.089E-04	5.5%
18	0.954- 0.956	6.84E+01	2.04%	8.46E-06	6.524E+01	4.756E-06	4.7%
17	0.956- 0.999	5.74E+02	0.70%	7.10E-05	5.303E+02	3.866E-05	7.8%
16	0.999- 1.002	5.40E+03	0.24%	6.68E-04	5.406E+03	3.940E-04	0.1%
15	1.002- 1.18	2.56E+03	0.34%	3.17E-04	2.473E+03	1.802E-04	3.5%
14	1.18- 1.2	1.63E+02	1.32%	2.01E-05	1.565E+02	1.141E-05	3.8%
13	1.2- 1.24	8.00E+02	0.60%	9.90E-05	7.938E+02	5.786E-05	0.8%
12	1.24- 1.26	6.66E+01	2.08%	8.24E-06	6.018E+01	4.387E-06	10.1%
11	1.26- 1.5	1.88E+03	0.40%	2.33E-04	1.834E+03	1.337E-04	2.5%
10	1.5- 1.52	4.09E+02	0.84%	5.05E-05	4.082E+02	2.975E-05	0.1%
9	1.52- 1.736	1.19E+03	0.50%	1.47E-04	1.166E+03	8.496E-05	2.0%
8	1.736- 1.74	3.80E+02	0.86%	4.70E-05	3.827E+02	2.789E-05	0.6%
7	1.74- 1.76	5.58E+01	2.26%	6.90E-06	5.353E+01	3.902E-06	4.2%
6	1.76- 1.83	2.06E+03	0.38%	2.55E-04	2.081E+03	1.517E-04	0.8%
5	1.83- 1.832	1.75E+02	1.28%	2.16E-05	1.764E+02	1.286E-05	1.0%
4	1.832- 2.21	1.26E+03	0.48%	1.55E-04	1.260E+03	9.187E-05	0.4%
3	2.21- 2.25	3.21E+02	0.94%	3.98E-05	3.233E+02	2.356E-05	0.6%
2	2.25- 2.749	2.65E+02	1.04%	3.28E-05	2.704E+02	1.971E-05	1.9%
1	2.749- 2.75	9.62E-01	17.28%	1.19E-07	9.836E-01	7.170E-08	2.2%
Total		8.08E+06	0.00%		1.37E+07		

**Lower bound for PENTRAN models was 0.29 MeV

APPENDIX A SOURCE BOOK

A.11. 50 year HEU Shell Source Inner Source Box

Top/Bottom Surfaces MCNP

Group	Energy Bounds (MeV)	Current Leakage (Photons/s)	2 sigma error	Normalized Leakage
24	0 -0.3 **	8.05E+06	0.00%	9.89E-01
23	0.3- 0.741	6.22E+04	0.06%	7.64E-03
22	0.741- 0.743	6.73E+02	0.66%	8.26E-05
21	0.743- 0.765	3.78E+02	0.88%	4.65E-05
20	0.765- 0.767	1.78E+03	0.40%	2.19E-04
19	0.767- 0.954	5.94E+03	0.22%	7.30E-04
18	0.954- 0.956	6.82E+01	2.06%	8.38E-06
17	0.956- 0.999	5.72E+02	0.70%	7.02E-05
16	0.999- 1.002	5.40E+03	0.24%	6.64E-04
15	1.002- 1.18	2.56E+03	0.34%	3.15E-04
14	1.18- 1.2	1.62E+02	1.34%	1.99E-05
13	1.2- 1.24	8.07E+02	0.60%	9.91E-05
12	1.24- 1.26	6.52E+01	2.10%	8.01E-06
11	1.26- 1.5	1.87E+03	0.40%	2.30E-04
10	1.5- 1.52	4.07E+02	0.84%	5.00E-05
9	1.52- 1.736	1.19E+03	0.50%	1.46E-04
8	1.736- 1.74	3.80E+02	0.86%	4.67E-05
7	1.74- 1.76	5.39E+01	2.30%	6.62E-06
6	1.76- 1.83	2.06E+03	0.38%	2.53E-04
5	1.83- 1.832	1.74E+02	1.28%	2.14E-05
4	1.832- 2.21	1.26E+03	0.48%	1.55E-04
3	2.21- 2.25	3.20E+02	0.94%	3.93E-05
2	2.25- 2.749	2.68E+02	1.04%	3.29E-05
1	2.749- 2.75	1.00E+00	16.90%	1.23E-07
Total		8.14E+06	0.00%	

**Lower bound for PENTRAN models was 0.29 MeV

APPENDIX A SOURCE BOOK

A.12. 50 year HEU Shell Source Outer Source Box

Side Surfaces		MCNP			PENTRAN		
Group	Energy Bounds (MeV)	Current Leakage (Photons/s)	2 sigma error	Normalized Leakage	Current Leakage (Photons/s)	Normalized Leakage	% difference
24	0 -0.3 **	7.30E+06	0.00%	9.87E-01	1.022E+07	9.930E-01	
23	0.3- 0.741	6.57E+04	0.06%	8.88E-03	4.781E+04	4.644E-03	31.5%
22	0.741- 0.743	6.39E+02	0.68%	8.64E-05	5.791E+02	5.625E-05	9.8%
21	0.743- 0.765	4.61E+02	0.78%	6.23E-05	3.773E+02	3.664E-05	20.0%
20	0.765- 0.767	1.67E+03	0.42%	2.26E-04	1.525E+03	1.482E-04	9.1%
19	0.767- 0.954	6.24E+03	0.22%	8.43E-04	5.444E+03	5.288E-04	13.5%
18	0.954- 0.956	7.08E+01	2.02%	9.57E-06	6.217E+01	6.039E-06	13.0%
17	0.956- 0.999	6.63E+02	0.66%	8.96E-05	5.684E+02	5.522E-05	15.3%
16	0.999- 1.002	5.17E+03	0.24%	6.99E-04	4.786E+03	4.649E-04	7.7%
15	1.002- 1.18	2.66E+03	0.32%	3.60E-04	2.382E+03	2.313E-04	11.0%
14	1.18- 1.2	1.74E+02	1.28%	2.36E-05	1.563E+02	1.518E-05	10.9%
13	1.2- 1.24	8.13E+02	0.60%	1.10E-04	7.460E+02	7.246E-05	8.6%
12	1.24- 1.26	7.77E+01	1.92%	1.05E-05	6.707E+01	6.515E-06	14.7%
11	1.26- 1.5	1.99E+03	0.38%	2.69E-04	1.806E+03	1.754E-04	9.5%
10	1.5- 1.52	4.15E+02	0.84%	5.61E-05	3.862E+02	3.751E-05	7.2%
9	1.52- 1.736	1.27E+03	0.48%	1.71E-04	1.159E+03	1.126E-04	8.9%
8	1.736- 1.74	3.84E+02	0.86%	5.19E-05	3.607E+02	3.504E-05	6.2%
7	1.74- 1.76	6.18E+01	2.16%	8.36E-06	5.540E+01	5.381E-06	10.9%
6	1.76- 1.83	2.10E+03	0.36%	2.84E-04	1.974E+03	1.918E-04	6.1%
5	1.83- 1.832	1.77E+02	1.28%	2.39E-05	1.668E+02	1.620E-05	5.8%
4	1.832- 2.21	1.30E+03	0.46%	1.76E-04	1.223E+03	1.188E-04	6.4%
3	2.21- 2.25	3.30E+02	0.94%	4.46E-05	3.115E+02	3.026E-05	5.6%
2	2.25- 2.749	2.77E+02	1.02%	3.75E-05	2.648E+02	2.572E-05	4.6%
1	2.749- 2.75	1.06E+00	16.44%	1.44E-07	9.619E-01	9.343E-08	9.9%
Total		7.39E+06	0.00%		1.030E+07		

**Lower bound for PENTRAN models was 0.29 MeV

APPENDIX A SOURCE BOOK

A.12. 50 year HEU Shell Source Outer Source Box

Top/Bottom Surfaces

MCNP

Group	Energy Bounds (MeV)	Current Leakage (Photons/s)	2 sigma error	Normalized Leakage
24	0 -0.3 **	4.24E+06	0.00%	9.88E-01
23	0.3- 0.741	3.76E+04	0.08%	8.76E-03
22	0.741- 0.743	3.57E+02	0.90%	8.31E-05
21	0.743- 0.765	2.60E+02	1.06%	6.07E-05
20	0.765- 0.767	9.40E+02	0.56%	2.19E-04
19	0.767- 0.954	3.51E+03	0.28%	8.17E-04
18	0.954- 0.956	3.98E+01	2.68%	9.28E-06
17	0.956- 0.999	3.68E+02	0.88%	8.58E-05
16	0.999- 1.002	2.91E+03	0.32%	6.77E-04
15	1.002- 1.18	1.49E+03	0.44%	3.47E-04
14	1.18- 1.2	9.86E+01	1.70%	2.30E-05
13	1.2- 1.24	4.58E+02	0.80%	1.07E-04
12	1.24- 1.26	4.33E+01	2.58%	1.01E-05
11	1.26- 1.5	1.11E+03	0.50%	2.59E-04
10	1.5- 1.52	2.33E+02	1.10%	5.43E-05
9	1.52- 1.736	7.08E+02	0.64%	1.65E-04
8	1.736- 1.74	2.15E+02	1.16%	5.00E-05
7	1.74- 1.76	3.37E+01	2.92%	7.85E-06
6	1.76- 1.83	1.17E+03	0.50%	2.72E-04
5	1.83- 1.832	9.91E+01	1.70%	2.31E-05
4	1.832- 2.21	7.27E+02	0.62%	1.69E-04
3	2.21- 2.25	1.83E+02	1.26%	4.25E-05
2	2.25- 2.749	1.54E+02	1.36%	3.59E-05
1	2.749- 2.75	5.74E-01	22.36%	1.34E-07
Total		4.29E+06	0.00%	

**Lower bound for PENTRAN models was 0.29 MeV

APPENDIX A SOURCE BOOK

A.13. 50 year HEU Shell Spatial Distributions at Outer Source Box surfaces

TOP/BOTTOM PLANE OF BOX

X-axis distribution

Location (cm)	Normalization
-30	0.000E+00
-24	6.788E-02
-18	9.008E-02
-12	1.048E-01
-6	1.149E-01
0	1.224E-01
6	1.224E-01
12	1.149E-01
18	1.048E-01
24	9.008E-02
30	6.788E-02

Y-axis distribution

Location (cm)	Normalization
-30	0.000E+00
-24	6.788E-02
-18	9.008E-02
-12	1.048E-01
-6	1.149E-01
0	1.224E-01
6	1.224E-01
12	1.149E-01
18	1.048E-01
24	9.008E-02
30	6.788E-02

SIDE PLANES OF BOX

X/Y-axis distribution

Location (cm)	Normalization
-30	0.000E+00
-24	7.099E-02
-18	8.470E-02
-12	1.002E-01
-6	1.164E-01
0	1.277E-01
6	1.277E-01
12	1.164E-01
18	1.002E-01
24	8.470E-02
30	7.099E-02

Z-axis distribution

Location (cm)	Normalization
-68.5	0.000E+00
-33	3.676E-02
-27.5	4.622E-02
-22	5.786E-02
-16.5	7.105E-02
-11	8.499E-02
-5.5	9.764E-02
0	1.055E-01
5.5	1.055E-01
11	9.764E-02
16.5	8.499E-02
22	7.105E-02
27.5	5.786E-02
33	4.622E-02
38.5	3.676E-02

APPENDIX A SOURCE BOOK

A.14. 50 year HEU Solid Source Inner Source Box

Side Surfaces		MCNP		PENTRAN			
Group	Energy Bounds (MeV)	Current Leakage (Photons/s)	2 sigma error	Normalized Leakage	Current Leakage (Photons/s)	Normalized Leakage	% difference
24	0 -0.3 **	2.19E+06	0.02%	9.89E-01	3.679E+06	9.943E-01	
23	0.3- 0.741	1.73E+04	0.12%	7.78E-03	1.322E+04	3.573E-03	26.5%
22	0.741- 0.743	1.88E+02	1.24%	8.49E-05	1.844E+02	4.983E-05	2.1%
21	0.743- 0.765	1.19E+02	1.56%	5.37E-05	9.636E+01	2.605E-05	21.1%
20	0.765- 0.767	4.98E+02	0.76%	2.25E-04	4.894E+02	1.323E-04	1.8%
19	0.767- 0.954	1.80E+03	0.40%	8.09E-04	1.620E+03	4.379E-04	10.3%
18	0.954- 0.956	2.09E+01	3.72%	9.40E-06	1.908E+01	5.158E-06	8.9%
17	0.956- 0.999	1.89E+02	1.24%	8.52E-05	1.633E+02	4.413E-05	14.6%
16	0.999- 1.002	1.57E+03	0.42%	7.07E-04	1.547E+03	4.181E-04	1.4%
15	1.002- 1.18	8.15E+02	0.60%	3.67E-04	7.488E+02	2.024E-04	8.4%
14	1.18- 1.2	5.54E+01	2.28%	2.50E-05	4.934E+01	1.334E-05	11.6%
13	1.2- 1.24	2.53E+02	1.06%	1.14E-04	2.413E+02	6.521E-05	4.7%
12	1.24- 1.26	2.49E+01	3.40%	1.12E-05	2.078E+01	5.616E-06	17.9%
11	1.26- 1.5	6.32E+02	0.68%	2.85E-04	5.858E+02	1.583E-04	7.5%
10	1.5- 1.52	1.31E+02	1.48%	5.88E-05	1.276E+02	3.448E-05	2.3%
9	1.52- 1.736	4.10E+02	0.84%	1.85E-04	3.817E+02	1.032E-04	7.1%
8	1.736- 1.74	1.22E+02	1.54%	5.49E-05	1.201E+02	3.247E-05	1.5%
7	1.74- 1.76	2.01E+01	3.78%	9.08E-06	1.824E+01	4.932E-06	9.9%
6	1.76- 1.83	6.62E+02	0.66%	2.99E-04	6.577E+02	1.778E-04	0.7%
5	1.83- 1.832	5.52E+01	2.28%	2.49E-05	5.562E+01	1.503E-05	0.8%
4	1.832- 2.21	4.16E+02	0.84%	1.88E-04	4.081E+02	1.103E-04	1.9%
3	2.21- 2.25	1.05E+02	1.66%	4.71E-05	1.040E+02	2.811E-05	0.5%
2	2.25- 2.749	8.90E+01	1.80%	4.01E-05	8.825E+01	2.385E-05	0.9%
1	2.749- 2.75	2.87E-01	31.62%	1.29E-07	3.203E-01	8.657E-08	10.9%
Total		2.22E+06	0.02%		3.700E+06		

**Lower bound for PENTRAN models was 0.29 MeV

APPENDIX A SOURCE BOOK

A.14. 50 year HEU Solid Source Inner Source Box

Top/Bottom Surfaces		MCNP		
Group	Energy Bounds (MeV)	Current Leakage (Photons/s)	2 sigma error	Normalized Leakage
24	0 -0.3 **	2.20E+06	0.02%	9.89E-01
23	0.3- 0.741	1.73E+04	0.12%	7.77E-03
22	0.741- 0.743	1.89E+02	1.24%	8.51E-05
21	0.743- 0.765	1.20E+02	1.54%	5.41E-05
20	0.765- 0.767	5.02E+02	0.76%	2.26E-04
19	0.767- 0.954	1.80E+03	0.40%	8.09E-04
18	0.954- 0.956	2.05E+01	3.74%	9.21E-06
17	0.956- 0.999	1.89E+02	1.24%	8.52E-05
16	0.999- 1.002	1.57E+03	0.42%	7.05E-04
15	1.002- 1.18	8.14E+02	0.60%	3.67E-04
14	1.18- 1.2	5.45E+01	2.30%	2.45E-05
13	1.2- 1.24	2.55E+02	1.06%	1.15E-04
12	1.24- 1.26	2.50E+01	3.40%	1.12E-05
11	1.26- 1.5	6.29E+02	0.68%	2.83E-04
10	1.5- 1.52	1.30E+02	1.48%	5.87E-05
9	1.52- 1.736	4.08E+02	0.84%	1.83E-04
8	1.736- 1.74	1.21E+02	1.54%	5.45E-05
7	1.74- 1.76	2.00E+01	3.78%	9.02E-06
6	1.76- 1.83	6.62E+02	0.66%	2.98E-04
5	1.83- 1.832	5.60E+01	2.26%	2.52E-05
4	1.832- 2.21	4.19E+02	0.82%	1.89E-04
3	2.21- 2.25	1.04E+02	1.66%	4.67E-05
2	2.25- 2.749	8.95E+01	1.80%	4.03E-05
1	2.749- 2.75	3.37E-01	29.18%	1.52E-07
Total		2.22E+06	0.02%	

**Lower bound for PENTRAN models was 0.29 MeV

APPENDIX A SOURCE BOOK

A.15. 50 year HEU Solid Source Outer Source Box

Side Surfaces		MCNP			PENTRAN		
Group	Energy Bounds (MeV)	Current Leakage (Photons/s)	2 sigma error	Normalized Leakage	Current Leakage (Photons/s)	Normalized Leakage	% difference
24	0 -0.3 **	2.07E+06	0.02%	9.87E-01	2.807E+06	9.927E-01	
23	0.3- 0.741	1.84E+04	0.12%	8.77E-03	1.316E+04	4.652E-03	33.1%
22	0.741- 0.743	1.79E+02	1.26%	8.56E-05	1.617E+02	5.720E-05	10.3%
21	0.743- 0.765	1.43E+02	1.42%	6.84E-05	1.127E+02	3.985E-05	23.9%
20	0.765- 0.767	4.70E+02	0.78%	2.24E-04	4.262E+02	1.507E-04	9.7%
19	0.767- 0.954	1.90E+03	0.38%	9.07E-04	1.597E+03	5.649E-04	17.3%
18	0.954- 0.956	2.17E+01	3.64%	1.04E-05	1.844E+01	6.520E-06	16.2%
17	0.956- 0.999	2.16E+02	1.16%	1.03E-04	1.765E+02	6.240E-05	20.3%
16	0.999- 1.002	1.52E+03	0.44%	7.24E-04	1.385E+03	4.897E-04	9.0%
15	1.002- 1.18	8.53E+02	0.58%	4.07E-04	7.313E+02	2.586E-04	15.3%
14	1.18- 1.2	5.99E+01	2.18%	2.86E-05	4.984E+01	1.763E-05	18.4%
13	1.2- 1.24	2.57E+02	1.06%	1.23E-04	2.294E+02	8.113E-05	11.4%
12	1.24- 1.26	2.91E+01	3.14%	1.39E-05	2.311E+01	8.171E-06	23.0%
11	1.26- 1.5	6.70E+02	0.66%	3.20E-04	5.825E+02	2.060E-04	13.9%
10	1.5- 1.52	1.33E+02	1.46%	6.37E-05	1.218E+02	4.308E-05	9.1%
9	1.52- 1.736	4.38E+02	0.82%	2.09E-04	3.824E+02	1.352E-04	13.5%
8	1.736- 1.74	1.24E+02	1.52%	5.90E-05	1.142E+02	4.037E-05	7.9%
7	1.74- 1.76	2.21E+01	3.60%	1.06E-05	1.894E+01	6.698E-06	15.6%
6	1.76- 1.83	6.76E+02	0.66%	3.23E-04	6.290E+02	2.224E-04	7.2%
5	1.83- 1.832	5.68E+01	2.24%	2.71E-05	5.302E+01	1.875E-05	6.9%
4	1.832- 2.21	4.34E+02	0.82%	2.07E-04	3.991E+02	1.411E-04	8.4%
3	2.21- 2.25	1.08E+02	1.64%	5.14E-05	1.009E+02	3.569E-05	6.5%
2	2.25- 2.749	9.28E+01	1.76%	4.43E-05	8.699E+01	3.076E-05	6.5%
1	2.749- 2.75	3.23E-01	29.82%	1.54E-07	3.151E-01	1.114E-07	2.5%
Total		2.09E+06	0.02%		2.828E+06		

**Lower bound for PENTRAN models was 0.29 MeV

APPENDIX A SOURCE BOOK

A.15. 50 year HEU Solid Source Outer Source Box

Top/Bottom Surfaces MCNP

Group	Energy Bounds (MeV)	Current Leakage (Photons/s)	2 sigma error	Normalized Leakage
24	0 -0.3 **	1.20E+06	0.0001	9.874E-01
23	0.3- 0.741	1.05E+04	0.0008	8.666E-03
22	0.741- 0.743	1.01E+02	0.0084	8.354E-05
21	0.743- 0.765	8.15E+01	0.0094	6.721E-05
20	0.765- 0.767	2.67E+02	0.0052	2.202E-04
19	0.767- 0.954	1.07E+03	0.0026	8.807E-04
18	0.954- 0.956	1.21E+01	0.0243	1.002E-05
17	0.956- 0.999	1.20E+02	0.0077	9.935E-05
16	0.999- 1.002	8.50E+02	0.0029	7.011E-04
15	1.002- 1.18	4.76E+02	0.0039	3.929E-04
14	1.18- 1.2	3.28E+01	0.0148	2.703E-05
13	1.2- 1.24	1.46E+02	0.007	1.205E-04
12	1.24- 1.26	1.59E+01	0.0212	1.311E-05
11	1.26- 1.5	3.73E+02	0.0044	3.079E-04
10	1.5- 1.52	7.44E+01	0.0098	6.137E-05
9	1.52- 1.736	2.44E+02	0.0054	2.009E-04
8	1.736- 1.74	6.87E+01	0.0102	5.668E-05
7	1.74- 1.76	1.20E+01	0.0245	9.898E-06
6	1.76- 1.83	3.80E+02	0.0043	3.131E-04
5	1.83- 1.832	3.22E+01	0.0149	2.653E-05
4	1.832- 2.21	2.43E+02	0.0054	2.004E-04
3	2.21- 2.25	5.95E+01	0.011	4.903E-05
2	2.25- 2.749	5.20E+01	0.0118	4.285E-05
1	2.749- 2.75	1.58E-01	0.2132	1.302E-07
Total		1.21E+06	0.0001	

**Lower bound for PENTRAN models was 0.29 MeV

APPENDIX A SOURCE BOOK

A.16. 50 year HEU Solid Spatial Distributions at Outer Source Box surfaces

TOP/BOTTOM PLANE OF BOX

X-axis distribution

Location (cm) Normalization

-30	0.000E+00
-24	1.259E-01
-18	1.184E-01
-12	1.099E-01
-6	9.430E-02
0	6.988E-02
6	8.920E-02
12	1.184E-01
18	1.099E-01
24	9.430E-02
30	6.988E-02

Y-axis distribution

Location (cm) Normalization

-30	0.000E+00
-24	1.259E-01
-18	1.184E-01
-12	1.099E-01
-6	9.430E-02
0	6.988E-02
6	8.920E-02
12	1.184E-01
18	1.099E-01
24	9.430E-02
30	6.988E-02

SIDE PLANES OF BOX

X/Y-axis distribution

Location (cm) Normalization

-30	0.000E+00
-24	7.369E-02
-18	8.675E-02
-12	1.013E-01
-6	1.141E-01
0	1.242E-01
6	1.242E-01
12	1.141E-01
18	1.013E-01
24	8.675E-02
30	7.369E-02

Z-axis distribution

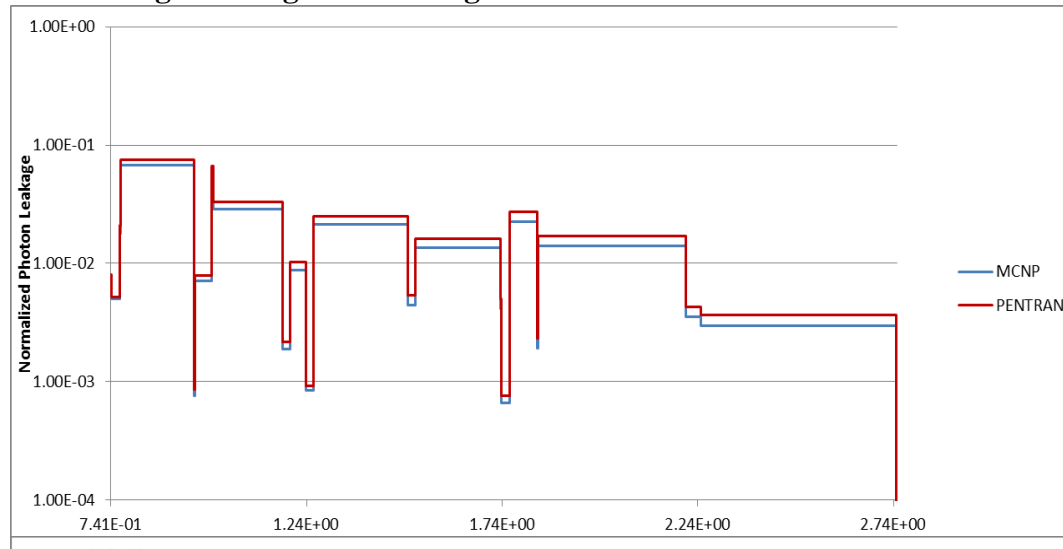
Location (cm) Normalization

-38.5	0.000E+00
-33	3.647E-02
-27.5	4.647E-02
-22	5.894E-02
-16.5	7.199E-02
-11	8.492E-02
-5.5	9.650E-02
0	1.047E-01
5.5	1.047E-01
11	9.650E-02
16.5	8.492E-02
22	7.199E-02
27.5	5.894E-02
33	4.647E-02
38.5	3.647E-02

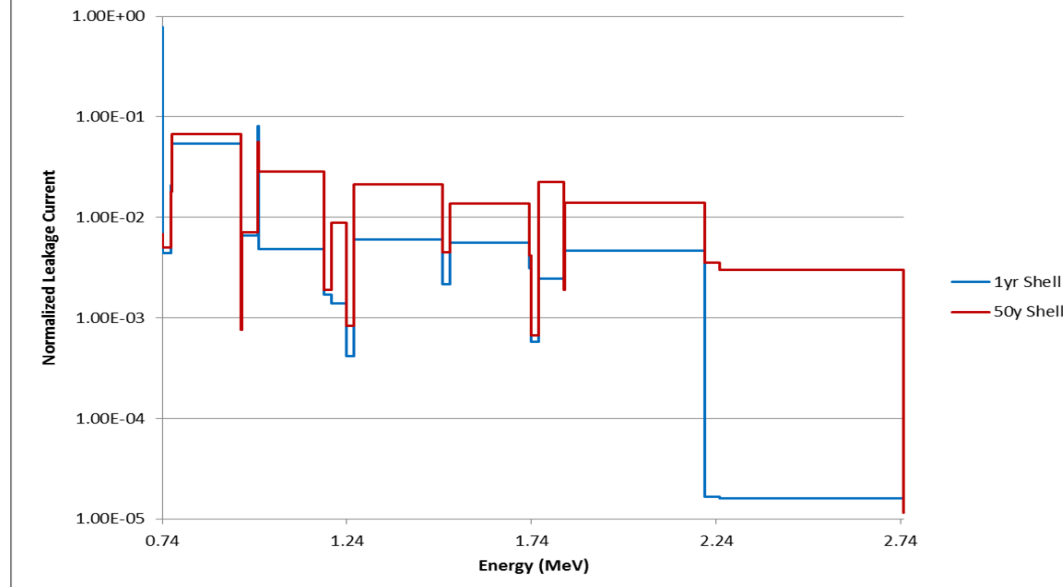
APPENDIX A SOURCE BOOK

Figure A.3. HEU 50 year Shell Outer Source Box Histograms of gamma leakage

MCNP vs PENTRAN for 50yr Shell



1yr vs. 50yr Shell



APPENDIX A SOURCE BOOK

A.17. 75 year HEU Shell Source Inner Source Box

Side Surfaces		MCNP		
Group	Energy Bounds (MeV)	Current Leakage (Photons/s)	2 sigma error	Normalized Leakage
24	0 -0.3 **	8.00E+06	0.00%	9.85E-01
23	0.3- 0.741	7.64E+04	0.06%	9.40E-03
22	0.741- 0.743	6.99E+02	0.64%	8.61E-05
21	0.743- 0.765	5.44E+02	0.72%	6.71E-05
20	0.765- 0.767	2.14E+03	0.36%	2.64E-04
19	0.767- 0.954	8.75E+03	0.18%	1.08E-03
18	0.954- 0.956	8.13E+01	1.88%	1.00E-05
17	0.956- 0.999	8.19E+02	0.60%	1.01E-04
16	0.999- 1.002	5.40E+03	0.24%	6.65E-04
15	1.002- 1.18	5.35E+03	0.24%	6.59E-04
14	1.18- 1.2	2.30E+02	1.12%	2.83E-05
13	1.2- 1.24	1.69E+03	0.42%	2.09E-04
12	1.24- 1.26	1.17E+02	1.56%	1.45E-05
11	1.26- 1.5	3.76E+03	0.28%	4.63E-04
10	1.5- 1.52	7.41E+02	0.62%	9.12E-05
9	1.52- 1.736	2.24E+03	0.36%	2.76E-04
8	1.736- 1.74	6.07E+02	0.68%	7.48E-05
7	1.74- 1.76	8.05E+01	1.88%	9.91E-06
6	1.76- 1.83	4.44E+03	0.26%	5.46E-04
5	1.83- 1.832	2.04E+02	1.18%	2.52E-05
4	1.832- 2.21	2.45E+03	0.34%	3.02E-04
3	2.21- 2.25	7.14E+02	0.64%	8.80E-05
2	2.25- 2.749	5.99E+02	0.70%	7.37E-05
1	2.749- 2.75	9.63E-01	17.28%	1.19E-07
Total		8.12E+06	0.00%	

**Lower bound for PENTRAN models was 0.29 MeV

APPENDIX A SOURCE BOOK

A.17. 75 year HEU Shell Source Inner Source Box

Top/Bottom Surfaces		MCNP		
Group	Energy Bounds (MeV)	Current Leakage (Photons/s)	2 sigma error	Normalized Leakage
24	0 -0.3 **	8.06E+06	0.00%	9.86E-01
23	0.3- 0.741	7.64E+04	0.06%	9.34E-03
22	0.741- 0.743	6.91E+02	0.64%	8.45E-05
21	0.743- 0.765	5.43E+02	0.72%	6.64E-05
20	0.765- 0.767	2.14E+03	0.36%	2.61E-04
19	0.767- 0.954	8.77E+03	0.18%	1.07E-03
18	0.954- 0.956	8.02E+01	1.90%	9.81E-06
17	0.956- 0.999	8.20E+02	0.60%	1.00E-04
16	0.999- 1.002	5.41E+03	0.24%	6.61E-04
15	1.002- 1.18	5.35E+03	0.24%	6.54E-04
14	1.18- 1.2	2.29E+02	1.12%	2.80E-05
13	1.2- 1.24	1.70E+03	0.42%	2.08E-04
12	1.24- 1.26	1.18E+02	1.56%	1.44E-05
11	1.26- 1.5	3.76E+03	0.28%	4.60E-04
10	1.5- 1.52	7.47E+02	0.62%	9.14E-05
9	1.52- 1.736	2.25E+03	0.36%	2.75E-04
8	1.736- 1.74	6.04E+02	0.68%	7.38E-05
7	1.74- 1.76	8.00E+01	1.90%	9.78E-06
6	1.76- 1.83	4.43E+03	0.26%	5.41E-04
5	1.83- 1.832	2.04E+02	1.18%	2.49E-05
4	1.832- 2.21	2.44E+03	0.34%	2.99E-04
3	2.21- 2.25	7.17E+02	0.64%	8.77E-05
2	2.25- 2.749	5.99E+02	0.70%	7.33E-05
1	2.749- 2.75	1.01E+00	16.90%	1.23E-07
Total		8.18E+06	0.00%	

**Lower bound for PENTRAN models was 0.29 MeV

APPENDIX A SOURCE BOOK

A.18. 75 year HEU Shell Source Outer Source Box

Side Surfaces		MCNP		
Group	Energy Bounds (MeV)	Current Leakage (Photons/s)	2 sigma error	Normalized Leakage
24	0 -0.3 **	7.31E+06	0.00%	9.83E-01
23	0.3- 0.741	8.12E+04	0.06%	1.09E-02
22	0.741- 0.743	6.62E+02	0.66%	8.91E-05
21	0.743- 0.765	6.67E+02	0.66%	8.97E-05
20	0.765- 0.767	2.02E+03	0.38%	2.71E-04
19	0.767- 0.954	9.23E+03	0.18%	1.24E-03
18	0.954- 0.956	8.39E+01	1.86%	1.13E-05
17	0.956- 0.999	9.53E+02	0.54%	1.28E-04
16	0.999- 1.002	5.18E+03	0.24%	6.97E-04
15	1.002- 1.18	5.54E+03	0.22%	7.45E-04
14	1.18- 1.2	2.57E+02	1.06%	3.46E-05
13	1.2- 1.24	1.72E+03	0.40%	2.31E-04
12	1.24- 1.26	1.42E+02	1.42%	1.91E-05
11	1.26- 1.5	3.98E+03	0.26%	5.35E-04
10	1.5- 1.52	7.55E+02	0.62%	1.02E-04
9	1.52- 1.736	2.39E+03	0.34%	3.22E-04
8	1.736- 1.74	6.11E+02	0.68%	8.22E-05
7	1.74- 1.76	9.18E+01	1.76%	1.23E-05
6	1.76- 1.83	4.50E+03	0.26%	6.05E-04
5	1.83- 1.832	2.06E+02	1.18%	2.77E-05
4	1.832- 2.21	2.55E+03	0.34%	3.42E-04
3	2.21- 2.25	7.35E+02	0.62%	9.89E-05
2	2.25- 2.749	6.24E+02	0.68%	8.40E-05
1	2.749- 2.75	1.06E+00	16.44%	1.43E-07
Total		7.43E+06	0.00%	

**Lower bound for PENTRAN models was 0.29 MeV

APPENDIX A SOURCE BOOK

A.18. 75 year HEU Shell Source Outer Source Box

Top/Bottom Surfaces		MCNP		
Group	Energy Bounds (MeV)	Current Leakage (Photons/s)	2 sigma error	Normalized Leakage
24	0 -0.3 **	4.24E+06	0.00%	9.84E-01
23	0.3- 0.741	4.65E+04	0.08%	1.08E-02
22	0.741- 0.743	3.69E+02	0.88%	8.54E-05
21	0.743- 0.765	3.77E+02	0.88%	8.72E-05
20	0.765- 0.767	1.13E+03	0.50%	2.61E-04
19	0.767- 0.954	5.20E+03	0.24%	1.21E-03
18	0.954- 0.956	4.78E+01	2.46%	1.11E-05
17	0.956- 0.999	5.31E+02	0.74%	1.23E-04
16	0.999- 1.002	2.91E+03	0.32%	6.75E-04
15	1.002- 1.18	3.11E+03	0.30%	7.20E-04
14	1.18- 1.2	1.43E+02	1.42%	3.30E-05
13	1.2- 1.24	9.61E+02	0.54%	2.23E-04
12	1.24- 1.26	7.97E+01	1.90%	1.85E-05
11	1.26- 1.5	2.22E+03	0.36%	5.15E-04
10	1.5- 1.52	4.25E+02	0.82%	9.85E-05
9	1.52- 1.736	1.34E+03	0.46%	3.11E-04
8	1.736- 1.74	3.41E+02	0.92%	7.91E-05
7	1.74- 1.76	5.08E+01	2.38%	1.18E-05
6	1.76- 1.83	2.52E+03	0.34%	5.83E-04
5	1.83- 1.832	1.16E+02	1.58%	2.68E-05
4	1.832- 2.21	1.41E+03	0.46%	3.27E-04
3	2.21- 2.25	4.10E+02	0.84%	9.50E-05
2	2.25- 2.749	3.46E+02	0.92%	8.01E-05
1	2.749- 2.75	5.75E-01	22.36%	1.33E-07
Total		4.32E+06	0.00%	

**Lower bound for PENTRAN models was 0.29 MeV

APPENDIX A SOURCE BOOK

A.19. 75 year HEU Solid Source Inner Source Box

Side Surfaces	MCNP			
Group	Energy Bounds (MeV)	Current Leakage (Photons/s)	2 sigma error	Normalized Leakage
24	0 -0.3 **	1.54E+06	0.02%	9.79E-01
23	0.3- 0.741	2.02E+04	0.12%	1.29E-02
22	0.741- 0.743	1.89E+02	1.24%	1.20E-04
21	0.743- 0.765	1.75E+02	1.28%	1.11E-04
20	0.765- 0.767	5.78E+02	0.70%	3.67E-04
19	0.767- 0.954	2.61E+03	0.34%	1.66E-03
18	0.954- 0.956	2.51E+01	3.38%	1.59E-05
17	0.956- 0.999	2.71E+02	1.04%	1.72E-04
16	0.999- 1.002	1.53E+03	0.44%	9.73E-04
15	1.002- 1.18	1.67E+03	0.42%	1.06E-03
14	1.18- 1.2	8.01E+01	1.90%	5.09E-05
13	1.2- 1.24	5.24E+02	0.74%	3.33E-04
12	1.24- 1.26	4.50E+01	2.52%	2.86E-05
11	1.26- 1.5	1.25E+03	0.48%	7.94E-04
10	1.5- 1.52	2.34E+02	1.10%	1.49E-04
9	1.52- 1.736	7.70E+02	0.62%	4.89E-04
8	1.736- 1.74	1.91E+02	1.22%	1.21E-04
7	1.74- 1.76	3.01E+01	3.10%	1.91E-05
6	1.76- 1.83	1.41E+03	0.46%	8.94E-04
5	1.83- 1.832	6.43E+01	2.12%	4.08E-05
4	1.832- 2.21	8.08E+02	0.60%	5.13E-04
3	2.21- 2.25	2.32E+02	1.12%	1.47E-04
2	2.25- 2.749	1.97E+02	1.20%	1.25E-04
1	2.749- 2.75	3.02E-01	30.86%	1.92E-07
Total		1.57E+06	0.02%	

**Lower bound for PENTRAN models was 0.29 MeV

APPENDIX A SOURCE BOOK

A.19. 75 year HEU Solid Source Inner Source Box

Top/Bottom Surfaces	MCNP			
Group	Energy Bounds (MeV)	Current Leakage (Photons/s)	2 sigma error	Normalized Leakage
24	0 -0.3 **	1.54E+06	0.02%	9.79E-01
23	0.3- 0.741	2.02E+04	0.12%	1.28E-02
22	0.741- 0.743	1.87E+02	1.24%	1.19E-04
21	0.743- 0.765	1.74E+02	1.28%	1.10E-04
20	0.765- 0.767	5.78E+02	0.70%	3.66E-04
19	0.767- 0.954	2.62E+03	0.34%	1.66E-03
18	0.954- 0.956	2.43E+01	3.44%	1.54E-05
17	0.956- 0.999	2.73E+02	1.02%	1.73E-04
16	0.999- 1.002	1.53E+03	0.44%	9.73E-04
15	1.002- 1.18	1.67E+03	0.42%	1.06E-03
14	1.18- 1.2	7.95E+01	1.90%	5.04E-05
13	1.2- 1.24	5.25E+02	0.74%	3.33E-04
12	1.24- 1.26	4.48E+01	2.54%	2.84E-05
11	1.26- 1.5	1.25E+03	0.48%	7.95E-04
10	1.5- 1.52	2.37E+02	1.10%	1.50E-04
9	1.52- 1.736	7.63E+02	0.62%	4.84E-04
8	1.736- 1.74	1.90E+02	1.22%	1.20E-04
7	1.74- 1.76	3.02E+01	3.08%	1.91E-05
6	1.76- 1.83	1.40E+03	0.46%	8.90E-04
5	1.83- 1.832	6.49E+01	2.10%	4.11E-05
4	1.832- 2.21	8.04E+02	0.60%	5.10E-04
3	2.21- 2.25	2.31E+02	1.12%	1.46E-04
2	2.25- 2.749	1.96E+02	1.22%	1.24E-04
1	2.749- 2.75	3.02E-01	30.86%	1.91E-07
Total		1.58E+06	0.02%	

**Lower bound for PENTRAN models was 0.29 MeV

APPENDIX A SOURCE BOOK

A.20. 75 year HEU Solid Source Outer Source Box

Side Surfaces	MCNP			
Group	Energy Bounds (MeV)	Current Leakage (Photons/s)	2 sigma error	Normalized Leakage
24	0 -0.3 **	1.48E+06	0.02%	9.77E-01
23	0.3- 0.741	2.17E+04	0.12%	1.44E-02
22	0.741- 0.743	1.82E+02	1.26%	1.20E-04
21	0.743- 0.765	2.12E+02	1.16%	1.40E-04
20	0.765- 0.767	5.49E+02	0.72%	3.63E-04
19	0.767- 0.954	2.77E+03	0.32%	1.83E-03
18	0.954- 0.956	2.65E+01	3.30%	1.75E-05
17	0.956- 0.999	3.12E+02	0.96%	2.06E-04
16	0.999- 1.002	1.48E+03	0.44%	9.77E-04
15	1.002- 1.18	1.74E+03	0.40%	1.15E-03
14	1.18- 1.2	8.97E+01	1.80%	5.92E-05
13	1.2- 1.24	5.33E+02	0.74%	3.52E-04
12	1.24- 1.26	5.34E+01	2.32%	3.52E-05
11	1.26- 1.5	1.33E+03	0.46%	8.76E-04
10	1.5- 1.52	2.41E+02	1.10%	1.59E-04
9	1.52- 1.736	8.20E+02	0.60%	5.41E-04
8	1.736- 1.74	1.93E+02	1.22%	1.28E-04
7	1.74- 1.76	3.35E+01	2.92%	2.21E-05
6	1.76- 1.83	1.43E+03	0.44%	9.47E-04
5	1.83- 1.832	6.56E+01	2.10%	4.33E-05
4	1.832- 2.21	8.43E+02	0.58%	5.56E-04
3	2.21- 2.25	2.40E+02	1.10%	1.58E-04
2	2.25- 2.749	2.06E+02	1.18%	1.36E-04
1	2.749- 2.75	3.74E-01	27.74%	2.47E-07
Total		1.52E+06	0.02%	

**Lower bound for PENTRAN models was 0.29 MeV

APPENDIX A SOURCE BOOK

A.20. 75 year HEU Solid Source Outer Source Box

Top/Bottom Surfaces		MCNP		
Group	Energy Bounds (MeV)	Current Leakage (Photons/s)	2 sigma error	Normalized Leakage
24	0 -0.3 **	8.57E+05	0.02%	9.77E-01
23	0.3- 0.741	1.25E+04	0.16%	1.42E-02
22	0.741- 0.743	1.00E+02	1.70%	1.14E-04
21	0.743- 0.765	1.18E+02	1.56%	1.35E-04
20	0.765- 0.767	3.07E+02	0.96%	3.49E-04
19	0.767- 0.954	1.56E+03	0.42%	1.78E-03
18	0.954- 0.956	1.49E+01	4.38%	1.70E-05
17	0.956- 0.999	1.76E+02	1.28%	2.00E-04
16	0.999- 1.002	8.29E+02	0.58%	9.45E-04
15	1.002- 1.18	9.73E+02	0.54%	1.11E-03
14	1.18- 1.2	4.94E+01	2.42%	5.63E-05
13	1.2- 1.24	3.01E+02	0.98%	3.43E-04
12	1.24- 1.26	2.95E+01	3.12%	3.36E-05
11	1.26- 1.5	7.41E+02	0.62%	8.45E-04
10	1.5- 1.52	1.34E+02	1.46%	1.53E-04
9	1.52- 1.736	4.54E+02	0.80%	5.18E-04
8	1.736- 1.74	1.08E+02	1.62%	1.23E-04
7	1.74- 1.76	1.90E+01	3.88%	2.16E-05
6	1.76- 1.83	8.02E+02	0.60%	9.14E-04
5	1.83- 1.832	3.68E+01	2.80%	4.19E-05
4	1.832- 2.21	4.67E+02	0.78%	5.33E-04
3	2.21- 2.25	1.33E+02	1.48%	1.51E-04
2	2.25- 2.749	1.13E+02	1.60%	1.29E-04
1	2.749- 2.75	1.72E-01	40.82%	1.96E-07
Total		8.77E+05	0.02%	

**Lower bound for PENTRAN models was 0.29 MeV

APPENDIX A SOURCE BOOK

A.21. 1 year WGPu Shell Gamma spectrum Inner Source Box

Side Surfaces

MCNP

Group Energy Bounds **Intrinsic Current Leakage** $\sigma_{\text{intrinsic}}$ **Current Leakage** σ_{leakage} **sigma error** σ_{error} **total Current Leakage** σ_{total} **Current Leakage** σ_{sig} **sigma error** σ_{sig} **normalized Leakage**

	(MeV)	(Photons/s)		(Photons/s)		(Photons/s)		(Photons/s)	
24	0 -0.3 **	1.85E+09	0.10%	2.43E+04	0.00%	1.85E+09	0.10%	9.906E-01	
23	0.3- 0.741	1.72E+07	0.04%	7.58E+04	0.00%	1.73E+07	0.04%	9.253E-03	
22	0.741- 0.743	6.36E+03	0.04%	3.28E+02	0.06%	6.68E+03	0.07%	3.572E-06	
21	0.743- 0.765	5.56E+04	0.02%	3.57E+03	0.02%	5.92E+04	0.03%	3.164E-05	
20	0.765- 0.767	4.15E+04	0.04%	3.21E+02	0.06%	4.18E+04	0.07%	2.234E-05	
19	0.767- 0.954	5.81E+04	0.02%	2.97E+04	0.00%	8.78E+04	0.02%	4.691E-05	
18	0.954- 0.956	7.50E+02	0.04%	2.69E+02	0.06%	1.02E+03	0.07%	5.443E-07	
17	0.956- 0.999	1.83E+03	0.06%	5.42E+03	0.02%	7.25E+03	0.06%	3.876E-06	
16	0.999- 1.002	6.63E+02	0.04%	3.65E+02	0.06%	1.03E+03	0.07%	5.494E-07	
15	1.002- 1.18	4.35E+03	0.04%	2.47E+04	0.00%	2.91E+04	0.04%	1.554E-05	
14	1.18- 1.2	4.19E+02	0.16%	2.01E+03	0.02%	2.43E+03	0.16%	1.296E-06	
13	1.2- 1.24	8.15E+02	0.10%	3.87E+03	0.02%	4.69E+03	0.10%	2.506E-06	
12	1.24- 1.26	2.18E+04	0.02%	1.86E+03	0.02%	2.36E+04	0.03%	1.262E-05	
11	1.26- 1.5	1.68E+03	0.06%	1.89E+04	0.00%	2.05E+04	0.06%	1.098E-05	
10	1.5- 1.52	1.39E+02	0.18%	1.32E+03	0.04%	1.46E+03	0.18%	7.783E-07	
9	1.52- 1.736	1.48E+03	0.06%	1.29E+04	0.00%	1.44E+04	0.06%	7.680E-06	
8	1.736- 1.74	2.71E+01	0.40%	1.97E+02	0.08%	2.24E+02	0.41%	1.199E-07	
7	1.74- 1.76	1.25E+04	0.02%	9.73E+02	0.04%	1.35E+04	0.04%	7.206E-06	
6	1.76- 1.83	1.66E+02	0.10%	3.26E+03	0.02%	3.42E+03	0.10%	1.829E-06	
5	1.83- 1.832	6.03E+00	0.48%	9.24E+01	0.12%	9.84E+01	0.49%	5.258E-08	
4	1.832- 2.21	8.71E+02	0.04%	1.42E+04	0.00%	1.50E+04	0.04%	8.038E-06	
3	2.21- 2.25	3.95E+03	0.02%	3.90E+03	0.02%	7.85E+03	0.03%	4.194E-06	
2	2.25- 2.749	4.05E+03	0.02%	1.21E+04	0.02%	1.62E+04	0.03%	8.633E-06	
1	2.749- 2.75	4.61E+03	0.02%	1.80E+01	0.26%	4.62E+03	0.26%	2.471E-06	
Total		1.87E+09	0.10%	2.40E+05	0.00%	1.87E+09	0.10%		

**Lower bound for PENTRAN models was 0.29 MeV

APPENDIX A SOURCE BOOK

A.21. 1 year WGPu Shell Gamma spectrum Inner Source Box

Top/Bottom Surfaces MCNP
Group Energy BoundsIntrinsic Current Leakage² sigma error

	(MeV)	(Photons/s)	
24	0 -0.3 **	1.86E+09	0.10%
23	0.3- 0.741	1.72E+07	0.04%
22	0.741- 0.743	6.36E+03	0.04%
21	0.743- 0.765	5.56E+04	0.02%
20	0.765- 0.767	4.15E+04	0.04%
19	0.767- 0.954	5.81E+04	0.02%
18	0.954- 0.956	7.50E+02	0.04%
17	0.956- 0.999	1.83E+03	0.06%
16	0.999- 1.002	6.63E+02	0.04%
15	1.002- 1.18	4.35E+03	0.04%
14	1.18- 1.2	4.19E+02	0.16%
13	1.2- 1.24	8.16E+02	0.10%
12	1.24- 1.26	2.18E+04	0.02%
11	1.26- 1.5	1.68E+03	0.06%
10	1.5- 1.52	1.39E+02	0.18%
9	1.52- 1.736	1.48E+03	0.06%
8	1.736- 1.74	2.71E+01	0.40%
7	1.74- 1.76	1.25E+04	0.02%
6	1.76- 1.83	1.66E+02	0.10%
5	1.83- 1.832	6.04E+00	0.48%
4	1.832- 2.21	8.71E+02	0.04%
3	2.21- 2.25	3.95E+03	0.02%
2	2.25- 2.749	4.05E+03	0.02%
1	2.749- 2.75	4.61E+03	0.02%
Total		1.87E+09	0.10%

**Lower bound for PENTRAN models was 0.29 MeV

APPENDIX A SOURCE BOOK

A.22. 1 year WGPu Shell Gamma Spectrum Outer Source Box

Side Surfaces

Group Energy Bound intrinsic Current Leakage² sigma error produced Current Leakage² sigma error total Current Leakage² sigma error normalized Leakage²

	(MeV)	(Photons/s)		(Photons/s)		(Photons/s)		(Photons/s)	
24	0 -0.3 **	1.75E+09	0.10%	0.00E+00	0.00%	1.75E+09	0.10%	9.90E-01	
23	0.3- 0.741	1.77E+07	0.04%	6.44E+03	0.02%	1.77E+07	0.04%	1.00E-02	
22	0.741- 0.743	6.07E+03	0.04%	1.44E+04	0.01%	2.04E+04	0.04%	1.16E-05	
21	0.743- 0.765	5.32E+04	0.04%	5.73E+01	0.21%	5.33E+04	0.21%	3.01E-05	
20	0.765- 0.767	3.90E+04	0.04%	6.24E+02	0.06%	3.96E+04	0.07%	2.24E-05	
19	0.767- 0.954	5.79E+04	0.02%	5.60E+01	0.21%	5.79E+04	0.21%	3.28E-05	
18	0.954- 0.956	7.32E+02	0.04%	5.50E+03	0.02%	6.23E+03	0.04%	3.52E-06	
17	0.956- 0.999	2.03E+03	0.06%	4.61E+01	0.23%	2.07E+03	0.24%	1.17E-06	
16	0.999- 1.002	6.57E+02	0.04%	9.31E+02	0.05%	1.59E+03	0.06%	8.98E-07	
15	1.002- 1.18	5.21E+03	0.04%	6.28E+01	0.20%	5.27E+03	0.20%	2.98E-06	
14	1.18- 1.2	5.15E+02	0.14%	4.14E+03	0.02%	4.66E+03	0.14%	2.63E-06	
13	1.2- 1.24	1.01E+03	0.10%	3.41E+02	0.08%	1.35E+03	0.13%	7.61E-07	
12	1.24- 1.26	2.15E+04	0.02%	7.02E+02	0.06%	2.22E+04	0.06%	1.25E-05	
11	1.26- 1.5	2.09E+03	0.04%	3.17E+02	0.09%	2.40E+03	0.10%	1.36E-06	
10	1.5- 1.52	1.72E+02	0.16%	3.36E+03	0.03%	3.54E+03	0.16%	2.00E-06	
9	1.52- 1.736	1.83E+03	0.04%	2.25E+02	0.10%	2.06E+03	0.11%	1.16E-06	
8	1.736- 1.74	3.36E+01	0.36%	2.21E+03	0.03%	2.25E+03	0.36%	1.27E-06	
7	1.74- 1.76	1.27E+04	0.02%	3.39E+01	0.27%	1.27E+04	0.27%	7.19E-06	
6	1.76- 1.83	2.07E+02	0.10%	1.68E+02	0.12%	3.74E+02	0.16%	2.12E-07	
5	1.83- 1.832	7.20E+00	0.44%	5.86E+02	0.06%	5.93E+02	0.44%	3.35E-07	
4	1.832- 2.21	1.09E+03	0.04%	1.58E+01	0.39%	1.10E+03	0.39%	6.24E-07	
3	2.21- 2.25	4.08E+03	0.02%	2.46E+03	0.03%	6.54E+03	0.04%	3.70E-06	
2	2.25- 2.749	4.31E+03	0.02%	6.55E+02	0.05%	4.97E+03	0.05%	2.81E-06	
1	2.749- 2.75	4.80E+03	0.02%	2.10E+03	0.03%	6.91E+03	0.04%	3.91E-06	
Total		1.77E+09	0.10%	3.05E+00	0.89%	1.77E+09	0.90%		

**Lower bound for PENTRAN models was 0.29 MeV

APPENDIX A SOURCE BOOK

A.22. 1 year WGPu Shell Gamma Spectrum Outer Source Box

Top/Bottom Surfaces

Group Energy Bounds Intrinsic Current Leakage sigma error produced Current Leakage sigma error total Current Leakage sigma error normalized Leakage

	(MeV)	(Photons/s)		(Photons/s)		(Photons/s)		(Photons/s)	
24	0 -0.3 **	1.01E+09	0.12%	4.37E+03	0.04%	1.01E+09	0.13%	9.90E-01	
23	0.3- 0.741	1.01E+07	0.04%	9.74E+03	0.04%	1.01E+07	0.06%	9.84E-03	
22	0.741- 0.743	3.41E+03	0.06%	3.78E+01	0.50%	3.45E+03	0.50%	3.36E-06	
21	0.743- 0.765	2.99E+04	0.04%	4.14E+02	0.16%	3.03E+04	0.16%	2.96E-05	
20	0.765- 0.767	2.19E+04	0.04%	3.70E+01	0.52%	2.20E+04	0.52%	2.14E-05	
19	0.767- 0.954	3.25E+04	0.04%	3.67E+03	0.04%	3.62E+04	0.06%	3.53E-05	
18	0.954- 0.956	4.11E+02	0.06%	3.04E+01	0.56%	4.42E+02	0.56%	4.32E-07	
17	0.956- 0.999	1.14E+03	0.06%	6.12E+02	0.12%	1.75E+03	0.13%	1.71E-06	
16	0.999- 1.002	3.69E+02	0.06%	4.11E+01	0.48%	4.10E+02	0.48%	4.00E-07	
15	1.002- 1.18	2.91E+03	0.06%	2.72E+03	0.06%	5.63E+03	0.08%	5.50E-06	
14	1.18- 1.2	2.86E+02	0.18%	2.24E+02	0.20%	5.10E+02	0.27%	4.98E-07	
13	1.2- 1.24	5.59E+02	0.14%	4.64E+02	0.14%	1.02E+03	0.20%	1.00E-06	
12	1.24- 1.26	1.20E+04	0.04%	2.08E+02	0.22%	1.22E+04	0.22%	1.20E-05	
11	1.26- 1.5	1.17E+03	0.06%	2.22E+03	0.06%	3.39E+03	0.08%	3.31E-06	
10	1.5- 1.52	9.60E+01	0.22%	1.48E+02	0.26%	2.44E+02	0.34%	2.38E-07	
9	1.52- 1.736	1.02E+03	0.06%	1.45E+03	0.08%	2.47E+03	0.10%	2.41E-06	
8	1.736- 1.74	1.86E+01	0.48%	2.22E+01	0.66%	4.07E+01	0.82%	3.98E-08	
7	1.74- 1.76	7.09E+03	0.02%	1.10E+02	0.30%	7.20E+03	0.30%	7.03E-06	
6	1.76- 1.83	1.15E+02	0.12%	3.86E+02	0.16%	5.01E+02	0.20%	4.90E-07	
5	1.83- 1.832	4.02E+00	0.60%	1.04E+01	0.96%	1.44E+01	1.13%	1.41E-08	
4	1.832- 2.21	6.02E+02	0.06%	1.61E+03	0.08%	2.21E+03	0.10%	2.16E-06	
3	2.21- 2.25	2.28E+03	0.02%	4.28E+02	0.12%	2.71E+03	0.12%	2.64E-06	
2	2.25- 2.749	2.40E+03	0.02%	1.38E+03	0.08%	3.78E+03	0.08%	3.69E-06	
1	2.749- 2.75	2.68E+03	0.02%	2.00E+00	2.22%	2.68E+03	2.22%	2.62E-06	
Total		1.02E+09	0.12%	3.03E+04	0.02%	1.02E+09	0.12%		

**Lower bound for PENTRAN models was 0.29 MeV

APPENDIX A SOURCE BOOK

A.23. 1 year WGPu Shell Neutron Spectrum Outer Source Box

Side Surfaces

Group	Energy Bound	neutron Current	Leakage	σ_{f}	Normalized Leakage	Group	Energy Bound	neutron Current	Leakage	σ_{f}	Normalized Leakage
47	0 -1E-7	3.10E+01	0.0034	2.23E-04		21	6.08E-1 - 7.43E-1	7.48E+03	0.0002	5.38E-02	
46	1E-7 - 4.14E-7	4.08E+01	0.003	2.94E-04		20	7.43E-1 - 8.21E-1	4.13E+03	0.0004	2.97E-02	
45	4.14E-7 - 8.76E-7	2.73E+01	0.0038	1.97E-04		19	8.21E-1 - 1	8.48E+03	0.0002	6.10E-02	
44	8.76E-7 - 1.86E-6	3.48E+01	0.0034	2.51E-04		18	1 - 1.35	1.46E+04	0.0002	1.05E-01	
43	1.86E-6 - 5.04E-6	6.24E+01	0.0026	4.49E-04		17	1.35 - 1.65	1.09E+04	0.0002	7.83E-02	
42	5.04E-6 - 1.07E-5	6.44E+01	0.0024	4.63E-04		16	1.65 - 1.92	8.44E+03	0.0002	6.07E-02	
41	1.07E-5 - 3.73E-5	1.54E+02	0.0016	1.11E-03		15	1.92 - 2.23	8.24E+03	0.0002	5.93E-02	
40	3.73E-5 - 1.01E-4	1.84E+02	0.0014	1.32E-03		14	2.23 - 2.35	2.85E+03	0.0004	2.05E-02	
39	1.01E-4 - 2.14E-4	1.91E+02	0.0014	1.37E-03		13	2.35 - 2.37	4.85E+02	0.001	3.49E-03	
38	2.14E-4 - 4.54E-4	2.40E+02	0.0012	1.72E-03		12	2.37 - 2.47	2.42E+03	0.0004	1.74E-02	
37	4.54E-4 - 1.58E-3	6.05E+02	0.0008	4.35E-03		11	2.47 - 2.73	5.27E+03	0.0002	3.79E-02	
36	1.58E-3 - 3.35E-3	5.25E+02	0.0008	3.78E-03		10	2.73 - 3.01	4.72E+03	0.0002	3.40E-02	
35	3.35E-3 - 7.1E-3	7.31E+02	0.0008	5.26E-03		9	3.01 - 3.68	8.19E+03	0.0002	5.89E-02	
34	7.1E-3 - 1.5E-2	1.01E+03	0.0006	7.26E-03		8	3.68 - 4.97	8.66E+03	0.0002	6.23E-02	
33	1.5E-2 - 2.19E-2	6.77E+02	0.0008	4.87E-03		7	4.97 - 6.07	3.23E+03	0.0004	2.33E-02	
32	2.19E-2 - 2.42E-2	2.14E+02	0.0014	1.54E-03		6	6.07 - 7.41	1.65E+03	0.0004	1.19E-02	
31	2.42E-2 - 2.61E-2	1.84E+02	0.0014	1.32E-03		5	7.41 - 8.61	5.45E+02	0.0008	3.92E-03	
30	2.61E-2 - 3.18E-2	4.29E+02	0.001	3.08E-03		4	8.61 - 10	2.41E+02	0.0012	1.74E-03	
29	3.18E-2 - 4.09E-2	6.41E+02	0.0008	4.62E-03		3	10 - 12.2	1.08E+02	0.002	7.77E-04	
28	4.09E-2 - 6.74E-2	1.79E+03	0.0004	1.29E-02		2	12.2 - 14.2	1.97E+01	0.0044	1.42E-04	
27	6.74E-2 - 1.11E-1	2.64E+03	0.0004	1.90E-02		1	14.2 - 19.64	5.58E+00	0.0084	4.02E-05	
26	1.11E-1 - 1.83E-1	4.18E+03	0.0004	3.01E-02		Total			1.39E+05		
25	1.83E-1 - 2.97E-1	6.64E+03	0.0002	4.78E-02							
24	2.97E-1 - 3.69E-1	4.26E+03	0.0004	3.07E-02							
23	3.69E-1 - 4.98E-1	6.70E+03	0.0002	4.82E-02							
22	4.98E-1 - 6.08E-1	6.09E+03	0.0002	4.38E-02							

APPENDIX A SOURCE BOOK

A.23. 1 year WGPu Shell Neutron Spectrum Outer Source Box

Top/Bottom Surfaces

Group	Energy	Bound	neutron Current	Leakage	σ_{f}	error	normalized Leakage	Group	Energy	Bound	neutron Current	Leakage	σ_{f}	error	normalized Leakage
47	0 - 1E-7	2.23E+01	0.40%	2.39E-04				21	6.08E-1 - 7.43E-1	5.04E+03		0.02%		5.41E-02	
46	1E-7 - 4.14E-7	3.02E+01	0.36%	3.24E-04				20	7.43E-1 - 8.21E-1	2.77E+03		0.04%		2.97E-02	
45	4.14E-7 - 8.76E-7	2.05E+01	0.44%	2.20E-04				19	8.21E-1 - 1	5.70E+03		0.02%		6.12E-02	
44	8.76E-7 - 1.86E-6	2.61E+01	0.38%	2.80E-04				18	1 - 1.35	9.79E+03		0.02%		1.05E-01	
43	1.86E-6 - 5.04E-6	4.67E+01	0.30%	5.01E-04				17	1.35 - 1.65	7.28E+03		0.02%		7.81E-02	
42	5.04E-6 - 1.07E-5	4.78E+01	0.28%	5.13E-04				16	1.65 - 1.92	5.64E+03		0.02%		6.05E-02	
41	1.07E-5 - 3.73E-5	1.15E+02	0.18%	1.23E-03				15	1.92 - 2.23	5.48E+03		0.02%		5.88E-02	
40	3.73E-5 - 1.01E-4	1.35E+02	0.18%	1.45E-03				14	2.23 - 2.35	1.89E+03		0.04%		2.03E-02	
39	1.01E-4 - 2.14E-4	1.40E+02	0.16%	1.50E-03				13	2.35 - 2.37	3.22E+02		0.12%		3.46E-03	
38	2.14E-4 - 4.54E-4	1.74E+02	0.16%	1.87E-03				12	2.37 - 2.47	1.61E+03		0.06%		1.73E-02	
37	4.54E-4 - 1.58E-3	4.35E+02	0.10%	4.66E-03				11	2.47 - 2.73	3.49E+03		0.04%		3.75E-02	
36	1.58E-3 - 3.35E-3	3.71E+02	0.10%	3.98E-03				10	2.73 - 3.01	3.13E+03		0.04%		3.36E-02	
35	3.35E-3 - 7.1E-3	5.11E+02	0.08%	5.48E-03				9	3.01 - 3.68	5.46E+03		0.02%		5.86E-02	
34	7.1E-3 - 1.5E-2	6.94E+02	0.08%	7.45E-03				8	3.68 - 4.97	5.76E+03		0.02%		6.18E-02	
33	1.5E-2 - 2.19E-2	4.60E+02	0.10%	4.94E-03				7	4.97 - 6.07	2.14E+03		0.04%		2.29E-02	
32	2.19E-2 - 2.42E-2	1.46E+02	0.16%	1.57E-03				6	6.07 - 7.41	1.09E+03		0.06%		1.17E-02	
31	2.42E-2 - 2.61E-2	1.26E+02	0.18%	1.35E-03				5	7.41 - 8.61	3.60E+02		0.10%		3.86E-03	
30	2.61E-2 - 3.18E-2	2.87E+02	0.12%	3.08E-03				4	8.61 - 10	1.59E+02		0.16%		1.71E-03	
29	3.18E-2 - 4.09E-2	4.30E+02	0.10%	4.61E-03				3	10 - 12.2	7.10E+01		0.24%		7.62E-04	
28	4.09E-2 - 6.74E-2	1.20E+03	0.06%	1.29E-02				2	12.2 - 14.2	1.29E+01		0.56%		1.39E-04	
27	6.74E-2 - 1.11E-1	1.77E+03	0.04%	1.90E-02				1	14.2 - 19.64	3.66E+00		1.04%		3.93E-05	
26	1.11E-1 - 1.83E-1	2.81E+03	0.04%	3.02E-02				Total			9.32E+04		0.00%		
25	1.83E-1 - 2.97E-1	4.47E+03	0.02%	4.80E-02											
24	2.97E-1 - 3.69E-1	2.87E+03	0.04%	3.08E-02											
23	3.69E-1 - 4.98E-1	4.53E+03	0.02%	4.86E-02											
22	4.98E-1 - 6.08E-1	4.12E+03	0.04%	4.42E-02											

APPENDIX A SOURCE BOOK

A.24. 1 year WGPu Solid Gamma Spectrum Inner Source Box

Side Surfaces

MCNP

Group Energy Bound Intrinsic Current Leakage sigma error induced Current Leakage sigma error total Current Leakage sigma error Normalized Leakage

	(MeV)	(Photons/s)		(Photons/s)		(Photons/s)		(Photons/s)	
24	0 -0.3 **	6.95E+08	0.16%	2.72E+04	0.02%	6.95E+08	0.16%	9.90E-01	
23	0.3- 0.741	6.54E+06	0.06%	8.66E+04	0.02%	6.63E+06	0.06%	9.44E-03	
22	0.741- 0.743	2.46E+03	0.06%	3.94E+02	0.14%	2.85E+03	0.15%	4.06E-06	
21	0.743- 0.765	2.16E+04	0.04%	4.30E+03	0.04%	2.59E+04	0.06%	3.68E-05	
20	0.765- 0.767	1.60E+04	0.04%	3.88E+02	0.14%	1.64E+04	0.15%	2.34E-05	
19	0.767- 0.954	2.33E+04	0.04%	3.67E+04	0.02%	6.00E+04	0.04%	8.55E-05	
18	0.954- 0.956	3.02E+02	0.06%	3.48E+02	0.16%	6.50E+02	0.17%	9.26E-07	
17	0.956- 0.999	8.22E+02	0.08%	7.04E+03	0.04%	7.87E+03	0.09%	1.12E-05	
16	0.999- 1.002	2.72E+02	0.08%	4.77E+02	0.14%	7.49E+02	0.16%	1.07E-06	
15	1.002- 1.18	2.14E+03	0.06%	3.18E+04	0.02%	3.40E+04	0.06%	4.84E-05	
14	1.18- 1.2	2.14E+02	0.22%	2.76E+03	0.06%	2.97E+03	0.23%	4.23E-06	
13	1.2- 1.24	4.18E+02	0.16%	5.36E+03	0.04%	5.78E+03	0.16%	8.23E-06	
12	1.24- 1.26	9.08E+03	0.04%	2.59E+03	0.06%	1.17E+04	0.07%	1.66E-05	
11	1.26- 1.5	9.44E+02	0.06%	2.67E+04	0.02%	2.77E+04	0.06%	3.94E-05	
10	1.5- 1.52	7.82E+01	0.24%	1.90E+03	0.06%	1.98E+03	0.25%	2.81E-06	
9	1.52- 1.736	8.34E+02	0.08%	1.85E+04	0.02%	1.94E+04	0.08%	2.76E-05	
8	1.736- 1.74	1.50E+01	0.52%	2.89E+02	0.16%	3.04E+02	0.54%	4.34E-07	
7	1.74- 1.76	5.47E+03	0.04%	1.43E+03	0.08%	6.89E+03	0.09%	9.82E-06	
6	1.76- 1.83	9.79E+01	0.14%	4.78E+03	0.04%	4.88E+03	0.15%	6.96E-06	
5	1.83- 1.832	3.37E+00	0.66%	1.35E+02	0.24%	1.39E+02	0.70%	1.97E-07	
4	1.832- 2.21	5.11E+02	0.06%	2.09E+04	0.02%	2.14E+04	0.06%	3.05E-05	
3	2.21- 2.25	1.77E+03	0.04%	4.70E+03	0.04%	6.47E+03	0.06%	9.21E-06	
2	2.25- 2.749	1.89E+03	0.02%	1.79E+04	0.02%	1.97E+04	0.03%	2.81E-05	
1	2.749- 2.75	2.07E+03	0.04%	2.66E+01	0.56%	2.10E+03	0.56%	2.99E-06	
Total		7.02E+08	0.16%	3.03E+05	0.02%	7.02E+08	0.16%		

APPENDIX A SOURCE BOOK

A.24. 1 year WGPu Solid Gamma Spectrum Inner Source Box

	Top/Bottom Surfaces	MCNP	Group Energy Bound	Intrinsic Current Leakage	sigma error	produced Current Leakage	sigma error	total Current Leakage	sigma error	Normalized Leakage
	(MeV)	(Photons/s)		(Photons/s)		(Photons/s)		(Photons/s)		
24	0 -0.3 **	6.96E+08	0.16%	2.72E+04	0.02%	6.96E+08	0.16%	9.90E-01		
23	0.3- 0.741	6.54E+06	0.06%	8.66E+04	0.02%	6.62E+06	0.06%	9.43E-03		
22	0.741- 0.743	2.46E+03	0.06%	3.93E+02	0.14%	2.85E+03	0.15%	4.06E-06		
21	0.743- 0.765	2.16E+04	0.04%	4.30E+03	0.04%	2.59E+04	0.06%	3.68E-05		
20	0.765- 0.767	1.60E+04	0.04%	3.89E+02	0.14%	1.64E+04	0.15%	2.34E-05		
19	0.767- 0.954	2.33E+04	0.04%	3.67E+04	0.02%	6.00E+04	0.04%	8.54E-05		
18	0.954- 0.956	3.03E+02	0.06%	3.48E+02	0.16%	6.51E+02	0.17%	9.26E-07		
17	0.956- 0.999	8.23E+02	0.08%	7.04E+03	0.04%	7.87E+03	0.09%	1.12E-05		
16	0.999- 1.002	2.72E+02	0.08%	4.77E+02	0.14%	7.49E+02	0.16%	1.07E-06		
15	1.002- 1.18	2.14E+03	0.06%	3.18E+04	0.02%	3.40E+04	0.06%	4.83E-05		
14	1.18- 1.2	2.14E+02	0.22%	2.76E+03	0.06%	2.97E+03	0.23%	4.23E-06		
13	1.2- 1.24	4.18E+02	0.16%	5.36E+03	0.04%	5.78E+03	0.16%	8.22E-06		
12	1.24- 1.26	9.08E+03	0.04%	2.59E+03	0.06%	1.17E+04	0.07%	1.66E-05		
11	1.26- 1.5	9.45E+02	0.06%	2.67E+04	0.02%	2.77E+04	0.06%	3.94E-05		
10	1.5- 1.52	7.83E+01	0.24%	1.90E+03	0.06%	1.98E+03	0.25%	2.81E-06		
9	1.52- 1.736	8.34E+02	0.08%	1.85E+04	0.02%	1.94E+04	0.08%	2.75E-05		
8	1.736- 1.74	1.49E+01	0.52%	2.90E+02	0.16%	3.04E+02	0.54%	4.33E-07		
7	1.74- 1.76	5.47E+03	0.04%	1.43E+03	0.08%	6.89E+03	0.09%	9.81E-06		
6	1.76- 1.83	9.78E+01	0.14%	4.79E+03	0.04%	4.88E+03	0.15%	6.95E-06		
5	1.83- 1.832	3.37E+00	0.66%	1.35E+02	0.24%	1.39E+02	0.70%	1.97E-07		
4	1.832- 2.21	5.11E+02	0.06%	2.09E+04	0.02%	2.14E+04	0.06%	3.05E-05		
3	2.21- 2.25	1.77E+03	0.04%	4.70E+03	0.04%	6.47E+03	0.06%	9.20E-06		
2	2.25- 2.749	1.89E+03	0.02%	1.79E+04	0.02%	1.97E+04	0.03%	2.81E-05		
1	2.749- 2.75	2.07E+03	0.04%	2.67E+01	0.56%	2.10E+03	0.56%	2.99E-06		
Total		7.02E+08	0.16%	3.03E+05	0.02%	7.03E+08	0.16%			

**Lower bound for PENTRAN models was 0.29 MeV

APPENDIX A SOURCE BOOK

A.25. 1 year WGPu Solid Gamma Spectrum Outer Source Box

Side Surfaces

MCNP

Group Energy Bound Intrinsic Current Leakage sigma error induced Current Leakage 2 sigma error total Current Leakage sigma error Normalized Leakage

	(MeV)	(Photons/s)		(Photons/s)		(Photons/s)		(Photons/s)
24	0 -0.3 **	6.63E+08	0.16%	4.64E+04	0.02%	6.63E+08	0.16%	9.89E-01
23	0.3- 0.741	6.73E+06	0.06%	1.04E+05	0.02%	6.83E+06	0.06%	1.02E-02
22	0.741- 0.743	2.35E+03	0.06%	4.34E+02	0.14%	2.79E+03	0.15%	4.16E-06
21	0.743- 0.765	2.07E+04	0.04%	4.74E+03	0.04%	2.54E+04	0.06%	3.79E-05
20	0.765- 0.767	1.51E+04	0.06%	4.27E+02	0.14%	1.55E+04	0.15%	2.32E-05
19	0.767- 0.954	2.33E+04	0.04%	4.29E+04	0.02%	6.62E+04	0.04%	9.89E-05
18	0.954- 0.956	2.97E+02	0.06%	3.75E+02	0.14%	6.71E+02	0.15%	1.00E-06
17	0.956- 0.999	9.12E+02	0.08%	7.57E+03	0.04%	8.49E+03	0.09%	1.27E-05
16	0.999- 1.002	2.71E+02	0.08%	5.13E+02	0.12%	7.83E+02	0.14%	1.17E-06
15	1.002- 1.18	2.52E+03	0.06%	3.35E+04	0.02%	3.60E+04	0.06%	5.37E-05
14	1.18- 1.2	2.56E+02	0.20%	2.92E+03	0.06%	3.18E+03	0.21%	4.75E-06
13	1.2- 1.24	5.00E+02	0.14%	6.06E+03	0.04%	6.56E+03	0.15%	9.79E-06
12	1.24- 1.26	8.99E+03	0.04%	2.76E+03	0.06%	1.17E+04	0.07%	1.75E-05
11	1.26- 1.5	1.13E+03	0.06%	2.97E+04	0.02%	3.08E+04	0.06%	4.60E-05
10	1.5- 1.52	9.35E+01	0.22%	2.02E+03	0.06%	2.12E+03	0.23%	3.16E-06
9	1.52- 1.736	9.95E+02	0.06%	1.98E+04	0.02%	2.08E+04	0.06%	3.11E-05
8	1.736- 1.74	1.79E+01	0.48%	3.10E+02	0.16%	3.28E+02	0.51%	4.89E-07
7	1.74- 1.76	5.55E+03	0.04%	1.53E+03	0.08%	7.08E+03	0.09%	1.06E-05
6	1.76- 1.83	1.17E+02	0.12%	5.34E+03	0.04%	5.46E+03	0.13%	8.15E-06
5	1.83- 1.832	3.93E+00	0.62%	1.44E+02	0.24%	1.48E+02	0.66%	2.21E-07
4	1.832- 2.21	6.13E+02	0.06%	2.25E+04	0.02%	2.31E+04	0.06%	3.45E-05
3	2.21- 2.25	1.83E+03	0.04%	4.93E+03	0.04%	6.76E+03	0.06%	1.01E-05
2	2.25- 2.749	2.01E+03	0.02%	1.93E+04	0.02%	2.14E+04	0.03%	3.19E-05
1	2.749- 2.75	2.16E+03	0.04%	2.85E+01	0.54%	2.19E+03	0.54%	3.27E-06
Total		6.69E+08	0.16%	3.59E+05	0.02%	6.70E+08	0.16%	

APPENDIX A SOURCE BOOK

A.25. 1 year WGPu Solid Gamma Spectrum Outer Source Box

	Top/Bottom Surfaces	MCNP	Group Energy Bound	Intrinsic Current Leakage	sigma err	produced Current Leakage	sigma erro	total Current Leakage	sigma erro	Normalized Leakage
	(MeV)	(Photons/s)		(Photons/s)		(Photons/s)		(Photons/s)		
24	0 -0.3 **	3.84E+08	0.20%	2.77E+04	0.02%	3.84E+08	0.20%	9.90E-01		
23	0.3- 0.741	3.82E+06	0.08%	6.12E+04	0.02%	3.89E+06	0.08%	1.00E-02		
22	0.741- 0.743	1.32E+03	0.08%	2.46E+02	0.18%	1.57E+03	0.20%	4.04E-06		
21	0.743- 0.765	1.16E+04	0.06%	2.70E+03	0.06%	1.43E+04	0.08%	3.69E-05		
20	0.765- 0.767	8.49E+03	0.06%	2.43E+02	0.18%	8.73E+03	0.19%	2.25E-05		
19	0.767- 0.954	1.31E+04	0.06%	2.46E+04	0.02%	3.77E+04	0.06%	9.71E-05		
18	0.954- 0.956	1.67E+02	0.08%	2.11E+02	0.20%	3.78E+02	0.22%	9.74E-07		
17	0.956- 0.999	5.12E+02	0.10%	4.26E+03	0.04%	4.78E+03	0.11%	1.23E-05		
16	0.999- 1.002	1.52E+02	0.10%	2.89E+02	0.16%	4.40E+02	0.19%	1.14E-06		
15	1.002- 1.18	1.41E+03	0.08%	1.88E+04	0.02%	2.02E+04	0.08%	5.21E-05		
14	1.18- 1.2	1.42E+02	0.26%	1.64E+03	0.08%	1.78E+03	0.27%	4.60E-06		
13	1.2- 1.24	2.78E+02	0.18%	3.44E+03	0.06%	3.72E+03	0.19%	9.58E-06		
12	1.24- 1.26	5.03E+03	0.04%	1.55E+03	0.08%	6.58E+03	0.09%	1.70E-05		
11	1.26- 1.5	6.32E+02	0.08%	1.68E+04	0.02%	1.74E+04	0.08%	4.48E-05		
10	1.5- 1.52	5.20E+01	0.30%	1.13E+03	0.08%	1.18E+03	0.31%	3.05E-06		
9	1.52- 1.736	5.53E+02	0.08%	1.11E+04	0.04%	1.17E+04	0.09%	3.00E-05		
8	1.736- 1.74	9.85E+00	0.66%	1.73E+02	0.22%	1.83E+02	0.70%	4.71E-07		
7	1.74- 1.76	3.10E+03	0.04%	8.56E+02	0.10%	3.96E+03	0.11%	1.02E-05		
6	1.76- 1.83	6.52E+01	0.16%	3.01E+03	0.06%	3.08E+03	0.17%	7.94E-06		
5	1.83- 1.832	2.20E+00	0.82%	8.05E+01	0.32%	8.27E+01	0.88%	2.13E-07		
4	1.832- 2.21	3.40E+02	0.08%	1.26E+04	0.04%	1.29E+04	0.09%	3.34E-05		
3	2.21- 2.25	1.02E+03	0.04%	2.76E+03	0.04%	3.78E+03	0.06%	9.74E-06		
2	2.25- 2.749	1.12E+03	0.04%	1.08E+04	0.04%	1.19E+04	0.06%	3.08E-05		
1	2.749- 2.75	1.21E+03	0.04%	1.60E+01	0.70%	1.22E+03	0.70%	3.15E-06		
Total		3.88E+08	0.20%	2.06E+05	0.02%	3.88E+08	0.20%			

**Lower bound for PENTRAN models was 0.29 MeV

APPENDIX A SOURCE BOOK

A.26. 1 year WGPu Solid Neutron Spectrum Outer Source Box

Side Surfaces

Group	Energy	Bound	neutron Current	Leakage	sigma error	normalized Leakage	Group	Energy	Bound	neutron Current	Leakage	sigma error	normalized Leakage
47	0 - 1E-7	2.87E+02	0.10%	2.46E-04			21	5.08E-1 - 7.43E-1	6.35E+04		0.02%		5.44E-02
46	1E-7 - 4.14E-7	3.72E+02	0.10%	3.19E-04			20	7.43E-1 - 8.21E-1	3.46E+04		0.02%		2.97E-02
45	4.14E-7 - 8.76E-7	2.47E+02	0.12%	2.12E-04			19	8.21E-1 - 1	6.95E+04		0.02%		5.95E-02
44	8.76E-7 - 1.86E-6	3.14E+02	0.10%	2.69E-04			18	1 - 1.35	1.15E+05		0.02%		9.89E-02
43	1.86E-6 - 5.04E-6	5.60E+02	0.08%	4.80E-04			17	1.35 - 1.65	8.44E+04		0.02%		7.23E-02
42	5.04E-6 - 1.07E-5	5.76E+02	0.08%	4.94E-04			16	1.65 - 1.92	6.52E+04		0.02%		5.58E-02
41	1.07E-5 - 3.73E-5	1.38E+03	0.06%	1.18E-03			15	1.92 - 2.23	6.37E+04		0.02%		5.45E-02
40	3.73E-5 - 1.01E-4	1.64E+03	0.04%	1.40E-03			14	2.23 - 2.35	2.26E+04		0.02%		1.94E-02
39	1.01E-4 - 2.14E-4	1.70E+03	0.04%	1.46E-03			13	2.35 - 2.37	3.80E+03		0.04%		3.25E-03
38	2.14E-4 - 4.54E-4	2.12E+03	0.04%	1.82E-03			12	2.37 - 2.47	1.87E+04		0.02%		1.60E-02
37	4.54E-4 - 1.58E-3	5.35E+03	0.02%	4.59E-03			11	2.47 - 2.73	4.16E+04		0.02%		3.56E-02
36	1.58E-3 - 3.35E-3	4.63E+03	0.04%	3.97E-03			10	2.73 - 3.01	3.74E+04		0.02%		3.21E-02
35	3.35E-3 - 7.1E-3	6.45E+03	0.02%	5.52E-03			9	3.01 - 3.68	6.72E+04		0.02%		5.76E-02
34	7.1E-3 - 1.5E-2	8.93E+03	0.02%	7.65E-03			8	3.68 - 4.97	7.42E+04		0.02%		6.36E-02
33	1.5E-2 - 2.19E-2	6.01E+03	0.02%	5.15E-03			7	4.97 - 6.07	3.04E+04		0.02%		2.60E-02
32	2.19E-2 - 2.42E-2	1.91E+03	0.04%	1.64E-03			6	6.07 - 7.41	1.71E+04		0.02%		1.47E-02
31	2.42E-2 - 2.61E-2	1.64E+03	0.04%	1.41E-03			5	7.41 - 8.61	6.33E+03		0.02%		5.42E-03
30	2.61E-2 - 3.18E-2	3.78E+03	0.04%	3.24E-03			4	8.61 - 10	3.06E+03		0.04%		2.62E-03
29	3.18E-2 - 4.09E-2	5.76E+03	0.02%	4.94E-03			3	10 - 12.2	1.53E+03		0.04%		1.31E-03
28	4.09E-2 - 6.74E-2	1.62E+04	0.02%	1.39E-02			2	12.2 - 14.2	3.12E+02		0.10%		2.67E-04
27	6.74E-2 - 1.11E-1	2.41E+04	0.02%	2.06E-02			1	14.2 - 19.64	9.50E+01		0.18%		8.14E-05
26	1.11E-1 - 1.83E-1	3.85E+04	0.02%	3.30E-02			Total			1.17E+06		0.02%	
25	1.83E-1 - 2.97E-1	6.15E+04	0.02%	5.27E-02									
24	2.97E-1 - 3.69E-1	3.90E+04	0.02%	3.35E-02									
23	3.69E-1 - 4.98E-1	6.02E+04	0.02%	5.16E-02									
22	4.98E-1 - 6.08E-1	5.34E+04	0.02%	4.57E-02									

APPENDIX A SOURCE BOOK

A.26. 1 year WGPu Solid Neutron Spectrum Outer Source Box

Top/Bottom Surfaces

Group	Energy Bound	neutron Current	Leakag	σ sigma erro	normalized Leakkag	Group	Energy Bound	neutron Current	Leakag	σ sigma erro	normalized Leakkag
47	0 -1E-7	1.88E+02	0.12%	2.76E-04		21	6.08E-1 - 7.43E-1	3.74E+04	0.02%	5.48E-02	
46	1E-7 - 4.14E-7	2.48E+02	0.12%	3.64E-04		20	7.43E-1 - 8.21E-1	2.02E+04	0.02%	2.96E-02	
45	4.14E-7 - 8.76E-7	1.66E+02	0.14%	2.43E-04		19	8.21E-1 - 1	4.07E+04	0.02%	5.97E-02	
44	8.76E-7 - 1.86E-6	2.11E+02	0.12%	3.09E-04		18	1 - 1.35	6.76E+04	0.02%	9.91E-02	
43	1.86E-6 - 5.04E-6	3.75E+02	0.10%	5.51E-04		17	1.35 - 1.65	4.89E+04	0.02%	7.17E-02	
42	5.04E-6 - 1.07E-5	3.85E+02	0.10%	5.64E-04		16	1.65 - 1.92	3.76E+04	0.02%	5.51E-02	
41	1.07E-5 - 3.73E-5	9.17E+02	0.06%	1.35E-03		15	1.92 - 2.23	3.65E+04	0.02%	5.36E-02	
40	3.73E-5 - 1.01E-4	1.08E+03	0.06%	1.59E-03		14	2.23 - 2.35	1.29E+04	0.02%	1.89E-02	
39	1.01E-4 - 2.14E-4	1.12E+03	0.06%	1.64E-03		13	2.35 - 2.37	2.16E+03	0.04%	3.17E-03	
38	2.14E-4 - 4.54E-4	1.39E+03	0.06%	2.03E-03		12	2.37 - 2.47	1.07E+04	0.02%	1.56E-02	
37	4.54E-4 - 1.58E-3	3.46E+03	0.04%	5.07E-03		11	2.47 - 2.73	2.37E+04	0.02%	3.47E-02	
36	1.58E-3 - 3.35E-3	2.95E+03	0.04%	4.32E-03		10	2.73 - 3.01	2.14E+04	0.02%	3.13E-02	
35	3.35E-3 - 7.1E-3	4.05E+03	0.04%	5.94E-03		9	3.01 - 3.68	3.87E+04	0.02%	5.67E-02	
34	7.1E-3 - 1.5E-2	5.51E+03	0.02%	8.08E-03		8	3.68 - 4.97	4.24E+04	0.02%	6.22E-02	
33	1.5E-2 - 2.19E-2	3.66E+03	0.04%	5.37E-03		7	4.97 - 6.07	1.72E+04	0.02%	2.53E-02	
32	2.19E-2 - 2.42E-2	1.16E+03	0.06%	1.70E-03		6	6.07 - 7.41	9.65E+03	0.02%	1.42E-02	
31	2.42E-2 - 2.61E-2	1.00E+03	0.06%	1.47E-03		5	7.41 - 8.61	3.58E+03	0.04%	5.24E-03	
30	2.61E-2 - 3.18E-2	2.28E+03	0.04%	3.34E-03		4	8.61 - 10	1.72E+03	0.04%	2.52E-03	
29	3.18E-2 - 4.09E-2	3.45E+03	0.04%	5.06E-03		3	10 - 12.2	8.59E+02	0.06%	1.26E-03	
28	4.09E-2 - 6.74E-2	9.71E+03	0.02%	1.42E-02		2	12.2 - 14.2	1.75E+02	0.14%	2.57E-04	
27	6.74E-2 - 1.11E-1	1.44E+04	0.02%	2.11E-02		1	14.2 - 19.64	5.34E+01	0.24%	7.83E-05	
26	1.11E-1 - 1.83E-1	2.30E+04	0.02%	3.37E-02		Total		6.82E+05	0.02%		
25	1.83E-1 - 2.97E-1	3.66E+04	0.02%	5.36E-02							
24	2.97E-1 - 3.69E-1	2.31E+04	0.02%	3.39E-02							
23	3.69E-1 - 4.98E-1	3.60E+04	0.02%	5.27E-02							
22	4.98E-1 - 6.08E-1	3.16E+04	0.02%	4.63E-02							

APPENDIX A SOURCE BOOK

A.27. 22.5 year WGPu Shell Gamma Spectrum Inner Source Box

Side Surfaces

MCNP

Group Energy Bound **Intrinsic Current Leakage** $\sigma_{\text{intrinsic}}$ **produced Current Leakage** σ_{produced} **total Current Leakage** σ_{total} **sigma error** σ_{error} **normalized Leakage**

	(MeV)	(Photons/s)	(Photons/s)	(Photons/s)	(Photons/s)	(Photons/s)	(Photons/s)
24	0 -0.3 **	2.45E+09	0.10%	4.18E+03	0.02%	2.45E+09	0.10%
23	0.3- 0.741	1.76E+07	0.04%	1.26E+04	0.02%	1.76E+07	0.04%
22	0.741- 0.743	7.56E+03	0.04%	5.46E+01	0.14%	7.62E+03	0.15%
21	0.743- 0.765	5.85E+04	0.02%	5.94E+02	0.04%	5.91E+04	0.04%
20	0.765- 0.767	4.20E+04	0.04%	5.34E+01	0.16%	4.20E+04	0.16%
19	0.767- 0.954	6.28E+04	0.02%	4.94E+03	0.02%	6.78E+04	0.03%
18	0.954- 0.956	9.71E+02	0.04%	4.47E+01	0.16%	1.02E+03	0.16%
17	0.956- 0.999	1.82E+03	0.06%	9.02E+02	0.04%	2.73E+03	0.07%
16	0.999- 1.002	5.85E+02	0.04%	6.07E+01	0.14%	6.46E+02	0.15%
15	1.002- 1.18	4.35E+03	0.04%	4.11E+03	0.02%	8.46E+03	0.04%
14	1.18- 1.2	4.19E+02	0.16%	3.34E+02	0.06%	7.53E+02	0.17%
13	1.2- 1.24	8.16E+02	0.10%	6.45E+02	0.04%	1.46E+03	0.11%
12	1.24- 1.26	2.18E+04	0.02%	3.09E+02	0.06%	2.21E+04	0.06%
11	1.26- 1.5	1.68E+03	0.06%	3.14E+03	0.02%	4.82E+03	0.06%
10	1.5- 1.52	1.39E+02	0.18%	2.19E+02	0.08%	3.58E+02	0.20%
9	1.52- 1.736	1.48E+03	0.06%	2.14E+03	0.02%	3.63E+03	0.06%
8	1.736- 1.74	2.71E+01	0.40%	3.28E+01	0.20%	5.99E+01	0.45%
7	1.74- 1.76	1.25E+04	0.02%	1.62E+02	0.08%	1.27E+04	0.08%
6	1.76- 1.83	1.66E+02	0.10%	5.42E+02	0.04%	7.08E+02	0.11%
5	1.83- 1.832	6.03E+00	0.48%	1.54E+01	0.28%	2.14E+01	0.56%
4	1.832- 2.21	8.71E+02	0.04%	2.36E+03	0.02%	3.23E+03	0.04%
3	2.21- 2.25	3.95E+03	0.02%	6.48E+02	0.04%	4.60E+03	0.04%
2	2.25- 2.749	4.05E+03	0.02%	2.01E+03	0.02%	6.07E+03	0.03%
1	2.749- 2.75	4.60E+03	0.02%	2.98E+00	0.64%	4.61E+03	0.64%
Total		2.47E+09	0.10%	4.01E+04	0.00%	2.47E+09	0.10%

**Lower bound for PENTRAN models was 0.29 MeV

APPENDIX A

SOURCE BOOK

A.27. 22.5 year WGpu Shell Gamma Spectrum Inner Source Box

Top/Bottom Surfaces

MCNP

Group Energy Bound intrinsic Current Leakage sigma errrorduced Current Leakage

	(MeV)	(Photons/s)	(Photons/s)	(Photons/s)	(Photons/s)	(Photons/s)
24	0 -0.3 **	2.45E+09	0.10%	4.21E+03	0.02%	2.45E+09
23	0.3- 0.741	1.76E+07	0.04%	1.26E+04	0.02%	1.76E+07
22	0.741- 0.743	7.56E+03	0.04%	5.45E+01	0.16%	7.62E+03
21	0.743- 0.765	5.86E+04	0.02%	5.93E+02	0.04%	5.91E+04
20	0.765- 0.767	4.20E+04	0.04%	5.33E+01	0.16%	4.20E+04
19	0.767- 0.954	6.28E+04	0.02%	4.94E+03	0.02%	6.78E+04
18	0.954- 0.956	9.72E+02	0.04%	4.46E+01	0.16%	1.02E+03
17	0.956- 0.999	1.82E+03	0.06%	9.01E+02	0.04%	2.72E+03
16	0.999- 1.002	5.85E+02	0.04%	6.06E+01	0.14%	6.46E+02
15	1.002- 1.18	4.35E+03	0.04%	4.11E+03	0.02%	8.46E+03
14	1.18- 1.2	4.19E+02	0.16%	3.34E+02	0.06%	7.52E+02
13	1.2- 1.24	8.16E+02	0.10%	6.45E+02	0.04%	1.46E+03
12	1.24- 1.26	2.18E+04	0.02%	3.09E+02	0.06%	2.21E+04
11	1.26- 1.5	1.68E+03	0.06%	3.14E+03	0.02%	4.82E+03
10	1.5- 1.52	1.39E+02	0.18%	2.19E+02	0.08%	3.58E+02
9	1.52- 1.736	1.48E+03	0.06%	2.14E+03	0.02%	3.63E+03
8	1.736- 1.74	2.71E+01	0.40%	3.28E+01	0.20%	6.00E+01
7	1.74- 1.76	1.25E+04	0.02%	1.62E+02	0.08%	1.27E+04
6	1.76- 1.83	1.66E+02	0.10%	5.42E+02	0.04%	7.08E+02
5	1.83- 1.832	6.04E+00	0.48%	1.54E+01	0.28%	2.14E+01
4	1.832- 2.21	8.71E+02	0.04%	2.36E+03	0.02%	3.23E+03
3	2.21- 2.25	3.95E+03	0.02%	6.48E+02	0.04%	4.60E+03
2	2.25- 2.749	4.05E+03	0.02%	2.01E+03	0.02%	6.07E+03
1	2.749- 2.75	4.60E+03	0.02%	2.98E+00	0.64%	4.61E+03
Total		2.47E+09	0.10%	4.01E+04	0.00%	2.47E+09
						0.10%
						1.0000E+00

**Lower bound for PENTRAN models was 0.29 MeV

APPENDIX A SOURCE BOOK

A.28. 22.5 year WGPu Shell Gamma spectrum Outer Source Box

Side Surfaces

Group Energy Bound Intrinsic Current Leaking² sigma error produced Current Leaking² sigma error total Current Leaking² sigma error normalized Leaking

	(MeV)	(Photons/s)		(Photons/s)		(Photons/s)		(Photons/s)	
24	0 -0.3 **	2.31E+09	0.10%	6.60E+03	0.02%	2.31E+09	0.10%	9.92E-01	
23	0.3- 0.741	1.81E+07	0.04%	1.49E+04	0.00%	1.81E+07	0.04%	7.75E-03	
22	0.741- 0.743	7.20E+03	0.04%	5.92E+01	0.14%	7.26E+03	0.15%	3.11E-06	
21	0.743- 0.765	5.60E+04	0.04%	6.45E+02	0.04%	5.66E+04	0.06%	2.43E-05	
20	0.765- 0.767	3.94E+04	0.04%	5.80E+01	0.14%	3.95E+04	0.15%	1.69E-05	
19	0.767- 0.954	6.25E+04	0.02%	5.69E+03	0.02%	6.82E+04	0.03%	2.92E-05	
18	0.954- 0.956	9.45E+02	0.04%	4.78E+01	0.16%	9.93E+02	0.16%	4.26E-07	
17	0.956- 0.999	2.02E+03	0.06%	9.63E+02	0.04%	2.98E+03	0.07%	1.28E-06	
16	0.999- 1.002	5.82E+02	0.06%	6.49E+01	0.14%	6.47E+02	0.15%	2.77E-07	
15	1.002- 1.18	5.21E+03	0.04%	4.29E+03	0.02%	9.50E+03	0.04%	4.07E-06	
14	1.18- 1.2	5.15E+02	0.14%	3.52E+02	0.06%	8.67E+02	0.15%	3.72E-07	
13	1.2- 1.24	1.01E+03	0.10%	7.25E+02	0.04%	1.73E+03	0.11%	7.42E-07	
12	1.24- 1.26	2.15E+04	0.02%	3.28E+02	0.06%	2.18E+04	0.06%	9.36E-06	
11	1.26- 1.5	2.09E+03	0.04%	3.48E+03	0.02%	5.57E+03	0.04%	2.39E-06	
10	1.5- 1.52	1.73E+02	0.16%	2.33E+02	0.08%	4.06E+02	0.18%	1.74E-07	
9	1.52- 1.736	1.84E+03	0.04%	2.29E+03	0.02%	4.12E+03	0.04%	1.77E-06	
8	1.736- 1.74	3.37E+01	0.36%	3.50E+01	0.18%	6.87E+01	0.40%	2.95E-08	
7	1.74- 1.76	1.27E+04	0.02%	1.73E+02	0.08%	1.29E+04	0.08%	5.52E-06	
6	1.76- 1.83	2.07E+02	0.10%	6.06E+02	0.04%	8.13E+02	0.11%	3.49E-07	
5	1.83- 1.832	7.20E+00	0.44%	1.63E+01	0.28%	2.35E+01	0.52%	1.01E-08	
4	1.832- 2.21	1.09E+03	0.04%	2.54E+03	0.02%	3.63E+03	0.04%	1.56E-06	
3	2.21- 2.25	4.08E+03	0.02%	6.77E+02	0.04%	4.76E+03	0.04%	2.04E-06	
2	2.25- 2.749	4.31E+03	0.02%	2.18E+03	0.02%	6.49E+03	0.03%	2.78E-06	
1	2.749- 2.75	4.80E+03	0.02%	3.18E+00	0.62%	4.80E+03	0.62%	2.06E-06	
Total		2.33E+09	0.10%	4.69E+04	0.00%	2.33E+09	0.10%		

**Lower bound for PENTRAN models was 0.29 MeV

APPENDIX A SOURCE BOOK

A.28. 22.5 year WGPu Shell Gamma spectrum Outer Source Box

Top/Bottom Surfaces

Group Energy Bound Intrinsic Current Leakage sigma error induced Current Leakage sigma error Total Current Leakage sigma error Normalized Leakage

	(MeV)	(Photons/s)	(Photons/s)	(Photons/s)	(Photons/s)	(Photons/s)	(Photons/s)
24	0 -0.3 **	1.34E+09	0.12%	3.95E+03	0.02%	1.34E+09	0.12% 9.92E-01
23	0.3- 0.741	1.03E+07	0.04%	8.67E+03	0.02%	1.03E+07	0.04% 7.61E-03
22	0.741- 0.743	4.05E+03	0.04%	3.36E+01	0.18%	4.08E+03	0.18% 3.02E-06
21	0.743- 0.765	3.15E+04	0.04%	3.66E+02	0.06%	3.18E+04	0.07% 2.36E-05
20	0.765- 0.767	2.22E+04	0.04%	3.28E+01	0.20%	2.22E+04	0.20% 1.64E-05
19	0.767- 0.954	3.51E+04	0.04%	3.25E+03	0.02%	3.84E+04	0.04% 2.84E-05
18	0.954- 0.956	5.31E+02	0.04%	2.69E+01	0.20%	5.58E+02	0.20% 4.13E-07
17	0.956- 0.999	1.14E+03	0.06%	5.42E+02	0.04%	1.68E+03	0.07% 1.24E-06
16	0.999- 1.002	3.27E+02	0.06%	3.64E+01	0.18%	3.63E+02	0.19% 2.69E-07
15	1.002- 1.18	2.92E+03	0.06%	2.41E+03	0.02%	5.32E+03	0.06% 3.94E-06
14	1.18- 1.2	2.86E+02	0.18%	1.98E+02	0.08%	4.84E+02	0.20% 3.59E-07
13	1.2- 1.24	5.60E+02	0.14%	4.11E+02	0.06%	9.71E+02	0.15% 7.19E-07
12	1.24- 1.26	1.20E+04	0.04%	1.84E+02	0.08%	1.22E+04	0.09% 9.06E-06
11	1.26- 1.5	1.17E+03	0.06%	1.97E+03	0.02%	3.13E+03	0.06% 2.32E-06
10	1.5- 1.52	9.60E+01	0.22%	1.31E+02	0.10%	2.27E+02	0.24% 1.68E-07
9	1.52- 1.736	1.02E+03	0.06%	1.28E+03	0.04%	2.30E+03	0.07% 1.70E-06
8	1.736- 1.74	1.86E+01	0.48%	1.96E+01	0.24%	3.82E+01	0.54% 2.83E-08
7	1.74- 1.76	7.10E+03	0.02%	9.70E+01	0.12%	7.19E+03	0.12% 5.33E-06
6	1.76- 1.83	1.15E+02	0.12%	3.42E+02	0.06%	4.57E+02	0.13% 3.38E-07
5	1.83- 1.832	4.02E+00	0.60%	9.12E+00	0.36%	1.31E+01	0.70% 9.73E-09
4	1.832- 2.21	6.02E+02	0.06%	1.42E+03	0.02%	2.02E+03	0.06% 1.50E-06
3	2.21- 2.25	2.28E+03	0.02%	3.78E+02	0.04%	2.66E+03	0.04% 1.97E-06
2	2.25- 2.749	2.40E+03	0.02%	1.22E+03	0.04%	3.62E+03	0.04% 2.68E-06
1	2.749- 2.75	2.68E+03	0.02%	1.79E+00	0.82%	2.68E+03	0.82% 1.98E-06
Total		1.35E+09	0.12%	2.70E+04	0.00%	1.35E+09	0.12%

**Lower bound for PENTRAN models was 0.29 MeV

APPENDIX A SOURCE BOOK

A.29. 22.5 year WGPu Shell Neutron Spectrum Outer Source Box

Side Surfaces

47 GROUP

Group	Energy Bounds (MeV)	Neutron Current Leakage (Neutrons/s)	2 sigma error	Normalized Leakage
47	0 -1E-7	3.14E+01	0.12%	2.19E-04
46	1E-7 - 4.14E-7	4.16E+01	0.10%	2.90E-04
45	4.14E-7 - 8.76E-7	2.79E+01	0.14%	1.95E-04
44	8.76E-7 - 1.86E-6	3.55E+01	0.12%	2.48E-04
43	1.86E-6 - 5.04E-6	6.38E+01	0.08%	4.45E-04
42	5.04E-6 - 1.07E-5	6.56E+01	0.08%	4.59E-04
41	1.07E-5 - 3.73E-5	1.58E+02	0.06%	1.10E-03
40	3.73E-5 - 1.01E-4	1.88E+02	0.06%	1.31E-03
39	1.01E-4 - 2.14E-4	1.95E+02	0.06%	1.36E-03
38	2.14E-4 - 4.54E-4	2.45E+02	0.04%	1.71E-03
37	4.54E-4 - 1.58E-3	6.18E+02	0.02%	4.32E-03
36	1.58E-3 - 3.35E-3	5.36E+02	0.04%	3.74E-03
35	3.35E-3 - 7.1E-3	7.47E+02	0.02%	5.21E-03
34	7.1E-3 - 1.5E-2	1.03E+03	0.02%	7.20E-03
33	1.5E-2 - 2.19E-2	6.91E+02	0.02%	4.83E-03
32	2.19E-2 - 2.42E-2	2.19E+02	0.04%	1.53E-03
31	2.42E-2 - 2.61E-2	1.89E+02	0.06%	1.32E-03
30	2.61E-2 - 3.18E-2	4.37E+02	0.04%	3.05E-03
29	3.18E-2 - 4.09E-2	6.55E+02	0.02%	4.58E-03
28	4.09E-2 - 6.74E-2	1.83E+03	0.02%	1.28E-02
27	6.74E-2 - 1.11E-1	2.71E+03	0.02%	1.89E-02
26	1.11E-1 - 1.83E-1	4.29E+03	0.02%	2.99E-02
25	1.83E-1 - 2.97E-1	6.82E+03	0.00%	4.76E-02
24	2.97E-1 - 3.69E-1	4.38E+03	0.02%	3.06E-02

Group	Energy Bounds (MeV)	Neutron Current Leakage (Neutrons/s)	2 sigma error	Normalized Leakage
23	3.69E-1 - 4.98E-1	6.88E+03	0.00%	4.81E-02
22	4.98E-1 - 6.08E-1	6.27E+03	0.00%	4.38E-02
21	5.08E-1 - 7.43E-1	7.70E+03	0.00%	5.38E-02
20	7.43E-1 - 8.21E-1	4.26E+03	0.02%	2.97E-02
19	8.21E-1 - 1	8.74E+03	0.00%	6.11E-02
17	1.35 - 1.65	1.12E+04	0.00%	7.84E-02
16	1.65 - 1.92	8.71E+03	0.00%	6.08E-02
15	1.92 - 2.23	8.50E+03	0.00%	5.94E-02
14	2.23 - 2.35	2.95E+03	0.02%	2.06E-02
13	2.35 - 2.37	5.01E+02	0.04%	3.50E-03
12	2.37 - 2.47	2.50E+03	0.02%	1.75E-02
11	2.47 - 2.73	5.44E+03	0.00%	3.80E-02
10	2.73 - 3.01	4.87E+03	0.02%	3.40E-02
9	3.01 - 3.68	8.45E+03	0.00%	5.90E-02
8	3.68 - 4.97	8.95E+03	0.00%	6.25E-02
7	4.97 - 6.07	3.34E+03	0.02%	2.34E-02
6	6.07 - 7.41	1.71E+03	0.02%	1.19E-02
5	7.41 - 8.61	5.64E+02	0.02%	3.94E-03
4	8.61 - 10	2.50E+02	0.04%	1.74E-03
3	10 - 12.2	1.12E+02	0.06%	7.79E-04
2	12.2 - 14.2	2.04E+01	0.16%	1.42E-04
1	14.2 - 19.64	5.80E+00	0.30%	4.05E-05
Total		1.43E+05	0.00%	
		average 2 sigma error	0.05%	

APPENDIX A SOURCE BOOK

A.29. 22.5 year WGPu Shell Neutron Spectrum Outer Source Box

Top/Bottom Surfaces

47 GROUP

Group	Energy Bounds (MeV)	Neutron Current Leakage (Neutrons/s)	2 sigma error	Normalized Leakage
47	0 -1E-7	2.07E+01	0.14%	2.48E-04
46	1E-7 - 4.14E-7	2.79E+01	0.14%	3.33E-04
45	4.14E-7 - 8.76E-7	1.88E+01	0.16%	2.25E-04
44	8.76E-7 - 1.86E-6	2.40E+01	0.14%	2.86E-04
43	1.86E-6 - 5.04E-6	4.30E+01	0.10%	5.14E-04
42	5.04E-6 - 1.07E-5	4.40E+01	0.10%	5.27E-04
41	1.07E-5 - 3.73E-5	1.05E+02	0.06%	1.26E-03
40	3.73E-5 - 1.01E-4	1.25E+02	0.06%	1.49E-03
39	1.01E-4 - 2.14E-4	1.29E+02	0.06%	1.54E-03
38	2.14E-4 - 4.54E-4	1.60E+02	0.06%	1.91E-03
37	4.54E-4 - 1.58E-3	4.00E+02	0.04%	4.78E-03
36	1.58E-3 - 3.35E-3	3.42E+02	0.04%	4.09E-03
35	3.35E-3 - 7.1E-3	4.70E+02	0.04%	5.62E-03
34	7.1E-3 - 1.5E-2	6.38E+02	0.02%	7.63E-03
33	1.5E-2 - 2.19E-2	4.23E+02	0.04%	5.05E-03
32	2.19E-2 - 2.42E-2	1.34E+02	0.06%	1.60E-03
31	2.42E-2 - 2.61E-2	1.16E+02	0.06%	1.38E-03
30	2.61E-2 - 3.18E-2	2.65E+02	0.04%	3.17E-03
29	3.18E-2 - 4.09E-2	3.94E+02	0.04%	4.71E-03
28	4.09E-2 - 6.74E-2	1.10E+03	0.02%	1.32E-02
27	6.74E-2 - 1.11E-1	1.62E+03	0.02%	1.94E-02
26	1.11E-1 - 1.83E-1	2.56E+03	0.02%	3.06E-02
25	1.83E-1 - 2.97E-1	4.06E+03	0.02%	4.85E-02
24	2.97E-1 - 3.69E-1	2.60E+03	0.02%	3.11E-02

47 GROUP

Group	Energy Bounds (MeV)	Neutron Current Leakage (Neutrons/s)	2 sigma error	Normalized Leakage
23	3.69E-1 - 4.98E-1	4.11E+03	0.02%	4.92E-02
22	4.98E-1 - 6.08E-1	3.71E+03	0.02%	4.44E-02
21	6.08E-1 - 7.43E-1	4.54E+03	0.02%	5.42E-02
20	7.43E-1 - 8.21E-1	2.49E+03	0.02%	2.98E-02
19	8.21E-1 - 1	5.13E+03	0.00%	6.13E-02
18	1 - 1.35	8.78E+03	0.00%	1.05E-01
16	1.65 - 1.92	5.03E+03	0.02%	6.01E-02
15	1.92 - 2.23	4.88E+03	0.02%	5.83E-02
14	2.23 - 2.35	1.68E+03	0.02%	2.01E-02
13	2.35 - 2.37	2.86E+02	0.04%	3.42E-03
12	2.37 - 2.47	1.43E+03	0.02%	1.71E-02
11	2.47 - 2.73	3.10E+03	0.02%	3.71E-02
10	2.73 - 3.01	2.78E+03	0.02%	3.33E-02
9	3.01 - 3.68	4.87E+03	0.02%	5.82E-02
8	3.68 - 4.97	5.12E+03	0.00%	6.12E-02
7	4.97 - 6.07	1.89E+03	0.02%	2.26E-02
6	6.07 - 7.41	9.63E+02	0.02%	1.15E-02
5	7.41 - 8.61	3.18E+02	0.04%	3.81E-03
4	8.61 - 10	1.41E+02	0.06%	1.68E-03
3	10 - 12.2	6.28E+01	0.08%	7.50E-04
2	12.2 - 14.2	1.15E+01	0.20%	1.37E-04
1	14.2 - 19.64	3.27E+00	0.38%	3.90E-05
Total		8.37E+04	0.00%	

APPENDIX A SOURCE BOOK

A.30. 22.5 year WGPu Shell 30 Group Neutron Spectrum Outer Source Box

Side Surfaces

30 GROUP

Group	Energy Bounds (MeV)	Neutron Current Leakage (Neutrons/s)	2 sigma error	Normalized Leakage	Group	Energy Bounds (MeV)	Neutron Current Leakage (Neutrons/s)	2 sigma error	Normalized Leakage
30	0- 1E-10	5.35E-05	141.62%	1.16E-09	6	7.5E-1 - 1.25	2.28E+04	0.00%	
29	1E-10 - 5E-10	1.40E-03	33.46%	3.04E-08	5	1.25 - 1.5	9.45E+03	0.02%	
28	5E-10 - 7.5E-10	2.11E-03	27.48%	4.57E-08	4	1.5 - 3	3.76E+04	0.00%	
27	7.5E-10 - 1.2E-9	1.03E-02	12.80%	2.24E-07	3	3 - 8.19	2.32E+04	0.00%	
26	1.2E-9 - 1.5E-9	7.47E-03	15.14%	1.62E-07	2	8.19 - 17.3	5.29E+02	0.06%	
25	1.5E-9 - 2.53E-8	5.79E+00	0.56%	1.26E-04	Total		4.61E+04	0.00%	
24	2.53E-8 - 3E-8	1.75E+00	1.02%	3.80E-05					
23	3E-8 - 4E-8	3.88E+00	0.68%	8.42E-05					
22	4E-8 - 5E-8	3.84E+00	0.68%	8.34E-05					
21	5E-8 - 7E-8	7.13E+00	0.50%	1.55E-04					
20	7E-8 - 1E-7	8.93E+00	0.46%	1.94E-04					
19	1E-7 - 1.25E-7	6.10E+00	0.56%	1.32E-04					
18	1.25E-7 - 1.75E-7	9.53E+00	0.44%	2.07E-04					
17	1.75E-7 - 3.5E-7	2.03E+01	0.30%	4.41E-04					
16	3.5E-7 - 6.25E-7	1.99E+01	0.32%	4.31E-04					
15	6.25E-7 - 1E-6	1.88E+01	0.32%	4.08E-04					
14	1E-6 - 1.3E-6	1.18E+01	0.40%	2.55E-04					
13	1.3E-6 - 3.05E-6	4.65E+01	0.20%	1.01E-03					
12	3.05E-6 - 3.7E-5	2.55E+02	0.08%	5.52E-03					
11	3.7E-5 - 1.55E-3	1.22E+03	0.04%	2.65E-02					
10	1.55E-3 - 1.3E-2	2.07E+03	0.04%	4.50E-02					
9	1.3E-2 - 4.5E-2	2.70E+03	0.02%	5.86E-02					
8	4.5E-2 - 2.7E-1	1.33E+04	0.02%	2.89E-01					
7	2.7E-1 - 7.5E-1	2.63E+04	0.00%	5.71E-01					

APPENDIX A SOURCE BOOK

A.31. 22.5 year WGPu Shell Spatial Distributions for Outer Source Box surfaces

PHOTONS

TOP/BOTTOM PLANE OF BOX

X-axis distribution

Location (cm) Normalization

-29.664	0
-25.638	0.022929627
-21.611	0.032067318
-18.255	0.036572398
-14.9	0.039556486
-11.544	0.041880245
-8.3112	0.043714313
-6.6063	0.045611449
-4.9015	0.046364426
-3.1966	0.047109178
-1.918	0.047852394
-0.63932	0.048174022
0	0.048168144
0.63932	0.048168144
1.918	0.048174022
3.1966	0.047852394
4.9015	0.047109178
6.6063	0.046364426
8.3112	0.045611449
11.544	0.043714313
14.9	0.041880245
18.255	0.039556486
21.611	0.036572398
25.638	0.032067318
29.664	0.022929627

Y-axis distribution

Location (cm) Normalization

-29.664	0
-25.638	0.022929627
-21.611	0.032067318
-18.255	0.036572398
-14.9	0.039556486
-11.544	0.041880245
-8.3112	0.043714313
-6.6063	0.045611449
-4.9015	0.046364426
-3.1966	0.047109178
-1.918	0.047852394
-0.63932	0.048174022
0	0.048168144
0.63932	0.048168144
1.918	0.048174022
3.1966	0.047852394
4.9015	0.047109178
6.6063	0.046364426
8.3112	0.045611449
11.544	0.043714313
14.9	0.041880245
18.255	0.039556486
21.611	0.036572398
25.638	0.032067318
29.664	0.022929627

SIDE PLANES OF BOX

X/Y-axis distribution

Location (cm) Normalization

-29.664	0
-26.309	0.033734897
-22.282	0.03687577
-18.255	0.042035364
-14.229	0.048043029
-10.873	0.051514961
-7.6719	0.053185094
-4.8304	0.057829542
-2.5573	0.0578155
-0.85243	0.059247934
0	0.059717907
0.85243	0.059717907
2.5573	0.059247934
4.8304	0.0578155
7.6719	0.057829542
10.873	0.053185094
14.229	0.051514961
18.255	0.048043029
22.282	0.042035364
26.309	0.03687577
29.664	0.033734897

Z-axis distribution

Location (cm) Normalization

-38.242	0
-36.094	0.019597339
-32.513	0.022045168
-28.933	0.025778524
-25.352	0.030317078
-21.772	0.034910583
-18.191	0.039732283
-14.611	0.044578034
-11.031	0.049313457
-7.2457	0.053295369
-3.8359	0.057552539
-1.2786	0.061055823
0	0.061823803
1.2786	0.061823803
3.8359	0.061055823
7.2457	0.057552539
11.031	0.053295369
14.611	0.049313457
18.191	0.044578034
21.772	0.039732283
25.352	0.034910583
28.933	0.030317078
32.513	0.025778524
36.094	0.022045168
38.242	0.019597339

APPENDIX A SOURCE BOOK

A.32. 22.5 year WGPu Solid Gamma Spectrum Inner Source Box

Side Surfaces

Group Energy Bound Intrinsic Current Leakage 2 sigma error induced Current Leakage 2 sigma error root total Current Leakage 2 sigma error normalized Leakage

	(MeV)	(Photons/s)		(Photons/s)		(Photons/s)		(Photons/s)	
24	0 -0.3 **	9.183E+08	0.16%	2.708E+04	0.02%	9.183E+08	0.16%	9.924E-01	
23	0.3- 0.741	6.668E+06	0.06%	8.639E+04	0.02%	6.754E+06	0.06%	7.299E-03	
22	0.741- 0.743	2.923E+03	0.06%	3.932E+02	0.14%	3.316E+03	0.15%	3.583E-06	
21	0.743- 0.765	2.267E+04	0.04%	4.290E+03	0.04%	2.696E+04	0.06%	2.914E-05	
20	0.765- 0.767	1.622E+04	0.04%	3.872E+02	0.14%	1.660E+04	0.15%	1.794E-05	
19	0.767- 0.954	2.517E+04	0.04%	3.657E+04	0.02%	6.175E+04	0.04%	6.673E-05	
18	0.954- 0.956	3.906E+02	0.06%	3.466E+02	0.16%	7.372E+02	0.17%	7.966E-07	
17	0.956- 0.999	8.195E+02	0.08%	7.025E+03	0.04%	7.844E+03	0.09%	8.477E-06	
16	0.999- 1.002	2.407E+02	0.08%	4.756E+02	0.14%	7.163E+02	0.16%	7.741E-07	
15	1.002- 1.18	2.142E+03	0.06%	3.174E+04	0.02%	3.388E+04	0.06%	3.662E-05	
14	1.18- 1.2	2.140E+02	0.22%	2.749E+03	0.06%	2.963E+03	0.23%	3.202E-06	
13	1.2- 1.24	4.180E+02	0.16%	5.346E+03	0.04%	5.764E+03	0.16%	6.229E-06	
12	1.24- 1.26	9.087E+03	0.04%	2.579E+03	0.06%	1.167E+04	0.07%	1.261E-05	
11	1.26- 1.5	9.448E+02	0.06%	2.667E+04	0.02%	2.762E+04	0.06%	2.984E-05	
10	1.5- 1.52	7.829E+01	0.24%	1.892E+03	0.06%	1.970E+03	0.25%	2.129E-06	
9	1.52- 1.736	8.343E+02	0.08%	1.847E+04	0.02%	1.931E+04	0.08%	2.086E-05	
8	1.736- 1.74	1.505E+01	0.52%	2.885E+02	0.16%	3.036E+02	0.54%	3.280E-07	
7	1.74- 1.76	5.469E+03	0.04%	1.423E+03	0.08%	6.892E+03	0.09%	7.448E-06	
6	1.76- 1.83	9.796E+01	0.14%	4.771E+03	0.04%	4.869E+03	0.15%	5.262E-06	
5	1.83- 1.832	3.366E+00	0.66%	1.347E+02	0.24%	1.381E+02	0.70%	1.492E-07	
4	1.832- 2.21	5.109E+02	0.06%	2.084E+04	0.02%	2.135E+04	0.06%	2.307E-05	
3	2.21- 2.25	1.768E+03	0.04%	4.686E+03	0.04%	6.454E+03	0.06%	6.975E-06	
2	2.25- 2.749	1.89E+03	0.02%	1.781E+04	0.02%	1.970E+04	0.03%	2.128E-05	
1	2.749- 2.75	2.07E+03	0.04%	2.651E+01	0.56%	2.097E+03	0.56%	2.266E-06	
Total		9.251E+08	0.16%	3.024E+05	0.02%	9.254E+08	0.16%		

**Lower bound for PENTRAN models was 0.29 MeV

APPENDIX A SOURCE BOOK

A.32. 22.5 year WGPu Solid Gamma Spectrum Inner Source Box

Top/Bottom Surfaces

Group Energy Bounds Intrinsic Current Leakage² sigma error produced Current Leakage² sigma error total Current Leakage² sigma error normalized Leakage²

	(MeV)	(Photons/s)		(Photons/s)		(Photons/s)		(Photons/s)	
24	0 -0.3 **	9.194E+08	0.16%	2.715E+04	0.02%	9.194E+08	0.16%	9.924E-01	
23	0.3- 0.741	6.666E+06	0.06%	8.640E+04	0.02%	6.752E+06	0.06%	7.288E-03	
22	0.741- 0.743	2.922E+03	0.06%	3.924E+02	0.14%	3.315E+03	0.15%	3.578E-06	
21	0.743- 0.765	2.268E+04	0.04%	4.290E+03	0.04%	2.697E+04	0.06%	2.911E-05	
20	0.765- 0.767	1.621E+04	0.04%	3.875E+02	0.14%	1.660E+04	0.15%	1.792E-05	
19	0.767- 0.954	2.518E+04	0.04%	3.657E+04	0.02%	6.176E+04	0.04%	6.666E-05	
18	0.954- 0.956	3.909E+02	0.06%	3.470E+02	0.16%	7.378E+02	0.17%	7.964E-07	
17	0.956- 0.999	8.196E+02	0.08%	7.024E+03	0.04%	7.843E+03	0.09%	8.466E-06	
16	0.999- 1.002	2.407E+02	0.08%	4.757E+02	0.14%	7.164E+02	0.16%	7.733E-07	
15	1.002- 1.18	2.143E+03	0.06%	3.173E+04	0.02%	3.388E+04	0.06%	3.657E-05	
14	1.18- 1.2	2.141E+02	0.22%	2.750E+03	0.06%	2.964E+03	0.23%	3.200E-06	
13	1.2- 1.24	4.180E+02	0.16%	5.345E+03	0.04%	5.763E+03	0.16%	6.220E-06	
12	1.24- 1.26	9.087E+03	0.04%	2.580E+03	0.06%	1.167E+04	0.07%	1.259E-05	
11	1.26- 1.5	9.451E+02	0.06%	2.667E+04	0.02%	2.761E+04	0.06%	2.981E-05	
10	1.5- 1.52	7.833E+01	0.24%	1.893E+03	0.06%	1.971E+03	0.25%	2.128E-06	
9	1.52- 1.736	8.345E+02	0.08%	1.847E+04	0.02%	1.931E+04	0.08%	2.084E-05	
8	1.736- 1.74	1.490E+01	0.52%	2.888E+02	0.16%	3.037E+02	0.54%	3.278E-07	
7	1.74- 1.76	5.471E+03	0.04%	1.424E+03	0.08%	6.895E+03	0.09%	7.442E-06	
6	1.76- 1.83	9.786E+01	0.14%	4.772E+03	0.04%	4.870E+03	0.15%	5.256E-06	
5	1.83- 1.832	3.369E+00	0.66%	1.349E+02	0.24%	1.383E+02	0.70%	1.492E-07	
4	1.832- 2.21	5.110E+02	0.06%	2.084E+04	0.02%	2.135E+04	0.06%	2.305E-05	
3	2.21- 2.25	1.768E+03	0.04%	4.684E+03	0.04%	6.452E+03	0.06%	6.964E-06	
2	2.25- 2.749	1.89E+03	0.02%	1.781E+04	0.02%	1.969E+04	0.03%	2.126E-05	
1	2.749- 2.75	2.07E+03	0.04%	2.664E+01	0.56%	2.097E+03	0.56%	2.264E-06	
Total		9.262E+08	0.16%	3.025E+05	0.02%	9.265E+08	0.16%		

**Lower bound for PENTRAN models was 0.29 MeV

APPENDIX A SOURCE BOOK

A.33. 22.5 year WGPu Solid Gamma Spectrum Outer Source Box

Side Surfaces

Group Energy Bounds Intrinsic Current Leakage sigma error produced Current Leakage sigma error total Current Leakage sigma error Normalized Leakage

	(MeV)	(Photons/s)		(Photons/s)		(Photons/s)		(Photons/s)	
24	0 -0.3 **	8.75E+08	0.16%	4.62E+04	0.02%	8.75E+08	0.16%	9.92E-01	
23	0.3- 0.741	6.86E+06	0.06%	1.04E+05	0.02%	6.97E+06	0.06%	7.89E-03	
22	0.741- 0.743	2.790E+03	0.06%	4.33E+02	0.14%	3.22E+03	0.15%	3.65E-06	
21	0.743- 0.765	2.173E+04	0.04%	4.73E+03	0.04%	2.65E+04	0.06%	3.00E-05	
20	0.765- 0.767	1.528E+04	0.06%	4.26E+02	0.14%	1.57E+04	0.15%	1.78E-05	
19	0.767- 0.954	2.514E+04	0.04%	4.28E+04	0.02%	6.79E+04	0.04%	7.70E-05	
18	0.954- 0.956	3.814E+02	0.06%	3.74E+02	0.14%	7.55E+02	0.15%	8.55E-07	
17	0.956- 0.999	9.085E+02	0.08%	7.55E+03	0.04%	8.46E+03	0.09%	9.59E-06	
16	0.999- 1.002	2.405E+02	0.08%	5.11E+02	0.12%	7.52E+02	0.14%	8.52E-07	
15	1.002- 1.18	2.520E+03	0.06%	3.34E+04	0.02%	3.59E+04	0.06%	4.07E-05	
14	1.18- 1.2	2.559E+02	0.20%	2.92E+03	0.06%	3.17E+03	0.21%	3.59E-06	
13	1.2- 1.24	5.004E+02	0.14%	6.04E+03	0.04%	6.54E+03	0.15%	7.41E-06	
12	1.24- 1.26	8.991E+03	0.04%	2.75E+03	0.06%	1.17E+04	0.07%	1.33E-05	
11	1.26- 1.5	1.133E+03	0.06%	2.96E+04	0.02%	3.07E+04	0.06%	3.48E-05	
10	1.5- 1.52	9.352E+01	0.22%	2.02E+03	0.06%	2.11E+03	0.23%	2.39E-06	
9	1.52- 1.736	9.953E+02	0.06%	1.98E+04	0.02%	2.08E+04	0.06%	2.35E-05	
8	1.736- 1.74	1.796E+01	0.48%	3.09E+02	0.16%	3.27E+02	0.51%	3.70E-07	
7	1.74- 1.76	5.555E+03	0.04%	1.52E+03	0.08%	7.08E+03	0.09%	8.02E-06	
6	1.76- 1.83	1.174E+02	0.12%	5.33E+03	0.04%	5.45E+03	0.13%	6.17E-06	
5	1.83- 1.832	3.929E+00	0.62%	1.43E+02	0.24%	1.47E+02	0.66%	1.67E-07	
4	1.832- 2.21	6.133E+02	0.06%	2.25E+04	0.02%	2.31E+04	0.06%	2.61E-05	
3	2.21- 2.25	1.830E+03	0.04%	4.92E+03	0.04%	6.75E+03	0.06%	7.65E-06	
2	2.25- 2.749	2.010E+03	0.02%	1.93E+04	0.02%	2.13E+04	0.03%	2.41E-05	
1	2.749- 2.75	2.162E+03	0.04%	2.84E+01	0.54%	2.19E+03	0.54%	2.48E-06	
Total		8.823E+08	0.16%	3.58E+05	0.02%	8.83E+08	0.16%		

**Lower bound for PENTRAN models was 0.29 MeV

APPENDIX A SOURCE BOOK

A.33. 22.5 year WGPu Solid Gamma Spectrum Outer Source Box

Top/Bottom Surfaces

Group Energy Bound Intrinsic Current Leakage² sigma error produced Current Leakage² sigma error total Current Leakage² sigma error normalized Leakage

	(MeV)	(Photons/s)		(Photons/s)		(Photons/s)		(Photons/s)	
24	0 -0.3 **	5.07E+08	0.20%	2.76E+04	0.02%	5.07E+08	0.20%	9.92E-01	
23	0.3- 0.741	3.90E+06	0.08%	6.10E+04	0.02%	3.96E+06	0.08%	7.75E-03	
22	0.741- 0.743	1.567E+03	0.08%	2.45E+02	0.18%	1.81E+03	0.20%	3.55E-06	
21	0.743- 0.765	1.222E+04	0.06%	2.69E+03	0.06%	1.49E+04	0.08%	2.92E-05	
20	0.765- 0.767	8.585E+03	0.06%	2.42E+02	0.18%	8.83E+03	0.19%	1.73E-05	
19	0.767- 0.954	1.413E+04	0.06%	2.45E+04	0.02%	3.86E+04	0.06%	7.56E-05	
18	0.954- 0.956	2.143E+02	0.08%	2.10E+02	0.20%	4.25E+02	0.22%	8.31E-07	
17	0.956- 0.999	5.106E+02	0.10%	4.25E+03	0.04%	4.76E+03	0.11%	9.31E-06	
16	0.999- 1.002	1.349E+02	0.12%	2.88E+02	0.16%	4.23E+02	0.20%	8.27E-07	
15	1.002- 1.18	1.411E+03	0.08%	1.88E+04	0.02%	2.02E+04	0.08%	3.94E-05	
14	1.18- 1.2	1.424E+02	0.26%	1.64E+03	0.08%	1.78E+03	0.27%	3.48E-06	
13	1.2- 1.24	2.782E+02	0.18%	3.43E+03	0.06%	3.71E+03	0.19%	7.25E-06	
12	1.24- 1.26	5.036E+03	0.04%	1.54E+03	0.08%	6.58E+03	0.09%	1.29E-05	
11	1.26- 1.5	6.328E+02	0.08%	1.67E+04	0.02%	1.73E+04	0.08%	3.39E-05	
10	1.5- 1.52	5.204E+01	0.30%	1.13E+03	0.08%	1.18E+03	0.31%	2.31E-06	
9	1.52- 1.736	5.533E+02	0.08%	1.11E+04	0.04%	1.16E+04	0.09%	2.27E-05	
8	1.736- 1.74	9.858E+00	0.66%	1.73E+02	0.22%	1.82E+02	0.70%	3.57E-07	
7	1.74- 1.76	3.106E+03	0.04%	8.54E+02	0.10%	3.96E+03	0.11%	7.74E-06	
6	1.76- 1.83	6.524E+01	0.16%	3.01E+03	0.06%	3.07E+03	0.17%	6.01E-06	
5	1.83- 1.832	2.202E+00	0.82%	8.03E+01	0.32%	8.25E+01	0.88%	1.61E-07	
4	1.832- 2.21	3.401E+02	0.08%	1.26E+04	0.04%	1.29E+04	0.09%	2.52E-05	
3	2.21- 2.25	1.021E+03	0.04%	2.75E+03	0.04%	3.77E+03	0.06%	7.37E-06	
2	2.25- 2.749	1.119E+03	0.04%	1.08E+04	0.04%	1.19E+04	0.06%	2.33E-05	
1	2.749- 2.75	1.206E+03	0.04%	1.60E+01	0.70%	1.22E+03	0.70%	2.39E-06	
Total		5.111E+08	0.20%	2.06E+05	0.02%	5.11E+08	0.20%		

**Lower bound for PENTRAN models was 0.29 MeV

APPENDIX A SOURCE BOOK

A.34. 22.5 year WGPu Solid Neutron Spectrum Outer Source Box

Side Surfaces

47 GROUP

Group	Energy Bounds	Neutron Current Leakage	2 sigma error	Normalized Leakage
	(MeV)	(Neutrons/s)		
47	0 -1E-7	2.86E+02	0.10%	2.46E-04
46	1E-7 - 4.14E-7	3.71E+02	0.10%	3.19E-04
45	4.14E-7 - 8.76E-7	2.47E+02	0.12%	2.12E-04
44	8.76E-7 - 1.86E-6	3.13E+02	0.10%	2.69E-04
43	1.86E-6 - 5.04E-6	5.59E+02	0.08%	4.80E-04
42	5.04E-6 - 1.07E-5	5.75E+02	0.08%	4.94E-04
41	1.07E-5 - 3.73E-5	1.38E+03	0.06%	1.18E-03
40	3.73E-5 - 1.01E-4	1.63E+03	0.04%	1.40E-03
39	1.01E-4 - 2.14E-4	1.69E+03	0.04%	1.46E-03
38	2.14E-4 - 4.54E-4	2.12E+03	0.04%	1.82E-03
37	4.54E-4 - 1.58E-3	5.34E+03	0.02%	4.59E-03
36	1.58E-3 - 3.35E-3	4.62E+03	0.04%	3.97E-03
35	3.35E-3 - 7.1E-3	6.43E+03	0.02%	5.52E-03
34	7.1E-3 - 1.5E-2	8.90E+03	0.02%	7.65E-03
33	1.5E-2 - 2.19E-2	5.99E+03	0.02%	5.15E-03
32	2.19E-2 - 2.42E-2	1.91E+03	0.04%	1.64E-03
31	2.42E-2 - 2.61E-2	1.64E+03	0.04%	1.41E-03
30	2.61E-2 - 3.18E-2	3.77E+03	0.04%	3.24E-03
29	3.18E-2 - 4.09E-2	5.75E+03	0.02%	4.94E-03
28	4.09E-2 - 6.74E-2	1.62E+04	0.02%	1.39E-02
27	6.74E-2 - 1.11E-1	2.40E+04	0.02%	2.06E-02
26	1.11E-1 - 1.83E-1	3.84E+04	0.02%	3.30E-02
25	1.83E-1 - 2.97E-1	6.13E+04	0.02%	5.27E-02
24	2.97E-1 - 3.69E-1	3.89E+04	0.02%	3.35E-02
23	3.69E-1 - 4.98E-1	6.00E+04	0.02%	5.16E-02

47 GROUP

Group	Energy Bounds	Neutron Current Leakage	2 sigma error	Normalized Leakage
	(MeV)	(Neutrons/s)		
22	4.98E-1 - 6.08E-1	5.32E+04	0.02%	4.57E-02
21	5.08E-1 - 7.43E-1	6.33E+04	0.02%	5.44E-02
20	7.43E-1 - 8.21E-1	3.45E+04	0.02%	2.97E-02
19	8.21E-1 - 1	6.93E+04	0.02%	5.95E-02
18	1 - 1.35	1.15E+05	0.02%	9.89E-02
17	1.35 - 1.65	8.42E+04	0.02%	7.23E-02
16	1.65 - 1.92	6.50E+04	0.02%	5.58E-02
15	1.92 - 2.23	6.35E+04	0.02%	5.45E-02
14	2.23 - 2.35	2.25E+04	0.02%	1.94E-02
13	2.35 - 2.37	3.79E+03	0.04%	3.25E-03
12	2.37 - 2.47	1.87E+04	0.02%	1.60E-02
11	2.47 - 2.73	4.15E+04	0.02%	3.56E-02
10	2.73 - 3.01	3.73E+04	0.02%	3.21E-02
9	3.01 - 3.68	6.70E+04	0.02%	5.76E-02
8	3.68 - 4.97	7.40E+04	0.02%	6.36E-02
7	4.97 - 6.07	3.03E+04	0.02%	2.60E-02
6	6.07 - 7.41	1.71E+04	0.02%	1.47E-02
5	7.41 - 8.61	6.31E+03	0.02%	5.42E-03
4	8.61 - 10	3.05E+03	0.04%	2.62E-03
3	10 - 12.2	1.52E+03	0.04%	1.31E-03
2	12.2 - 14.2	3.11E+02	0.10%	2.67E-04
1	14.2 - 19.64	9.47E+01	0.18%	8.14E-05
Total		1.16E+06	0.02%	

APPENDIX A SOURCE BOOK

A.34. 22.5 year WGPu Solid Neutron Spectrum Outer Source Box

Top/Bottom Surfaces

47 GROUP

Group	Energy Bounds	Neutron Current Leakage	2 sigma error	Normalized Leakage
	(MeV)	(Neutrons/s)		
47	0 -1E-7	1.88E+02	0.12%	2.76E-04
46	1E-7 - 4.14E-7	2.47E+02	0.12%	3.64E-04
45	4.14E-7 - 8.76E-7	1.65E+02	0.14%	2.43E-04
44	8.76E-7 - 1.86E-6	2.10E+02	0.12%	3.09E-04
43	1.86E-6 - 5.04E-6	3.74E+02	0.10%	5.50E-04
42	5.04E-6 - 1.07E-5	3.84E+02	0.10%	5.64E-04
41	1.07E-5 - 3.73E-5	9.15E+02	0.06%	1.35E-03
40	3.73E-5 - 1.01E-4	1.08E+03	0.06%	1.59E-03
39	1.01E-4 - 2.14E-4	1.11E+03	0.06%	1.64E-03
38	2.14E-4 - 4.54E-4	1.38E+03	0.06%	2.03E-03
37	4.54E-4 - 1.58E-3	3.45E+03	0.04%	5.07E-03
36	1.58E-3 - 3.35E-3	2.94E+03	0.04%	4.32E-03
35	3.35E-3 - 7.1E-3	4.04E+03	0.04%	5.94E-03
34	7.1E-3 - 1.5E-2	5.50E+03	0.02%	8.08E-03
33	1.5E-2 - 2.19E-2	3.65E+03	0.04%	5.37E-03
32	2.19E-2 - 2.42E-2	1.16E+03	0.06%	1.70E-03
31	2.42E-2 - 2.61E-2	1.00E+03	0.06%	1.47E-03
30	2.61E-2 - 3.18E-2	2.27E+03	0.04%	3.34E-03
29	3.18E-2 - 4.09E-2	3.44E+03	0.04%	5.06E-03
28	4.09E-2 - 6.74E-2	9.68E+03	0.02%	1.42E-02
27	6.74E-2 - 1.11E-1	1.43E+04	0.02%	2.11E-02
26	1.11E-1 - 1.83E-1	2.29E+04	0.02%	3.37E-02
25	1.83E-1 - 2.97E-1	3.65E+04	0.02%	5.36E-02
24	2.97E-1 - 3.69E-1	2.31E+04	0.02%	3.39E-02
23	3.69E-1 - 4.98E-1	3.59E+04	0.02%	5.27E-02

47 GROUP

Group	Energy Bounds	Neutron Current Leakage	2 sigma error	Normalized Leakage
	(MeV)	(Neutrons/s)		
22	4.98E-1 - 6.08E-1	3.15E+04	0.02%	4.63E-02
21	6.08E-1 - 7.43E-1	3.73E+04	0.02%	5.48E-02
20	7.43E-1 - 8.21E-1	2.02E+04	0.02%	2.96E-02
19	8.21E-1 - 1	4.06E+04	0.02%	5.97E-02
18	1 - 1.35	6.74E+04	0.02%	9.91E-02
17	1.35 - 1.65	4.87E+04	0.02%	7.17E-02
16	1.65 - 1.92	3.75E+04	0.02%	5.51E-02
15	1.92 - 2.23	3.64E+04	0.02%	5.35E-02
14	2.23 - 2.35	1.29E+04	0.02%	1.89E-02
13	2.35 - 2.37	2.16E+03	0.04%	3.17E-03
12	2.37 - 2.47	1.06E+04	0.02%	1.56E-02
11	2.47 - 2.73	2.36E+04	0.02%	3.47E-02
10	2.73 - 3.01	2.13E+04	0.02%	3.13E-02
9	3.01 - 3.68	3.86E+04	0.02%	5.67E-02
8	3.68 - 4.97	4.23E+04	0.02%	6.22E-02
7	4.97 - 6.07	1.72E+04	0.02%	2.53E-02
6	6.07 - 7.41	9.63E+03	0.02%	1.42E-02
5	7.41 - 8.61	3.57E+03	0.04%	5.24E-03
4	8.61 - 10	1.72E+03	0.04%	2.52E-03
3	10 - 12.2	8.57E+02	0.06%	1.26E-03
2	12.2 - 14.2	1.75E+02	0.14%	2.57E-04
1	14.2 - 19.64	5.33E+01	0.24%	7.84E-05
Total		6.80E+05	0.02%	

APPENDIX A SOURCE BOOK

A.35. 22.5 year WGPu Solid 30 Group Neutron Spectrum Outer Source Box

Side Surfaces

30 GROUP

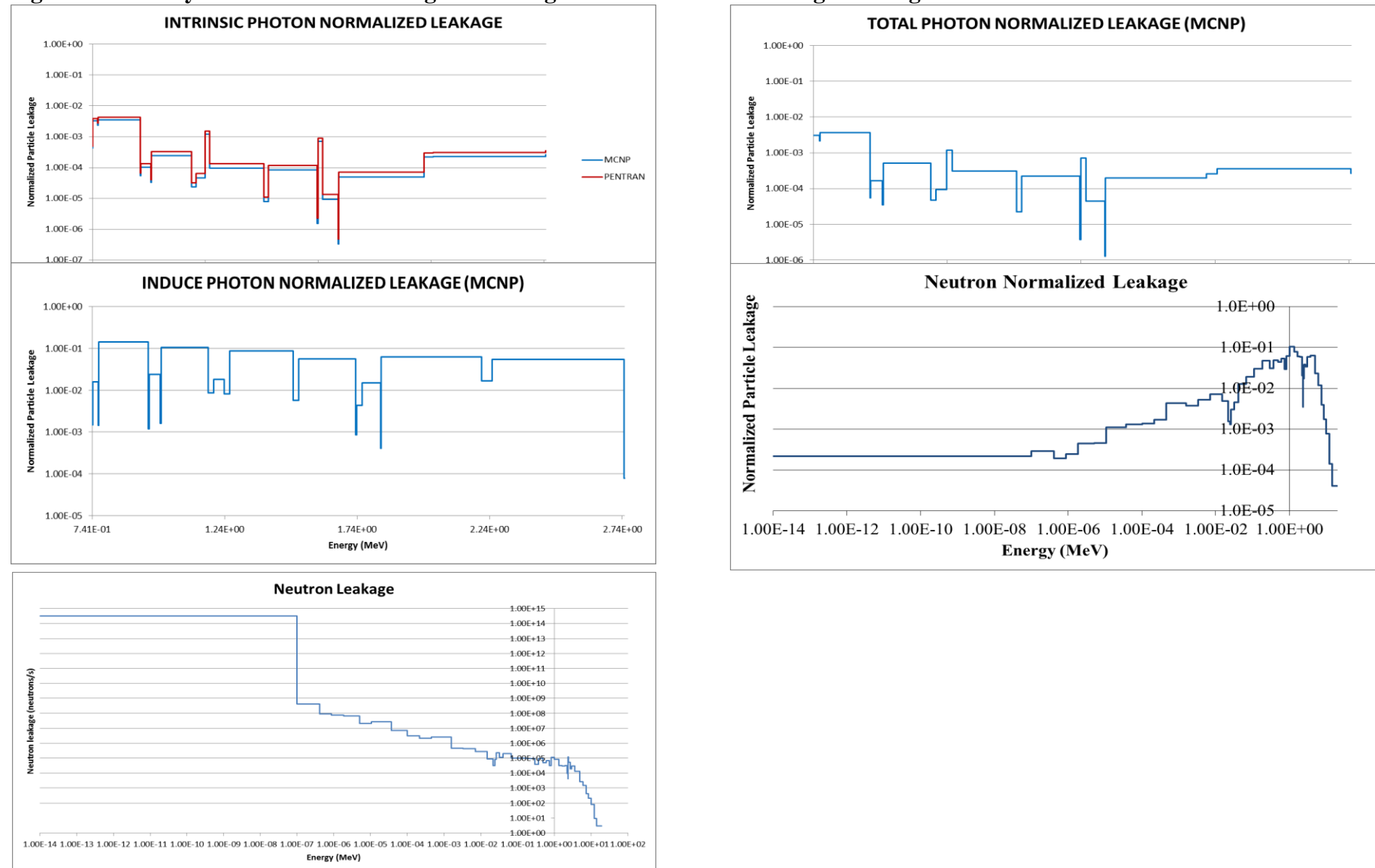
Group	Energy Bounds	Neutron Current Leakage	2 sigma error	Normalized Leakage
	(MeV)	(Neutrons/s)		
30	0- 1E-10	7.13E-04	53.40%	1.21E-09
29	1E-10 - 5E-10	1.52E-02	13.12%	2.59E-08
28	5E-10 - 7.5E-10	1.77E-02	12.26%	3.00E-08
27	7.5E-10 - 1.2E-9	9.31E-02	5.42%	1.58E-07
26	1.2E-9 - 1.5E-9	7.90E-02	5.94%	1.34E-07
25	1.5E-9 - 2.53E-8	5.33E+01	0.24%	9.05E-05
24	2.53E-8 - 3E-8	1.60E+01	0.42%	2.72E-05
23	3E-8 - 4E-8	3.55E+01	0.28%	6.03E-05
22	4E-8 - 5E-8	3.52E+01	0.30%	5.97E-05
21	5E-8 - 7E-8	6.51E+01	0.22%	1.11E-04
20	7E-8 - 1E-7	8.11E+01	0.20%	1.38E-04
19	1E-7 - 1.25E-7	5.50E+01	0.24%	9.34E-05
18	1.25E-7 - 1.75E-7	8.56E+01	0.20%	1.45E-04
17	1.75E-7 - 3.5E-7	1.81E+02	0.14%	3.07E-04
16	3.5E-7 - 6.25E-7	1.77E+02	0.14%	3.00E-04
15	6.25E-7 - 1E-6	1.67E+02	0.14%	2.83E-04
14	1E-6 - 1.3E-6	1.04E+02	0.18%	1.77E-04
13	1.3E-6 - 3.05E-6	4.09E+02	0.08%	6.95E-04
12	3.05E-6 - 3.7E-5	2.23E+03	0.04%	3.79E-03
11	3.7E-5 - 1.55E-3	1.06E+04	0.02%	1.80E-02
10	1.55E-3 - 1.3E-2	1.79E+04	0.02%	3.04E-02
9	1.3E-2 - 4.5E-2	2.35E+04	0.02%	3.99E-02
8	4.5E-2 - 2.7E-1	1.21E+05	0.02%	2.06E-01
7	2.7E-1 - 7.5E-1	2.30E+05	0.02%	3.90E-01
6	7.5E-1 - 1.25	1.82E+05	0.02%	3.09E-01

30 GROUP

Group	Energy Bounds	Neutron Current Leakage	2 sigma error	Normalized Leakage
	(MeV)	(Neutrons/s)		
5	1.25 - 1.5	7.32E+04	0.02%	1.24E-01
4	1.5 - 3	2.86E+05	0.02%	4.86E-01
3	3 - 8.19	1.92E+05	0.02%	3.25E-01
2	8.19 - 17.3	6.51E+03	0.02%	1.11E-02
1	17.3 - 20	8.61E+00	0.62%	1.46E-05
Total		5.89E+05	0.02%	1.00E+00

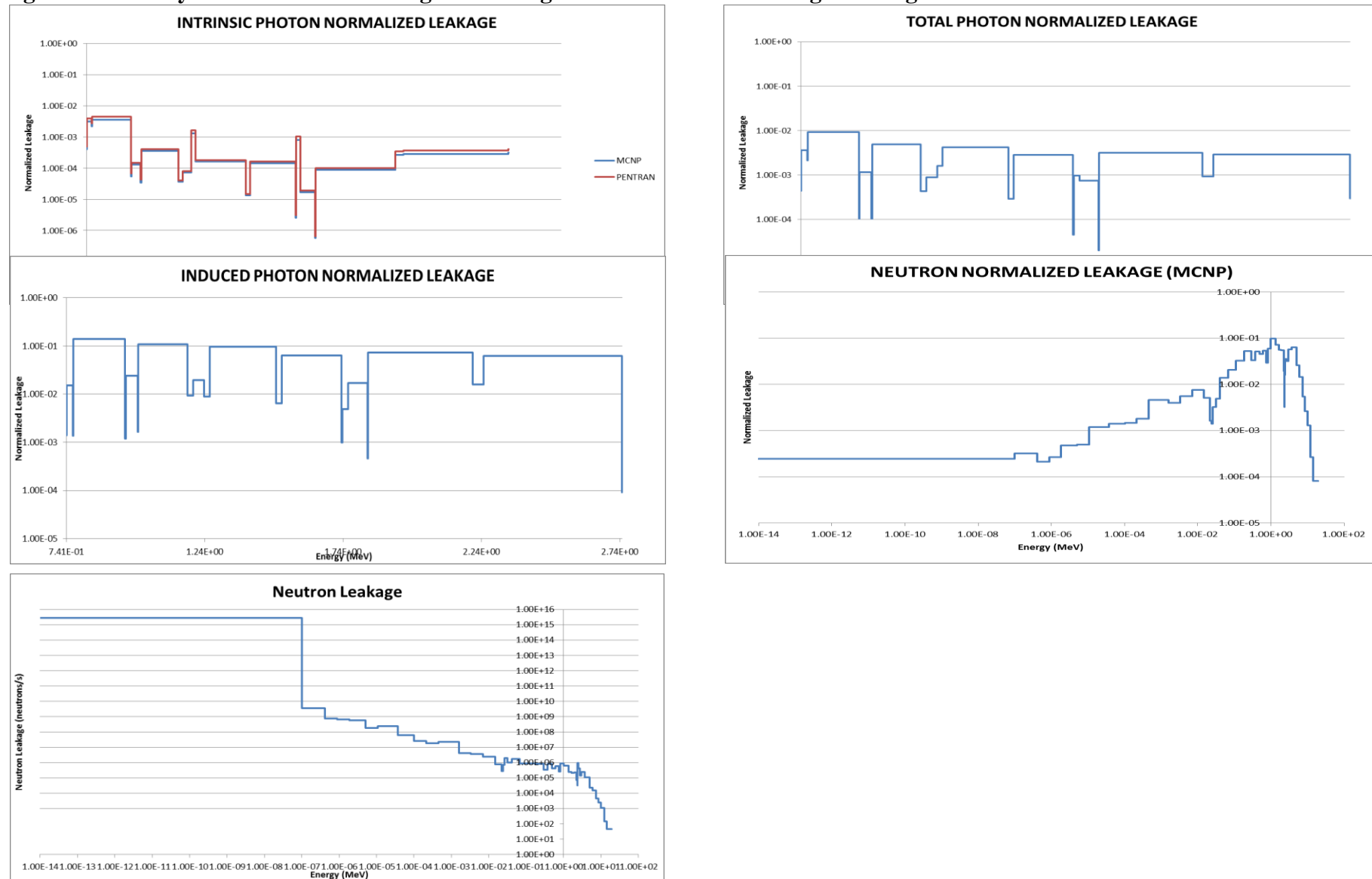
APPENDIX A SOURCE BOOK

Figure A.4. 22.5 year WGPu Shell Histograms for gamma and neutron leakages through outer source box side surfaces



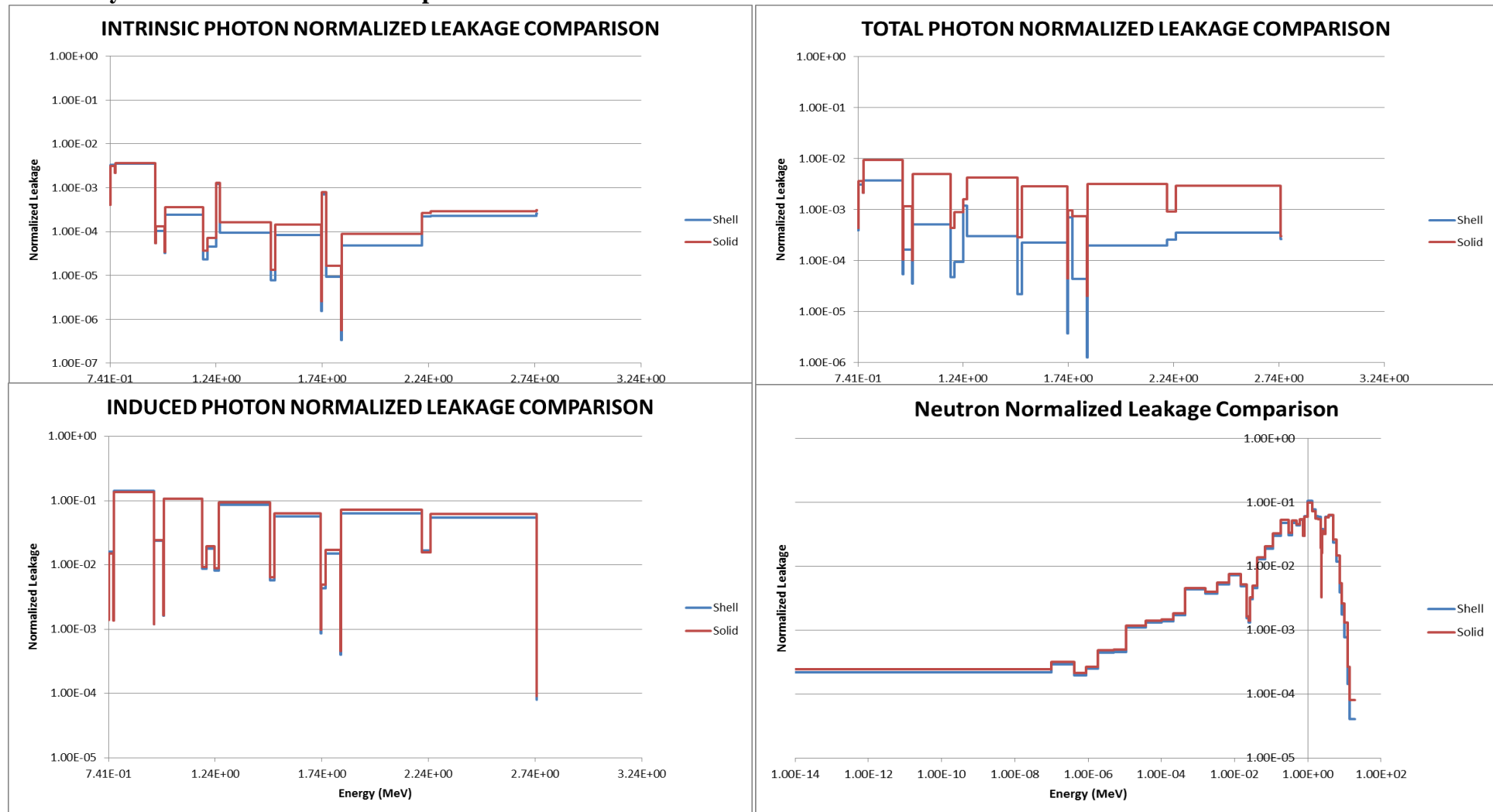
APPENDIX A SOURCE BOOK

Figure A.5. 22.5 year WGPu Solid Histograms for gamma and neutron leakages through outer source box side surfaces



APPENDIX A SOURCE BOOK

A.6. 22.5yr WGPu Solid vs. Shell Comparison



APPENDIX A SOURCE BOOK

A.36. 50 year WGPu Shell Gamma Spectrum Inner Source Box

Side Surfaces Side Surfaces

Group Energy Bound Intrinsic Current Leakage sigma error induced Current Leakage sigma error total Current Leakage sigma error Normalized Leakage

	(MeV)	(Photons/s)		(Photons/s)		(Photons/s)		(Photons/s)	
1	2.749- 2.75	2.62E+09	0.10%	4.16E+03	0.02%	2.62E+09	0.10%	9.93E-01	
2	2.25- 2.749	1.78E+07	0.04%	1.26E+04	0.02%	1.78E+07	0.04%	6.75E-03	
3	2.21- 2.25	7.673E+03	0.04%	5.44E+01	0.14%	7.73E+03	0.15%	2.93E-06	
4	1.832- 2.21	5.924E+04	0.02%	5.91E+02	0.04%	5.98E+04	0.04%	2.27E-05	
5	1.83- 1.832	4.104E+04	0.04%	5.31E+01	0.16%	4.11E+04	0.16%	1.56E-05	
6	1.76- 1.83	6.370E+04	0.02%	4.92E+03	0.02%	6.86E+04	0.03%	2.61E-05	
7	1.74- 1.76	1.035E+03	0.04%	4.45E+01	0.16%	1.08E+03	0.16%	4.10E-07	
8	1.736- 1.74	1.812E+03	0.06%	8.98E+02	0.04%	2.71E+03	0.07%	1.03E-06	
9	1.52- 1.736	5.029E+02	0.06%	6.05E+01	0.14%	5.63E+02	0.15%	2.14E-07	
10	1.5- 1.52	4.322E+03	0.04%	4.09E+03	0.02%	8.42E+03	0.04%	3.20E-06	
11	1.26- 1.5	4.176E+02	0.16%	3.32E+02	0.06%	7.50E+02	0.17%	2.85E-07	
12	1.24- 1.26	8.136E+02	0.10%	6.42E+02	0.04%	1.46E+03	0.11%	5.53E-07	
13	1.2- 1.24	2.169E+04	0.02%	3.08E+02	0.06%	2.20E+04	0.06%	8.35E-06	
14	1.18- 1.2	1.677E+03	0.06%	3.13E+03	0.02%	4.80E+03	0.06%	1.82E-06	
15	1.002- 1.18	1.391E+02	0.18%	2.18E+02	0.08%	3.57E+02	0.20%	1.36E-07	
16	0.999- 1.002	1.478E+03	0.06%	2.13E+03	0.02%	3.61E+03	0.06%	1.37E-06	
17	0.956- 0.999	2.720E+01	0.40%	3.26E+01	0.20%	5.98E+01	0.45%	2.27E-08	
18	0.954- 0.956	1.248E+04	0.02%	1.61E+02	0.08%	1.26E+04	0.08%	4.80E-06	
19	0.767- 0.954	1.672E+02	0.10%	5.40E+02	0.04%	7.07E+02	0.11%	2.68E-07	
20	0.765- 0.767	6.031E+00	0.48%	1.53E+01	0.28%	2.14E+01	0.56%	8.11E-09	
21	0.743- 0.765	8.685E+02	0.04%	2.35E+03	0.02%	3.22E+03	0.04%	1.22E-06	
22	0.741- 0.743	3.937E+03	0.02%	6.45E+02	0.04%	4.58E+03	0.04%	1.74E-06	
23	0.3- 0.741	4.041E+03	0.02%	2.00E+03	0.02%	6.04E+03	0.03%	2.30E-06	
24	0 -0.3 **	4.588E+03	0.02%	2.97E+00	0.64%	4.59E+03	0.64%	1.74E-06	
Total		2.633E+09	0.10%	3.99E+04	0.00%	2.63E+09	0.10%		

**Lower bound for PENTRAN models was 0.29 MeV

APPENDIX A SOURCE BOOK

A.36. 50 year WGPu Shell Gamma Spectrum Inner Source Box

Top/Bottom Surfaces

Group Energy Bound Intrinsic Current Leakage 2 sigma error introduced Current Leakage 2 sigma error Total Current Leakage 2 sigma error Normalized Leakage

	(MeV)	(Photons/s)		(Photons/s)		(Photons/s)		(Photons/s)	
1	2.749- 2.75	2.62E+09	0.10%	4.20E+03	0.02%	2.62E+09	0.10%	9.93E-01	
2	2.25- 2.749	1.78E+07	0.04%	1.26E+04	0.02%	1.78E+07	0.04%	6.74E-03	
3	2.21- 2.25	7.673E+03	0.04%	5.43E+01	0.16%	7.73E+03	0.16%	2.93E-06	
4	1.832- 2.21	5.925E+04	0.02%	5.91E+02	0.04%	5.98E+04	0.04%	2.27E-05	
5	1.83- 1.832	4.103E+04	0.04%	5.31E+01	0.16%	4.11E+04	0.16%	1.56E-05	
6	1.76- 1.83	6.370E+04	0.02%	4.92E+03	0.02%	6.86E+04	0.03%	2.60E-05	
7	1.74- 1.76	1.035E+03	0.04%	4.45E+01	0.16%	1.08E+03	0.16%	4.09E-07	
8	1.736- 1.74	1.811E+03	0.06%	8.97E+02	0.04%	2.71E+03	0.07%	1.03E-06	
9	1.52- 1.736	5.028E+02	0.06%	6.04E+01	0.14%	5.63E+02	0.15%	2.14E-07	
10	1.5- 1.52	4.323E+03	0.04%	4.09E+03	0.02%	8.41E+03	0.04%	3.19E-06	
11	1.26- 1.5	4.175E+02	0.16%	3.32E+02	0.06%	7.50E+02	0.17%	2.84E-07	
12	1.24- 1.26	8.140E+02	0.10%	6.42E+02	0.04%	1.46E+03	0.11%	5.52E-07	
13	1.2- 1.24	2.170E+04	0.02%	3.08E+02	0.06%	2.20E+04	0.06%	8.35E-06	
14	1.18- 1.2	1.677E+03	0.06%	3.13E+03	0.02%	4.80E+03	0.06%	1.82E-06	
15	1.002- 1.18	1.392E+02	0.18%	2.18E+02	0.08%	3.57E+02	0.20%	1.35E-07	
16	0.999- 1.002	1.478E+03	0.06%	2.13E+03	0.02%	3.61E+03	0.06%	1.37E-06	
17	0.956- 0.999	2.721E+01	0.40%	3.27E+01	0.20%	5.99E+01	0.45%	2.27E-08	
18	0.954- 0.956	1.248E+04	0.02%	1.61E+02	0.08%	1.26E+04	0.08%	4.80E-06	
19	0.767- 0.954	1.672E+02	0.10%	5.40E+02	0.04%	7.07E+02	0.11%	2.68E-07	
20	0.765- 0.767	6.044E+00	0.48%	1.53E+01	0.28%	2.13E+01	0.56%	8.10E-09	
21	0.743- 0.765	8.689E+02	0.04%	2.35E+03	0.02%	3.21E+03	0.04%	1.22E-06	
22	0.741- 0.743	3.936E+03	0.02%	6.45E+02	0.04%	4.58E+03	0.04%	1.74E-06	
23	0.3- 0.741	4.041E+03	0.02%	2.00E+03	0.02%	6.04E+03	0.03%	2.29E-06	
24	0 -0.3 **	4.588E+03	0.02%	2.97E+00	0.64%	4.59E+03	0.64%	1.74E-06	
Total		2.636E+09	0.10%	4.00E+04	0.00%	2.64E+09	0.10%		

**Lower bound for PENTRAN models was 0.29 MeV

APPENDIX A SOURCE BOOK

A.37. 50 year WGPu Shell Gamma Spectrum Outer Source Box

Side Surfaces

Group Energy Bound Intrinsic Current Leakage² sigma error produced Current Leakage² sigma error total Current Leakage² sigma error Normalized Leakage

	(MeV)	(Photons/s)		(Photons/s)		(Photons/s)	
1	2.749- 2.75	2.47E+09	0.10%	6.58E+03	0.02%	2.47E+09	0.10%
2	2.25- 2.749	1.82E+07	0.04%	1.48E+04	0.00%	1.83E+07	0.04%
3	2.21- 2.25	7.305E+03	0.04%	5.90E+01	0.14%	7.36E+03	0.15%
4	1.832- 2.21	5.662E+04	0.04%	6.42E+02	0.04%	5.73E+04	0.06%
5	1.83- 1.832	3.858E+04	0.04%	5.77E+01	0.14%	3.86E+04	0.15%
6	1.76- 1.83	6.334E+04	0.02%	5.66E+03	0.02%	6.90E+04	0.03%
7	1.74- 1.76	1.006E+03	0.04%	4.76E+01	0.16%	1.05E+03	0.16%
8	1.736- 1.74	2.008E+03	0.06%	9.59E+02	0.04%	2.97E+03	0.07%
9	1.52- 1.736	5.025E+02	0.06%	6.47E+01	0.14%	5.67E+02	0.15%
10	1.5- 1.52	5.181E+03	0.04%	4.27E+03	0.02%	9.45E+03	0.04%
11	1.26- 1.5	5.132E+02	0.14%	3.51E+02	0.06%	8.64E+02	0.15%
12	1.24- 1.26	1.004E+03	0.10%	7.22E+02	0.04%	1.73E+03	0.11%
13	1.2- 1.24	2.142E+04	0.02%	3.27E+02	0.06%	2.17E+04	0.06%
14	1.18- 1.2	2.083E+03	0.04%	3.46E+03	0.02%	5.55E+03	0.04%
15	1.002- 1.18	1.722E+02	0.16%	2.32E+02	0.08%	4.04E+02	0.18%
16	0.999- 1.002	1.830E+03	0.04%	2.28E+03	0.02%	4.11E+03	0.04%
17	0.956- 0.999	3.371E+01	0.36%	3.49E+01	0.18%	6.86E+01	0.40%
18	0.954- 0.956	1.265E+04	0.02%	1.73E+02	0.08%	1.28E+04	0.08%
19	0.767- 0.954	2.079E+02	0.10%	6.03E+02	0.04%	8.11E+02	0.11%
20	0.765- 0.767	7.204E+00	0.44%	1.63E+01	0.28%	2.35E+01	0.52%
21	0.743- 0.765	1.085E+03	0.04%	2.53E+03	0.02%	3.61E+03	0.04%
22	0.741- 0.743	4.069E+03	0.02%	6.74E+02	0.04%	4.74E+03	0.04%
23	0.3- 0.741	4.301E+03	0.02%	2.17E+03	0.02%	6.47E+03	0.03%
24	0 -0.3 **	4.785E+03	0.02%	3.17E+00	0.62%	4.79E+03	0.62%
Total		2.488E+09	0.10%	4.67E+04	0.00%	2.49E+09	0.10%

**Lower bound for PENTRAN models was 0.29 MeV

APPENDIX A SOURCE BOOK

A.37. 50 year WGPu Shell Gamma Spectrum Outer Source Box

Top/Bottom Surfaces

Group Energy Bound Intrinsic Current Leakage² sigma error produced Current Leakage² sigma error Total Current Leakage² sigma error Normalized Leakage

	(MeV)	(Photons/s)		(Photons/s)		(Photons/s)		(Photons/s)	
1	2.749- 2.75	1.43E+09	0.24%	3.94E+03	0.02%	1.43E+09	0.24%	9.93E-01	
2	2.25- 2.749	1.04E+07	0.08%	8.63E+03	0.02%	1.04E+07	0.08%	7.21E-03	
3	2.21- 2.25	4.104E+03	0.08%	3.35E+01	0.18%	4.14E+03	0.20%	2.87E-06	
4	1.832- 2.21	3.183E+04	0.08%	3.65E+02	0.06%	3.22E+04	0.10%	2.23E-05	
5	1.83- 1.832	2.168E+04	0.08%	3.27E+01	0.20%	2.17E+04	0.22%	1.51E-05	
6	1.76- 1.83	3.557E+04	0.08%	3.24E+03	0.02%	3.88E+04	0.08%	2.69E-05	
7	1.74- 1.76	5.650E+02	0.08%	2.68E+01	0.20%	5.92E+02	0.22%	4.11E-07	
8	1.736- 1.74	1.128E+03	0.12%	5.40E+02	0.04%	1.67E+03	0.13%	1.16E-06	
9	1.52- 1.736	2.821E+02	0.16%	3.63E+01	0.18%	3.18E+02	0.24%	2.21E-07	
10	1.5- 1.52	2.899E+03	0.12%	2.40E+03	0.02%	5.30E+03	0.12%	3.68E-06	
11	1.26- 1.5	2.855E+02	0.36%	1.97E+02	0.08%	4.82E+02	0.37%	3.35E-07	
12	1.24- 1.26	5.583E+02	0.28%	4.10E+02	0.06%	9.68E+02	0.29%	6.72E-07	
13	1.2- 1.24	1.200E+04	0.08%	1.83E+02	0.08%	1.22E+04	0.11%	8.46E-06	
14	1.18- 1.2	1.163E+03	0.12%	1.96E+03	0.02%	3.12E+03	0.12%	2.17E-06	
15	1.002- 1.18	9.585E+01	0.44%	1.30E+02	0.10%	2.26E+02	0.45%	1.57E-07	
16	0.999- 1.002	1.015E+03	0.12%	1.28E+03	0.04%	2.29E+03	0.13%	1.59E-06	
17	0.956- 0.999	1.860E+01	0.96%	1.95E+01	0.24%	3.81E+01	0.99%	2.65E-08	
18	0.954- 0.956	7.073E+03	0.04%	9.65E+01	0.12%	7.17E+03	0.13%	4.98E-06	
19	0.767- 0.954	1.157E+02	0.24%	3.40E+02	0.06%	4.56E+02	0.25%	3.17E-07	
20	0.765- 0.767	4.017E+00	1.20%	9.08E+00	0.36%	1.31E+01	1.25%	9.09E-09	
21	0.743- 0.765	6.003E+02	0.12%	1.41E+03	0.02%	2.01E+03	0.12%	1.40E-06	
22	0.741- 0.743	2.270E+03	0.04%	3.77E+02	0.04%	2.65E+03	0.06%	1.84E-06	
23	0.3- 0.741	2.395E+03	0.04%	1.21E+03	0.04%	3.61E+03	0.06%	2.50E-06	
24	0 -0.3 **	2.668E+03	0.04%	1.78E+00	0.82%	2.67E+03	0.82%	1.85E-06	
Total		1.441E+09	0.24%	2.69E+04	0.00%	1.44E+09	0.24%		

**Lower bound for PENTRAN models was 0.29 MeV

APPENDIX A SOURCE BOOK

A.38. 50 year WG⁶Pu Shell Neutron Spectrum Outer Source Box

Side Surfaces

47 GROUP

Group	Energy Bounds	Neutron Current Leakage	2 sigma error	Normalized Leakage
	(MeV)	(Neutrons/s)		
47	0 -1E-7	3.1262E+01	0.12%	2.19E-04
46	1E-7 - 4.14E-7	4.1418E+01	0.10%	2.91E-04
45	4.14E-7 - 8.76E-7	2.7778E+01	0.14%	1.95E-04
44	8.76E-7 - 1.86E-6	3.5365E+01	0.12%	2.48E-04
43	1.86E-6 - 5.04E-6	6.3519E+01	0.08%	4.46E-04
42	5.04E-6 - 1.07E-5	6.5372E+01	0.08%	4.59E-04
41	1.07E-5 - 3.73E-5	1.5711E+02	0.06%	1.10E-03
40	3.73E-5 - 1.01E-4	1.8685E+02	0.06%	1.31E-03
39	1.01E-4 - 2.14E-4	1.9428E+02	0.06%	1.36E-03
38	2.14E-4 - 4.54E-4	2.4370E+02	0.04%	1.71E-03
37	4.54E-4 - 1.58E-3	6.1572E+02	0.02%	4.32E-03
36	1.58E-3 - 3.35E-3	5.3380E+02	0.04%	3.74E-03
35	3.35E-3 - 7.1E-3	7.4351E+02	0.02%	5.21E-03
34	7.1E-3 - 1.5E-2	1.0266E+03	0.02%	7.20E-03
33	1.5E-2 - 2.19E-2	6.8862E+02	0.02%	4.83E-03
32	2.19E-2 - 2.42E-2	2.1844E+02	0.04%	1.53E-03
31	2.42E-2 - 2.61E-2	1.8797E+02	0.06%	1.32E-03
30	2.61E-2 - 3.18E-2	4.3537E+02	0.04%	3.05E-03
29	3.18E-2 - 4.09E-2	6.5267E+02	0.02%	4.58E-03
28	4.09E-2 - 6.74E-2	1.8268E+03	0.02%	1.28E-02
27	6.74E-2 - 1.11E-1	2.6956E+03	0.02%	1.89E-02
26	1.11E-1 - 1.83E-1	4.2702E+03	0.02%	3.00E-02
25	1.83E-1 - 2.97E-1	6.7879E+03	0.00%	4.76E-02
24	2.97E-1 - 3.69E-1	4.3622E+03	0.02%	3.06E-02
23	3.69E-1 - 4.98E-1	6.8552E+03	0.00%	4.81E-02

47 GROUP

Group	Energy Bounds	Neutron Current Leakage	2 sigma error	Normalized Leakage
	(MeV)	(Neutrons/s)		
22	4.98E-1 - 6.08E-1	6.2436E+03	0.00%	4.38E-02
21	6.08E-1 - 7.43E-1	7.6714E+03	0.00%	5.38E-02
20	7.43E-1 - 8.21E-1	4.2400E+03	0.02%	2.97E-02
19	8.21E-1 - 1	8.7047E+03	0.00%	6.11E-02
18	1 - 1.35	1.4945E+04	0.00%	1.05E-01
17	1.35 - 1.65	1.1180E+04	0.00%	7.84E-02
16	1.65 - 1.92	8.6745E+03	0.00%	6.08E-02
15	1.92 - 2.23	8.4677E+03	0.00%	5.94E-02
14	2.23 - 2.35	2.9340E+03	0.02%	2.06E-02
13	2.35 - 2.37	4.9923E+02	0.04%	3.50E-03
12	2.37 - 2.47	2.4925E+03	0.02%	1.75E-02
11	2.47 - 2.73	5.4191E+03	0.00%	3.80E-02
10	2.73 - 3.01	4.8521E+03	0.02%	3.40E-02
9	3.01 - 3.68	8.4146E+03	0.00%	5.90E-02
8	3.68 - 4.97	8.9142E+03	0.00%	6.25E-02
7	4.97 - 6.07	3.3299E+03	0.02%	2.34E-02
6	6.07 - 7.41	1.6984E+03	0.02%	1.19E-02
5	7.41 - 8.61	5.6138E+02	0.02%	3.94E-03
4	8.61 - 10	2.4848E+02	0.04%	1.74E-03
3	10 - 12.2	1.1103E+02	0.06%	7.79E-04
2	12.2 - 14.2	2.0271E+01	0.16%	1.42E-04
1	14.2 - 19.64	5.7788E+00	0.30%	4.05E-05
Total		1.43E+05	0.00%	

APPENDIX A SOURCE BOOK

A.38. 50 year WGPu Shell Neutron Spectrum Outer Source Box

Top/Bottom Surfaces

47 GROUP

Group	Energy Bounds	Neutron Current Leakage	2 sigma error	Normalized Leakage
	(MeV)	(Neutrons/s)		
47	0 -1E-7	2.06E+01	0.14%	2.47E-04
46	1E-7 - 4.14E-7	2.78E+01	0.14%	3.33E-04
45	4.14E-7 - 8.76E-7	1.87E+01	0.16%	2.25E-04
44	8.76E-7 - 1.86E-6	2.39E+01	0.14%	2.87E-04
43	1.86E-6 - 5.04E-6	4.28E+01	0.10%	5.13E-04
42	5.04E-6 - 1.07E-5	4.38E+01	0.10%	5.26E-04
41	1.07E-5 - 3.73E-5	1.05E+02	0.06%	1.26E-03
40	3.73E-5 - 1.01E-4	1.24E+02	0.06%	1.49E-03
39	1.01E-4 - 2.14E-4	1.28E+02	0.06%	1.54E-03
38	2.14E-4 - 4.54E-4	1.59E+02	0.06%	1.91E-03
37	4.54E-4 - 1.58E-3	3.98E+02	0.04%	4.78E-03
36	1.58E-3 - 3.35E-3	3.41E+02	0.04%	4.09E-03
35	3.35E-3 - 7.1E-3	4.68E+02	0.04%	5.62E-03
34	7.1E-3 - 1.5E-2	6.36E+02	0.02%	7.63E-03
33	1.5E-2 - 2.19E-2	4.21E+02	0.04%	5.05E-03
32	2.19E-2 - 2.42E-2	1.33E+02	0.06%	1.60E-03
31	2.42E-2 - 2.61E-2	1.15E+02	0.06%	1.38E-03
30	2.61E-2 - 3.18E-2	2.64E+02	0.04%	3.17E-03
29	3.18E-2 - 4.09E-2	3.93E+02	0.04%	4.72E-03
28	4.09E-2 - 6.74E-2	1.10E+03	0.02%	1.32E-02
27	6.74E-2 - 1.11E-1	1.61E+03	0.02%	1.94E-02
26	1.11E-1 - 1.83E-1	2.55E+03	0.02%	3.06E-02
25	1.83E-1 - 2.97E-1	4.04E+03	0.02%	4.85E-02
24	2.97E-1 - 3.69E-1	2.59E+03	0.02%	3.11E-02
23	3.69E-1 - 4.98E-1	4.10E+03	0.02%	4.92E-02

47 GROUP

Group	Energy Bounds	Neutron Current Leakage	2 sigma error	Normalized Leakage
	(MeV)	(Neutrons/s)		
22	4.98E-1 - 6.08E-1	3.70E+03	0.02%	4.44E-02
21	6.08E-1 - 7.43E-1	4.52E+03	0.02%	5.42E-02
20	7.43E-1 - 8.21E-1	2.48E+03	0.02%	2.98E-02
19	8.21E-1 - 1	5.10E+03	0.00%	6.13E-02
18	1 - 1.35	8.75E+03	0.00%	1.05E-01
17	1.35 - 1.65	6.47E+03	0.00%	7.77E-02
16	1.65 - 1.92	5.01E+03	0.02%	6.01E-02
15	1.92 - 2.23	4.86E+03	0.02%	5.83E-02
14	2.23 - 2.35	1.68E+03	0.02%	2.01E-02
13	2.35 - 2.37	2.85E+02	0.04%	3.42E-03
12	2.37 - 2.47	1.42E+03	0.02%	1.71E-02
11	2.47 - 2.73	3.09E+03	0.02%	3.71E-02
10	2.73 - 3.01	2.77E+03	0.02%	3.33E-02
9	3.01 - 3.68	4.84E+03	0.02%	5.82E-02
8	3.68 - 4.97	5.10E+03	0.00%	6.12E-02
7	4.97 - 6.07	1.89E+03	0.02%	2.26E-02
6	6.07 - 7.41	9.59E+02	0.02%	1.15E-02
5	7.41 - 8.61	3.17E+02	0.04%	3.80E-03
4	8.61 - 10	1.40E+02	0.06%	1.68E-03
3	10 - 12.2	6.25E+01	0.08%	7.50E-04
2	12.2 - 14.2	1.14E+01	0.20%	1.37E-04
1	14.2 - 19.64	3.24E+00	0.38%	3.89E-05
Total		8.33E+04	0.00%	

APPENDIX A SOURCE BOOK

A.39. 50 year WGPu Solid Gamma Spectrum Inner Source Box

Side Surfaces

Group Energy Boundntrinsic Current Leakage² sigma error Induced Current Leakage¹ sigma erro' total Current Leakage² sigma erro' formalized Leakage³

	(MeV)	(Photons/s)		(Photons/s)		(Photons/s)		(Photons/s)	
24	0 -0.3 **	9.81E+08	0.16%	2.70E+04	0.02%	9.805E+08	0.16%	9.928E-01	
23	0.3- 0.741	6.74E+06	0.06%	8.60E+04	0.02%	6.823E+06	0.06%	6.909E-03	
22	0.741- 0.743	2.965E+03	0.06%	3.92E+02	0.14%	3.356E+03	0.15%	3.398E-06	
21	0.743- 0.765	2.294E+04	0.04%	4.27E+03	0.04%	2.722E+04	0.06%	2.756E-05	
20	0.765- 0.767	1.586E+04	0.04%	3.85E+02	0.14%	1.625E+04	0.15%	1.645E-05	
19	0.767- 0.954	2.552E+04	0.04%	3.64E+04	0.02%	6.194E+04	0.04%	6.272E-05	
18	0.954- 0.956	4.158E+02	0.06%	3.45E+02	0.16%	7.609E+02	0.17%	7.705E-07	
17	0.956- 0.999	8.144E+02	0.08%	7.00E+03	0.04%	7.810E+03	0.09%	7.908E-06	
16	0.999- 1.002	2.078E+02	0.08%	4.74E+02	0.14%	6.814E+02	0.16%	6.899E-07	
15	1.002- 1.18	2.130E+03	0.06%	3.16E+04	0.02%	3.374E+04	0.06%	3.416E-05	
14	1.18- 1.2	2.134E+02	0.22%	2.74E+03	0.06%	2.951E+03	0.23%	2.988E-06	
13	1.2- 1.24	4.169E+02	0.16%	5.32E+03	0.04%	5.741E+03	0.16%	5.813E-06	
12	1.24- 1.26	9.058E+03	0.04%	2.57E+03	0.06%	1.163E+04	0.07%	1.177E-05	
11	1.26- 1.5	9.422E+02	0.06%	2.66E+04	0.02%	2.750E+04	0.06%	2.785E-05	
10	1.5- 1.52	7.813E+01	0.24%	1.88E+03	0.06%	1.962E+03	0.25%	1.986E-06	
9	1.52- 1.736	8.318E+02	0.08%	1.84E+04	0.02%	1.923E+04	0.08%	1.947E-05	
8	1.736- 1.74	1.507E+01	0.52%	2.87E+02	0.16%	3.024E+02	0.54%	3.062E-07	
7	1.74- 1.76	5.451E+03	0.04%	1.42E+03	0.08%	6.868E+03	0.09%	6.954E-06	
6	1.76- 1.83	9.834E+01	0.14%	4.75E+03	0.04%	4.850E+03	0.15%	4.910E-06	
5	1.83- 1.832	3.365E+00	0.66%	1.34E+02	0.24%	1.376E+02	0.70%	1.393E-07	
4	1.832- 2.21	5.095E+02	0.06%	2.08E+04	0.02%	2.126E+04	0.06%	2.153E-05	
3	2.21- 2.25	1.762E+03	0.04%	4.67E+03	0.04%	6.429E+03	0.06%	6.509E-06	
2	2.25- 2.749	1.881E+03	0.02%	1.77E+04	0.02%	1.961E+04	0.03%	1.986E-05	
1	2.749- 2.75	2.063E+03	0.04%	2.64E+01	0.56%	2.090E+03	0.56%	2.116E-06	
Total		9.873E+08	0.16%	3.01E+05	0.02%	9.876E+08	0.16%		

**Lower bound for PENTRAN models was 0.29 MeV

APPENDIX A SOURCE BOOK

A.39. 50 year WGPu Solid Gamma Spectrum Inner Source Box

Top/Bottom Surfaces

Group Energy Bounds Intrinsic Current Leakage sigma error produced Current Leakage sigma error total Current Leakage sigma error normalized Leakage

	(MeV)	(Photons/s)		(Photons/s)		(Photons/s)		(Photons/s)	
24	0 -0.3 **	9.82E+08	0.16%	2.70E+04	0.02%	9.82E+08	0.16%	9.93E-01	
23	0.3- 0.741	6.73E+06	0.06%	8.60E+04	0.02%	6.82E+06	0.06%	6.90E-03	
22	0.741- 0.743	2.965E+03	0.06%	3.91E+02	0.14%	3.36E+03	0.15%	3.39E-06	
21	0.743- 0.765	2.295E+04	0.04%	4.27E+03	0.04%	2.72E+04	0.06%	2.75E-05	
20	0.765- 0.767	1.586E+04	0.04%	3.86E+02	0.14%	1.62E+04	0.15%	1.64E-05	
19	0.767- 0.954	2.553E+04	0.04%	3.64E+04	0.02%	6.19E+04	0.04%	6.26E-05	
18	0.954- 0.956	4.161E+02	0.06%	3.45E+02	0.16%	7.62E+02	0.17%	7.70E-07	
17	0.956- 0.999	8.146E+02	0.08%	6.99E+03	0.04%	7.81E+03	0.09%	7.90E-06	
16	0.999- 1.002	2.078E+02	0.08%	4.74E+02	0.14%	6.81E+02	0.16%	6.89E-07	
15	1.002- 1.18	2.130E+03	0.06%	3.16E+04	0.02%	3.37E+04	0.06%	3.41E-05	
14	1.18- 1.2	2.134E+02	0.22%	2.74E+03	0.06%	2.95E+03	0.23%	2.99E-06	
13	1.2- 1.24	4.169E+02	0.16%	5.32E+03	0.04%	5.74E+03	0.16%	5.80E-06	
12	1.24- 1.26	9.058E+03	0.04%	2.57E+03	0.06%	1.16E+04	0.07%	1.18E-05	
11	1.26- 1.5	9.426E+02	0.06%	2.66E+04	0.02%	2.75E+04	0.06%	2.78E-05	
10	1.5- 1.52	7.817E+01	0.24%	1.88E+03	0.06%	1.96E+03	0.25%	1.99E-06	
9	1.52- 1.736	8.321E+02	0.08%	1.84E+04	0.02%	1.92E+04	0.08%	1.94E-05	
8	1.736- 1.74	1.492E+01	0.52%	2.88E+02	0.16%	3.03E+02	0.54%	3.06E-07	
7	1.74- 1.76	5.453E+03	0.04%	1.42E+03	0.08%	6.87E+03	0.09%	6.95E-06	
6	1.76- 1.83	9.824E+01	0.14%	4.75E+03	0.04%	4.85E+03	0.15%	4.90E-06	
5	1.83- 1.832	3.369E+00	0.66%	1.34E+02	0.24%	1.38E+02	0.70%	1.39E-07	
4	1.832- 2.21	5.097E+02	0.06%	2.08E+04	0.02%	2.13E+04	0.06%	2.15E-05	
3	2.21- 2.25	1.762E+03	0.04%	4.66E+03	0.04%	6.43E+03	0.06%	6.50E-06	
2	2.25- 2.749	1.881E+03	0.02%	1.77E+04	0.02%	1.96E+04	0.03%	1.98E-05	
1	2.749- 2.75	2.064E+03	0.04%	2.65E+01	0.54%	2.09E+03	0.54%	2.11E-06	
Total		9.885E+08	0.16%	3.01E+05	0.02%	9.89E+08	0.16%	1.00E+00	

**Lower bound for PENTRAN models was 0.29 MeV

APPENDIX A SOURCE BOOK

A.40. 50 year WGPu Solid Gamma Spectrum Outer Source Box

Side Surfaces

Group Energy Bound Intrinsic Current Leakage 2 sigma error produced Current Leakage 2 sigma error total Current Leakage 2 sigma error Normalized Leakage

	(MeV)	(Photons/s)		(Photons/s)		(Photons/s)		(Photons/s)	
24	0 - 0.3 **	9.35E+08	0.16%	4.60E+04	0.02%	9.35E+08	0.16%	9.92E-01	
23	0.3- 0.741	6.93E+06	0.06%	1.04E+05	0.02%	7.04E+06	0.06%	7.47E-03	
22	0.741- 0.743	2.830E+03	0.06%	4.31E+02	0.14%	3.26E+03	0.15%	3.46E-06	
21	0.743- 0.765	2.199E+04	0.04%	4.71E+03	0.04%	2.67E+04	0.06%	2.83E-05	
20	0.765- 0.767	1.494E+04	0.06%	4.24E+02	0.14%	1.54E+04	0.15%	1.63E-05	
19	0.767- 0.954	2.548E+04	0.04%	4.26E+04	0.02%	6.81E+04	0.04%	7.23E-05	
18	0.954- 0.956	4.055E+02	0.06%	3.72E+02	0.14%	7.78E+02	0.15%	8.26E-07	
17	0.956- 0.999	9.030E+02	0.08%	7.52E+03	0.04%	8.42E+03	0.09%	8.94E-06	
16	0.999- 1.002	2.086E+02	0.10%	5.09E+02	0.12%	7.18E+02	0.16%	7.62E-07	
15	1.002- 1.18	2.507E+03	0.06%	3.32E+04	0.02%	3.57E+04	0.06%	3.79E-05	
14	1.18- 1.2	2.551E+02	0.20%	2.90E+03	0.06%	3.16E+03	0.21%	3.35E-06	
13	1.2- 1.24	4.990E+02	0.14%	6.02E+03	0.04%	6.52E+03	0.15%	6.92E-06	
12	1.24- 1.26	8.962E+03	0.04%	2.74E+03	0.06%	1.17E+04	0.07%	1.24E-05	
11	1.26- 1.5	1.130E+03	0.06%	2.94E+04	0.02%	3.06E+04	0.06%	3.25E-05	
10	1.5- 1.52	9.332E+01	0.22%	2.01E+03	0.06%	2.10E+03	0.23%	2.23E-06	
9	1.52- 1.736	9.924E+02	0.06%	1.97E+04	0.02%	2.07E+04	0.06%	2.19E-05	
8	1.736- 1.74	1.797E+01	0.48%	3.08E+02	0.16%	3.26E+02	0.51%	3.46E-07	
7	1.74- 1.76	5.536E+03	0.04%	1.52E+03	0.08%	7.05E+03	0.09%	7.49E-06	
6	1.76- 1.83	1.177E+02	0.12%	5.31E+03	0.04%	5.42E+03	0.13%	5.76E-06	
5	1.83- 1.832	3.927E+00	0.62%	1.43E+02	0.24%	1.47E+02	0.66%	1.56E-07	
4	1.832- 2.21	6.117E+02	0.06%	2.24E+04	0.02%	2.30E+04	0.06%	2.44E-05	
3	2.21- 2.25	1.824E+03	0.04%	4.90E+03	0.04%	6.72E+03	0.06%	7.14E-06	
2	2.25- 2.749	2.003E+03	0.02%	1.92E+04	0.02%	2.12E+04	0.03%	2.25E-05	
1	2.749- 2.75	2.155E+03	0.04%	2.83E+01	0.54%	2.18E+03	0.54%	2.32E-06	
Total		9.416E+08	0.16%	3.56E+05	0.02%	9.42E+08	0.16%	1.00E+00	

**Lower bound for PENTRAN models was 0.29 MeV

APPENDIX A SOURCE BOOK

A.40. 50 year WGPu Solid Gamma Spectrum Outer Source Box

Top/Bottom Surfaces

Group Energy Bound Intrinsic Current Leakage sigma error produced Current Leakage sigma error total Current Leakage sigma error Normalized Leakage

	(MeV)	(Photons/s)		(Photons/s)		(Photons/s)		(Photons/s)	
24	0 -0.3 **	5.41E+08	0.20%	2.75E+04	0.02%	5.41E+08	0.002009975	9.92E-01	
23	0.3- 0.741	3.94E+06	0.08%	6.08E+04	0.02%	4.00E+06	0.000824621	7.33E-03	
22	0.741- 0.743	1.590E+03	0.08%	2.44E+02	0.18%	1.83E+03	0.001969772	3.36E-06	
21	0.743- 0.765	1.236E+04	0.06%	2.68E+03	0.06%	1.50E+04	0.000848528	2.76E-05	
20	0.765- 0.767	8.397E+03	0.06%	2.41E+02	0.18%	8.64E+03	0.001897367	1.58E-05	
19	0.767- 0.954	1.432E+04	0.06%	2.44E+04	0.02%	3.87E+04	0.000632456	7.10E-05	
18	0.954- 0.956	2.278E+02	0.08%	2.10E+02	0.20%	4.37E+02	0.002154066	8.02E-07	
17	0.956- 0.999	5.075E+02	0.10%	4.23E+03	0.04%	4.74E+03	0.001077033	8.69E-06	
16	0.999- 1.002	1.170E+02	0.12%	2.87E+02	0.16%	4.04E+02	0.002	7.40E-07	
15	1.002- 1.18	1.403E+03	0.08%	1.87E+04	0.02%	2.01E+04	0.000824621	3.68E-05	
14	1.18- 1.2	1.420E+02	0.26%	1.63E+03	0.08%	1.77E+03	0.002720294	3.25E-06	
13	1.2- 1.24	2.774E+02	0.18%	3.42E+03	0.06%	3.69E+03	0.001897367	6.77E-06	
12	1.24- 1.26	5.020E+03	0.04%	1.54E+03	0.08%	6.56E+03	0.000894427	1.20E-05	
11	1.26- 1.5	6.310E+02	0.08%	1.66E+04	0.02%	1.73E+04	0.000824621	3.16E-05	
10	1.5- 1.52	5.193E+01	0.30%	1.12E+03	0.08%	1.18E+03	0.003104835	2.16E-06	
9	1.52- 1.736	5.516E+02	0.08%	1.10E+04	0.04%	1.16E+04	0.000894427	2.12E-05	
8	1.736- 1.74	9.864E+00	0.64%	1.72E+02	0.22%	1.82E+02	0.00676757	3.33E-07	
7	1.74- 1.76	3.095E+03	0.04%	8.51E+02	0.10%	3.95E+03	0.001077033	7.23E-06	
6	1.76- 1.83	6.543E+01	0.16%	2.99E+03	0.06%	3.06E+03	0.001708801	5.61E-06	
5	1.83- 1.832	2.201E+00	0.82%	7.99E+01	0.32%	8.21E+01	0.008802272	1.51E-07	
4	1.832- 2.21	3.391E+02	0.08%	1.25E+04	0.04%	1.29E+04	0.000894427	2.36E-05	
3	2.21- 2.25	1.018E+03	0.04%	2.74E+03	0.04%	3.76E+03	0.000565685	6.88E-06	
2	2.25- 2.749	1.115E+03	0.04%	1.08E+04	0.04%	1.19E+04	0.000565685	2.17E-05	
1	2.749- 2.75	1.202E+03	0.04%	1.59E+01	0.70%	1.22E+03	0.007011419	2.23E-06	
Total		5.454E+08	0.20%	2.05E+05	0.02%	5.46E+08	0.002009975	1.00E+00	

**Lower bound for PENTRAN models was 0.29 MeV

APPENDIX A SOURCE BOOK

A.41. 50 year WGPu Solid Neutron Spectrum Outer Source Box

Side Surfaces

47 GROUP

Group	Energy Bounds	Neutron Current Leakage	2 sigma error	Normalized Leakage
	(MeV)	(Neutrons/s)		
47	0 -1E-7	2.85E+02	0.001	2.46E-04
46	1E-7 - 4.14E-7	3.70E+02	0.001	3.19E-04
45	4.14E-7 - 8.76E-7	2.46E+02	0.0012	2.12E-04
44	8.76E-7 - 1.86E-6	3.12E+02	0.001	2.69E-04
43	1.86E-6 - 5.04E-6	5.57E+02	0.0008	4.80E-04
42	5.04E-6 - 1.07E-5	5.72E+02	0.0008	4.94E-04
41	1.07E-5 - 3.73E-5	1.37E+03	0.0006	1.18E-03
40	3.73E-5 - 1.01E-4	1.63E+03	0.0004	1.40E-03
39	1.01E-4 - 2.14E-4	1.69E+03	0.0004	1.46E-03
38	2.14E-4 - 4.54E-4	2.11E+03	0.0004	1.82E-03
37	4.54E-4 - 1.58E-3	5.32E+03	0.0002	4.59E-03
36	1.58E-3 - 3.35E-3	4.60E+03	0.0004	3.97E-03
35	3.35E-3 - 7.1E-3	6.40E+03	0.0002	5.52E-03
34	7.1E-3 - 1.5E-2	8.87E+03	0.0002	7.65E-03
33	1.5E-2 - 2.19E-2	5.97E+03	0.0002	5.15E-03
32	2.19E-2 - 2.42E-2	1.90E+03	0.0004	1.64E-03
31	2.42E-2 - 2.61E-2	1.63E+03	0.0004	1.41E-03
30	2.61E-2 - 3.18E-2	3.75E+03	0.0004	3.24E-03
29	3.18E-2 - 4.09E-2	5.72E+03	0.0002	4.94E-03
28	4.09E-2 - 6.74E-2	1.61E+04	0.0002	1.39E-02
27	6.74E-2 - 1.11E-1	2.39E+04	0.0002	2.06E-02
26	1.11E-1 - 1.83E-1	3.82E+04	0.0002	3.30E-02
25	1.83E-1 - 2.97E-1	6.11E+04	0.0002	5.27E-02
24	2.97E-1 - 3.69E-1	3.88E+04	0.0002	3.35E-02
23	3.69E-1 - 4.98E-1	5.98E+04	0.0002	5.16E-02

47 GROUP

Group	Energy Bounds	Neutron Current Leakage	2 sigma error	Normalized Leakage
	(MeV)	(Neutrons/s)		
22	4.98E-1 - 6.08E-1	5.30E+04	0.0002	4.57E-02
21	5.08E-1 - 7.43E-1	6.31E+04	0.0002	5.44E-02
20	7.43E-1 - 8.21E-1	3.44E+04	0.0002	2.97E-02
19	8.21E-1 - 1	6.90E+04	0.0002	5.95E-02
18	1 - 1.35	1.15E+05	0.0002	9.89E-02
17	1.35 - 1.65	8.38E+04	0.0002	7.23E-02
16	1.65 - 1.92	6.47E+04	0.0002	5.58E-02
15	1.92 - 2.23	6.32E+04	0.0002	5.45E-02
14	2.23 - 2.35	2.25E+04	0.0002	1.94E-02
13	2.35 - 2.37	3.77E+03	0.0004	3.25E-03
12	2.37 - 2.47	1.86E+04	0.0002	1.60E-02
11	2.47 - 2.73	4.13E+04	0.0002	3.56E-02
10	2.73 - 3.01	3.72E+04	0.0002	3.21E-02
9	3.01 - 3.68	6.67E+04	0.0002	5.76E-02
8	3.68 - 4.97	7.37E+04	0.0002	6.36E-02
7	4.97 - 6.07	3.02E+04	0.0002	2.60E-02
6	6.07 - 7.41	1.70E+04	0.0002	1.47E-02
5	7.41 - 8.61	6.29E+03	0.0002	5.42E-03
4	8.61 - 10	3.04E+03	0.0004	2.62E-03
3	10 - 12.2	1.52E+03	0.0004	1.31E-03
2	12.2 - 14.2	3.09E+02	0.001	2.67E-04
1	14.2 - 19.64	9.43E+01	0.0018	8.14E-05
Total		1.16E+06	0.0002	1.00E+00

APPENDIX A SOURCE BOOK

A.41. 50 year WGPu Solid Neutron Spectrum Outer Source Box

Top/Bottom Surfaces

47 GROUP

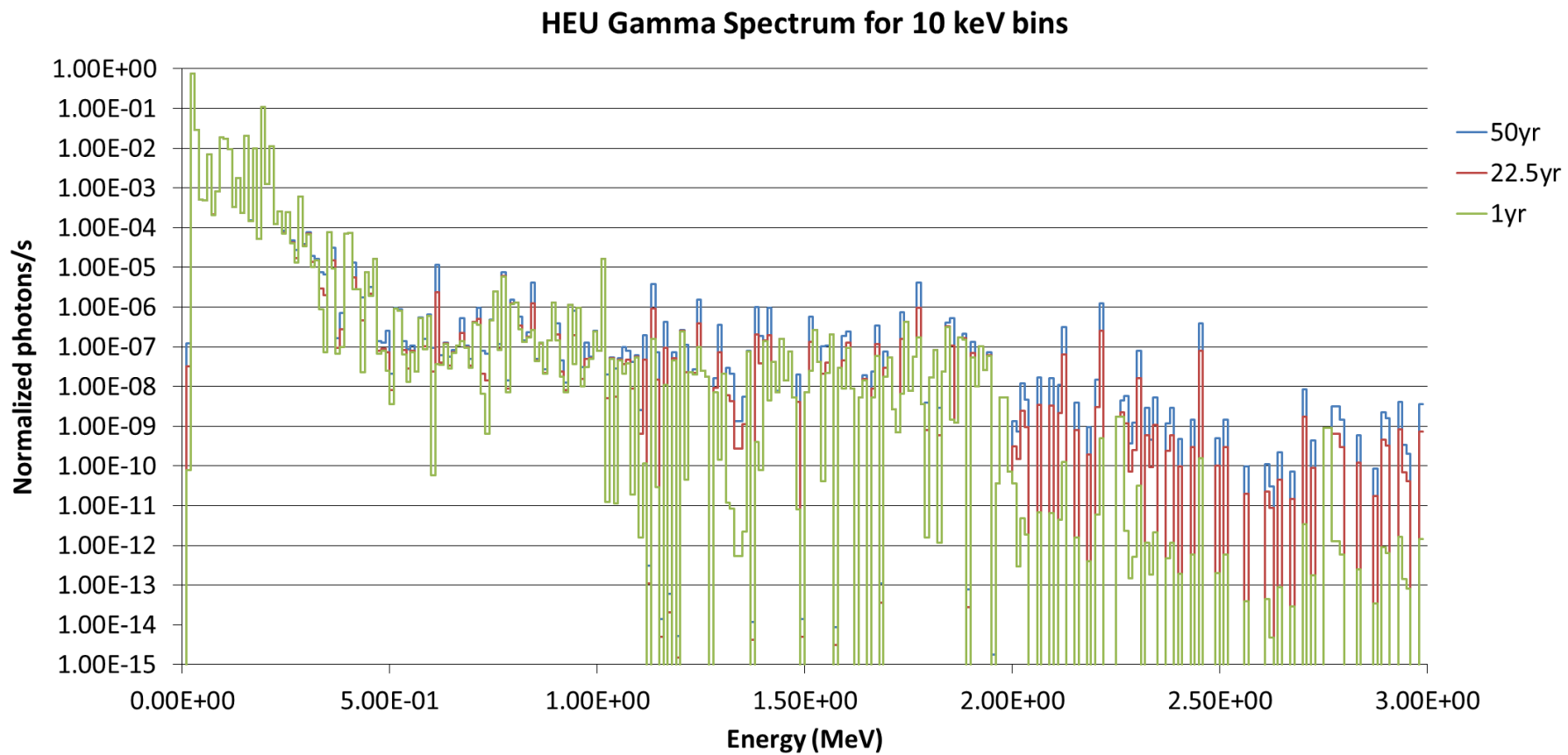
Group	Energy Bounds (MeV)	Neutron Current Leakage (Neutrons/s)	2 sigma error	Normalized Leakage
47	0 -1E-7	1.87E+02	0.12%	2.76E-04
46	1E-7 - 4.14E-7	2.46E+02	0.12%	3.64E-04
45	4.14E-7 - 8.76E-7	1.65E+02	0.14%	2.43E-04
44	8.76E-7 - 1.86E-6	2.09E+02	0.12%	3.09E-04
43	1.86E-6 - 5.04E-6	3.73E+02	0.10%	5.50E-04
42	5.04E-6 - 1.07E-5	3.82E+02	0.10%	5.64E-04
41	1.07E-5 - 3.73E-5	9.11E+02	0.06%	1.35E-03
40	3.73E-5 - 1.01E-4	1.08E+03	0.06%	1.59E-03
39	1.01E-4 - 2.14E-4	1.11E+03	0.06%	1.64E-03
38	2.14E-4 - 4.54E-4	1.38E+03	0.06%	2.03E-03
37	4.54E-4 - 1.58E-3	3.43E+03	0.04%	5.07E-03
36	1.58E-3 - 3.35E-3	2.93E+03	0.04%	4.32E-03
35	3.35E-3 - 7.1E-3	4.03E+03	0.04%	5.94E-03
34	7.1E-3 - 1.5E-2	5.47E+03	0.02%	8.08E-03
33	1.5E-2 - 2.19E-2	3.64E+03	0.04%	5.37E-03
32	2.19E-2 - 2.42E-2	1.15E+03	0.06%	1.70E-03
31	2.42E-2 - 2.61E-2	9.95E+02	0.06%	1.47E-03
30	2.61E-2 - 3.18E-2	2.27E+03	0.04%	3.34E-03
29	3.18E-2 - 4.09E-2	3.43E+03	0.04%	5.06E-03
28	4.09E-2 - 6.74E-2	9.64E+03	0.02%	1.42E-02
27	6.74E-2 - 1.11E-1	1.43E+04	0.02%	2.11E-02
26	1.11E-1 - 1.83E-1	2.28E+04	0.02%	3.37E-02
25	1.83E-1 - 2.97E-1	3.63E+04	0.02%	5.36E-02
24	2.97E-1 - 3.69E-1	2.30E+04	0.02%	3.39E-02
23	3.69E-1 - 4.98E-1	3.57E+04	0.02%	5.27E-02

47 GROUP

Group	Energy Bounds (MeV)	Neutron Current Leakage (Neutrons/s)	2 sigma error	Normalized Leakage
22	4.98E-1 - 6.08E-1	3.14E+04	0.02%	4.63E-02
21	6.08E-1 - 7.43E-1	3.71E+04	0.02%	5.48E-02
20	7.43E-1 - 8.21E-1	2.01E+04	0.02%	2.96E-02
19	8.21E-1 - 1	4.04E+04	0.02%	5.97E-02
18	1 - 1.35	6.71E+04	0.02%	9.91E-02
17	1.35 - 1.65	4.85E+04	0.02%	7.17E-02
16	1.65 - 1.92	3.73E+04	0.02%	5.51E-02
15	1.92 - 2.23	3.63E+04	0.02%	5.35E-02
14	2.23 - 2.35	1.28E+04	0.02%	1.89E-02
13	2.35 - 2.37	2.15E+03	0.04%	3.17E-03
12	2.37 - 2.47	1.06E+04	0.02%	1.56E-02
11	2.47 - 2.73	2.35E+04	0.02%	3.47E-02
10	2.73 - 3.01	2.12E+04	0.02%	3.13E-02
9	3.01 - 3.68	3.84E+04	0.02%	5.67E-02
8	3.68 - 4.97	4.21E+04	0.02%	6.22E-02
7	4.97 - 6.07	1.71E+04	0.02%	2.53E-02
6	6.07 - 7.41	9.59E+03	0.02%	1.42E-02
5	7.41 - 8.61	3.55E+03	0.04%	5.24E-03
4	8.61 - 10	1.71E+03	0.04%	2.52E-03
3	10 - 12.2	8.53E+02	0.06%	1.26E-03
2	12.2 - 14.2	1.74E+02	0.14%	2.57E-04
1	14.2 - 19.64	5.31E+01	0.24%	7.84E-05
Total		6.77E+05	0.02%	

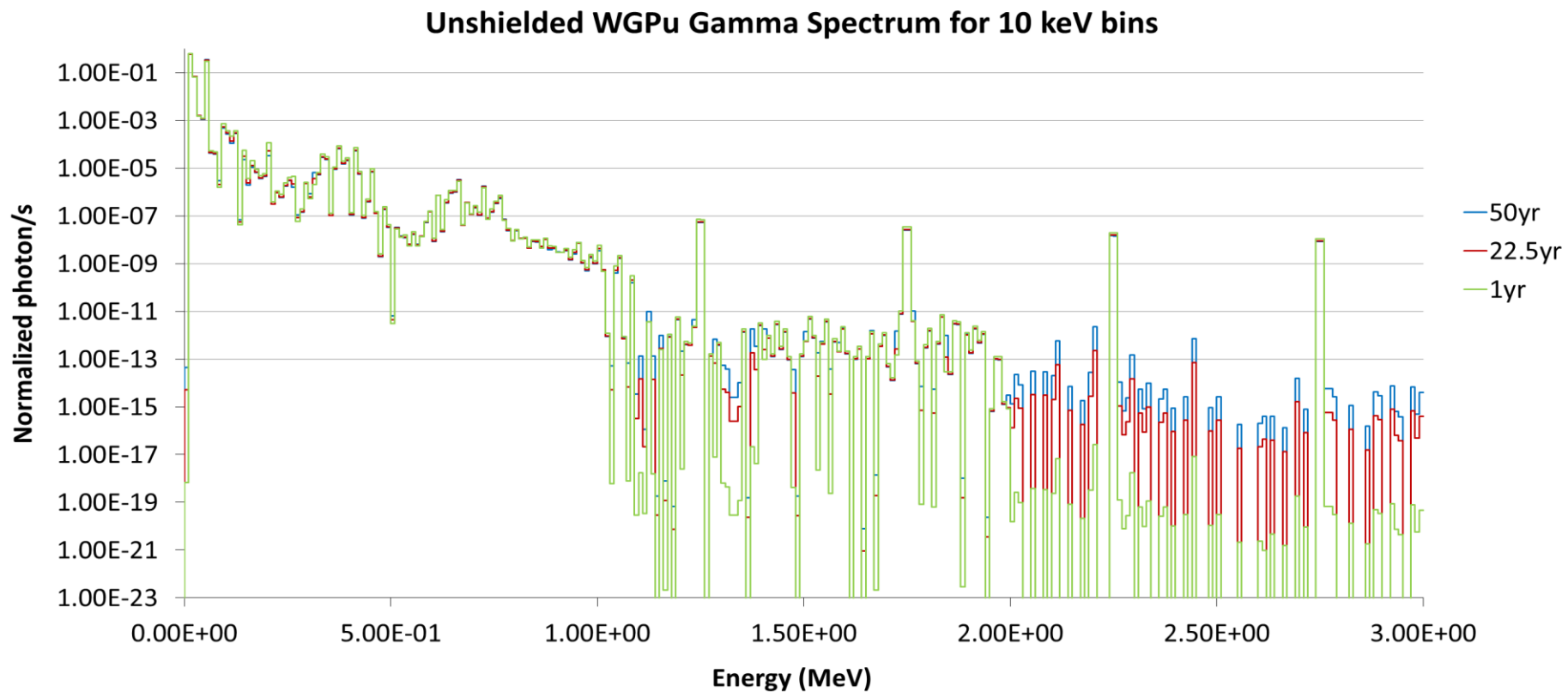
APPENDIX A SOURCE BOOK

Figure A.7. HEU 10keV binned unshielded 25kg mass gamma spectrum



APPENDIX A SOURCE BOOK

Figure A.8. WGPu 10keV binned unshielded 8kg mass gamma spectrum



APPENDIX A SOURCE BOOK

A.42. 25kg HEU unshielded

PHOTONS		Photons/s					Normalized				
Group	Energy Bounds (MeV)	1.0 y	22.5 y	50.0 y	75.0 y	100.0 y	1.0 y	22.5 y	50.0 y	75.0 y	100.0 y
1	0.290 - 0.300	7.64E+05	8.00E+05	8.80E+05	9.81E+05	1.11E+06	2.454E-01	2.396E-01	2.193E-01	1.992E-01	1.818E-01
2	0.300 - 0.741	2.00E+06	2.14E+06	2.54E+06	3.06E+06	3.70E+06	6.421E-01	6.398E-01	6.322E-01	6.214E-01	6.091E-01
3	0.741 - 0.743	2.57E+04	2.57E+04	2.59E+04	2.61E+04	2.64E+04	8.262E-03	7.710E-03	6.449E-03	5.298E-03	4.338E-03
4	0.743 - 0.765	1.15E+03	1.22E+03	1.48E+03	1.90E+03	2.46E+03	3.680E-04	3.641E-04	3.699E-04	3.851E-04	4.052E-04
5	0.765 - 0.767	5.50E+04	5.80E+04	6.77E+04	8.10E+04	9.77E+04	1.768E-02	1.737E-02	1.689E-02	1.645E-02	1.607E-02
6	0.767 - 0.954	6.87E+04	8.28E+04	1.28E+05	1.88E+05	2.60E+05	2.208E-02	2.481E-02	3.193E-02	3.809E-02	4.282E-02
7	0.954 - 0.956	1.37E+03	1.39E+03	1.47E+03	1.56E+03	1.65E+03	4.393E-04	4.174E-04	3.662E-04	3.165E-04	2.721E-04
8	0.956 - 0.999	4.04E+03	4.24E+03	5.02E+03	6.23E+03	7.92E+03	1.299E-03	1.270E-03	1.251E-03	1.266E-03	1.303E-03
9	0.999 - 1.000	1.56E+05	1.56E+05	1.56E+05	1.56E+05	1.56E+05	5.020E-02	4.678E-02	3.891E-02	3.171E-02	2.568E-02
10	1.000 - 1.180	4.08E+03	1.35E+04	5.00E+04	1.06E+05	1.84E+05	1.311E-03	4.042E-03	1.245E-02	2.159E-02	3.030E-02
11	1.180 - 1.200	2.39E+03	2.42E+03	2.51E+03	2.62E+03	2.73E+03	7.677E-04	7.249E-04	6.257E-04	5.312E-04	4.489E-04
12	1.200 - 1.240	1.48E+03	4.61E+03	1.69E+04	3.61E+04	6.27E+04	4.743E-04	1.381E-03	4.213E-03	7.325E-03	1.032E-02
13	1.240 - 1.260	3.17E+02	3.17E+02	3.17E+02	3.17E+02	3.17E+02	1.018E-04	9.493E-05	7.897E-05	6.435E-05	5.211E-05
14	1.260 - 1.500	5.50E+03	1.05E+04	3.03E+04	6.11E+04	1.04E+05	1.768E-03	3.158E-03	7.553E-03	1.241E-02	1.709E-02
15	1.500 - 1.520	2.82E+03	3.87E+03	8.01E+03	1.45E+04	2.34E+04	9.062E-04	1.160E-03	1.996E-03	2.935E-03	3.852E-03
16	1.520 - 1.740	5.64E+03	8.11E+03	1.78E+04	3.29E+04	5.40E+04	1.812E-03	2.429E-03	4.440E-03	6.689E-03	8.881E-03
17	1.740 - 1.740	3.97E+03	4.69E+03	7.55E+03	1.20E+04	1.82E+04	1.274E-03	1.406E-03	1.883E-03	2.440E-03	2.997E-03
18	1.740 - 1.760	6.27E+02	6.27E+02	6.27E+02	6.27E+02	6.27E+02	2.015E-04	1.878E-04	1.562E-04	1.273E-04	1.031E-04
19	1.760 - 1.830	2.85E+03	1.04E+04	4.00E+04	8.61E+04	1.50E+05	9.146E-04	3.110E-03	9.964E-03	1.749E-02	2.472E-02
20	1.830 - 1.830	2.98E+03	3.07E+03	3.43E+03	4.00E+03	4.79E+03	9.576E-04	9.203E-04	8.560E-04	8.125E-04	7.876E-04
21	1.830 - 2.210	5.31E+03	8.70E+03	2.20E+04	4.28E+04	7.18E+04	1.705E-03	2.607E-03	5.492E-03	8.698E-03	1.180E-02
22	2.210 - 2.250	1.91E+01	1.21E+03	5.88E+03	1.32E+04	2.33E+04	6.122E-06	3.623E-04	1.466E-03	2.673E-03	3.833E-03
23	2.250 - 2.749	1.68E+01	9.57E+02	4.65E+03	1.04E+04	1.84E+04	5.383E-06	2.867E-04	1.158E-03	2.113E-03	3.027E-03
24	2.749 - 2.750	1.73E+01	1.73E+01	1.73E+01	1.73E+01	1.73E+01	5.550E-06	5.175E-06	4.305E-06	3.510E-06	2.842E-06
total		3.11E+06	3.34E+06	4.01E+06	4.92E+06	6.08E+06					

APPENDIX A SOURCE BOOK

A.43. 8 kg WGPu Unshielded Source Gammas (0.29 - 2.75 MeV)

PHOTONS

Group	Energy Bounds (MeV)	Photons/s				Normalized			
		1.0 y	10.0 y	22.5 y	50.0 y	1.0 y	10.0 y	22.5 y	50.0 y
1	0.290 - 0.300	1.26E+07	1.48E+07	1.84E+07	2.70E+07	1.461E-02	1.699E-02	2.078E-02	2.994E-02
2	0.300 - 0.741	8.43E+08	8.52E+08	8.59E+08	8.68E+08	9.778E-01	9.753E-01	9.715E-01	9.625E-01
3	0.741 - 0.743	2.36E+05	2.64E+05	2.84E+05	2.88E+05	2.743E-04	3.029E-04	3.205E-04	3.190E-04
4	0.743 - 0.765	2.03E+06	2.09E+06	2.13E+06	2.16E+06	2.352E-03	2.392E-03	2.412E-03	2.395E-03
5	0.765 - 0.767	1.57E+06	1.59E+06	1.59E+06	1.55E+06	1.823E-03	1.819E-03	1.796E-03	1.722E-03
6	0.767 - 0.954	1.63E+06	1.71E+06	1.77E+06	1.80E+06	1.891E-03	1.961E-03	2.003E-03	1.994E-03
7	0.954 - 0.956	2.09E+04	2.47E+04	2.75E+04	2.94E+04	2.430E-05	2.824E-05	3.111E-05	3.260E-05
8	0.956 - 0.999	2.60E+04	2.59E+04	2.59E+04	2.57E+04	3.017E-05	2.971E-05	2.923E-05	2.850E-05
9	0.999 - 1.002	1.70E+04	1.60E+04	1.48E+04	1.25E+04	1.974E-05	1.837E-05	1.673E-05	1.383E-05
10	1.002 - 1.180	1.65E+04	1.67E+04	1.66E+04	1.62E+04	1.919E-05	1.908E-05	1.879E-05	1.798E-05
11	1.180 - 1.200	2.09E+01	2.09E+01	2.09E+01	2.09E+01	2.421E-08	2.389E-08	2.358E-08	2.314E-08
12	1.200 - 1.240	1.28E+01	1.30E+01	1.42E+01	2.68E+01	1.490E-08	1.483E-08	1.603E-08	2.969E-08
13	1.240 - 1.260	5.03E+05	5.03E+05	5.03E+05	5.02E+05	5.836E-04	5.766E-04	5.688E-04	5.559E-04
14	1.260 - 1.500	4.80E+01	4.81E+01	5.01E+01	7.03E+01	5.566E-08	5.513E-08	5.662E-08	7.796E-08
15	1.500 - 1.520	2.46E+01	2.46E+01	2.51E+01	2.93E+01	2.855E-08	2.822E-08	2.832E-08	3.247E-08
16	1.520 - 1.736	4.92E+01	4.93E+01	5.03E+01	6.04E+01	5.708E-08	5.644E-08	5.681E-08	6.691E-08
17	1.736 - 1.740	3.46E+01	3.46E+01	3.49E+01	3.79E+01	4.017E-08	3.967E-08	3.948E-08	4.195E-08
18	1.740 - 1.760	2.42E+05	2.42E+05	2.42E+05	2.41E+05	2.808E-04	2.774E-04	2.738E-04	2.676E-04
19	1.760 - 1.830	2.47E+01	2.50E+01	2.80E+01	5.83E+01	2.869E-08	2.865E-08	3.161E-08	6.466E-08
20	1.830 - 1.832	2.60E+01	2.60E+01	2.61E+01	2.64E+01	3.020E-08	2.980E-08	2.945E-08	2.929E-08
21	1.832 - 2.210	4.63E+01	4.64E+01	4.77E+01	6.14E+01	5.372E-08	5.315E-08	5.396E-08	6.807E-08
22	2.210 - 2.250	6.99E+04	6.99E+04	6.99E+04	6.96E+04	8.104E-05	8.006E-05	7.897E-05	7.717E-05
23	2.250 - 2.749	6.23E+04	6.24E+04	6.23E+04	6.21E+04	7.229E-05	7.142E-05	7.045E-05	6.885E-05
24	2.749 - 2.750	7.94E+04	7.94E+04	7.93E+04	7.91E+04	9.206E-05	9.091E-05	8.967E-05	8.761E-05
total		8.62E+08	8.73E+08	8.85E+08	9.02E+08				

APPENDIX A SOURCE BOOK

A.44. 8 kg WGPu Unshielded Source Gammas (1.0×10^{-13} - 3.0 MeV)

PHOTONS		Photons/s				Normalized			
Group	Energy Bounds (MeV)	1.0 y	10.0 y	22.5 y	50.0 y	1.0 y	10.0 y	22.5 y	50.0 y
1	1.0E-13 - 0.300	6.59E+11	7.79E+11	8.72E+11	9.31E+11	9.986E-01	9.988E-01	9.989E-01	9.990E-01
2	0.300 - 0.660	8.95E+08	9.02E+08	9.09E+08	9.21E+08	1.356E-03	1.156E-03	1.042E-03	9.888E-04
3	0.660 - 0.870	1.98E+07	2.26E+07	2.47E+07	2.61E+07	2.994E-05	2.893E-05	2.834E-05	2.799E-05
4	0.870 - 1.000	1.82E+05	1.92E+05	1.98E+05	1.98E+05	2.761E-07	2.460E-07	2.268E-07	2.122E-07
5	1.000 - 1.080	2.51E+04	2.48E+04	2.43E+04	2.29E+04	3.802E-08	3.185E-08	2.785E-08	2.459E-08
6	1.080 - 1.240	1.09E+03	1.01E+03	9.27E+02	7.97E+02	1.643E-09	1.300E-09	1.063E-09	8.552E-10
7	1.240 - 1.250	2.53E+05	2.53E+05	2.53E+05	2.52E+05	3.825E-07	3.240E-07	2.895E-07	2.703E-07
8	1.250 - 1.300	2.47E+05	2.47E+05	2.47E+05	2.46E+05	3.734E-07	3.163E-07	2.827E-07	2.639E-07
9	1.300 - 1.410	1.91E+01	1.92E+01	2.07E+01	3.59E+01	2.890E-11	2.464E-11	2.371E-11	3.856E-11
10	1.410 - 1.450	1.87E+01	1.87E+01	1.89E+01	2.13E+01	2.831E-11	2.397E-11	2.170E-11	2.287E-11
11	1.450 - 1.490	7.15E+00	7.15E+00	7.16E+00	7.32E+00	1.083E-11	9.165E-12	8.211E-12	7.858E-12
12	1.490 - 1.740	9.21E+01	9.22E+01	9.38E+01	1.11E+02	1.394E-10	1.181E-10	1.075E-10	1.194E-10
13	1.740 - 1.750	1.21E+05	1.22E+05	1.22E+05	1.21E+05	1.839E-07	1.558E-07	1.392E-07	1.300E-07
14	1.750 - 1.860	1.17E+05	1.18E+05	1.18E+05	1.17E+05	1.778E-07	1.506E-07	1.347E-07	1.257E-07
15	1.860 - 1.890	2.74E+01	2.74E+01	2.74E+01	2.79E+01	4.146E-11	3.508E-11	3.141E-11	2.999E-11
16	1.890 - 1.990	2.15E+01	2.15E+01	2.15E+01	2.22E+01	3.253E-11	2.752E-11	2.469E-11	2.381E-11
17	1.990 - 2.210	5.78E-03	8.41E-02	8.76E-01	9.05E+00	8.759E-15	1.078E-13	1.004E-12	9.710E-12
18	2.210 - 2.230	4.70E-05	4.61E-02	5.12E-01	5.32E+00	7.114E-17	5.910E-14	5.866E-13	5.705E-12
19	2.230 - 2.250	6.95E+04	6.96E+04	6.95E+04	6.93E+04	1.053E-07	8.920E-08	7.970E-08	7.440E-08
20	2.250 - 2.440	6.64E+04	6.65E+04	6.64E+04	6.62E+04	1.006E-07	8.520E-08	7.613E-08	7.107E-08
21	2.440 - 2.500	2.93E-05	2.87E-02	3.19E-01	3.31E+00	4.432E-17	3.682E-14	3.654E-13	3.554E-12
22	2.500 - 2.740	8.16E-07	8.14E-04	9.05E-03	9.38E-02	1.236E-18	1.043E-15	1.038E-14	1.007E-13
23	2.740 - 2.750	3.97E+04	3.98E+04	3.97E+04	3.96E+04	6.019E-08	5.096E-08	4.553E-08	4.249E-08
24	2.750 - 3.000	3.79E+04	3.80E+04	3.79E+04	3.78E+04	5.747E-08	4.865E-08	4.347E-08	4.057E-08
totals		6.60E+11	7.80E+11	8.73E+11	9.32E+11				

APPENDIX A SOURCE BOOK

A.45. 8 kg WGpu Unshielded Source Neutrons

NEUTRONS

47 Group

Group Energy Bounds (MeV)	Neutrons/s				Normalized			
	1.0 y	10.0 y	22.5 y	50.0 y	1.0 y	10.0 y	22.5 y	50.0 y
1 1.00E-11 - 1.00E-07	5.85E-06	5.84E-06	5.83E-06	5.80E-06	6.974E-11	6.969E-11	6.964E-11	6.958E-11
2 1.00E-07 - 4.14E-07	4.98E-05	4.98E-05	4.97E-05	4.95E-05	5.940E-10	5.937E-10	5.935E-10	5.934E-10
3 4.14E-07 - 8.76E-07	1.18E-04	1.18E-04	1.17E-04	1.17E-04	1.404E-09	1.404E-09	1.403E-09	1.404E-09
4 8.76E-07 - 1.86E-06	3.62E-04	3.62E-04	3.61E-04	3.60E-04	4.318E-09	4.316E-09	4.314E-09	4.314E-09
5 1.86E-06 - 5.04E-06	1.86E-03	1.86E-03	1.86E-03	1.85E-03	2.221E-08	2.221E-08	2.219E-08	2.218E-08
6 5.04E-06 - 1.07E-05	4.98E-03	4.97E-03	4.96E-03	4.94E-03	5.932E-08	5.928E-08	5.926E-08	5.924E-08
7 1.07E-05 - 3.73E-05	4.06E-02	4.05E-02	4.04E-02	4.03E-02	4.838E-07	4.835E-07	4.833E-07	4.831E-07
8 3.73E-05 - 1.01E-04	1.67E-01	1.67E-01	1.67E-01	1.66E-01	1.993E-06	1.993E-06	1.992E-06	1.993E-06
9 1.01E-04 - 2.14E-04	4.48E-01	4.47E-01	4.46E-01	4.45E-01	5.336E-06	5.335E-06	5.335E-06	5.334E-06
10 2.14E-04 - 4.54E-04	1.38E+00	1.38E+00	1.37E+00	1.37E+00	1.643E-05	1.643E-05	1.642E-05	1.641E-05
11 4.54E-04 - 1.58E-03	1.13E+01	1.13E+01	1.12E+01	1.12E+01	1.342E-04	1.342E-04	1.342E-04	1.341E-04
12 1.58E-03 - 3.35E-03	2.77E+01	2.76E+01	2.76E+01	2.75E+01	3.298E-04	3.296E-04	3.295E-04	3.294E-04
13 3.35E-03 - 7.10E-03	8.51E+01	8.49E+01	8.48E+01	8.45E+01	1.014E-03	1.014E-03	1.013E-03	1.013E-03
14 7.10E-03 - 1.50E-02	2.61E+02	2.61E+02	2.60E+02	2.59E+02	3.114E-03	3.113E-03	3.112E-03	3.112E-03
15 1.50E-02 - 2.19E-02	2.91E+02	2.91E+02	2.90E+02	2.89E+02	3.470E-03	3.470E-03	3.469E-03	3.468E-03
16 2.19E-02 - 2.42E-02	1.09E+02	1.09E+02	1.09E+02	1.09E+02	1.303E-03	1.303E-03	1.303E-03	1.302E-03
17 2.42E-02 - 2.61E-02	9.34E+01	9.33E+01	9.31E+01	9.27E+01	1.113E-03	1.113E-03	1.112E-03	1.112E-03
18 2.61E-02 - 3.18E-02	3.06E+02	3.06E+02	3.06E+02	3.04E+02	3.653E-03	3.653E-03	3.651E-03	3.651E-03
19 3.18E-02 - 4.09E-02	5.36E+02	5.36E+02	5.35E+02	5.33E+02	6.393E-03	6.391E-03	6.389E-03	6.389E-03
20 4.09E-02 - 6.74E-02	1.90E+03	1.90E+03	1.90E+03	1.89E+03	2.265E-02	2.265E-02	2.265E-02	2.264E-02
21 6.74E-02 - 1.11E-01	3.96E+03	3.96E+03	3.95E+03	3.93E+03	4.721E-02	4.721E-02	4.719E-02	4.719E-02
22 1.11E-01 - 1.83E-01	8.17E+03	8.16E+03	8.14E+03	8.11E+03	9.734E-02	9.734E-02	9.732E-02	9.730E-02
23 1.83E-01 - 2.97E-01	1.58E+04	1.58E+04	1.57E+04	1.57E+04	1.880E-01	1.879E-01	1.880E-01	1.880E-01
24 2.97E-01 - 3.69E-01	1.11E+04	1.11E+04	1.11E+04	1.11E+04	1.328E-01	1.328E-01	1.328E-01	1.328E-01
25 3.69E-01 - 4.98E-01	2.17E+04	2.16E+04	2.16E+04	2.15E+04	2.582E-01	2.582E-01	2.583E-01	2.583E-01
26 4.98E-01 - 6.08E-01	1.96E+04	1.96E+04	1.95E+04	1.94E+04	2.332E-01	2.333E-01	2.333E-01	2.332E-01

APPENDIX A SOURCE BOOK

A.45. 8 kg WG⁹⁴Pu Unshielded Source Neutrons

NEUTRONS

47 Group

Group	Energy Bounds (MeV)	Neutrons/s				Normalized			
		1.0 y	10.0 y	22.5 y	50.0 y	1.0 y	10.0 y	22.5 y	50.0 y
27	6.08E-01 - 7.43E-01	2.46E+04	2.46E+04	2.46E+04	2.45E+04	2.934E-01	2.934E-01	2.934E-01	2.935E-01
28	7.43E-01 - 8.21E-01	1.44E+04	1.44E+04	1.44E+04	1.43E+04	1.717E-01	1.717E-01	1.717E-01	1.718E-01
29	8.21E-01 - 1.00E+00	3.33E+04	3.33E+04	3.32E+04	3.31E+04	3.970E-01	3.971E-01	3.971E-01	3.971E-01
30	1.00E+00 - 1.35E+00	6.10E+04	6.09E+04	6.08E+04	6.06E+04	7.269E-01	7.271E-01	7.271E-01	7.270E-01
31	1.35E+00 - 1.65E+00	4.68E+04	4.67E+04	4.67E+04	4.65E+04	5.576E-01	5.575E-01	5.575E-01	5.574E-01
32	1.65E+00 - 1.92E+00	3.70E+04	3.70E+04	3.69E+04	3.68E+04	4.416E-01	4.414E-01	4.412E-01	4.411E-01
33	1.92E+00 - 2.23E+00	3.75E+04	3.74E+04	3.73E+04	3.72E+04	4.467E-01	4.464E-01	4.462E-01	4.461E-01
34	2.23E+00 - 2.35E+00	1.23E+04	1.23E+04	1.23E+04	1.22E+04	1.471E-01	1.470E-01	1.469E-01	1.468E-01
35	2.35E+00 - 2.37E+00	2.03E+03	2.03E+03	2.03E+03	2.02E+03	2.423E-02	2.421E-02	2.420E-02	2.420E-02
36	2.37E+00 - 2.47E+00	1.01E+04	1.01E+04	1.01E+04	1.01E+04	1.208E-01	1.206E-01	1.206E-01	1.206E-01
37	2.47E+00 - 2.73E+00	2.35E+04	2.35E+04	2.35E+04	2.34E+04	2.806E-01	2.804E-01	2.804E-01	2.803E-01
38	2.73E+00 - 3.01E+00	2.21E+04	2.21E+04	2.20E+04	2.19E+04	2.634E-01	2.632E-01	2.630E-01	2.630E-01
39	3.01E+00 - 3.68E+00	3.83E+04	3.82E+04	3.81E+04	3.80E+04	4.560E-01	4.558E-01	4.556E-01	4.554E-01
40	3.68E+00 - 4.97E+00	3.87E+04	3.87E+04	3.86E+04	3.84E+04	4.614E-01	4.613E-01	4.613E-01	4.612E-01
41	4.97E+00 - 6.07E+00	1.33E+04	1.33E+04	1.33E+04	1.33E+04	1.590E-01	1.591E-01	1.591E-01	1.591E-01
42	6.07E+00 - 7.41E+00	6.13E+03	6.13E+03	6.12E+03	6.10E+03	7.308E-02	7.315E-02	7.319E-02	7.318E-02
43	7.41E+00 - 8.61E+00	1.77E+03	1.76E+03	1.76E+03	1.75E+03	2.105E-02	2.104E-02	2.102E-02	2.101E-02
44	8.61E+00 - 1.00E+01	6.61E+02	6.60E+02	6.58E+02	6.55E+02	7.880E-03	7.874E-03	7.868E-03	7.861E-03
45	1.00E+01 - 1.22E+01	2.23E+02	2.23E+02	2.22E+02	2.21E+02	2.657E-03	2.655E-03	2.653E-03	2.650E-03
46	1.22E+01 - 1.42E+01	2.68E+01	2.67E+01	2.66E+01	2.65E+01	3.190E-04	3.187E-04	3.184E-04	3.179E-04
47	1.42E+01 - 1.96E+01	4.60E+00	4.59E+00	4.58E+00	4.56E+00	5.488E-05	5.481E-05	5.475E-05	5.465E-05
total		8.39E+04	8.38E+04	8.37E+04	8.34E+04				

APPENDIX A SOURCE BOOK

A.46. 8 kg WGPu unshielded source 30 group neutron spectrum

NEUTRONS

30 Group		22.5 y	22.5 y	30 Group		22.5 y	22.5 y
Group	Energy Bounds (MeV)	Neutrons/s	Normalized	Group	Energy Bounds (MeV)	Neutrons/s	Normalized
1	0.00E+00 - 1.00E-10	1.18E-09	3.472E-15	27	1.50E+00 - 3.00E+00	1.66E+05	4.896E-01
2	1.00E-10 - 5.00E-10	1.49E-09	4.370E-15	28	3.00E+00 - 8.19E+00	9.83E+04	2.894E-01
3	5.00E-10 - 7.50E-10	6.20E-10	1.825E-15	29	8.19E+00 - 1.73E+01	1.33E+03	3.919E-03
4	7.50E-10 - 1.20E-09	9.18E-10	2.700E-15	30	1.73E+01 - 2.00E+01	1.90E-01	5.600E-07
5	1.20E-09 - 1.50E-09	5.32E-10	1.565E-15	totals		3.40E+05	
6	1.50E-09 - 2.53E-08	5.11E-07	1.503E-12				
7	2.53E-08 - 3.00E-08	2.07E-07	6.103E-13				
8	3.00E-08 - 4.00E-08	5.15E-07	1.515E-12				
9	4.00E-08 - 5.00E-08	6.02E-07	1.771E-12				
10	5.00E-08 - 7.00E-08	1.42E-06	4.190E-12				
11	7.00E-08 - 1.00E-07	2.65E-06	7.798E-12				
12	1.00E-07 - 1.25E-07	2.65E-06	7.783E-12				
13	1.25E-07 - 1.75E-07	6.12E-06	1.802E-11				
14	1.75E-07 - 3.50E-07	2.83E-05	8.339E-11				
15	3.50E-07 - 6.25E-07	6.07E-05	1.787E-10				
16	6.25E-07 - 1.00E-06	1.07E-04	3.157E-10				
17	1.00E-06 - 1.30E-06	1.02E-04	3.004E-10				
18	1.30E-06 - 3.05E-06	8.12E-04	2.389E-09				
19	3.05E-06 - 3.70E-05	4.62E-02	1.358E-07				
20	3.70E-05 - 1.55E-03	1.28E+01	3.761E-05				
21	1.55E-03 - 1.30E-02	2.98E+02	8.763E-04				
22	1.30E-02 - 4.50E-02	1.67E+03	4.923E-03				
23	4.50E-02 - 2.70E-01	2.55E+04	7.489E-02				
24	2.70E-01 - 7.50E-01	8.21E+04	2.417E-01				
25	7.50E-01 - 1.25E+00	8.98E+04	2.643E-01				
26	1.25E+00 - 1.50E+00	4.08E+04	1.201E-01				

APPENDIX B

SAMPLE MCNP SOURCE BOX INPUT

Simple Sourcebox 1yr HEU

```
c
c -----CELLS-----
c
1 0 -1           IMP:P=1 $Source Box
2 1 -0.00120479 1 -2 IMP:P=2 $Air Surrounding box
3 1 -0.00120479 2 -3 IMP:P=1 $Air between Sphere and Outer Space
4 0 3           IMP:P=0 $Outer Space Void

c -----SURFACES-----
1 rpp -30 30 -30 30 -30 30      $Box
2 rpp -31 31 -31 31 -40 40      $Sphere for Tally
3 rpp -75 75 -75 75 -75 75      $Outer Space Box

c -----DATA-----
c
MODE P
SDEF ERG=d1 CEL=1 x=d2 y=d3 z=d4
c
c -----Energy Distribution-----
#   SI1      SP1
    h        d
    0.00    0.00
    3.000E-01 9.913E-01
    7.410E-01 6.871E-03
    7.430E-01 8.408E-05
    7.650E-01 3.865E-05
    7.670E-01 1.834E-04
    9.540E-01 4.726E-04
    9.560E-01 7.822E-06
    9.990E-01 5.759E-05
    1.002E+00 7.010E-04
    1.180E+00 4.210E-05
    1.200E+00 1.489E-05
    1.240E+00 1.210E-05
    1.260E+00 3.655E-06
    1.500E+00 5.284E-05
    1.520E+00 1.894E-05
    1.736E+00 4.859E-05
```

1.740E+00	2.698E-05
1.760E+00	5.036E-06
1.830E+00	2.153E-04
1.832E+00	2.085E-04
2.210E+00	4.047E-04
2.250E+00	1.433E-07
2.749E+00	1.394E-07
2.750E+00	1.443E-07

c

c -----X-Axis Distribution-----

#	SI2	SP2
	h	d
-30	0.0000E+00	
-24	7.0319E-02	
-18	8.4472E-02	
-12	1.0066E-01	
-6	1.1681E-01	
0	1.2774E-01	
6	1.2774E-01	
12	1.1681E-01	
18	1.0066E-01	
24	8.4472E-02	
30	7.0319E-02	

c -----Y-Axis Distribution-----

#	SI3	SP3
	h	d
-30	0.0000E+00	
-24	7.0319E-02	
-18	8.4472E-02	
-12	1.0066E-01	
-6	1.1681E-01	
0	1.2774E-01	
6	1.2774E-01	
12	1.1681E-01	
18	1.0066E-01	
24	8.4472E-02	
30	7.0319E-02	

c -----Z-Axis Distribution-----

#	SI4	SP4
	h	d
-30	0.0000E+00	
-24	7.0319E-02	
-18	8.4472E-02	
-12	1.0066E-01	
-6	1.1681E-01	
0	1.2774E-01	

```

6    1.2774E-01
12   1.1681E-01
18   1.0066E-01
24   8.4472E-02
30   7.0319E-02

c
c -----Tally definitions-----
c
e0  7.41000E-01
    7.43000E-01
    7.65000E-01
    7.67000E-01
    0.954
    0.956
    0.999
    1.002
    1.18
    1.2
    1.24
    1.26
    1.5
    1.52
    1.736
    1.74
    1.76
    1.83
    1.832
    2.21
    2.25
    2.749
    2.75

c
c0  0 1
c
fc1  Particles through surrounding sphere
f1:p 2.1 2.2 2.3 2.4 2.5 2.6
fm1  4.83E7
c
FMESH4:P GEOM=rec ORIGIN=-50 -50 -50
IMESH=-40
-30
-20
-10
0.0
10
20

```

30
40
50
JMESH=-40
-30
-20
-10
0.0
10
20
30
40
50
KMESH=-40
-30
-20
-10
0.0
10
20
30
40
50
FACTOR=3.2966E5
c
c
c -----MATERIALS-----
c
c -----AIR p=0.00120479g/cc -----
M1 6000.04p -0.0126 \$Carbon
7000.04p -76.508 \$Nitrogen
8000.04p -23.4793 \$Oxygen
c
nps 1E8
RAND GEN 4
print 110

APPENDIX C

SAMPLE MCNP GEB INPUT

Model of 22.5yr WGPu solid

C

c Cell Cards

```
1 1 -19.6      -1    IMP:P=1 $inside of shell
2 2 -2.702      1 -2    IMP:P=1 $Aluminum Shielding
3 5 -0.00120479 2 -3    IMP:P=1 $Inner source box
4 5 -0.00120479 3 -4    IMP:P=1 $Inner container
5 3 -0.24       4 -5 3  IMP:P=1 $Packing material
6 4 -8.03       5 -6    IMP:P=1 $Steel Drum
7 5 -0.00120479 6 -7    IMP:P=1 $Outer source box
8 5 -0.00120479 7 9 -8  IMP:P=1 $air
9 0            8    IMP:P=0 $outer space void
10 6 -4.51      -9   IMP:P=1 $CsI detector
```

c Surface Cards

```
1 so 4.581
2 so 5.581
3 rpp -5.582 5.582 -5.582 5.582 -5.582 5.582
4 rcc 0 0 -33.1 0 0 66.2 19.924
5 rcc 0 0 -38.1 0 0 76.2 26.924
6 rcc 0 0 -38.222 0 0 76.444 27.046
7 rpp -27.05 27.05 -27.05 27.05 -38.23 38.23
8 rpp -37 30 -30 30 -38.6 38.6
9 rpp -36 -32 -2 2 -4 4
```

C DATA Cards

C

```
M1 94000.04p 1    $WGPu
M2 13000.04p 1    $Aluminum
M3 1000.04p 1    $Hydrogen
       6000.04p 1    $Carbon
       8000.04p 1    $Oxygen
M4 6000.04p -0.08  $Carbon
       14000.04p -1.0 $Silicon
       15000.04p -0.045 $Phosphorus
       24000.04p -17.0 $Chromium
       25000.04p -2.0  $Manganese
       26000.04p -65.375 $Iron
```

```

28000.04p -12 $Nickel
42000.04p -2.5 $Molybdenum
M5 6000.04p -0.0126 $Carbon
    7000.04p -76.508 $Nitrogen
    8000.04p -23.4793 $Oxygen
M6 55000.04p 0.0147471
    53000.04p 0.0147471
    11000.04p 1.4747e-5

```

c

mode P

sdef POS=0 0 0 RAD=d2 par=2 cell=1 erg=d1

#	Si1	SP1	SB1
	h	d	d
	0.29	0	0
	3.000E-01	2.0778E-02	0.002202643
	7.410E-01	9.7151E-01	0.002202643
	7.430E-01	3.2048E-04	0.002202643
	7.650E-01	2.4124E-03	0.002202643
	7.670E-01	1.7963E-03	0.002202643
	9.540E-01	2.0032E-03	0.00660793
	9.560E-01	3.1110E-05	0.00660793
	9.990E-01	2.9234E-05	0.00660793
	1.002E+00	1.6731E-05	0.033039648
	1.180E+00	1.8788E-05	0.033039648
	1.200E+00	2.3581E-08	0.033039648
	1.240E+00	1.6030E-08	0.033039648
	1.260E+00	5.6884E-04	0.033039648
	1.500E+00	5.6624E-08	0.033039648
	1.520E+00	2.8318E-08	0.033039648
	1.736E+00	5.6805E-08	0.033039648
	1.740E+00	3.9475E-08	0.088105727
	1.760E+00	2.7380E-04	0.088105727
	1.830E+00	3.1607E-08	0.088105727
	1.832E+00	2.9448E-08	0.088105727
	2.210E+00	5.3957E-08	0.088105727
	2.250E+00	7.8974E-05	0.088105727
	2.749E+00	7.0450E-05	0.088105727
	2.750E+00	8.9668E-05	0.088105727

c

SI2 0 4.58

SP2 -21 2

c -----

c Tally definitions

c -----

c Default Tally Energy structure: BUGLE-96 basis

e0 0.29

3.000E-01
7.410E-01
7.430E-01
7.650E-01
7.670E-01
9.540E-01
9.560E-01
9.990E-01
1.002E+00
1.180E+00
1.200E+00
1.240E+00
1.260E+00
1.500E+00
1.520E+00
1.736E+00
1.740E+00
1.760E+00
1.830E+00
1.832E+00
2.210E+00
2.250E+00
2.749E+00
2.750E+00

c

C0 0 1

NONU

c

c ---CsI(Na) Detector Pulse Height, with E broadening---

f18:P (10)

ft18 geb -0.00725 0.07322 0.31329 \$Gaussian energy broadening a b c

e18 0 1.000E-05 0.001 2998i 3.0

c

c ---Pulse height tally with GEB for detector in 24 group structure---

f28:P (10)

ft28 geb -0.00725 0.07322 0.31329 \$Gaussian energy broadening a b c

e28 0.29

3.00000E-01

7.41000E-01

7.43000E-01

7.65000E-01

7.67000E-01

0.954

0.956

0.999

1.002

```
1.18
1.2
1.24
1.26
1.5
1.52
1.736
1.74
1.76
1.83
1.832
2.21
2.25
2.749
2.75

c
c ---Flux Tally inside of detector---
f34:P (10)
fm34 8.846e8 $tally multiplier
c
ctme 800
print
```

REFERENCES

- [1] GOTTLIEB, S., "Debating terrorism and counterterrorism: conflicting perspectives on causes, contexts, and responses," 2nd ed. pp.169- 170, 2009.
- [2] GOSNELL, T.B., "Uranium measurements and attributes," Presented at the 41st annual meeting of the Institute of Nuclear Materials Management, New Orleans, LA, 2000.
- [3] MOSS, C.E, GOULDING, C.A., HOLLAS, C.L., AND MYERS, W.L., "Neutron detectors for active interrogation of highly enriched uranium," IEEE Transactions on Nuclear Science., vol. 51, pp. 1677-1681, 2004.
- [4] LITTLE, R.C., CHADWICH, M.B., AND MYERS, W.L., "Detection of highly enriched uranium through active interrogation," Presented at the 11th International Conference on Nuclear Reaction Mechanisms, Varenna, Italy, 2006.
- [5] House Hearing, 109 Congress, "Detecting nuclear weapons and radiological materials: how effective is available technology?" Joint hearing before subcommittee on prevention of nuclear and biological attack with the subcommittee on emergency preparedness, and science, and technology of the committee on homeland security House of Representatives first session, (2005). SN: 109-23.
- [6] Los Alamos National Laboratory, "MCNP5: Monte Carlo N-Particle Transport Code Including MCNP5 1.60 and MCNPX 2.7.0 & Data Libraries," *RSICC Data Library Collection*, C00740 MNYCP 08, 5.0 ed., Los Alamos, New Mexico (2011).
- [7] SJODEN, G., AND HAGHIGHAT, A., "PENTRAN - A 3-D Cartesian Parallel SN Code with Angular, Energy, and Spatial Decomposition", Proceedings of the Joint International Conference on Mathematical Methods and Supercomputing for Nuclear Applications, p. 553, Saratoga Springs, NY, October 5-10, 1997.
- [8] HAGHIGHAT, A., SJODEN, G., KUCUBOYACI, V., "Effectiveness of PENTRAN's Unique Numerics for Simulation of the Kobayashi Benchmarks", Special Issue, Progress in Nuclear Energy Journal, 3D Radiation Transport Benchmarks for Simple Geometries with Void Region, 39, 2, (2001), ISSN 0149-1970.

- [9] COURAU, T., AND SJODEN, G., "3D Neutron Transport and HPC: A PWR Full Core Calculation Using PENTRAN Sn Code and IBM BLUEGENE/P Computers", Progress in NUCLEAR SCIENCE and TECHNOLOGY, Vol. 2, pp.628-633 2011.
- [10] International Atomic Energy Agency, "IAEA Safeguards Glossary" Vol. 3. Vienna, Austria (2001).
- [11] HIGGINSON, M.C., "Westinghouse Hanford Company Special Nuclear Material Vault Storage Study," Westinghouse Hanford Company, U. S. Department of Energy, Ed. 1, 1996.
- [12] HANSEN, L.F., "A Comparison of the Shielding Performances of the AT-400A, Model FL, and Model AL-R8 Containers," Defense Programs 2nd Annual Packaging Workshop, San Francisco, CA, 1995.
- [13] Ed: QUIRK, W.C., JUNE, K., ROBERT, D., VORE, L.D., KROOPNIK, H., GLEASON, K., MCELROY, L., "Dismantling the Cold War Arsenal," Lawrence Livermore National Laboratory, Springfield, Virginia, 1993.
- [14] FAHRENHOLTZ, J.C., "Development of an automated pit packaging system for Pantex," *Sandia National Laboratory*, SAND--97-2163, ON: DE98000061, TRN: 97:005374, 1997.
- [15] YI, C., "PENMSHXP: Parallel Environment Automated Mesh Generator," 2.67b ed., Computational Radiation Transport Laboratory (CRiTCEL), Georgia Institute of Technology, 2011.
- [17] Oak Ridge National Laboratory, "SCALE6: A Comprehensive Modeling and Simulation Suite for Nuclear Safety Analysis and Design; Includes ORIGEN (Source & Executables)," RSICC Data Library Collection, C00785-MNYCP-00, 6.0 ed., (2009).
- [16] "The Modern Pit Facility (MPF)," American Physical Society Panel on Public Affairs (2004).
- [18] WHITE, J.E., "Bugle-96: Coupled 47 Neutron, 20 Gamma-Ray Group Cross Section Library Derived from ENDF-B/VI for LWR Shielding and Pressure Vessel Dosimetry Applications," RSICC Data Library Collection, D00185-ALLCP-00, 1996.

- [19] SJODEN, G., MANISCALCO, J., CHAPMAN, M., "Recent advances in the use of ASEDRa in post processing scintillator spectra for resolution enhancement", Journal of Radioanalytical and Nuclear Chemistry: Volume 291, Issue 2 (2012), Page 365-371.
- [20] REILLY, D.E., ENSSLIN, N., SMITH, H.A., SAMPSON, T.E., "PANDA: Passive Nondestructive Assay of Nuclear Materials," U. S. Nuclear Regulatory Commission Office of Nuclear Regulatory Research, NUREG/CR-550, Washington, D.C., 1991.
- [21] GHITA, G., SJODEN, G., BACIAK, J., "Computational and experimental validation of a WGPu neutron leakage source using a shielded PuBe (a,n) neutron source," Nuclear Technology Vol 168, Nov 2009.
- [22] MOLINAR, M.P., "SNM neutron detection using a time-gated synthetic aperture hybrid approach," Presented at the International Conference on Mathematics and Computations Methods Applied to Nuclear Science and Engineering. Sun Valley, ID, 2013.
- [22] GHITA, G., SJODEN, G., BACIAK, J., "On Neutron Spectroscopy Using Gas Proportional Detectors Optimized By Transport Theory," Nuclear Technology, Vol 168, pp. 620-628, 2009.
- [23] SJODEN, G., AND YI, C., "Transport simulation and validation of a synthetic aperture SNM detection system" ("T-SADS") Quarterly Report to NNSA, NA-22, July 2011.
- [24] CHIN, M., "The design of a mobile synthetic aperture collimated gamma detector for passive HEU sources," M.S. Thesis (in progress). 2013.